POLITECNICO DI MILANO

Dipartimento di Elettrotecnica
Dipartimento Energia

Scuola di Dottorato

Dottorato di Ricerca in Ingegneria Elettrica – XXIV Ciclo

Tesi di Dottorato

Ph.D. Thesis

VOLTAGE CONTROL IN MV NETWORKS WITH HIGH DG PRESENCE USING A REAL-TIME DIGITAL SIMULATOR

Candidato

Gianluca Sapienza

Matricola *738754*

Relatore

Dario Zaninelli

Tutor e Coordinatore
del Corso di Dottorato
Alberto Berizzi

Correlatori
Ettore De Berardinis
Paola Petroni

Summary

Introduction

The widespread of the Distributed Generation (DG), installed in Medium Voltage (MV) Distribution Networks, impacts the future development of modern Electrical Power Systems. A massive DG installation, typically based on Renewable Energy, completely changes power flows and, consecutively, network voltages and energy losses.

Focusing on the MV network, we can say that today DG normally exchanges only active power to the grid, i.e. it works at unitary power factor. However, due to the MV grid resistance/reactance ratio, network voltages are also influenced by active power injections. Therefore, in case of high active power injection, high voltage levels may occurs so potentially causing DG disconnection by means of interface relay tripping.

Controlling the grid voltage, the above mentioned problems should be solved. Moreover, voltage regulation allows to increase the network hosting capacity.

In this PhD Thesis, which has been developed in collaboration with Enel Distribuzione S.p.A. (the major Italian DSO), an MV grid Voltage Control Criteria is proposed, discussed and analyzed using a Real-Time Digital Simulator (RTDS). The Voltage Control Criteria consists in three voltage control strategies, which works in correlate way:

1. MV busbar voltage regulation in Primary Substation
2. "Local" Voltage Control, along feeders
3. "Centralized" Voltage Control, which involves the entire MV grid

The MV busbar voltage regulation in Primary Substation, which is treated in Chapter 1, allows to maintain the MV busbar to the minimum admissible voltage set-point. It is based on "daily load flow" calculation performed by the Distribution Management System (DMS) by means of load curves derived from the Electronic Meters.

The Local Voltage Control allows to control voltage along feeders, at the DG delivery point, varying the exchanged reactive power as a function of the delivery point voltage. Two local regulation functions will be presented: the UPG and the RQV. Both functions will be treated in Chapter 2.

The "Centralized" Voltage Control allows to support the Local Voltage Control. In case of Local Voltage Control is not able to maintain the voltage between pre-defined limits, the Centralized Voltage Control try to help generators "in difficulty" asking the "closest" generators

to operate. The "closest" concept is based on a Sensitivity Approach particularized for radial distribution feeders. The Centralized Voltage Control will be presented in Chapter 3.

The proposed Voltage Control Criteria will be applied to the "Ciccalento" MV line, located in the Italian Puglia region, and fed by the "San Giovanni Rotondo" Primary Substation. The "Ciccalento" line has been taken into account for the "POI-P3" Pilot Project (the Italian acronym of "Interregional Operative Project") on Smart Grids, funded by the Italian Ministry of Economic Development, which involves some GD plants in four Regions of the South of Italy.

Before the real field application in the pilot project, Real-Time Digital Simulations have been used to validate the presented criteria. Analysis have been performed using the Real-Time Digital Simulator installed in the Enel Distribuzione Test Center of Milan (Italy). The RTDS model of the considered grid is presented in Chapter 4. Numerical results have been shown in Chapter 5.

Finally, in Chapter 6, the MV network Sensitivity Approach has been generalized for a four-wires LV network, in order to extend the Centralized Voltage Control to LV application.

Chapter 1

Distributed Generation influence on MV busbar Voltage Regulation Criteria

1.1 INTRODUCTION TO CHAPTER 1

Medium voltage distribution networks (MVDN) work typically in a radial configuration. The supply point is the MV busbar of the primary substation.

The HV/MV transformer of the primary substation is equipped with an on-load tap changer (OLTC) driven by an automatic voltage regulator (AVR). This system allow to regulate the voltage along the MV feeders of the MVDN setting a particular voltage set-point on the MV busbar. Typically this set-point can be constant or variable with a function which depends on the transformer MV side current. In the first case we can say that the voltage is "constant regulated". In the second case we can say that the voltage is "compound regulated".

The compounded busbar regulation can crate problem with DG, as shown in the follow. However a completely constant busbar voltage regulation, e.g. daily constant regulation, is not possible because in case of high DG injected power can produces over-voltages. The proposed busbar regulation criteria, which will be applied to the MV grid of the POI-P3 pilot project on Smart Grids, is presented in this chapter. It consists in a "busbar set-point daily profile calculation" performed using load flow algorithms implemented in the Distribution Management System (DMS).

1.2 COMPOUND VOLTAGE REGULATION AT THE MV BUSBAR

1.2.1 The total compound

The compound voltage regulation allow to regulate the voltage, on a particular line section, regulating a voltage in another section. For example, referring to Fig. 1.2-1-a the (compounded) AVR can maintain a constant voltage E_L^* at the load busbar (LB) performing the regulation at the MV busbar (MVB). It is clear that the MV busbar voltage must be variable in function of the load. In other words its set-point must be:

$$E_B^* = f\left(P_L, \cos\varphi_L\right) \Rightarrow E_B^* = f\left(A_L\right) \tag{1.1}$$

where A_L is the load apparent power.

The set-point voltage E_B^* can be calculated using the approximate voltage drop formula. Referring to Fig. 1.2-1-b, which represents the single-phase equivalent circuit of Fig. 1.2-1-a, we can write:

$$E_B^* = E_L^* + I_l \left(R_l \cos \varphi_L + X_l \sin \varphi_L \right) \tag{1.2}$$

where:

- E_L^*, R_l and X_l are constant values set into the AVR
- the line current I_l can be measured using a current transformer (CT) installed at the MVB section
- the power factor $\cos \varphi_L$ cannot be measured at the MVB section; in substitution of this variable, the power factor $\cos \varphi_L'$ can be used, i.e.:

$$E_B^* = E_L^* + I_l \left(R_l \cos \varphi_L' + X_l \sin \varphi_L' \right) \tag{1.3}$$

otherwise, in term of line-to-line parameters:

$$V_B^* = V_L^* + \sqrt{3} I_l \left(R_l \cos \varphi_L' + X_l \sin \varphi_L' \right) \tag{1.4}$$

The equation (1.4) represents the *compound function*. The *tap positioner* implemented in the AVR choose the OLTC tap in order to obtain a voltage error referred to the measured voltage V_B:

$$e_V = V_B^* - V_B \tag{1.5}$$

close to zero. The small difference between V_B and V_B^* (from which we can have $e_V \cong 0$) is due to the discrete tap regulation ΔV_{OLTC} and is not taken into account in this treatment because it creates only a difference $\pm \Delta V_{OLTC}$ on the load voltage (and this difference is a small percentage of the power system rated voltage).

According to (1.4) and (1.5), the block diagram of the AVR is represented in Fig. 1.2-2.

It is important to note that if (1.4) is implemented as a compound function, we obtain a *total compound effect*. In other words, from the load point of view and in steady-state, the supply equals to an ideal voltage source with phase voltage E_L^* connected to the load with a zero-impedance line (as reported in Fig. 1.2-3-a). The volt-ampère (V-I) characteristic "viewed" from the load is reported in Fig. 1.2-3-c and the MV busbar voltage set-point necessary to obtain the V-I characteristic (calculated using (1.4)) is stretched in Fig. 1.2-3-b.

Fig. 1.2-1. MV distribution line with OLTC on the MV busbar. Power system schematic (a), and single-phase equivalent circuit (b).

Fig. 1.2-2. AVR of the OLTC.

$$\sqrt{3}\left(R_l \cos\varphi_L{}' + X_l \sin\varphi_L{}'\right)$$

Fig. 1.2-3. **The *total compound effect* in terms of equivalent circuit (a), the MV busbar voltage set-point (b), and the load "viewed" volt-ampère characteristic (c).**

1.2.2 The partial compound

Sometimes it is necessary to have, at load terminals, a *partial compound effect*. In the practice this operation mode is called "*with compound function enabled*". This king of voltage regulation avoid that the voltage overcomes the maximum admissible voltage in all network nodes. In fact, as said before, if we want to regulate the end of the line at constant voltage, we need to increase the busbar voltage after a load increment. If the line is very long, or the load is very heavy, the needed busbar voltage can be extremely high and can overcomes the maximum admissible voltage. This problem can be avoided using the partial compound. It is clear that we cannot regulate the load node at constant voltage value. In the follow the compound regulation is described.

The V-I characteristic of the circuit depicted in Fig. 1.2-1-b, is:

$$V_L = V_B - \sqrt{3}I_l\left(R_l \cos\varphi_L + X_l \sin\varphi_L\right) \tag{1.6}$$

and in terms of MV busbar voltage set-point (in order to obtain V_L at the load) we can write:

$$V_B^* = V_L + \sqrt{3}I_l\left(R_l \cos\varphi_L + X_l \sin\varphi_L\right) \tag{1.7}$$

Let us now suppose that the desired partial compounded V-I characteristic is:

$$V_L = V_L^* - \sqrt{3} I_l \left(k R_l \cos \varphi_L + k X_l \sin \varphi_L \right) \tag{1.8}$$

where $0 \le k \le 1$ is an impedance reduction factor.

Substituting (1.8) in (1.6) it is possible to calculate in order to have, at the load terminals, the partial compounded characteristic described by (1.8). We have:

$$\begin{aligned} V_B^* &= V_L^* + \sqrt{3} I_l \left((1-k) \cdot R_l \cos \varphi_L + (1-k) \cdot X_l \sin \varphi_L \right) = \\ &= V_L^* + \sqrt{3} I_l \left(\alpha \cdot R_l \cos \varphi_L + \alpha \cdot X_l \sin \varphi_L \right) \end{aligned} \tag{1.9}$$

where:

$$(1-k) \triangleq \alpha \tag{1.10}$$

is the *compound factor*. In particular we can say that:

$$\begin{cases} \alpha = 0 \ (k=1) \ \textit{no compound} \\ 0 < \alpha < 1 \ \textit{partial compound effect} \\ \alpha = 1 \ (k=0) \ \textit{total compound effect} \end{cases} \tag{1.11}$$

As said before, the power factor $\cos \varphi_L$ cannot be measured at the MVB section; in substitution of this variable, the power factor $\cos \varphi_L'$ can be used. We have:

$$V_B^* = V_L^* + \sqrt{3} I_l \left(\alpha \cdot R_l \cos \varphi_L' + \alpha \cdot X_l \sin \varphi_L' \right) \tag{1.12}$$

In terms of equivalent circuit, α (or k) regulates the line impedance (see (1.8) and (1.10)). The consequent equivalent circuit is reported in Fig. 1.2-4-a. The V-I characteristic "viewed" from the load is reported in Fig. 1.2-4-c (A_l is the load apparent power) and the MV busbar voltage set-point necessary to obtain the V-I characteristic (calculated using (1.12)) is stretched in Fig. 1.2-4-b.

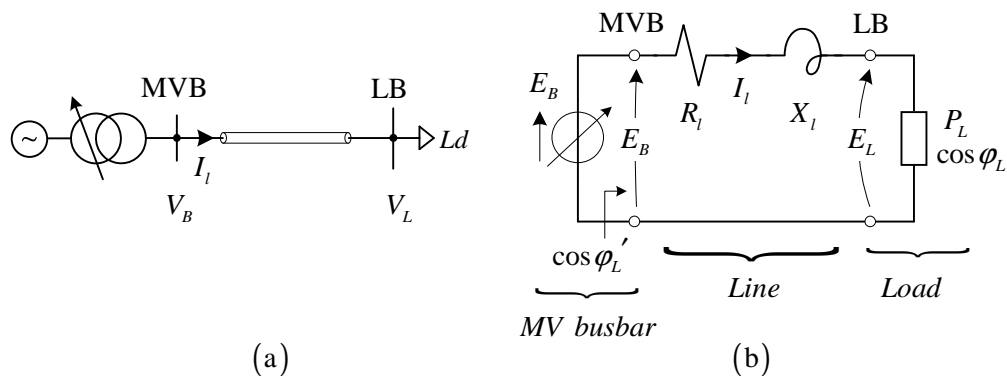The complete AVR block diagram, with partial compound, is reported in Fig. 1.2-5.
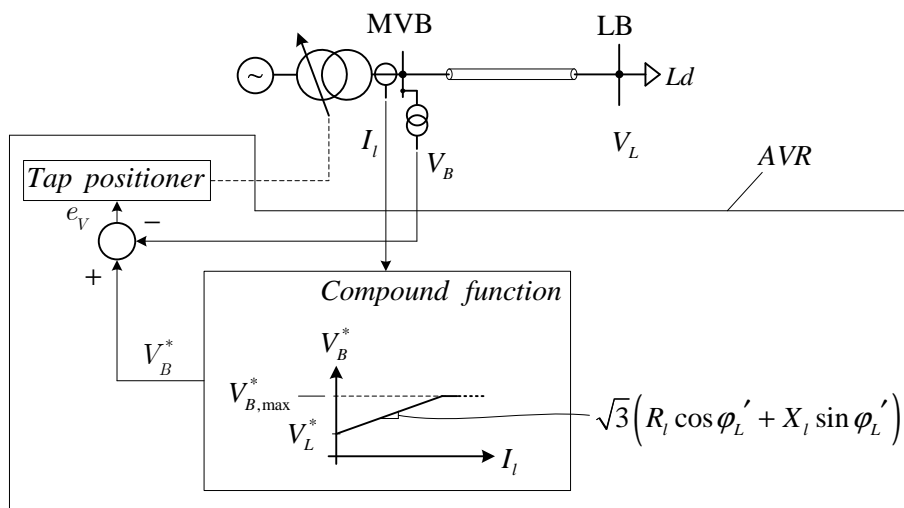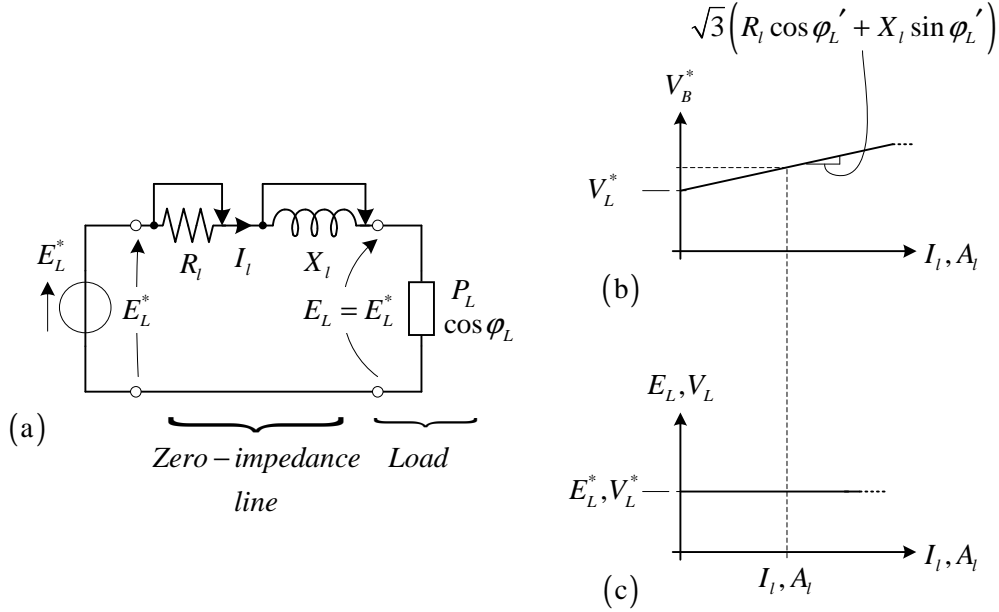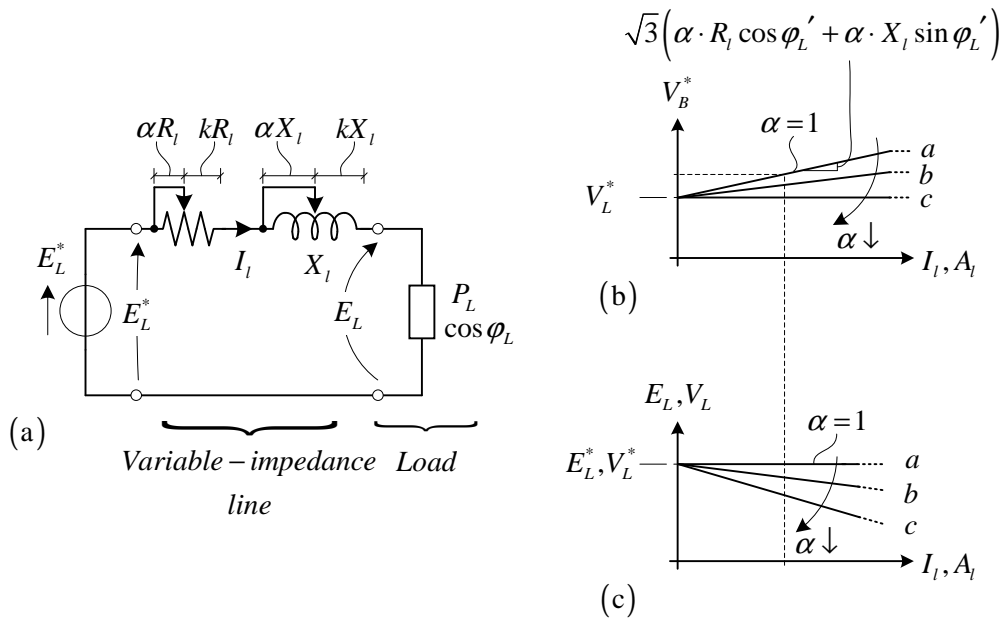
Fig. 1.2-4. The *partial compound effect* in terms of equivalent circuit (a), the MV busbar voltage set-point (b), and the load "viewed" volt-ampère characteristic (c).
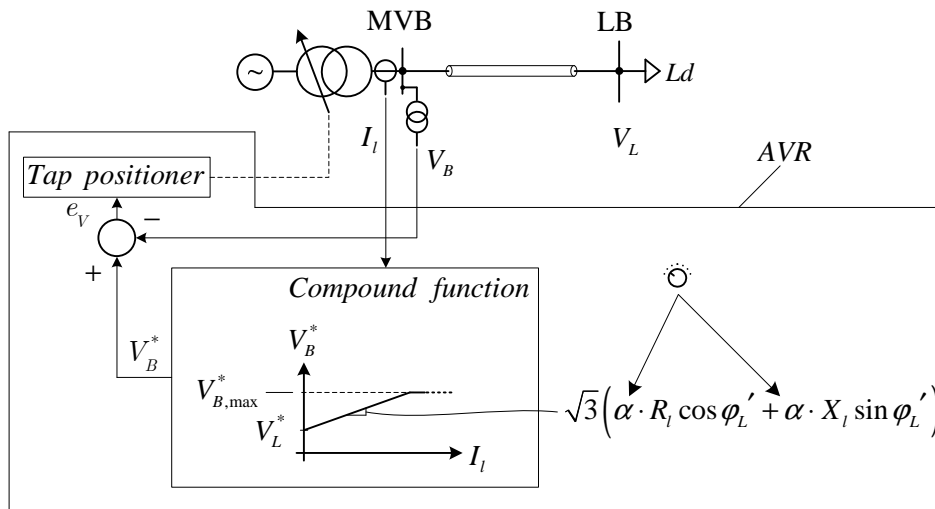

Fig. 1.2-5. AVR of the OLTC with the *partial compound effect*.

1.2.3 Compound effect in terms of V-I characteristic

The total and partial compound effect can be reviewed in terms of V-I characteristics. For both cases the analyzed single-phase equivalent circuit is that depicted in Fig. 1.2-1, where, as said before, the AVR acts on the MV busbar voltage E_B. In normal operation this voltage equals the set-point E_B^*.

The external characteristic (or source characteristic), "viewed" at LB terminals, is:

$$E_L = E_B^* - I_l \left(R_l \cos \varphi_L' + X_l \sin \varphi_L' \right) \tag{1.13}$$

which is represented in Fig. 1.2-6 (functions *a*, *b*, *c*, *d*) for constant load power factor. For each characteristic, the *fictitious* short circuit current is:

$$I_{SC} = I_l \big|_{E_{L=0}} = \frac{E_B^*}{\left(R_l \cos \varphi_L' + X_l \sin \varphi_L' \right)} \tag{1.14}$$

This current is *fictitious* because is not the real short circuit at LB terminals.

Let us now suppose that the AVR is set to obtain the total compound effect (section 1.2.1), in order to have E_L^* on the load LB side. The situation is represented in Fig. 1.2-6-a. If $I_{l,1}$ is the load current, the working point of the power system is p_1. Let us now suppose a load increment. The new current is $I_{l,2}$ and the new working point will be p_2. In the first case the AVR set the voltage busbar at $E_{B,1}^*$ and the external characteristic at LB is *a*; in the second case the set-point will be $E_{B,2}^*$ and the external characteristic at LB is *b*.

If the AVR is set to obtain the partial compound effect (section 1.2.2), the situation is sketched in Fig. 1.2-6-b. If $I_{l,1}$ is the load current, the working point of the power system is p_3. Let us now suppose the same load increment of the previous case. The new current is $I_{l,2}$ and the new working point will be p_4. These points lie on the V-I compounded characteristic (similar to *b*, *c* depicted in Fig. 1.2-4) relative to the AVR. In the first case the AVR set the voltage busbar at $E_{B,1}^*$ and the external characteristic at LB is *c*; in the second case the set-point will be $E_{B,2}^*$ and the external characteristic at LB is *d*. The set-point difference:

$$\Delta E_B^* = E_{B,2}^* - E_{B,1}^* \tag{1.15}$$

of this second case is less than the same difference relative to the first case. In other words, if a compound function is set in the AVR, at the same load current increment follows a voltage less set-point variation.
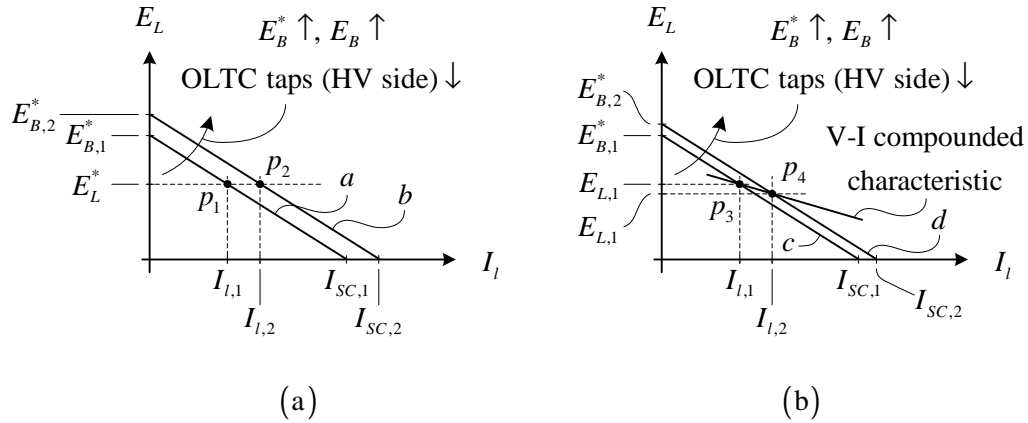
Fig. 1.2-6. Compound effect in terms of V-I characteristic. Total compound (a) and partial compound (b)

1.2.4 Compound regulation on the entire MV network

The previous example refers to a single MV line. It is important to note that the compound voltage regulation is normally implemented in transformers (equipped with OLTC) which feed, by means the MV busbar, an entire distribution network. The compound regulation is necessary to compensate the voltage drops along the MV feeders. The situation is sketched in Fig. 1.2-7.

In this case, all of the principles illustrated in the sections 1.2.1 and 1.2.2 are still valid, but the resistance R_l and the reactance X_l have a different meaning. They can be calculated using the concept of *electrical barycentre* of the lines supplied by the MV busbar.
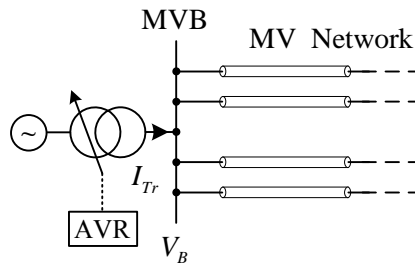
Fig. 1.2-7. Compound regulation on the entire MV network.

1.3 DISTRIBUTED GENERATION EFFECT ON THE MV BUSBAR VOLTAGE REGULATION

1.3.1 DG effect in terms of voltage compound regulation

Let us now suppose that the MVDN is active, i.e. some distributed generators (DG) are present. Moreover let us suppose that the AVR have the compound function enabled (the AVR sense the machine current I_{Tr} and the MV busbar voltage V_B). Fig. 1.3-1 represents a very

simple situation. Let us suppose that the generator is initially out of service (because, for example, the renewable primary energy is not present now) and that the load can be modeled using the constant-current model (with current I_{l2}). According to Fig. 1.2-6-b the voltage on the load busbar (LB) is sketched in Fig. 1.3-2-a. To the load current I_{l2} corresponds the voltage V_L' and, in this case, the transformer current coincides with the loads current.

When the generator begins its service, it tends to compensate the load and the transformer current tends to decrease (let us suppose that the generator power is comparable to the load power). The MV busbar voltage set-point follows this current decrease, as reported in Fig. 1.2-4-b and the same effect occurs on the load voltage, according to Fig. 1.2-6-b. In other words the load voltage became $V_L'' < V_L'$.
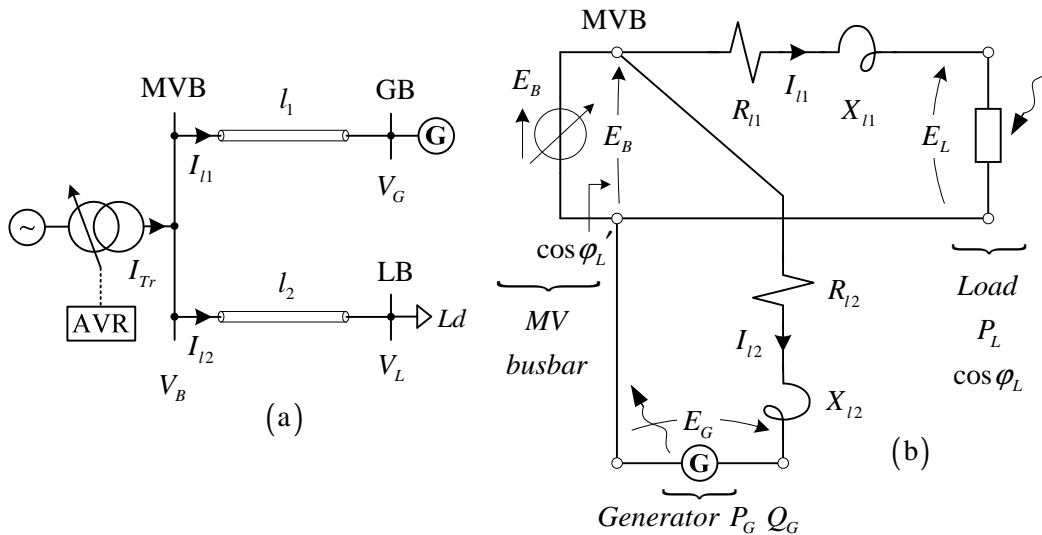
Fig. 1.3-1. Simple MVDN with GD presence. MVDN schematic (a) and single-phase equivalent circuit (b).
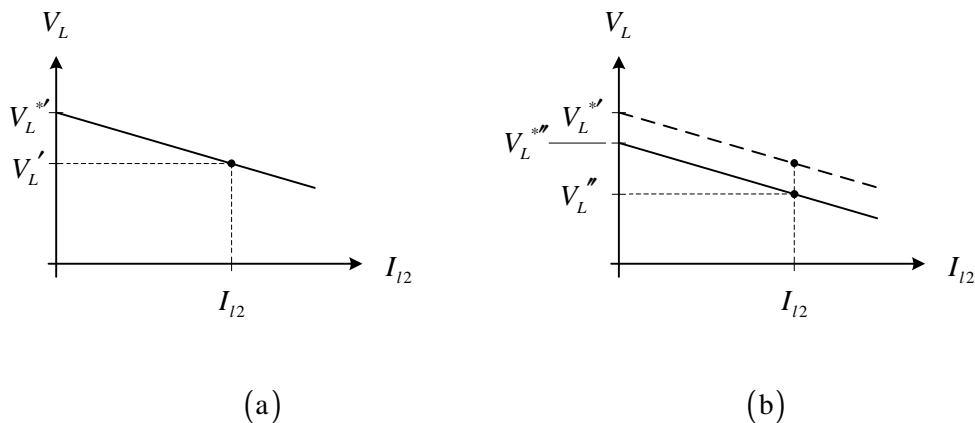
Fig. 1.3-2. Compound effect on MVDN with GD presence. Without and with generator (a), (b).

14

The voltage reduction from V_L' to V_L'' can be a problem from the load point of view. In other words the voltage compound regulation can create problems when the in the network some DGs are present, i.e. this technique cannot be used in the Smart Grids context.

1.3.2 DG effect with constant MV busbar voltage: the proposed approach to regulate the MV busbar in primary substation

As said before, the voltage compound regulation can create problems with DGs. The new approach, proposed in this treatment, consists to maintain the MV busbar to a constant voltage. The necessary AVR voltage set-point is calculated using the Enel Distribuzione Distribution Management System (DMS) as follow: let us suppose that all of the DGs of the MVDN are out of service, i.e. also loads are connected to the grid (the described situation is represented in Fig. 1.3-3 where the dot-sketched generators represent the devices out of service). The MV busbar voltage set-point E_B^* must be calculated in order to guarantee that the voltage on the *critical node* (CN), i.e. the network node which have the less voltage, is at least equal to the minimum admissible voltage $V_{\min}$ [1]:

$$V_{CN} \geq V_{\min} \tag{1.16}$$
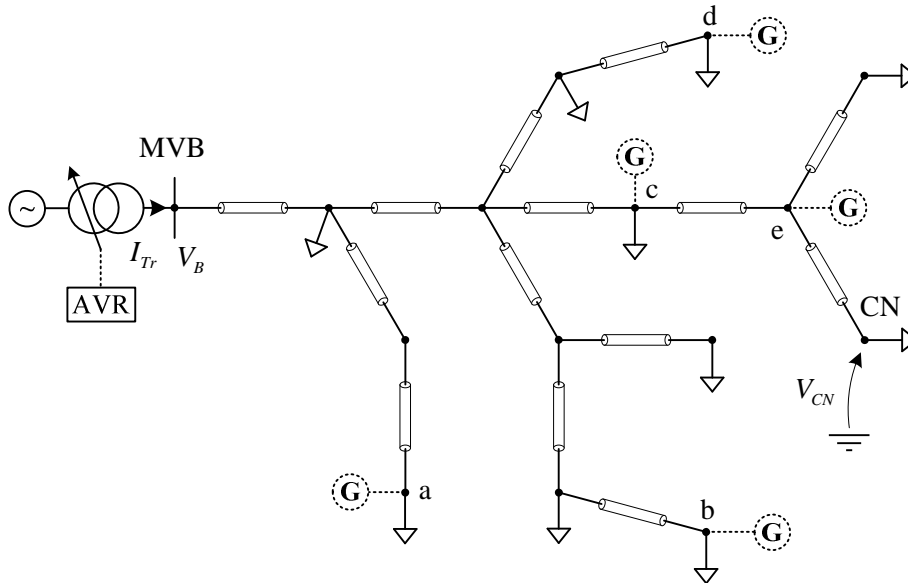
Fig. 1.3-3. MVDN with constant-regulated busbar and critical node concept.

In other words when the busbar is set to E_B^*, all of the nodes work correctly in terms of voltage. If we switch-on one generator, and wait that the AVR act on the OLTC in order to

---

[1] In this PhD work, the chosen value of $V_{\min}$ is 0.96 p.u.

maintain to E_B^* the MV busbar, i.e. the new steady-state condition occurs, the voltage grow up in all network nodes with respect to the initial condition. This phenomena occurs also if the generators inject only active power, i.e. it works at unitary power factor, due to the non-negligible value of the network series resistance with respect to the series inductive reactance.

If we want to reduce a nodal voltage along the feeder, we needs to locally absorb reactive power. In this last case the network "see" the DG like a real generator in terms of active power and like an inductor in terms of reactive power. Fig. 1.3-4 expose schematically these concepts, referred on a node of the grid depicted in Fig. 1.3-3.

The E_B^* calculation procedure, which is performed by the DMS, can be described using the following steps:

1. deactivate all of generators
2. run a load flow satisfying (1.16), for the entire day
3. calculate the daily E_B^* profile
4. send the daily E_B^* profile to the AVR which stores it in a memory

It is clear that the loads power PQ profile must be known in order to compute the MV busbar set-point using the load flow. This is not a problem in the Enel Distribuzione network because all of the loads are represented with a daily profile (defined every quarter of hour[2]) stored in the DMS database. The load daily profiles are built reading the electronic meters installed at the customers delivery points. Fig. 1.3-5 represent the MV busbar voltage set-point calculation scheme. The loads daily profile is composed by 96 values. Then also the E_B^* profile is composed by 96 voltage values.

In this paragraph the proposed criteria to regulate the MV primary substation busbar has been presented. In the following chapters, voltage regulation criteria necessary to regulates the nodal voltages along feeders will be presented.
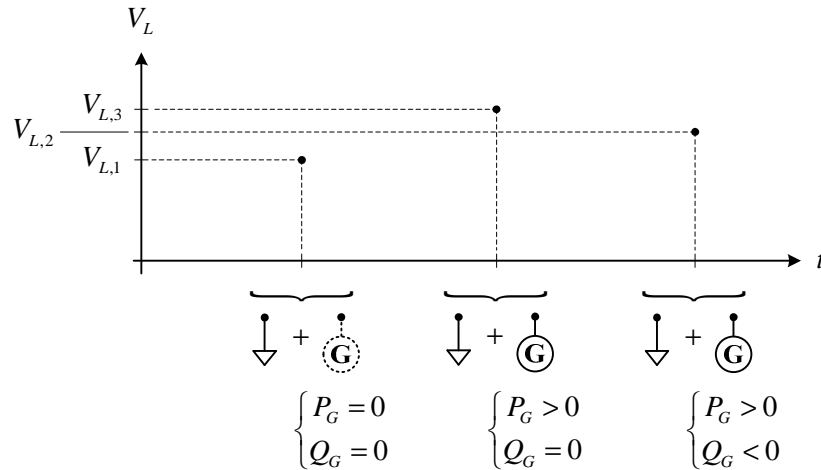
Fig. 1.3-4. Voltage variation in the node.

---

[2] Then a daily load profile is defined by 96 values
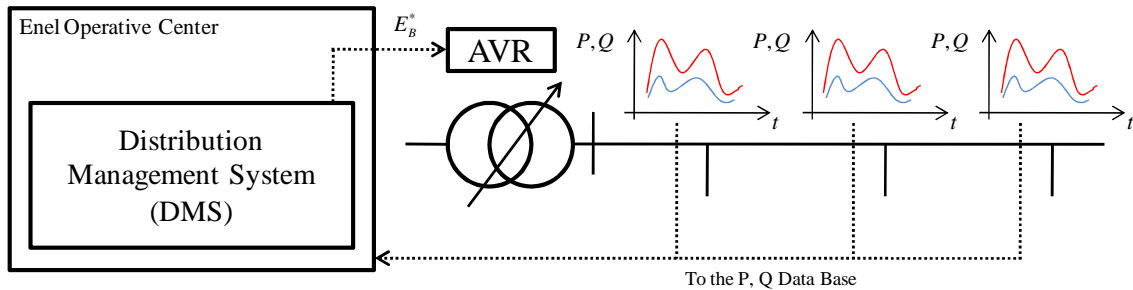
Fig. 1.3-5. MV busbar voltage set-point calculation scheme.

1.4 REFERENCES

[1] R. Marconato, "Electric Power Systems Vol. II" CEI, Milano, 2008.

[2] F. Cottignoli, A. Baccarini, "Elettrotecnica Generale", Edizioni Calderini, Bologna.

[3] F. Cottignoli, A. Baccarini, "Macchine Elettriche", Edizioni Calderini, Bologna.

[4] F. Cottignoli, A. Baccarini, "Misure elettriche ed elettrotecniche", 3 voll., Edizioni Calderini, Bologna, 1970.

[5] F. Cottignoli, A. Baccarini, "Guida al laboratorio di misure elettriche", 2 voll., E-dizioni Calderini, Bologna, 1971.

[6] P. Kundur, "Power System Stability and Control" McGraw-Hill, 1994.

[7] F. Saccomanno, "Electric Power Systems" Wiley-Interscience IEEE Press, Piscataway, NJ, 2003.

[8] G. Andersson, "Modeling and Analysis of Electric Power Systems" Lecture 227-0526-00, ITET ETH Zürich, 2008, Zürich.

[9] P.M. Anderson, "Power System Protection," IEEE Press, Piscataway, NJ, 1999.

[10] L. L. Grigsby, "Electric Power Generation, Transmission and Distribution", CRC Press-Taylor & Francis Group, Boca Raton, 2006.

[11] Radial Distribution Test Feeders, Distribution System Analysis Subcommittee Report.

Chapter 2

Proposed Local Voltage Control along MV Lines

2.1 Introduction to Chapter 2

The voltage control strategy designed for the Enel Distribuzione POI-P3 pilot project on Smart Grids, consists in three types of regulations:

- the Primary Substation MV Busbar Voltage Regulation, described in Chapter 1
- the Local Voltage Regulation, which is treated in this Chapter
- the Centralized (or remote) Voltage Regulation, which will be explained in Chapter 3

The local voltage regulation acts on distributed generator in function of the local delivery point (or "interconnection point") voltage. In the proposed approach there are two types of possible local voltage controls:

- the UPG regulation, which is a threshold-based control strategy. It changes the generator power-factor set-point when the voltage exceeds some thresholds. The UPG is described in Paragraph 2.2
- the RQV regulation, which is a droop-based control strategy. It changes the generator reactive power set-point in function of the interconnection point voltage. The RQV is treated in Paragraph 2.3

Generally, the local voltage regulation try to locally adjust the delivery point voltage in case of both "high voltage" and "low voltage". However it is possible that the voltage exceeds its limits also after the local voltage action. In this case the Centralized Voltage Regulation must act in order to try a new voltage adjustment. The Centralized Voltage Regulation is hierarchically higher than the Local Voltage Regulation. It is based on a "Sensitivity Table" which is related to the "electrical proximity" concept. The Centralized Voltage Regulation is performed by a DMS functionality called "Voltage Control System" (VCS) which will be treated in Chapter 3.

2.2 The "UPG" Local Voltage Control Technique

It is well known that, if reactive power is absorbed from the network, its voltage decreases. This simple concept can be used to reduce the network voltage, in case of high voltage, varying the absorbed reactive power when the voltage exceeds a particular threshold. Moreover the

reactive power can be generated, in case of low voltage, when the network voltage is less than a minimum threshold. The UPG local voltage regulation technique is based on this simple concepts, and can be classified as a threshold-based local voltage control.

In order to explain the UPG function, let us consider Fig. 2.2-1, which represents high voltage case. Let us suppose an interconnection point voltage V_{MT} increment, that can occur in case of high generated power injection or load losing. When V_{MT} exceeds the threshold V_{2S-UPG}, for the time period T_{2S-UPG}, the UPG switches its controlled generator "reactive power absorption mode" (RAM = ON). The RAM corresponds to a constant inductive power factor generator operation; in other words when RAM is ON, the UPG send an inductive power factor set-point to the generator regulators, and it absorbs reactive power from the network proportionally to the generated active power P_g. The RAM inductive power factor set-point is $\cos\varphi_{g,ind}$. Considering a positive generated reactive power Q_g, when the RAM is ON we can write:

$$Q_g = -P_g \tan\varphi_{g,ind} \tag{2.1}$$

where $\tan\varphi_{g,ind}$ is the tangent which corresponds to the phase angle $\varphi_{g,ind}$. In other words Q_g is a constant percentage of P_g. For example, if $\cos\varphi_{g,ind} = 0.9$, then:

$$Q_g = -P_g \tan\varphi_{g,ind} = -0.4843 P_g \tag{2.2}$$

In other words Q_g represents, in absolute value, the 48.43 % of P_g.

After the RAM mode activation, V_{MT} tends to decrease, due to the reactive power absorbed from the network. However no "bounce" problems can occurs due to:

- the network resistance/reactance ratio, which is variable from 0,75 to 1,65 in medium voltage distribution network
- the concept explained by (2.2) (Q_g is always a constant percentage of P_g)

These observations allow to avoid bounce problems: an active power injection causes a voltage increment but the reactive power absorption due to the RAM causes a voltage decrement which is less than the voltage increment. We can say that the voltage decrement is a percentage of the voltage increment[3].

---

[3] This concept can be also derived from the Sensitivity theory explained in Chapter 3.
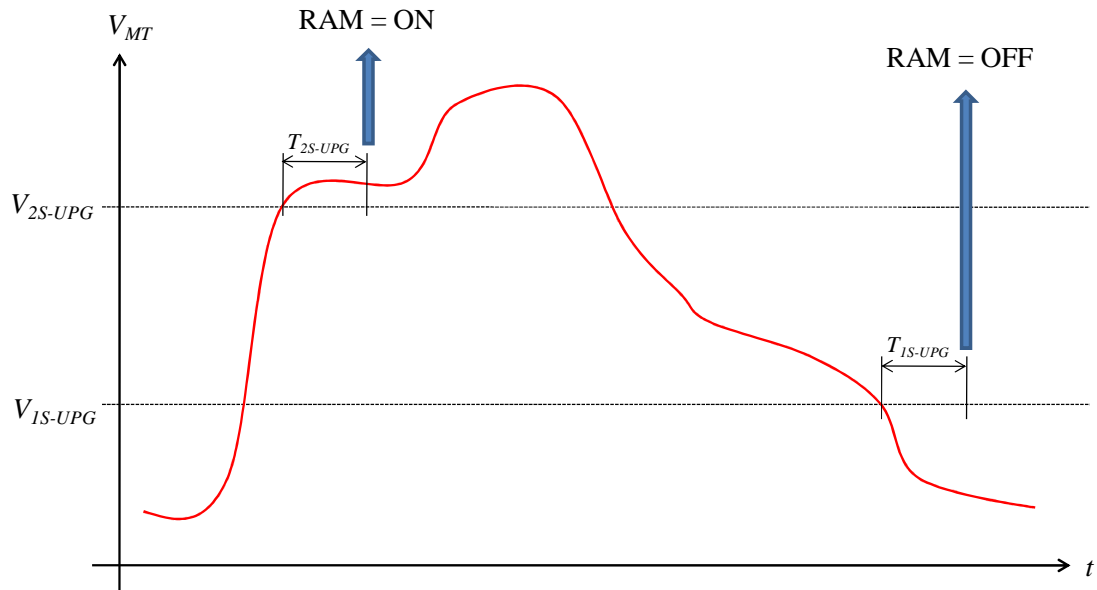
Fig. 2.2-1. The UPG thresholds in case of high voltage

The RAM is switched-off when V_{MT} remains under the threshold V_{1S-UPG} for the time T_{1S-UPG}, as reported in Fig. 2.2-1.

The low voltage case is represented in Fig. 2.2-2 and can be treated in the analogous way of the high voltage case, substituting the RAM function with the "reactive power generation mode" (RGM).
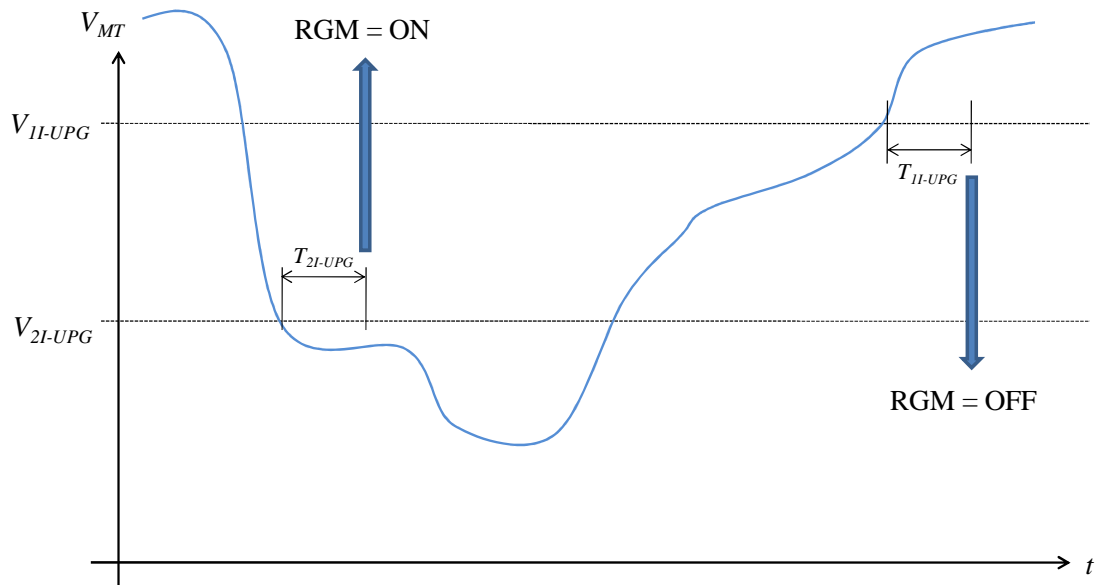

Fig. 2.2-2. The UPG thresholds in case of low voltage

When V_{MT} is under the threshold V_{2I-UPG}, for the time period T_{2I-UPG}, the UPG switches its controlled generator "reactive power generation mode" (RGM = ON). The RGM corresponds to a constant capacitive power factor generator operation; in other words when RGM is ON, the UPG send a capacitive power factor set-point to the generator regulators, and it injects reactive power in the network proportionally to the generated active power P_g. The RGM inductive power factor set-point is $\cos\varphi_{g,cap}$. Considering a positive generated reactive power Q_g, when the RGM is ON we can write:

$$Q_g = P_g \tan\varphi_{g,cap} \tag{2.3}$$

where $\tan\varphi_{g,cap}$ is the tangent which corresponds to the phase angle $\varphi_{g,cap}$. In other words Q_g is a constant percentage of P_g. After the RGM mode activation, V_{MT} tends to increase, due to the reactive power injected in the network. Likewise to the high voltage case, the bouncing problems are avoided by the resistance/reactance network ratio and by the reactive power like a percentage of the active power concept. The RAM is switched-off when V_{MT} exceeds the threshold V_{1I-UPG} for the time T_{1I-UPG}.

The power factor set-points generated by the RAM and RGM functions, comes to the controlled plant via the IRE device, which is described in Paragraph 2.3.

The UPG try to locally mitigate high and low voltage conditions. However, if the local RAM/RGM activation cannot be able to restore the correct voltage value, the Centralized Voltage Control, based on the Sensitivity technique, act its strategy choosing the "Best Generator (BG)", as described in Chapter 3.

The VCS is able to know the plants voltage status thanks to the UPG which sent, to the VCS, the binary signal VFLS in case of highest voltage, and the signal VFLI in case of lowest voltage level.

In particular, the VFLS signal is active (VFLS = 1) when V_{MT} exceeds the voltage threshold V_{2S-VCS} for the time period T_{2S-VCS}, as reported in Fig. 2.2-3. The VFLS de-activation (VFLS = 0) is performed when V_{MT} remains under the voltage threshold V_{1S-VCS} for the time period T_{1S-VCS}.
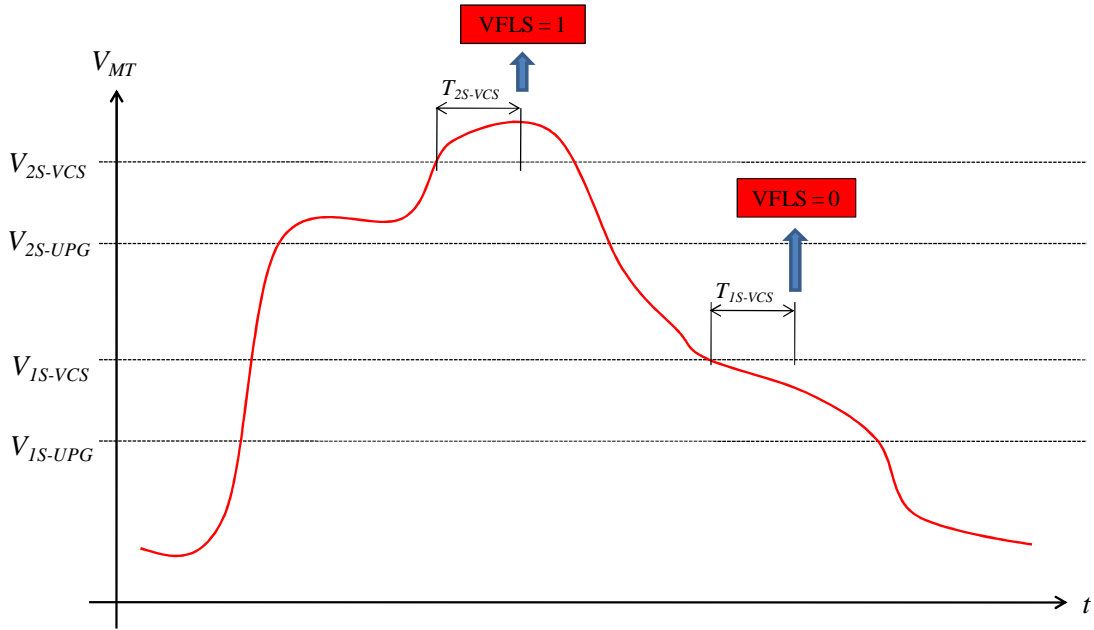
Fig. 2.2-3. The UPG/VCS thresholds in case of high voltage

The analogous procedure can be applied to the lowest voltage level case, as reported in Fig. 2.2-5. In this case the VFLI signal is active (VFLI = 1) when V_{MT} is under the voltage threshold V_{2I-VCS} for the time period T_{2I-VCS}, as reported in Fig. 2.2-5. The VFLI de-activation (VFLI = 0) is performed when V_{MT} exceeds the voltage threshold V_{1I-VCS} for the time period T_{1I-VCS}.

Fig. 2.2-4 represents the UPG characteristics is the voltage-power factor plane in case of high (Fig. 2.2-4-a) and low (Fig. 2.2-4-b) voltage.
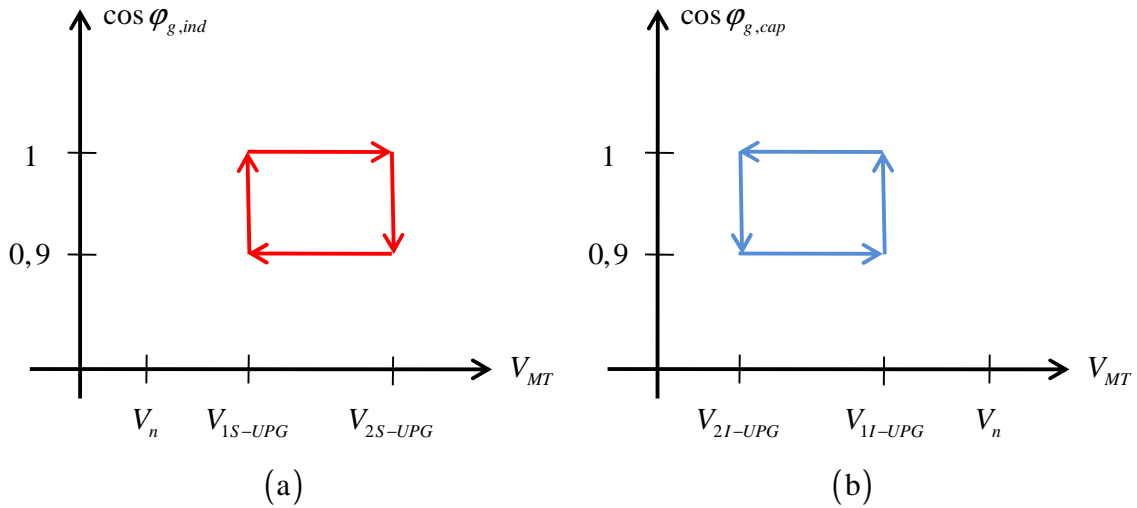
Fig. 2.2-4. The UPG characteristics is the voltage-power factor plane in case of high (a) and low (b) voltage

All of the described function have been implemented in the RTDS environment, using the RTDS "C-Builder tool", which allow to program the model blocks using the C language. The UPG dynamical RTDS block is reported in Fig. 2.2-6, where input and output signals have been defined using the IEC 61850 criteria (signals are characterized by value and activation bit).
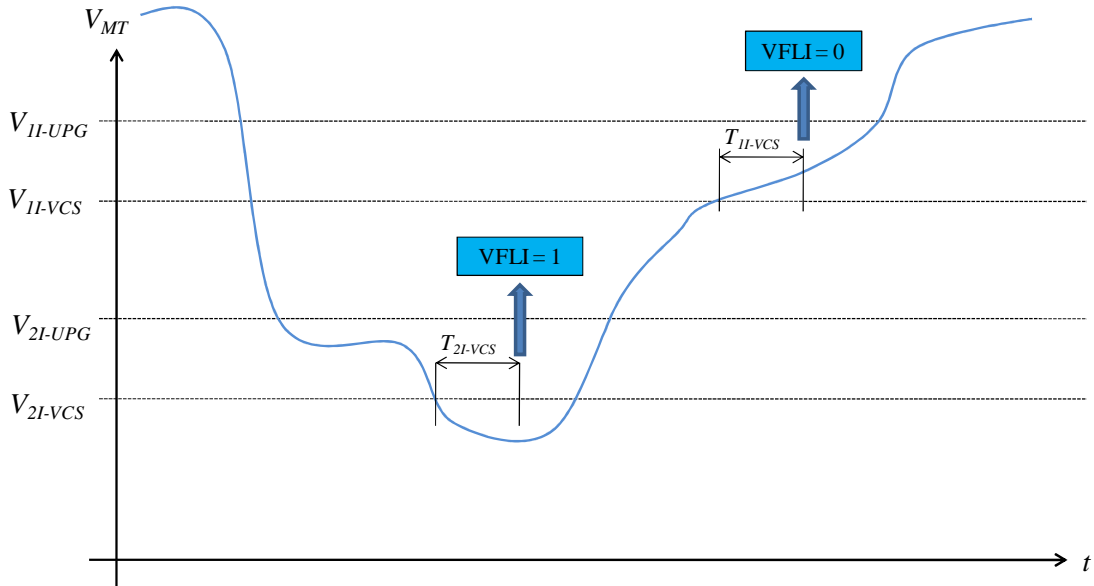
Fig. 2.2-5. The UPG/VCS thresholds in case of low voltage
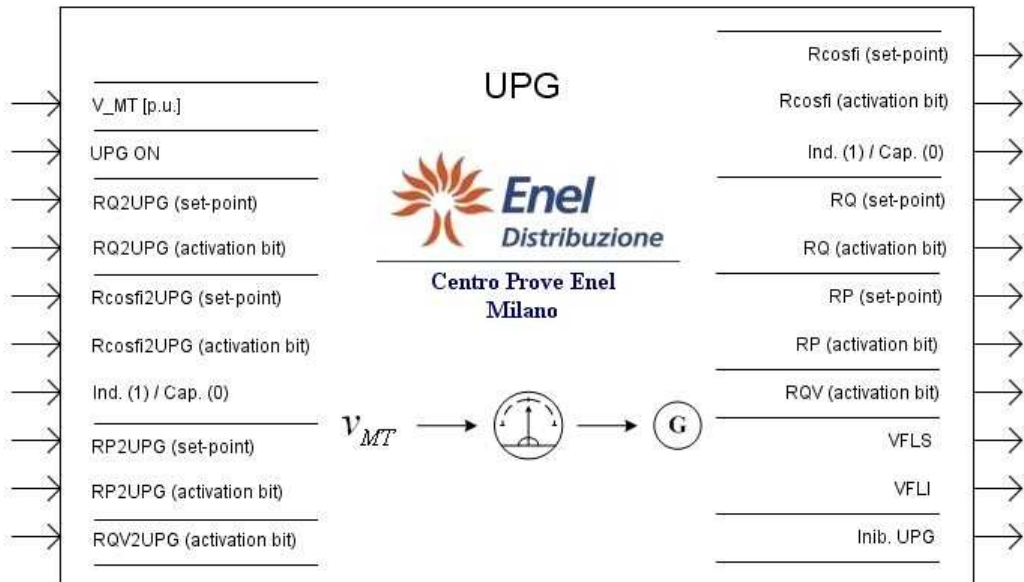
Fig. 2.2-6. The UPG block implemented in the RTDS environment

In particular:

- V_MT is the measured interconnection point voltage;
- UPG ON is the "main UPG switch" which allows to completely de-activate the UPG functions;
- RQ2UPG (set-point) is the remote reactive power set-point which can be supplied by the Enel Control Center in case of remote set-point controlling necessity;
- RQ2UPG (activation bit) is the RQ2UPG (set-point) activation bit; RQ2UPG (set-point) can be applied to the controlled plant only if RQ2UPG (set-point) = 1; moreover RQ2UPG (set-point) = 1 de-activates the UPG;
- Rcosfi2UPG (set-point) is the remote power factor set-point which can be supplied by the Enel Control Center in case of remote set-point controlling necessity. The power factor typology (inductive or capacitive) is defined by the "Ind. (1) / Cap. (0)" bit (signal = 1 corresponds to an inductive power factor, signal = 0 corresponds to a capacitive power factor);
- Rcosfi2UPG (activation bit) is the Rcosfi2UPG (set-point) activation bit; Rcosfi2UPG (set-point) can be applied to the controlled plant only if Rcosfi2UPG (set-point) = 1;
- RP2UPG (set-point) is the remote active power set-point which can be supplied by the Enel Control Center in case of remote set-point controlling necessity;
- RP2UPG (activation bit) is the RP2UPG (set-point) activation bit; RP2UPG (set-point) can be applied to the controlled plant only if RP2UPG (set-point) = 1;
- RQV2UPG (activation bit) is the signal which de-activate de UPG (leaving activated the VFLS/VLFI signals) and activate the RQV function implemented in the IRE device (see Paragraph 2.3). The RQV activation is performed by the RQV (activation bit) signal, which is always equal to RQV2UPG (activation bit);
- Rcosfi (set-point) is the power factor set-point generated by the RAM and by the RGM
- Rcosfi (activation bit) is the RAM/RGM activation bit. When one of this functions is activated, Rcosfi (activation bit) = 1;
- Ind. (1) / Cap. (0) is the bit which describe the Rcosfi (set-point) typology; when the Rcosfi (set-point) is due to the RAM, Ind. (1) / Cap. (0) equals 1 (inductive power factor). When the Rcosfi (set-point) is due to the RGM, Ind. (1) / Cap. (0) equals 0 (capacitive power factor);
- RQ (set-point) is equal to RQ2UPG (set-point). It is the (remote) reactive power set-point which is sent to the generator regulators
- RQ (activation bit) is equal to RQ2UPG (activation bit). It is the activation bit of the (remote) reactive power set-point
- RP (set-point) and RP (activation bit), are analogue to RQ (set-point) and RQ (activation bit) substituting Q with P
- RQV (activation bit) is equal to RQV2UPG (activation bit)
- VFLS and VFLI are VFLS and VFLI threshold signals

- Inib. UPG is the inhibition UPG signal. The UPG is inhibited when V_MT is very low

The subdivision in "set-point" and "activation bit" is based on the Enel IEC 61850 protocol profile philosophy.

The UPG parameters, used in the POI-P3 project simulations, will be presented in Chapter 4.

2.3 THE "RQV" LOCAL VOLTAGE CONTROL TECHNIQUE

As said in Paragraph 2.2, the UPG regulates the generators voltage acting a constant power factor, i.e. the reactive power exchanged with the network is direct proportional to the generated active power. Another modality to locally regulate the generator voltage can be performed proportionally varying the reactive power in function to the generator voltage. In other words we can define a reactive power-voltage droop. This local voltage regulation mode, which is described in this chapter, is called RQV technique. After the theoretical treatment of the RQV regulation technique, a numerical simulation using the RTDS will be explained, in order to validate the presented theory. In the POI-P3 pilot project the RQV local voltage regulation is implemented in the IRE ("Energy Regulation Interface") device, which has been implemented in the RTDS simulation environment using the "C-Builder" tool.

2.3.1 Definition of Q-V curves

2.3.1.1 Network Q-V curves

Generally, Q-V curves relate the voltage magnitude to the reactive power. These curves can be defined also for the network and generators. In the first case the curve parameters depend to the network data. In the second case the curve parameters are defined by the reactive power regulator in the steady-state condition.

In order to study the Q-V curves, we can consider Fig. 2.3-1, where the network is represented by means the Thévenin equivalent circuit (in this figure we have line-to-line voltages and three phase powers). In particular:

- V_r is the Thévenin equivalent voltage source (or the "network equivalent voltage"), which coincides to the no-load voltage.
- V_g is the voltage at the interconnection point (or "power delivery point")
- P_g is the active power at the interconnection point
- Q_g is the reactive power at the interconnection point
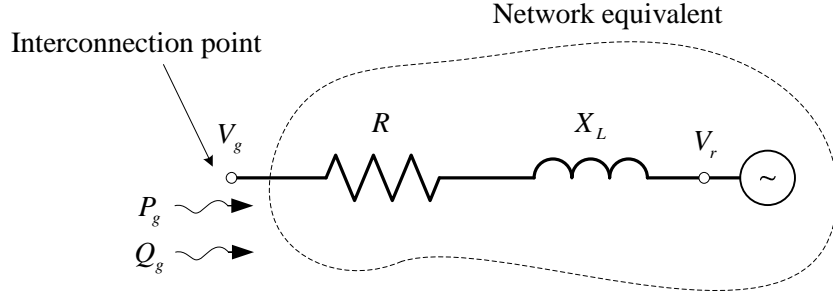
Fig. 2.3-1. The network equivalent

Using the industrial voltage drop calculation formula, we can obtain:

$$V_g = V_r + P_g \frac{R}{V_g} + Q_g \frac{X}{V_g} \tag{2.4}$$

but V_g is normally close to the network rated voltage V_n. Then the previous relation can be approximated to:

$$V_g \cong V_r + P_g \frac{R}{V_n} + Q_g \frac{X}{V_n} = Q_g \frac{X}{V_n} + \left(P_g \frac{R}{V_n} + V_r \right) \tag{2.5}$$

This equation indicates that, for small voltage variations, the interconnection point voltage linearly varies in function of the exchanged reactive power with a proportional relationship. In particular:

- $\dfrac{X}{V_n}$ is the slope (measured in $\left[\dfrac{V}{VAr} \right]$)

- $P_g \dfrac{R}{V_n} + V_r$ is the intercept in the origin (measured in $\left[V \right]$). Then this parameter

    depends to the equivalent network voltage and to the exchanged active power.

The slope indicates the reactive power-voltage "natural droop" of the network. Fig. 2.3-2 graphically indicates (2.5).
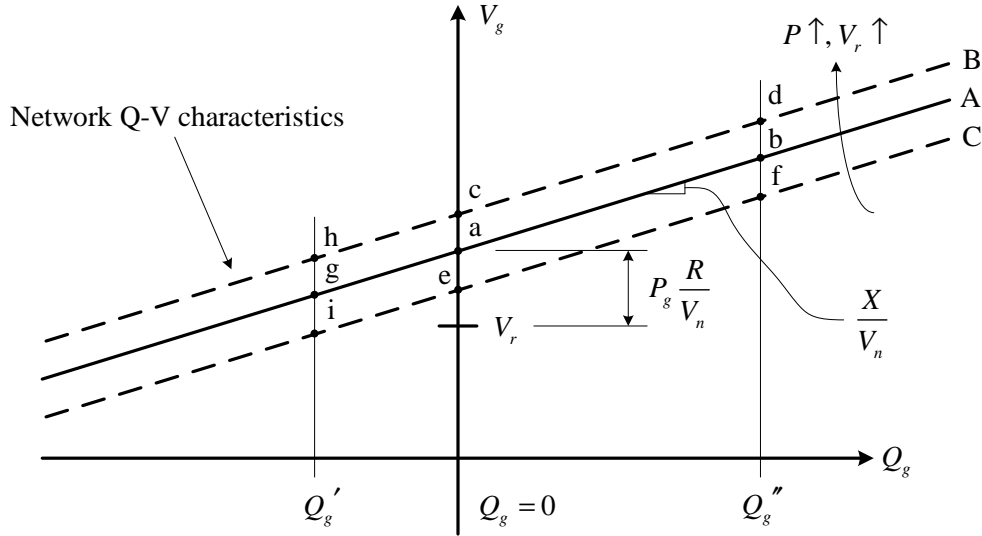
Fig. 2.3-2. The network characteristic

Increasing P_g or V_r, the network Q-V curve is shifted along the y axis forming a curves family. Related to the reactive power exchanged to the interconnection point, we have a variation of the working point and so the voltage V_g change its magnitude.

Now we can consider the $P_g = \text{cost}$ condition. This hypothesis maintains the treatment generality. Increasing the equivalent network voltage the Q-V curve is shifted to the positive y, only in function to V_g. For example, if $Q_g = 0$, the working point changes from "a" to "c".

Similarly, if the generator absorbs $Q_g{}'$, the consequent voltage will be less than the previous case, and the working point changes from "g" to "h". Analogous behavior occurs in case of V_r decrement and/or in case of $Q_g{}''$ reactive power generation.

2.3.1.2 Generator Q-V curves

As said before, the Q-V generator curves depend to the behavior of the reactive power regulator in steady-state condition.

Fig. 2.3-3 indicates network-generator coupling, in terms of Q-V curves. The D characteristic, with β droop, is a result of the reactive power regulator settings. This is the generator Q-V curve.

If A is the network Q-V curve, the actual working point will be "d". Increasing the equivalent network voltage (this condition corresponds to the curve B), the new working point will be "b".

It is important to note that now the voltage variation ΔV_g at the interconnection point is less with respect to the equivalent network voltage ΔV_r. This is the advantage of a regulation with Q-V droop.

$$\Delta V_g < \Delta V_r \ , \ \ \Delta Q_g \neq 0$$
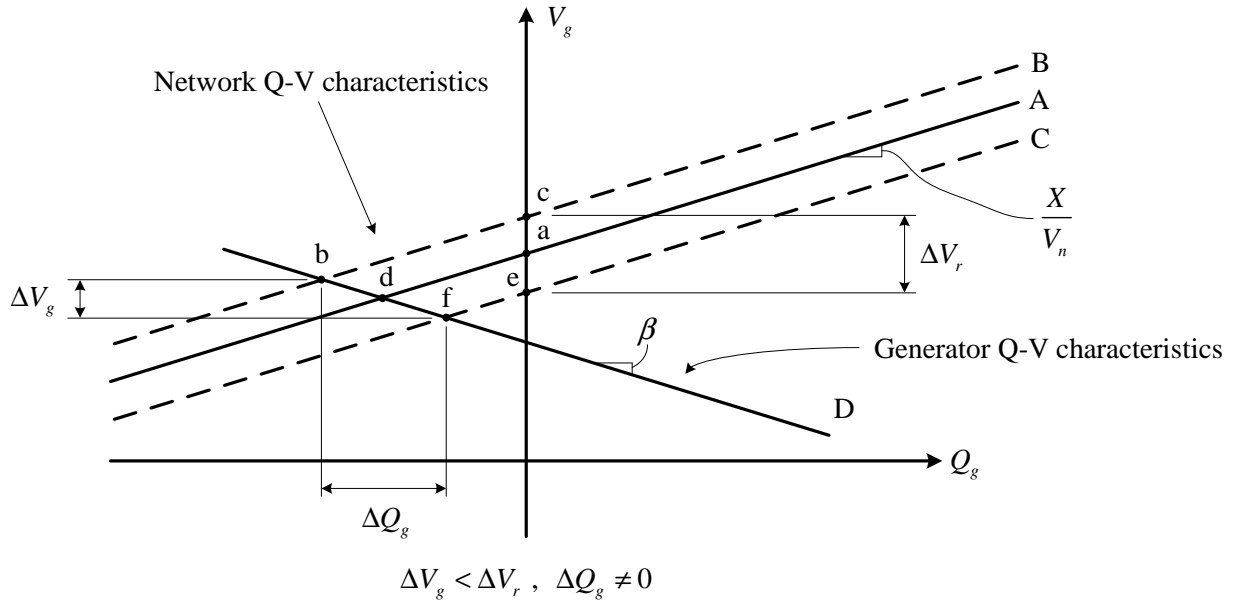
Fig. 2.3-3. The network-generator coupling, in terms of Q-V curves

If no regulation is activated, i.e. the generator not varies the reactive power, we exactly obtain:

$$\Delta V_g = \Delta V_r \tag{2.6}$$

It is clear that, in order to perform the described Q-V regulation, reactive power always must be exchanged, also when the generator voltage is close to its rated value. Generally, in order to obtain the "reduced" ΔV_g variation, ΔQ_g must be exchanged. To avoid this inconvenient, we can define a "voltage dead-band" (or "no regulation band", see Fig. 2.3-8 and Fig. 2.3-9); this solution will be discussed in the follow.

The discussed generator Q-V curve works good also in case of V_r decrement, as reported in Fig. 2.3-4. In this case the new working point will be "f", and the consequent ΔV_g will be less than ΔV_r.
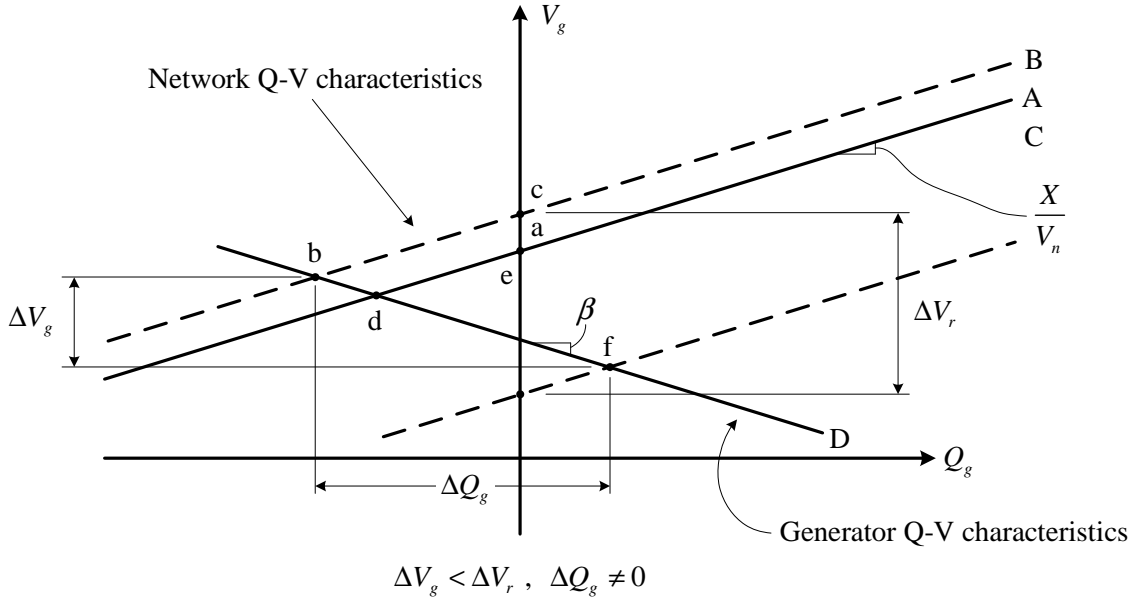
Fig. 2.3-4. The network-generator coupling, in terms of Q-V curves. The network voltage decrement case

2.3.1.3 Generator Q-V curve droop calculation

The ΔV_g reduction, with respect to ΔV_r, is related to β, which is set, as a parameter, into the reactive power regulator. Now we show a method to calculates this parameter, in function to the desired ΔV_g.

Fig. 2.3-5 show a "zoom" of the working area of Fig. 2.3-3. We can write:

$$\tan \gamma = \frac{\Delta V_g}{\Delta Q_g} \tag{2.7}$$

The slope β refers to the angle $-\gamma$, then the previous equation can be rewritten:

$$\tan \gamma = -\beta = \frac{\Delta V_g}{\Delta Q_g} \tag{2.8}$$

Similarly, for the generator, we have (Fig. 2.3-5):

$$\tan \delta = \frac{\Delta V_r - \Delta V_g}{\Delta Q_g} \tag{2.9}$$

and then:

$$\tan \delta = \frac{X}{V_n} = \frac{\Delta V_r - \Delta V_g}{\Delta Q_g} \tag{2.10}$$

Substituting (2.8) in (2.10) we can obtain:

$$\beta = -\left(\frac{\Delta V_g}{\Delta V_r - \Delta V_g} \right) \frac{X}{V_n} = -\frac{1}{\left(\dfrac{\Delta V_r}{\Delta V_g} - 1 \right)} \frac{X}{V_n} \tag{2.11}$$

Equation (2.11) allows to calculate the generator Q-V curve slope, in function to the $\Delta V_r / \Delta V_g$ ratio.

If we want a 0.5 times voltage variation at the interconnection point (with respect to the equivalent voltage variation or, which is the same, with respect to the absence of reactive power regulation), we must write:

$$\Delta V_g = \frac{1}{2} \Delta V_r \;\; \Rightarrow \;\; \frac{\Delta V_r}{\Delta V_g} = 2 \tag{2.12}$$

then, from (2.11):

$$\beta = -\frac{X}{V_n} \tag{2.13}$$

in other words, if the slope of the generator Q-V curve is equal (but with the negative sign) with respect to the network Q-V curve, we will guarantee the condition (2.13). In order to reach this goal, the equivalent network reactance (which corresponds to the short circuit reactance at the interconnection point) will be known.
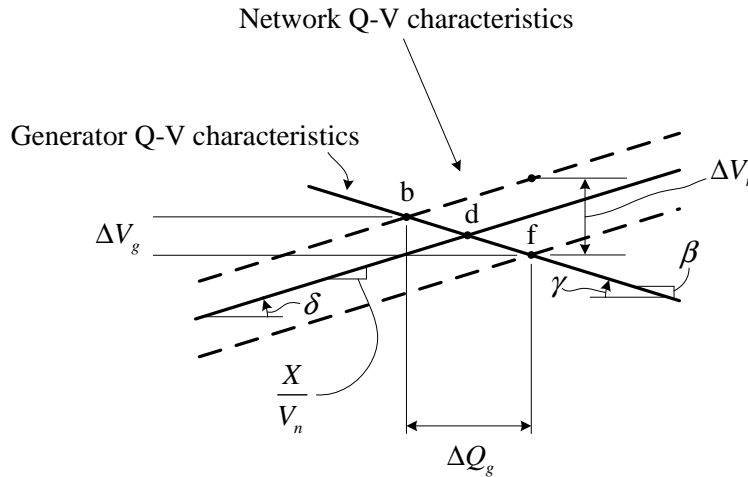

Fig. 2.3-5. Working point "zoom"

It is important to note that the term:

$$\tan \delta = \frac{X}{V_n} \tag{2.14}$$

used in (2.11) and (2.13), can be calculated using the sensitivity matrix presented in Chapter 3. In fact the term (2.14) represents the voltage variation, in the node *i*, in function of the reactive power variation in the same node (its units are V/VAr); in other words (2.14) represents the auto-sensitivity term (in absolute value). Using the sensitivity rule explained in Chapter 3, we can say that (2.14) "*is the arithmetic sum of the reactances of the branches in which the powers absorbed by node i flow, multiplied by* $1/V_n$".

From the electrotechnic point of view the previous observation corresponds to calculate the Thévenin reactance (or the short circuit reactance) viewed from the node *i*, neglecting load and generator contributions.

2.3.1.4 UPG and RQV regulation modalities in the Q-V plane

In the normal operation, a UPG controlled generator exchanges no reactive power. However it exchanges a reactive power proportional to the generated active power when the voltage exceeds its maximum threshold. Fig. 2.3-6 and Fig. 2.3-7 represent this behavior (in Fig. 2.3-7 the reactive power exchanged proportionally to the active power has been named $Q_{g,max}$). In Fig. 2.3-6 the normal operation is depicted; in this case no reactive power is exchanged and then $\Delta V_g = \Delta V_r$.

If the generator voltage reach its maximum admissible value, the UPG commutates the generator in order to absorb a reactive power related to the generated active power, and the working point will be "f" (see Fig. 2.3-7). The new V_g is less than V_r, and the difference is related to the reactive power, then to the generated active power.

$$\Delta V_g = \Delta V_r \ , \ \ \Delta Q_g = 0$$
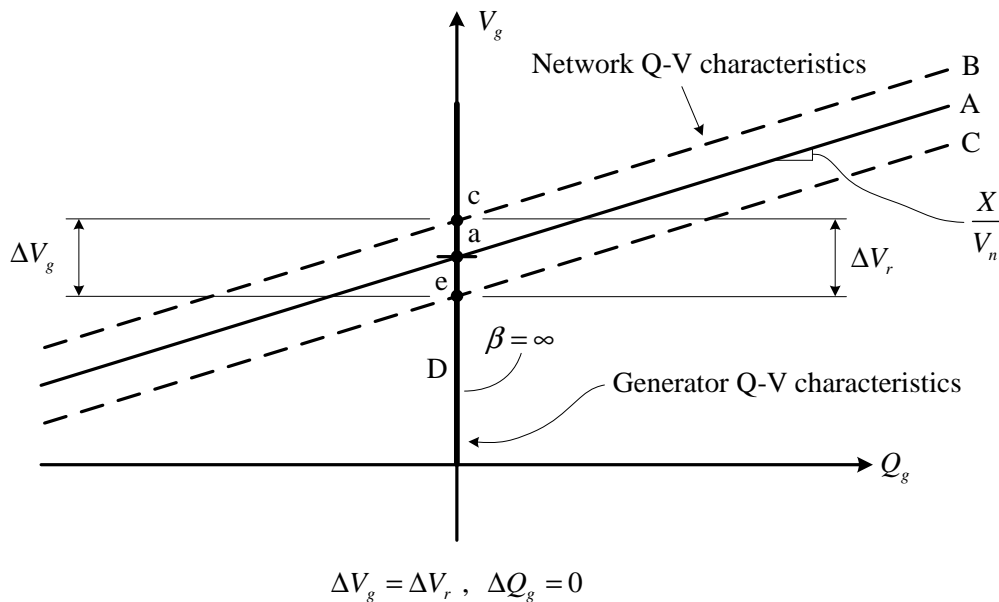
Fig. 2.3-6. Local UPG voltage control technique without reactive power absorption

The advantage with respect to the RQV regulation is that the UPG mode exchanges reactive power only if the voltage exceeds its maximum threshold. However the UPG deactivation thresholds must be carefully chosen in order to avoid continuous activations/deactivations of the UPG.
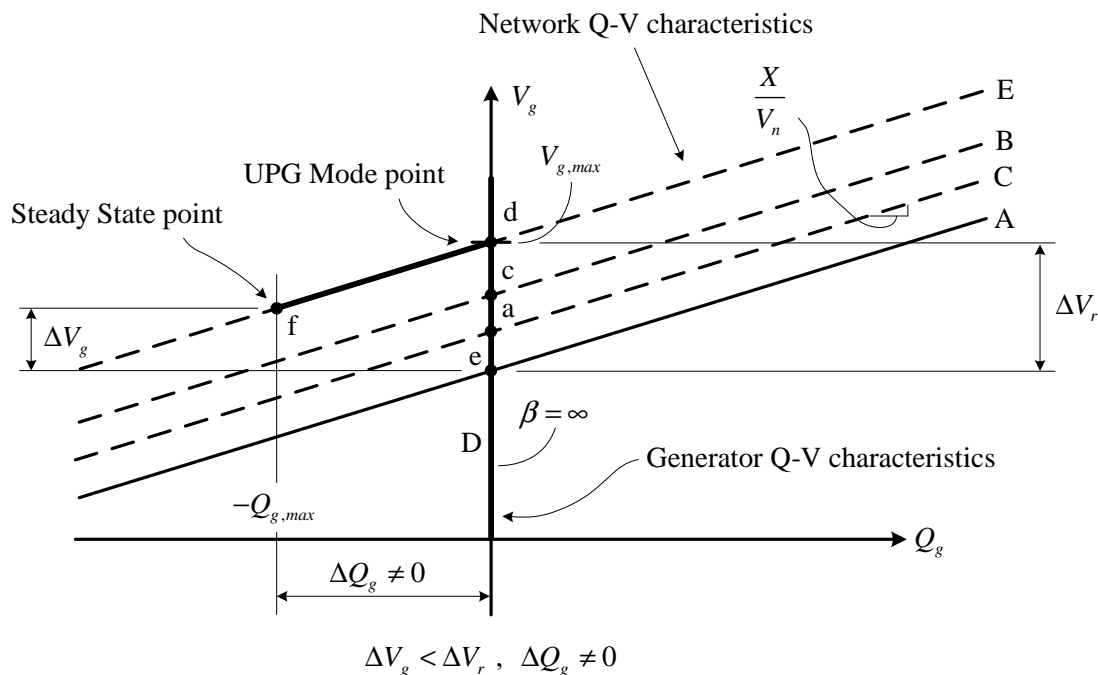
Fig. 2.3-7. Local UPG voltage control technique with maximum reactive power absorption

2.3.1.5 Voltage "dead-band" in the RQV regulation mode

As previously said, an RQV regulated generator always exchanges reactive power. A possible solution consists in a "dead-band" (or "no regulation band") definition, as depicted in Fig. 2.3-8. Using this technique, the RQV works in two sectors:

- if we have a voltage variation in the dead-band (defined by "c" and "e" limits), no reactive power is exchanged
- if we have a voltage variation outside the dead band, the generator is regulates using the Q-V curve. The slope calculation has been previously discussed.

$$\begin{cases} \Delta V_g = \Delta V_r \,, \quad \Delta Q_g = 0 \quad \text{in the No Regulation Band} \\ \Delta V_g < \Delta V_r \,, \quad \Delta Q_g \neq 0 \quad \text{out of the No Regulation Band} \end{cases}$$
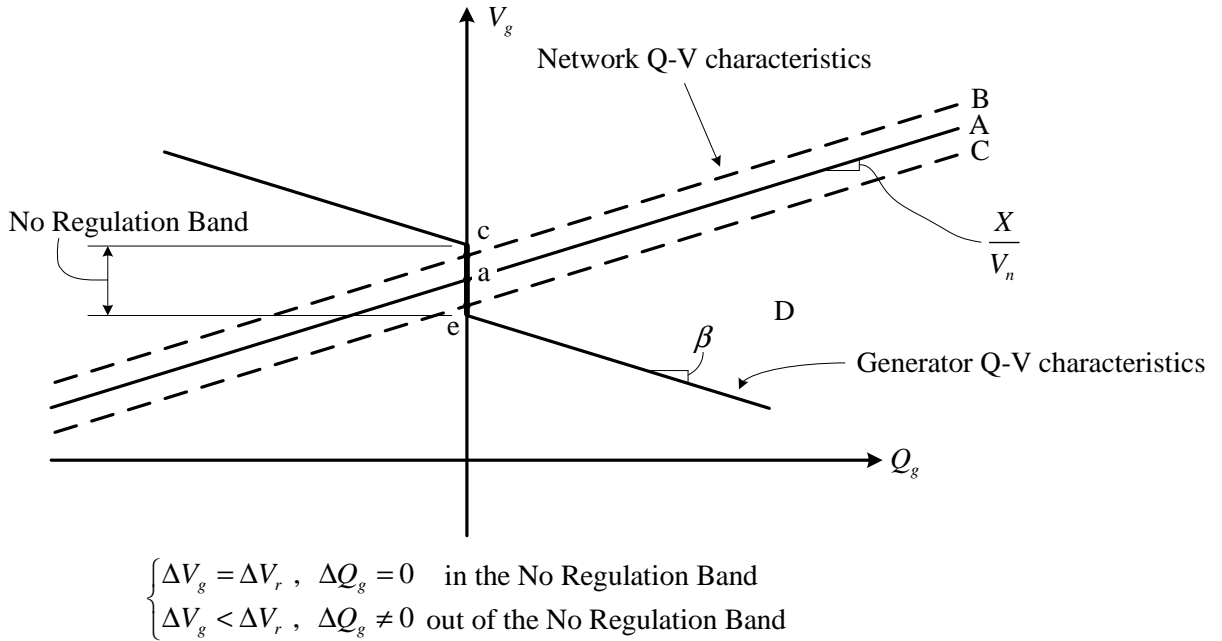
Fig. 2.3-8. Generator Q-V curves with dead-band

$$\begin{cases} \Delta V_g = \Delta V_r \,, \quad \Delta Q_g = 0 \quad \text{in the No Regulation Band} \\ \Delta V_g < \Delta V_r \,, \quad \Delta Q_g \neq 0 \quad \text{out of the No Regulation Band} \end{cases}$$

Fig. 2.3-9. Generator Q-V curves with dead-band and UPG regulation

The RQV and the UPG functions can be contemporarily used (however in this thesis this operation modality is not taken into account). In particular the RQV (with the dead-band) can be always activated and the UPG can operates only if the voltage is "very high". Let us now

consider Fig. 2.3-9; if the voltage at the interconnection point exceeds a maximum admissible value (which coincides to the point "g"), the generator is switched in UPG mode.

2.3.2 A numerical application using the Real-Time Digital Simulator (RTDS)

2.3.2.1 Network description

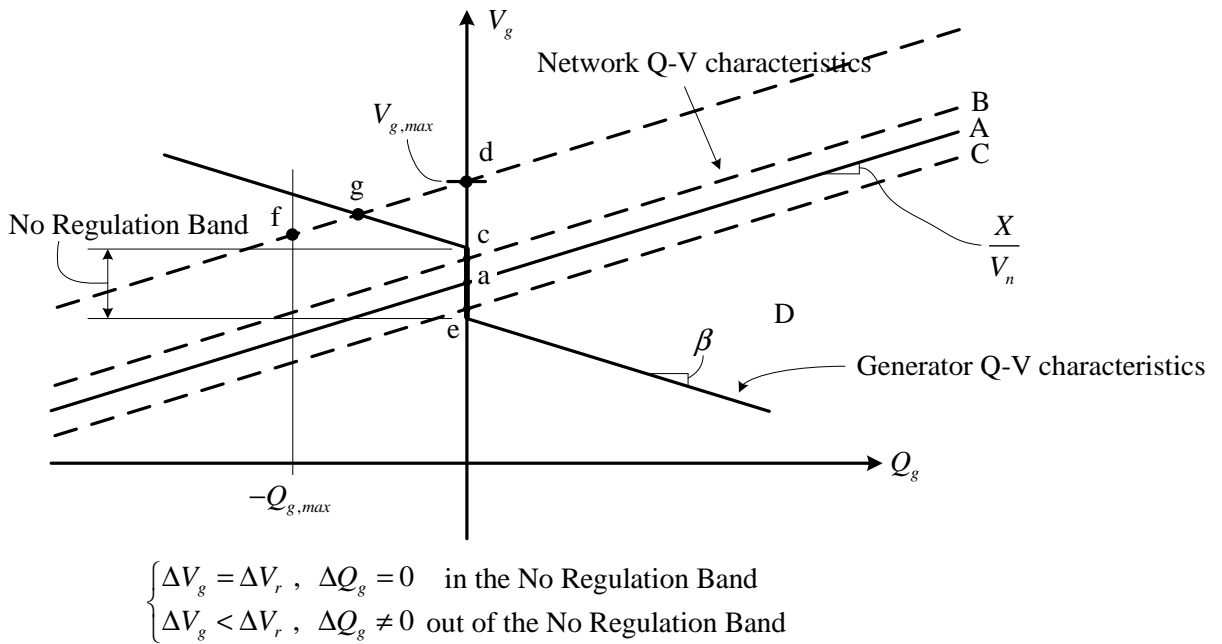In order to validate the previous discussed theory, a numerical application, using the Real-Time Digital Simulator (RTDS), installed in the Enel Test Center – Milano, is now presented. In spite of simplicity, but also maintaining the theory generality, the voltage dead-band is not implemented.

The network schematic is depicted in Fig. 2.3-10 and it is composed by:

- the HV network equivalent. In spite of simplicity this equivalent is an infinite bus with $V_n = 132$ kV rated voltage
- HV/MT transformer, named T1, which have the following characteristic:
    - $V_{AT,n} = 132$ kV
    - $V_{MT,n} = 132$ kV
    - $A_n = 40$ MVA
    - $V_{CC\%} = 15,5$ kV
- generator to grid coupling transformer, named T2, which have the following characteristic:
    - $V_{AT,n} = 20$ kV
    - $V_{MT,n} = 20$ kV
    - $A_n = 10$ MVA
    - $V_{CC\%} = 15,5$ kV
- synchronous generator, with PQ regulation, which have the following characteristic:
    - maximum generable active power $P_{max} = 5$ MW
    - maximum generable reactive power $Q_{max} = 5$ MVAr
    - maximum absorbable reactive power $Q_{min} = -5$ MVAr

Generator PQ regulators (depicted in Fig. 2.3-11) are contained on the "G1 Controls" block of Fig. 2.3-10.
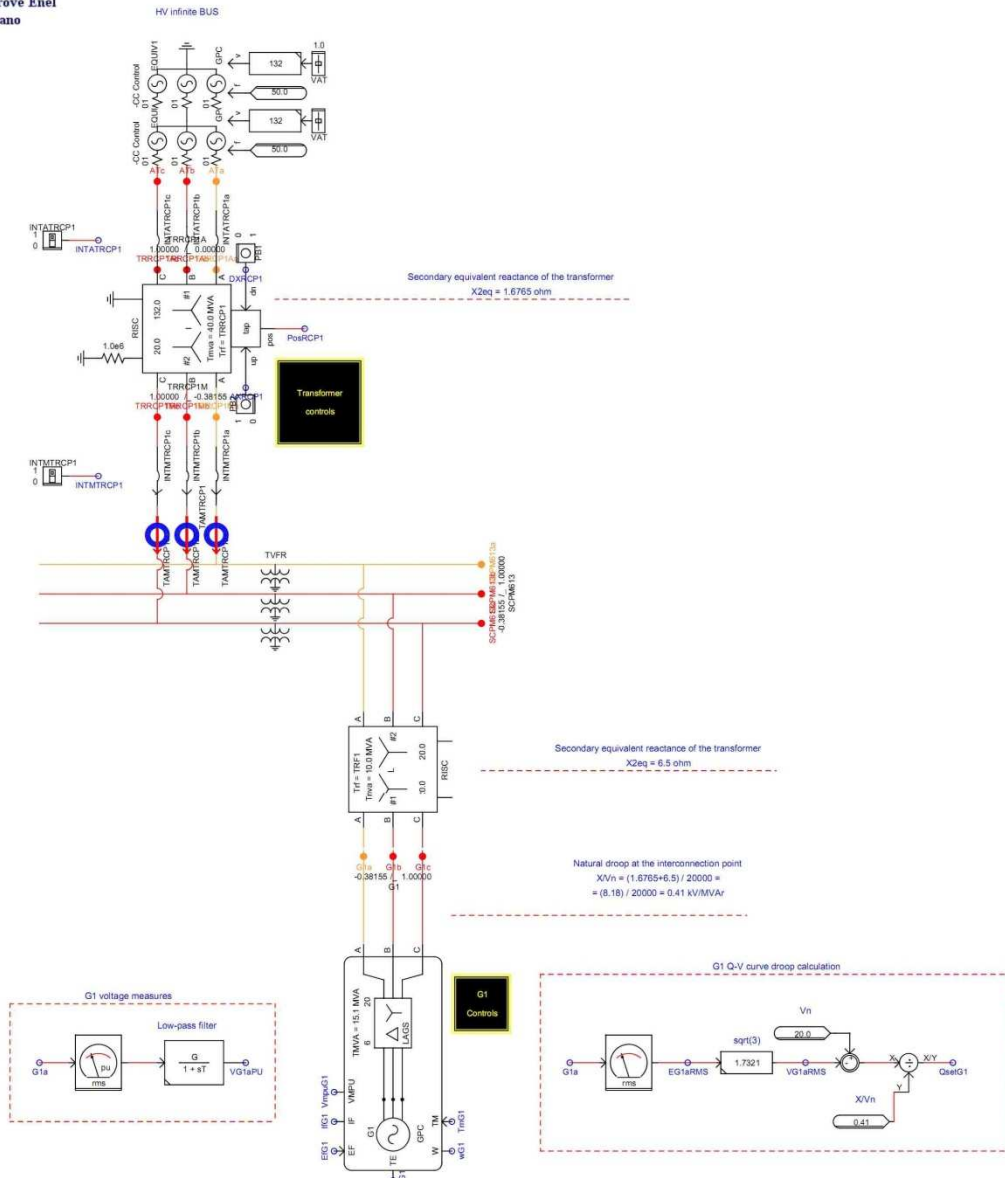
Fig. 2.3-10. The simulated network in RTDS
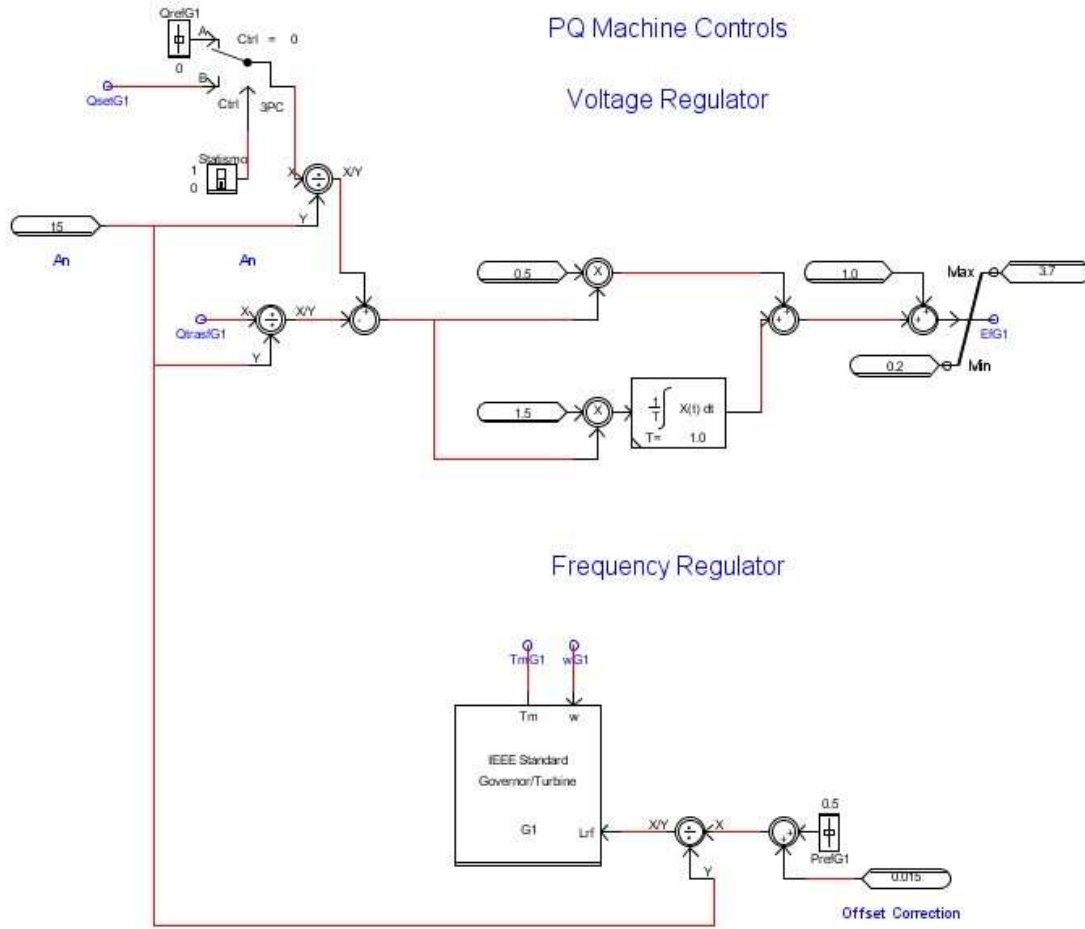
Fig. 2.3-11. Generator G1 PQ regulators

The group named "G1 voltage measures", depicted in Fig. 2.3-10, measures and converts in p.u. the generator voltage.

The group named "G1 Q-V curve droop calculation" calculates the reactive power regulator set-point (depicted in Fig. 2.3-11) by means the Q-V curve. The regulator is a proportional-integral (PI) type. The generator Q-V curve is calculated referring to the D characteristic represented in Fig. 2.3-3; the intercept in the origin of the this characteristic is $V_n = 20 \text{ kV}$. In other words the generator tends absorbs reactive power when the voltage at the interconnection is greater than the nominal voltage, while it generates reactive power when the voltage decreases. Then the Q-V equation is:

$$V_{g,mis} = \beta Q_{g,set} + V_n \tag{2.15}$$

36

where $V_{g,mis}$ is the line-to-line generator (measured) voltage, while $Q_{g,set}$ is the reactive power regulator set-point. As said before, (2.13) must be satisfied. Then, from (2.15), the reactive power regulator set-point is:

$$Q_{g,set} = \frac{V_n - V_{g,mis}}{X/V_n} \tag{2.16}$$

The previous equation is implemented in the group "G1 Q-V curve droop calculation".

Due to transformers T1 and T2, the reactance viewed at the interconnection point terminals, and the "network natural droop" are:

$$X = 8,18 \ \Omega \ \Rightarrow \ \frac{X}{V_n} = 0,41 \ \frac{\text{kV}}{\text{MVAr}} \tag{2.17}$$

The network natural droop can be also expressed in p.u. (in terms of voltage) obtaining $0,0205$ p.u./MVAr .

The reactive power regulator set-point can be also manually controlled, using a slider.

2.3.3 Numerical simulation results

Two study cases are now discussed. In the first case, the case A, no RQV regulation is implemented, and $Q_{g,set}$ is forced to zero. In the second case, the case B, the RQV regulation is switched on in order to implement the Q-V characteristic.

In both cases the generated active power set-point is 2 MW. Moreover an increment (5% with respect to the rated HV voltage, which corresponds to 0.05 p.u.) of the equivalent network voltage will be simulated, and the following parameters will be monitored:

- the voltage $V_{g,mis}$ at the interconnection point
- the generated reactive power
- the voltage $V_{g,mis}$ at the interconnection point, in function of the generated reactive power

2.3.3.1 Case A results

In this case, the reactive power regulator set-point is 0 MVAr, then the Q-V regulation is disabled.

Numerical results in case of network equivalent voltage increment

The voltage variation in the interconnection point follows the network equivalent voltage, as reported in Fig. 2.3-12. As depicted in Fig. 2.3-13, no reactive power is exchanged in steady-state operation, between the generator and the network. In the initial condition of the voltage

transient, the generator voltage is less than the network voltage. Then the generator is initially under-excited and absorbs reactive power.

Fig. 2.3-12. Interconnection point voltage

Fig. 2.3-14 shows the voltage at the interconnection point in function of the generated reactive power. The Q-V network characteristic is shifted along the y axis due to the network voltage increment.

Fig. 2.3-13. G1 generated reactive power

Fig. 2.3-14. Interconnection point voltage vs G1 generated reactive power

Numerical results in case of network equivalent voltage decrement

The voltage variation in the interconnection point follows the network equivalent voltage, as reported in Fig. 2.3-15. As depicted in Fig. 2.3-16, no reactive power is exchanged in steady-state operation, between the generator and the network. In the initial condition of the voltage transient, the generator voltage is greater than the network voltage. Then the generator is initially over-excited and generates reactive power.
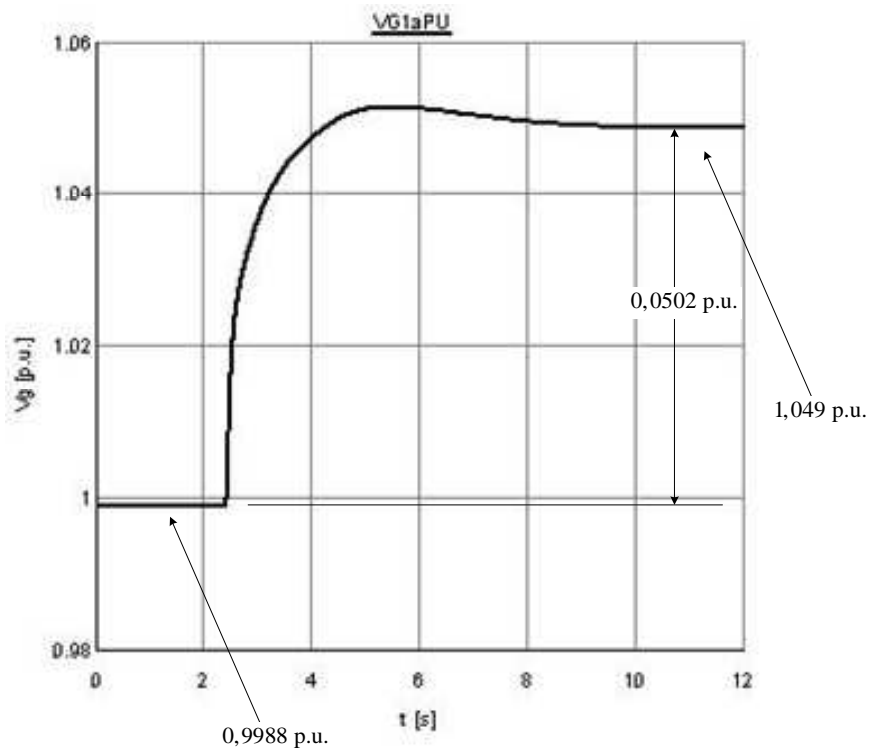
Fig. 2.3-17 shows the voltage at the interconnection point in function of the generated reactive power. The Q-V network characteristic is shifted along the y axis due to the network voltage decrement.
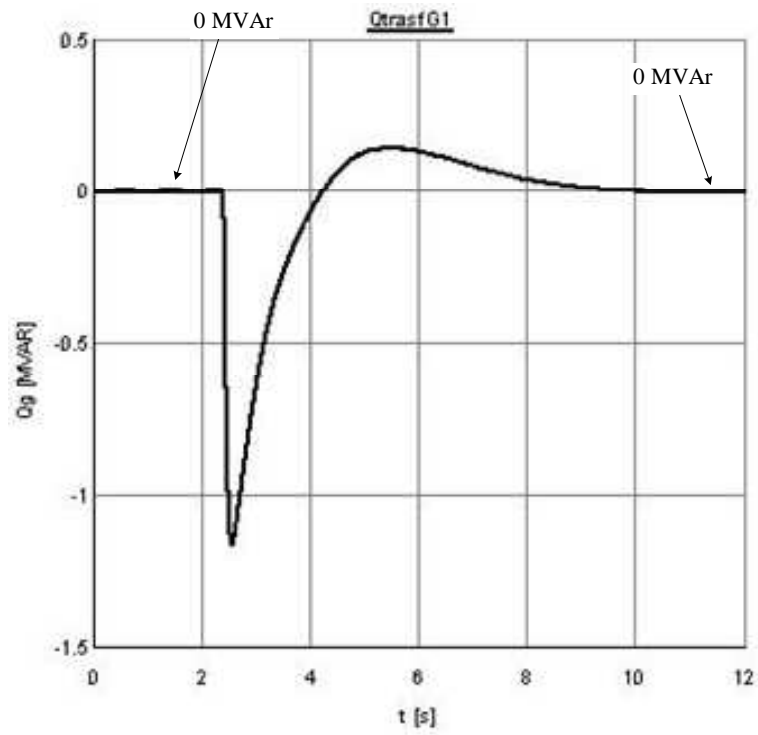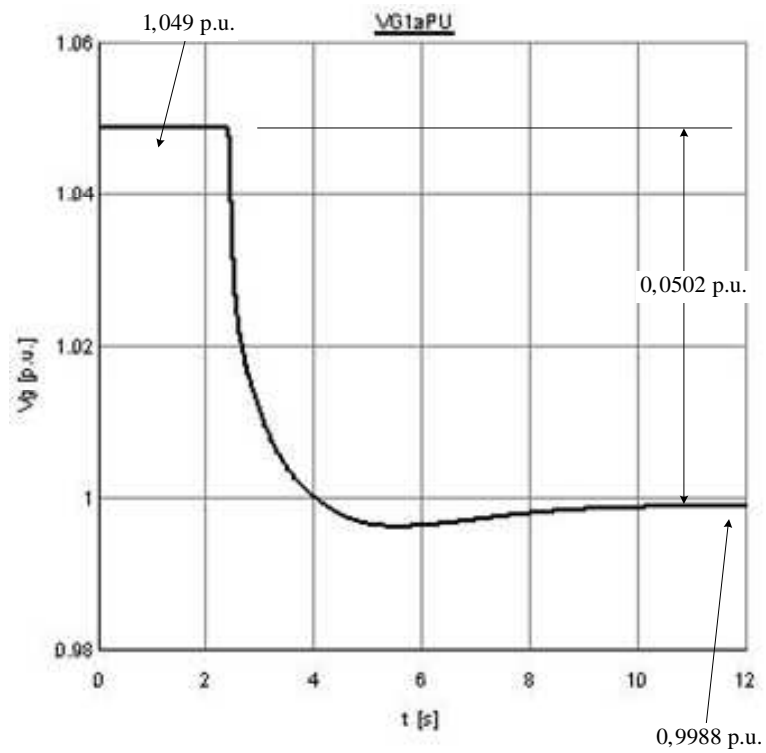
Fig. 2.3-15. Interconnection point voltage
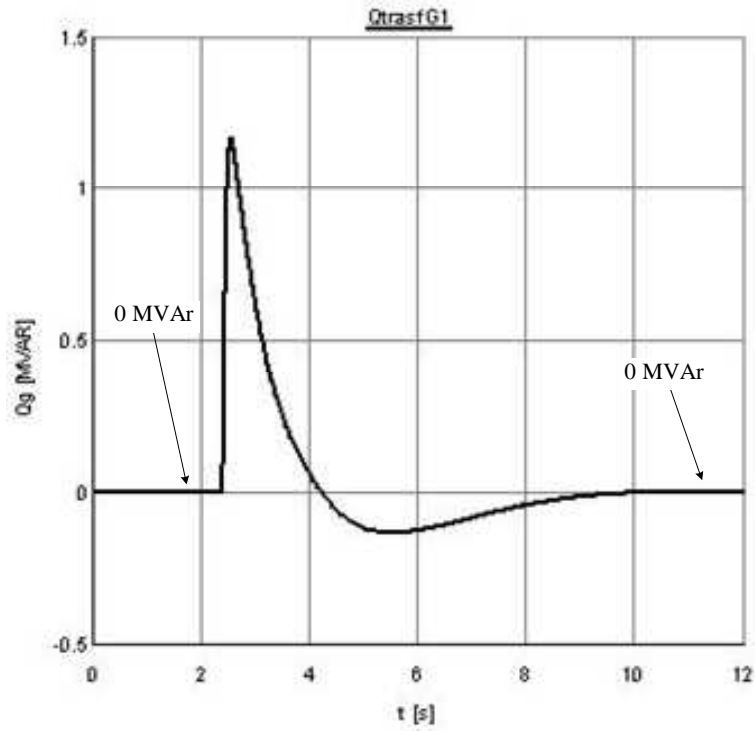
Fig. 2.3-16. G1 generated reactive power
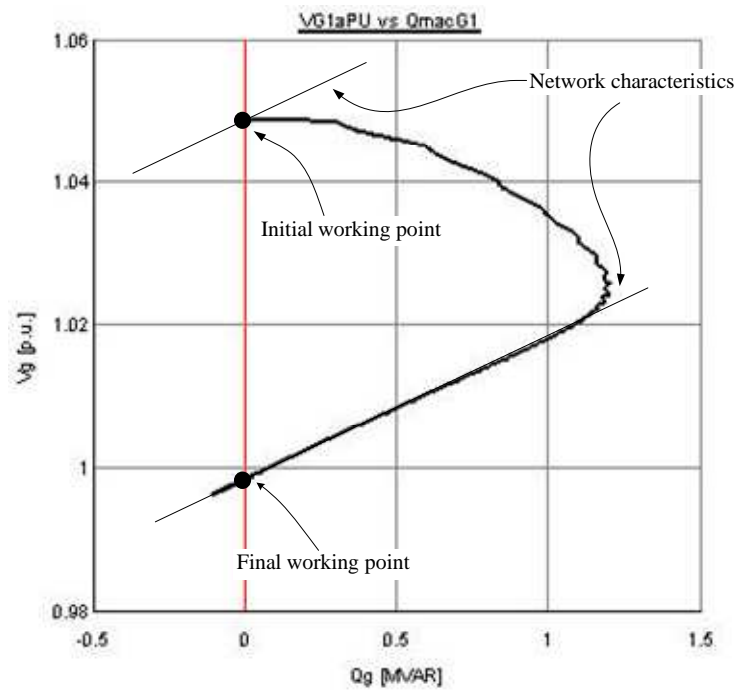
Fig. 2.3-17. Interconnection point voltage vs G1 generated reactive power

2.3.3.2 Case B results

In this case the reactive power regulator set-point is calculated using the group "G1 Q-V curve droop calculation" then the Q-V regulation is enabled.

Numerical results in case of network equivalent voltage increment

As reported in Fig. 2.3-18, the voltage variation at the interconnection point is reduced with respect to the equivalent network variation by 1/2 factor. The reactive power exchanged in steady-state is not zero, as depicted in Fig. 2.3-19.

The voltage at the interconnection point in function of the generator reactive power is depicted in Fig. 2.3-20. The final voltage, corresponding to the final working point, is less with respect to the case depicted in Fig. 2.3-14 due to the Q-V regulation.
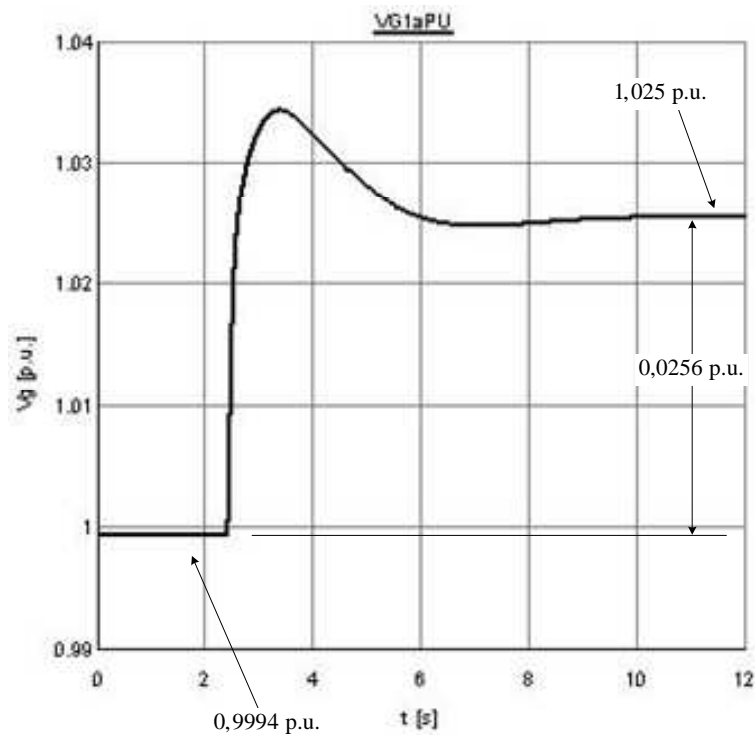
Fig. 2.3-18. Interconnection point voltage
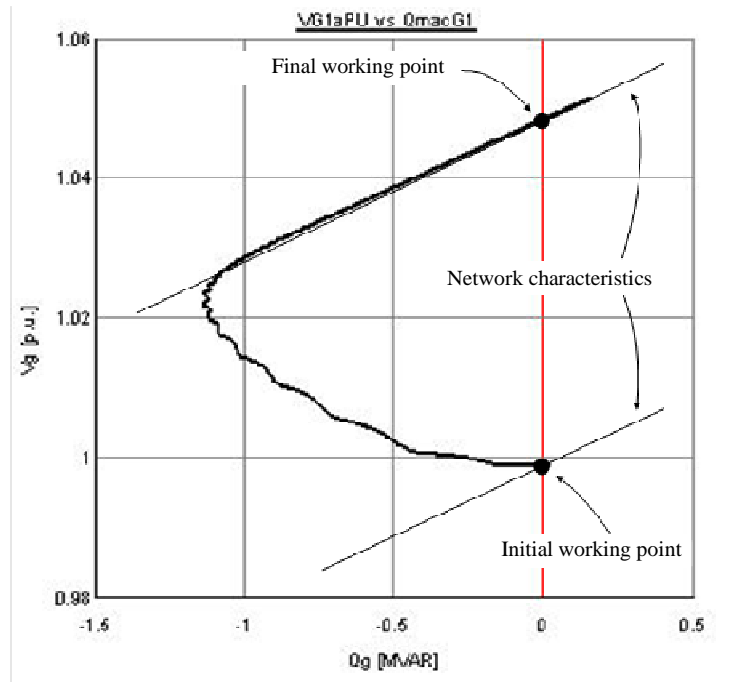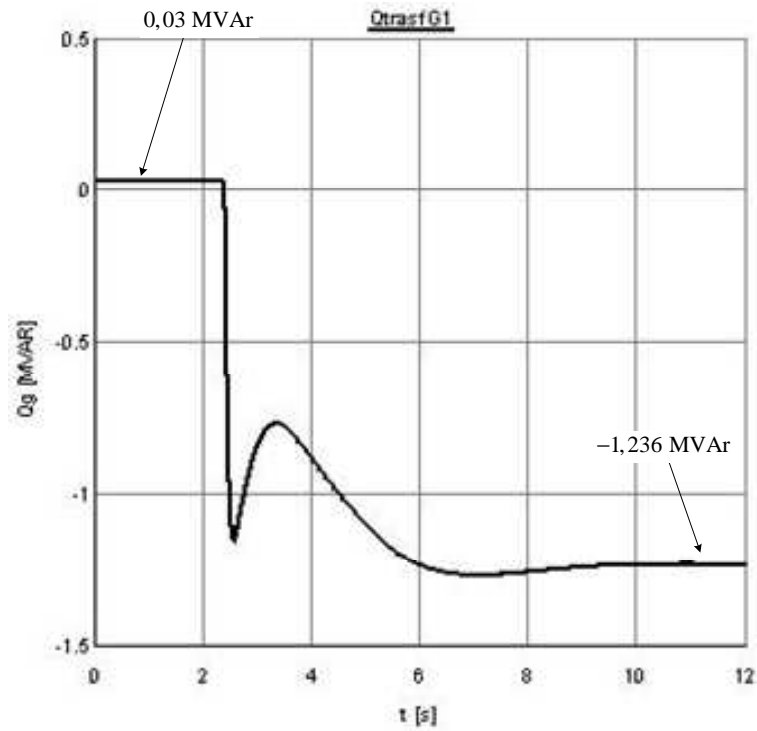
Fig. 2.3-19. G1 generated reactive power
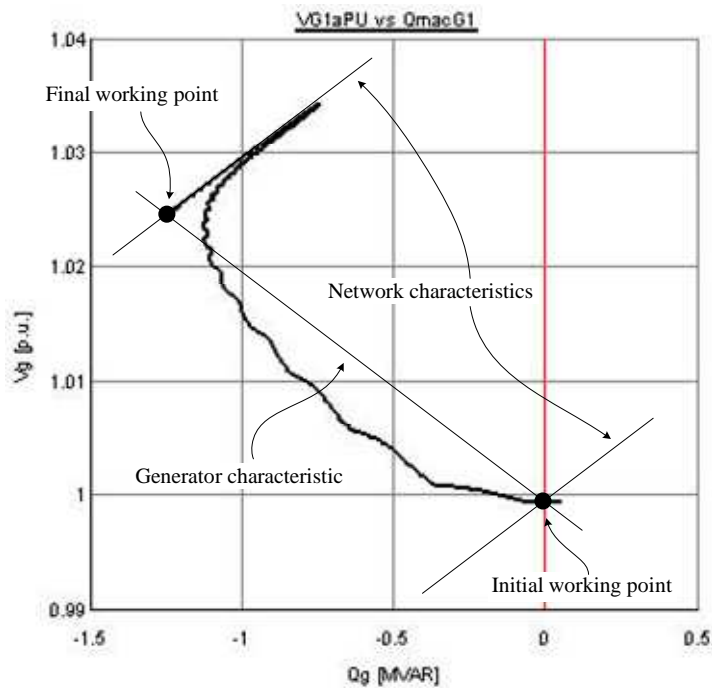
Fig. 2.3-20. Interconnection point voltage vs G1 generated reactive power

Numerical results in case of network equivalent voltage decrement

As reported Fig. 2.3-21 in the voltage variation at the interconnection point is reduced with respect to the equivalent network variation by 1/2 factor. The reactive power exchanged in steady-state is not zero, as depicted in Fig. 2.3-22.

The voltage at the interconnection point in function of the generator reactive power is depicted in Fig. 2.3-23. The final voltage, corresponding to the final working point, is less with respect to the case depicted in Fig. 2.3-17 due to the Q-V regulation.
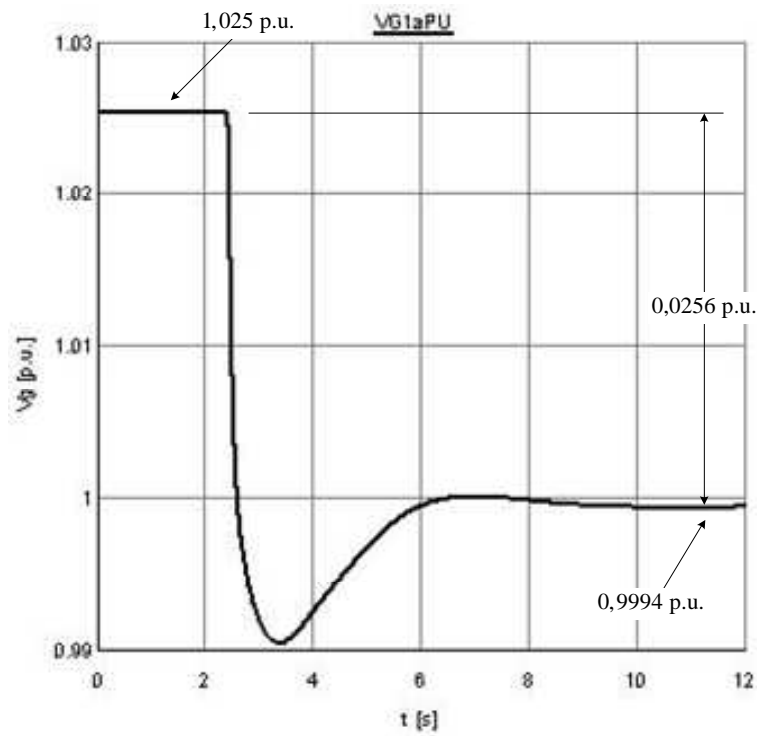
Fig. 2.3-21. Interconnection point voltage

0,03 MVAr

−1,236 MVAr
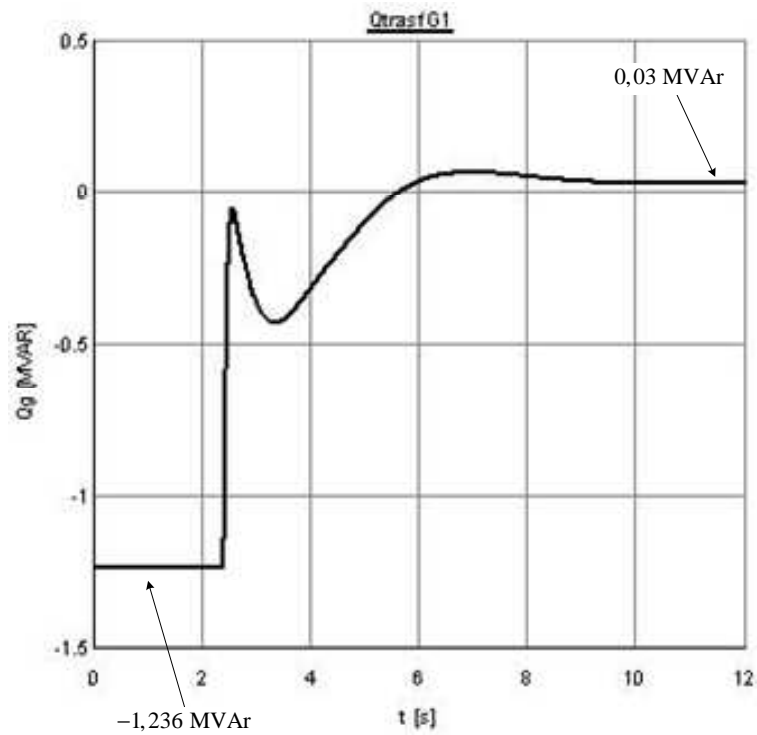
Fig. 2.3-22. G1 generated reactive power

Network characteristic

Initial working point

Generator characteristic

Final working point
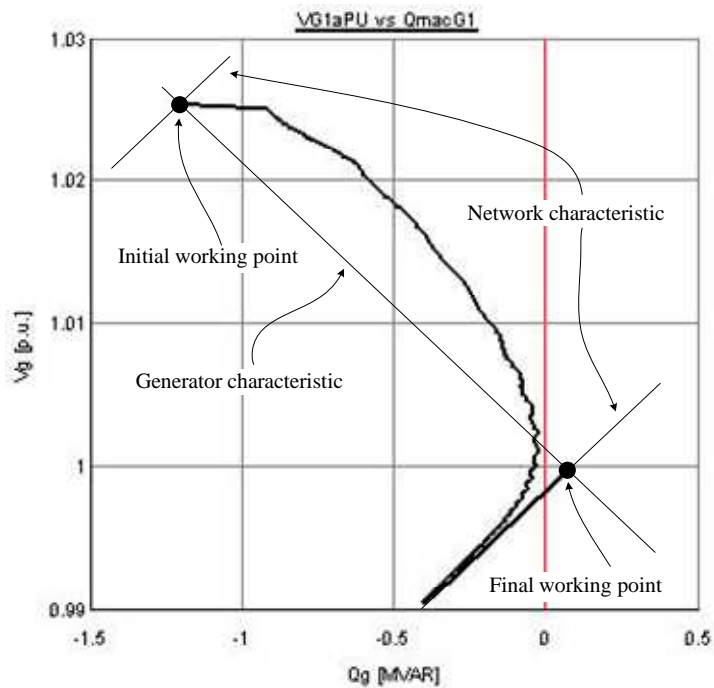
Fig. 2.3-23. Interconnection point voltage vs G1 generated reactive power

2.3.4 RQV implementation in the RTDS simulation environment

The presented RQV local voltage regulation technique has been implemented in the RTDS environment, using the C-builder tool (which allows to build the dynamic model blocks using the C programming language), in order to analyze the POI-P3 pilot project Enel grid.

The RQV block is reported in Fig. 2.3-24, where:

- V_MT is the interconnection point measured voltage input
- Pg is the generated power input. This input is necessary to activate the RQV only when the generator produces a minimum active power. In other word Pg it is necessary for the "active power lock-in (and lock-out)" function. In the simulations results of the POI-P3 pilot project, presented in Chapter 5, the lock-in and lock-out power are, respectively, the 5 % and the 4.5 % of the nominal apparent power A_n of each generator
- RQVact is the activation bit of the RQV function. If RQVact = 0, the RQV is always off
- Qout is the generator calculated reactive power set-point (when the value is positive, the generator absorbs reactive power from the network)
- RQVout_act is the output activation bit. RQVout_act is equal to RQVact

The RQV block calculates the reactive power set-point each T_{cycle}, which a calculation time period. Moreover the new set-point will be calculated only if the V_MT variation is greater than the voltage hysteresis ε_{V_MT}. This parameter must be set in function of the measuring voltage error; in the POI-P3 project the voltage is measured by the RGDM/IC device[4] which is characterized by $\varepsilon_V = \pm 0.5$ % voltage measuring error. The in the RQV we have set:

$$\varepsilon_{V\_MT} = 2\varepsilon_V = 1 \text{ %} \tag{2.18}$$

for all generators.

---

[4] The voltage is measured by the RGDM/IC and sent via the optical fiber to the IRE device, as reported in Fig. 2.3-25.
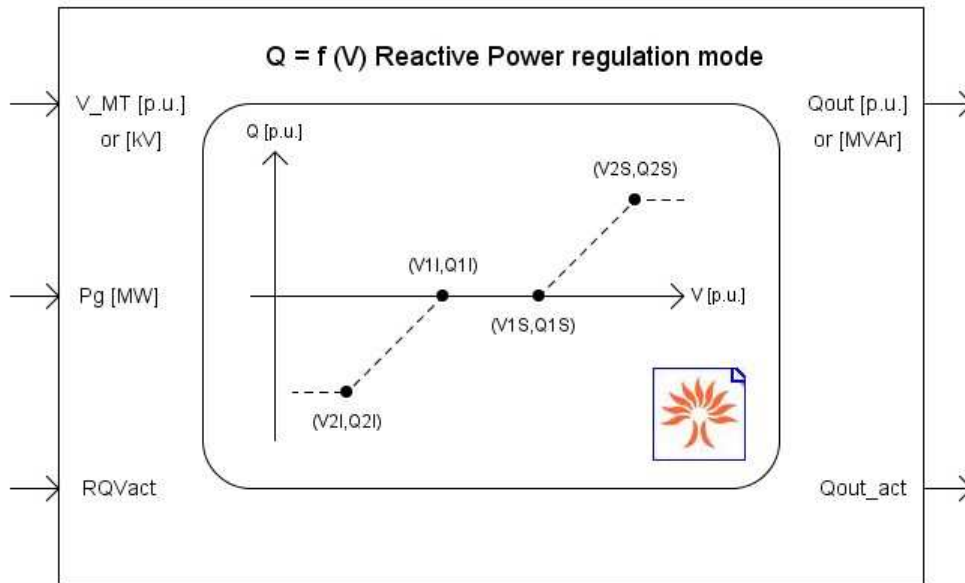
Fig. 2.3-24. The RQV block in the RTDS environment

The RQV parameters, used in the POI-P3 project simulations, will be presented in Chapter 4.

2.3.5 The IRE device

In the POI-P3 pilot project, the RQC function will be implemented in the IRE ("Energy Regulation Interface") device, designed by Enel Distribuzione. This device have several functions, summarized in the follow:

- it is necessary to interface the Enel communication infrastructure to the customer plant
- it allows to distribute the active/reactive set-points, generated by the Enel central control when the remote regulation is active, to the single generators which compose the generation plant. In other words the IRE also allows the voltage remote control
- it allows to communicate to the Enel central control the capability curves of generators and energy storage systems installed in the custom plant
- it implements the RQV regulation technique, using the interconnection point voltage measured by the RGDM/IC device. In other word IRE also allows to locally regulate the voltage
- it is able to sent to the generators the power factor set-point generated by the RGDM/IC device
- it is able to assign a priority to the voltage regulation. The remote voltage regulation have the maximum priority with respect to the local voltage control, i.e. UPG and RQV. It is also able to select the local voltage regulation technique (UPG or RQV)
- it is able to regulate the generated active power in function of the power system frequency, in order to improve the frequency stability

The Enel communication infrastructure of the POI-P3 pilot project, including the RQV local voltage regulation technique implemented in IRE, is reported in Fig. 2.3-25.
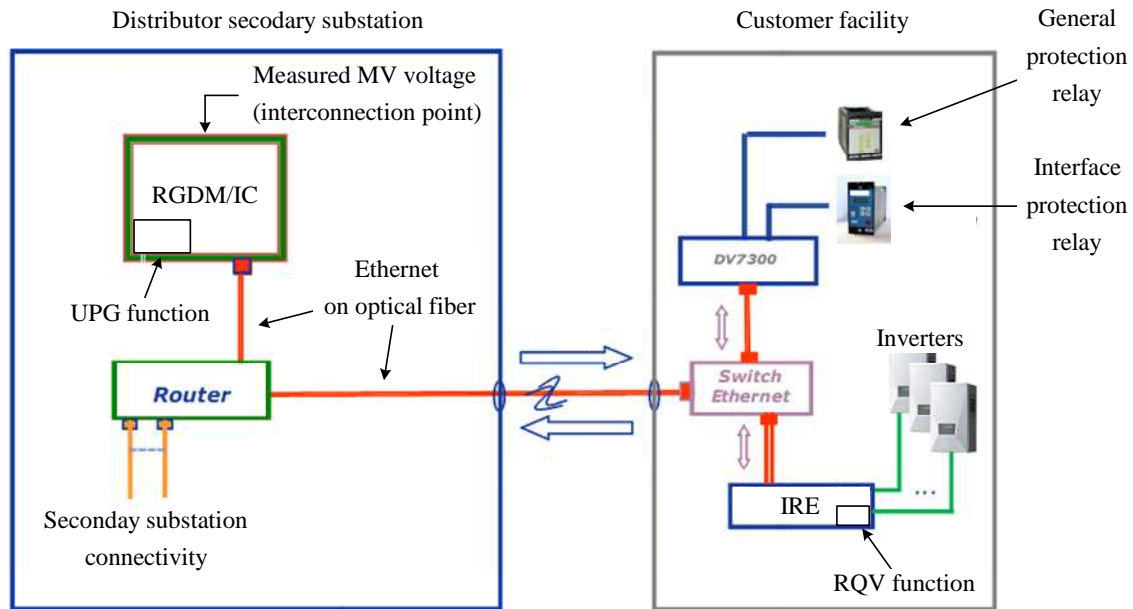
Fig. 2.3-25. Enel POI-P3 project distributor/customer communication infrastructure

2.4 REFERENCES

[1] R. Marconato, "Electric Power Systems Vol. II" CEI, Milano, 2008.

[2] P. Kundur, "Power System Stability and Control" McGraw-Hill, 1994.

[3] Y. Rosales Hernandez, T. Hiyama, "Distance Measure Based Rules for Voltage Regulation with Loss Reduction"

[4] F. Saccomanno, "Electric Power Systems" Wiley-Interscience IEEE Press, Piscataway, NJ, 2003.

[5] G. Andersson, "Modeling and Analysis of Electric Power Systems" Lecture 227-0526-00, ITET ETH Zürich, 2008, Zürich.

[6] Y. Abdel-Rady I. Mohamed E. F. El-Saadany "A Control Scheme for PWM Voltage-Source Distributed-Generation Inverters for Fast Load-Voltage Regulation and Effective Mitigation of Unbalanced Voltage Disturbances" IEEE Transactions on Industrial Electronics, Vol. 55, N. 5, May 2008 Page(s): 2072 – 2084.

[7] P. M. S. Carvalho, P. F. Correia, L. A. F. M. Ferreira, "Distributed Reactive Power Generation Control for Voltage Rise Mitigation in Distribution Networks," Power Systems, IEEE Transactions on Volume: 23 , Issue: 2, 2008 , Page(s): 766 – 772.

[8] P. N. Vovos, A. E. Kiprakis, A. R. Wallace, G. P. Harrison, "Centralized and Distributed Voltage Control: Impact on Distributed Generation Penetration," Power Systems, IEEE Transactions on Volume: 22, Issue: 1, 2007 , Page(s): 476 – 483.

[9] P.M. Anderson, "Power System Protection," IEEE Press, Piscataway, NJ, 1999.

[10]   N. Mohan, T. M. Undeland, W. P. Robbins, "Power electronics: converters, applications, and design", Wiley, 1995.

[11]   M. H. Rashid, "Power Electronics Handbook", Academic Press-Elsevier, 2007.

[12]   L. L. Grigsby, "Electric Power Generation, Transmission and Distribution", CRC Press-Taylor & Francis Group, Boca Raton, 2006.

[13]   F. A. Viawan, D. Karlsson, "Coordinated Voltage and Reactive Power Control in the Presence of Distributed Generation," PES General Meeting - Conversion and Delivery of Electrical Energy in the 21st Century, 2008 IEEE.

[14]   S. Corsi, "Wide Area Voltage Regulation & Protection" Paper accepted for presentation at 2009 IEEE Bucharest Power Tech Conference, June 28th - July 2nd, Bucharest, Romania.

[15]   A. Gandelli, S. Leva, A. P. Morando, "Topological Considerations on the Symmetrical Components Transformation, "Circuits and Systems I: Fundamental Theory and Applications, IEEE Transactions on Vol. 47, Issue 8, Aug. 2000 Page(s): 1202 – 1211.

[16]   Radial Distribution Test Feeders, Distribution System Analysis Subcommittee Report.

[17]   H. M. Ayres, L. C. P. da Silva, W. Freitas, M. C. de Almeida V. F. da Costa, "Evaluation of the Impact of Distributed Generation on Power Losses by Using a Sensitivity-Based Method," PES General Meeting, 2009 IEEE.

[18]   A. Kishore, E. F. Hill, "Static optimization of Reactive Power Sources by use of Sensitivity Parameters", Power Apparatus and Systems, IEEE Transactions on, Volume: PAS-90, Issue: 3, 1971, Page(s): 1166 – 1173.

Chapter 3

Proposed Centralized Voltage Control on MV Network

3.1 INTRODUCTION TO CHAPTER 3

As said in Chapter 2, it is possible that the voltage exceeds its limits also after the local voltage action. In this case the Local Voltage Regulation fails its goal[5]. Then the Centralized Voltage Regulation must act in order to try a new voltage adjustment. The Centralized Voltage Regulation, which is hierarchically higher than the Local Voltage Regulation, is based on a voltage Sensitivity analysis approach, which is treated in this Chapter. The Centralized Voltage Regulation is performed by a DMS functionality called "Voltage Control System" (VCS).

When a generator delivery point voltage exceeds the V_{2S-VCS} (or V_{2I-VCS}) limit, its UPG sent an "highest" (or "lowest") voltage signal[6] to the VCS, as described in Chapter 2. This signal is VFLS (or VFLI).

When the VCS receive this signals the VCS "calls" the "electrically closest" generator(s), requesting a reactive power variation in order to help the OTG. The "electrically closest" generator have the greatest influence on the OTG and will be called "best generator" (BG).

The "electrical closeness" concept is based on a Sensitivity approach which is implemented in the VCS. This proposed Sensitivity approach, which will be treated in this Chapter, is different from which applied in the HV grids, due to the typical radial topology of the MV network.

3.2 CLASSICAL SENSITIVITY THEORY OVERVIEW AND PROPOSED SENSITIVITY APPROACH

The classical Sensitivity theory used in HV network analysis to perform primary and secondary voltage regulation is based on the Jacobian Matrix and reveals the relationships between the nodal voltages (magnitude and phase) and the nodal power injections (active and

---

[5] The generator which have failed the local voltage control will be called "out of voltage threshold generator" (OTG).

[6] This signals, described in Chapter 2, are VFLS and VFLI. It is important to note that this signals will be sent to the VCS also when the UPG is disabled in order to activate the RQV regulation. in other words the VCS works correctly also in case of RQV local voltage regulation.

reactive). The relationships mentioned above are represented by the following matrix expression:

$$
\begin{bmatrix} [\Delta E] \\ [\Delta \vartheta] \end{bmatrix} = \begin{bmatrix} \left[\dfrac{\partial P}{\partial V}\right] & \left[\dfrac{\partial P}{\partial \vartheta}\right] \\ \left[\dfrac{\partial Q}{\partial V}\right] & \left[\dfrac{\partial Q}{\partial \vartheta}\right] \end{bmatrix}^{-1} \begin{bmatrix} [1] & [0] \\ [0] & [1] \end{bmatrix} \begin{bmatrix} [\Delta P^*] \\ [\Delta Q^*] \end{bmatrix}
\tag{3.1}
$$

where $[\Delta E]$ and $[\Delta \vartheta]$ are, respectively, the nodal voltage magnitudes (rms) and phase variations corresponding to the nodal active or reactive power injections $[\Delta P^*]$ and $[\Delta Q^*]$ ($[1]$ is the identity matrix).

Equation (3.1) can be rewritten in the following compact form:

$$
\begin{bmatrix} [\Delta E] \\ [\Delta \vartheta] \end{bmatrix} = [s] \begin{bmatrix} [\Delta P^*] \\ [\Delta Q^*] \end{bmatrix}
\tag{3.2}
$$

where:

$$
[s] \triangleq \begin{bmatrix} \left[\dfrac{\partial P}{\partial V}\right] & \left[\dfrac{\partial P}{\partial \vartheta}\right] \\ \left[\dfrac{\partial Q}{\partial V}\right] & \left[\dfrac{\partial Q}{\partial \vartheta}\right] \end{bmatrix}^{-1} \begin{bmatrix} [1] & [0] \\ [0] & [1] \end{bmatrix}
\tag{3.3}
$$

is the (injection) Sensitivity Matrix. The method described above is generally valid, but its computational complexity is too high for practical voltage analysis in MVDNs. For radial networks, only the voltage magnitude is needed to control the nodal voltages. The proposed theory is easier than classical theory, and it is suitable for radial MVDNs.

3.3 THE PROPOSED THEORY

In this Paragraph, the proposed theory for choosing the BG is outlined. The method is first described in general and considers the possibility of reactive power regulation for all nodes.

After the general treatment, the analysis focuses on a realistic network in which the reactive power can only be controlled in some nodes (generator nodes).

Let us consider the network depicted in Fig. 3.3-1, which is a four-node test MVDN.
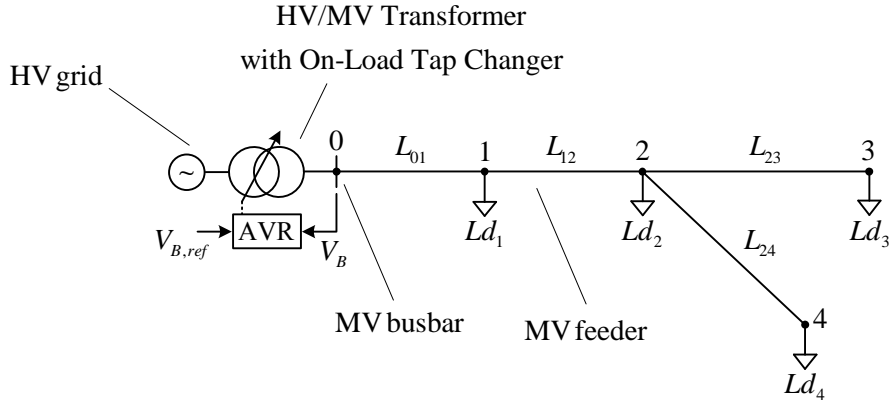
Fig. 3.3-1. The considered four nodes test MVDN

The general loads $Ld_1 \ldots Ld_4$ are represented using constant PQ models. Positive P (or Q) corresponds to the absorbed power by the load. Negative P (or Q) corresponds to the injected power in the network (i.e., the general load is really a generator). The per-phase equivalent circuit is shown in Fig. 3.3-2.

The lines $L_{01} \ldots L_{24}$ are modeled using the RL-direct sequence equivalent circuit, but the shunt admittances are neglected (as explained in the follow). The node 0 represents the MV busbar, which is regulated at a constant voltage value E_0 by the AVR of the OLTC. This reference voltage coincides with the rated value $E_0 = V_n / \sqrt{3}$.
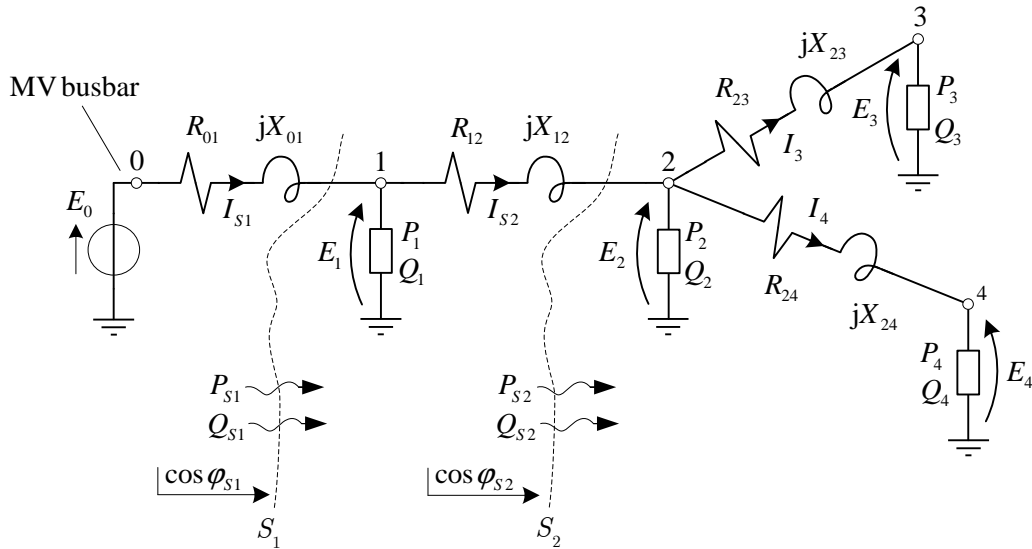
Fig. 3.3-2. The per-phase equivalent circuit

Because the busbar is regulated at E_0, we can characterize the generic node i using the difference V_{0i} between the magnitude of the busbar voltage and the node voltage E_i. In other words, we can write:

$$V_{0i} = E_0 - E_i \tag{3.4}$$

In radial networks, (3.4) can be calculated as the sum of the voltage differences between adjacent nodes from the ith node toward the MV busbar. For example, if $i = 3$ (see Fig. 3.3-2), (3.4) becomes:

$$V_{03} = E_0 - E_3 \tag{3.5}$$

By adding and subtracting E_1 and E_2 in (3.5), we obtain:

$$\begin{aligned} V_{03} &= (E_0 - E_1) + (E_1 - E_2) + (E_2 - E_3) = \\ &= V_{01} + V_{12} + V_{23} \end{aligned} \tag{3.6}$$

where V_{03} is the sum of the voltage differences V_{01}, V_{12} and V_{23}.

The voltage V_{23} can be calculated considering the network parameters and the line power flow as follows:

$$\begin{aligned} V_{23} &= E_2 - E_3 = R_{23}I_3 \cos\varphi_3 + X_{23}I_3 \sin\varphi_3 = \\ &= \frac{R_{23}E_3I_3 \cos\varphi_3 + X_{23}E_3I_3 \sin\varphi_3}{E_3} = \frac{R_{23}P_3 + X_{23}Q_3}{E_3} \end{aligned} \tag{3.7}$$

where $\cos\varphi_3$, P_3 and Q_3 are the power factor and the active and reactive (per-phase) powers of the load Ld_3, respectively. I_3, R_{23} and X_{23} are the current, resistance and reactance of the line L_3.

Normally, the nodal voltages are close to the rated voltage E_n. Applying this assumption to (3.7) leads to:

$$V_{23} \cong \frac{R_{23}P_3 + X_{23}Q_3}{E_n} \tag{3.8}$$

Similarly, considering nodes 1 and 2, we can write:

$$\begin{aligned} V_{12} &= E_1 - E_2 = R_{12}I_2 \cos\varphi_{S2} + X_{12}I_2 \sin\varphi_{S2} = \\ &= \frac{R_{12}E_2I_2 \cos\varphi_{S2} + X_{12}E_2I_2 \sin\varphi_{S2}}{E_2} \cong \frac{R_{12}P_{S2} + X_{12}Q_{S2}}{E_n} \end{aligned} \tag{3.9}$$

where P_{S2} and Q_{S2} are the active and reactive powers through the section S_2 and $\cos\varphi_{S2}$ is the power factor for the same section. For P_{S2} and Q_{S2}, we can write:

$$P_{S2} = P_2 + P_3 + P_4 + P_{R23} + P_{R24} \tag{3.10}$$

$$Q_{S2} = Q_2 + Q_3 + Q_4 + Q_{X23} + Q_{X24} \tag{3.11}$$

where P_{R23} and P_{R24} are the power losses in R_{23} and R_{24}, while Q_{X23} and Q_{X24} are the reactive powers absorbed by X_{23} and X_{24}. These active and reactive losses are negligible compared to the load powers. Applying this assumption to (3.9), (3.10) and (3.11) leads to:

$$P_{S2} \cong P_2 + P_3 + P_4 \tag{3.12}$$

$$Q_{S2} \cong Q_2 + Q_3 + Q_4 \tag{3.13}$$

and:

$$V_{12} \cong \frac{R_{12}\left(P_2 + P_3 + P_4\right) + X_{12}\left(Q_2 + Q_3 + Q_4\right)}{E_n} \tag{3.14}$$

Finally, the voltage difference V_{01} is:

$$V_{01} = E_0 - E_1 \cong \frac{R_{01}P_{S1} + X_{01}Q_{S1}}{E_n} \tag{3.15}$$

where:

$$P_{S1} \cong P_1 + P_2 + P_3 + P_4 \tag{3.16}$$

$$Q_{S1} \cong Q_1 + Q_2 + Q_3 + Q_4 \tag{3.17}$$

are the powers through section S_1.

Using (3.6) with (3.15), (3.9) and (3.8), we can say that V_{03} is a function of all loads and active and reactive powers, i.e., $P_1 \dots P_4$ and $Q_1 \dots Q_4$. The same observation is valid for E_3:

$$E_3 = E_0 - V_{03} = E_0 - \left(V_{01} + V_{12} + V_{23}\right) \tag{3.18}$$

because E_0 is constant. In other words, we can write:

$$E_3 = f\left(P_1, \dots, P_4, Q_1, \dots, Q_4\right) \tag{3.19}$$

Equation (3.19) shows that an active/reactive power variation (in the general j node) that is defined as:

$$\Delta P_j = P_j^f - P_j^0 \tag{3.20}$$

$$\Delta Q_j = Q_j^f - Q_j^0 \tag{3.21}$$

where P_j^f (Q_j^f) and P_j^0 (Q_j^0) are the final and initial power values, respectively, produces a voltage variation in node 3 that is defined as:

$$\Delta E_3 = E_3^f - E_3^0 \tag{3.22}$$

In this treatment, we only consider the reactive power variations (i.e., $\Delta P_j = 0$) because we assume that only the reactive power can be used to control the node voltages.

The variation ΔE_3 can be calculated by linearizing (3.19) and considering only the reactive power variations. In particular, we can write:

$$\Delta E_3 = \frac{\partial E_3}{\partial Q_1} \Delta Q_1 + \frac{\partial E_3}{\partial Q_2} \Delta Q_2 + $$
$$+ \frac{\partial E_3}{\partial Q_3} \Delta Q_3 + \frac{\partial E_3}{\partial Q_4} \Delta Q_4 \tag{3.23}$$

The terms $\partial E_i / \partial Q_j$ in (3.23) indicate the "gain" from the voltage variation ΔE_i in node i when a reactive power variation ΔQ_j occurs in node j. In other words, they are Sensitivity terms.

According to (3.18), we can obtain:

$$\frac{\partial E_3}{\partial Q_1} = -\frac{X_{01}}{E_n} \qquad \frac{\partial E_3}{\partial Q_2} = -\frac{X_{01} + X_{12}}{E_n}$$
$$\frac{\partial E_3}{\partial Q_3} = -\frac{X_{01} + X_{12} + X_{23}}{E_n} \qquad \frac{\partial E_3}{\partial Q_4} = -\frac{X_{01} + X_{12}}{E_n} \tag{3.24}$$

Substituting equation group (3.24) into (3.23) has important implications.

If we have a reactive injection in any node, i.e., $\Delta Q_j < 0$ (in this case $j = 1...4$), then $\Delta E_3 > 0$ in node 3 (i.e., the voltage increases). Then, if we were to reduce the voltage in any node, we must absorb reactive power from the network (i.e., $\Delta Q_j > 0$) by using, for example, the distributed generators.

If the above analysis that focuses on node 3 is extended to all network nodes, (3.23) has a general matrix relationship:

$$\begin{bmatrix} \Delta E_1 \\ \Delta E_2 \\ \Delta E_3 \\ \Delta E_4 \end{bmatrix} = \begin{bmatrix} \dfrac{\partial E_1}{\partial Q_1} & \dfrac{\partial E_1}{\partial Q_2} & \dfrac{\partial E_1}{\partial Q_3} & \dfrac{\partial E_1}{\partial Q_4} \\ \dfrac{\partial E_2}{\partial Q_1} & \dfrac{\partial E_2}{\partial Q_2} & \dfrac{\partial E_2}{\partial Q_3} & \dfrac{\partial E_2}{\partial Q_4} \\ \dfrac{\partial E_3}{\partial Q_1} & \dfrac{\partial E_3}{\partial Q_2} & \dfrac{\partial E_3}{\partial Q_3} & \dfrac{\partial E_3}{\partial Q_4} \\ \dfrac{\partial E_4}{\partial Q_1} & \dfrac{\partial E_4}{\partial Q_2} & \dfrac{\partial E_4}{\partial Q_3} & \dfrac{\partial E_4}{\partial Q_4} \end{bmatrix} \begin{bmatrix} \Delta Q_1 \\ \Delta Q_2 \\ \Delta Q_3 \\ \Delta Q_4 \end{bmatrix} \tag{3.25}$$

which in a compact form yields:

$$\left[\Delta E \right] = \left[s_Q \right] \left[\Delta Q \right] \tag{3.26}$$

where $\left[s_Q \right]$ is the reactive Sensitivity Matrix, $\left[\Delta Q \right]$ is the reactive power-variations vector and $\left[\Delta E \right]$ is the nodal voltages vector.

Calculating the partial derivatives contained in $\left[s_Q \right]$, we have:

$$\left[s_Q \right] = -\frac{1}{E_n} \begin{bmatrix} X_{01} & X_{01} & X_{01} & X_{01} \\ X_{01} & X_{01} + X_{12} & X_{01} + X_{12} & X_{01} + X_{12} \\ X_{01} & X_{01} + X_{12} & X_{01} + X_{12} + X_{23} & X_{01} + X_{12} \\ X_{01} & X_{01} + X_{12} & X_{01} + X_{12} & X_{01} + X_{12} + X_{24} \end{bmatrix} \tag{3.27}$$

After analyzing this form of (3.27), we can say that this matrix can be built using the following inspection rule:

"The element i, j is the arithmetic sum of the reactances of the branches in which both the powers absorbed by node i and node j flow multiplied by $-1/E_n$ ".

For example, in (3.27), the element 2, 4 is $-\left(X_{01} + X_{12} \right)/E_n$ because the powers delivered by node 2 and node 4 flow in branches 01 and 12.

It is important to note that if we would consider also the active power variation effect, for the above discussions (3.26) becomes:

$$[\Delta E] = \left[s_Q \right][\Delta Q] + \left[s_P \right][\Delta P] \tag{3.28}$$

where:

$$[\Delta P] = \begin{bmatrix} \Delta P_1 & \Delta P_2 & \Delta P_3 & \Delta P_4 \end{bmatrix}^T \tag{3.29}$$

is the active power variations vector and $\left[s_P \right]$ is the active power Sensitivity Matrix, that is formally identical to (3.27) but replacing the reactances with the resistances and maintaining the same subscript, i.e. X_{01} became R_{01} etc. Also the inspection rule is identical, considering the resistances instead of the reactances. Then the active power Sensitivity Matrix for the network of Fig. 3.3-2 is:

$$\left[s_P \right] = -\frac{1}{E_n} \begin{bmatrix} R_{01} & R_{01} & R_{01} & R_{01} \\ R_{01} & R_{01} + R_{12} & R_{01} + R_{12} & R_{01} + R_{12} \\ R_{01} & R_{01} + R_{12} & R_{01} + R_{12} + R_{23} & R_{01} + R_{12} \\ R_{01} & R_{01} + R_{12} & R_{01} + R_{12} & R_{01} + R_{12} + R_{24} \end{bmatrix} \tag{3.30}$$

Typically, in MVDNs, the resistance is not negligible if compared with the reactance. The consequence is that in (3.28) the matrix $\left[s_P \right]$ is not negligible compared with $\left[s_Q \right]$, hence an active power injection variation causes a voltage variation. In other words the so-called $P\theta - QV$ decoupling, that is typical of HV networks, is inexistent in MVDNs because the P variations are "coupled" with the voltage variations.

It is important to note that in the above presented theoretical treatment, lines have been modeled using the series RL equivalent circuit. Shunt capacitances have been neglected

considering this elements like constant reactive power generators ($\Delta Q_{cap} = 0$). This assumption creates a negligible error.

Equation (3.28) allows to calculate the phase voltage variation in function of the active and reactive power variation. Multiplying the left and the right side of (3.28) by $\sqrt{3}$ and multiplying and dividing the right side of the same equation by 3, (3.28) can be expressed in function of the three-phase parameters:

$$[\Delta V] = [s_{Q,t}][\Delta Q_t] + [s_{P,t}][\Delta P_t] \tag{3.31}$$

where $[\Delta V]$ is the line-to-line voltage variation vector and $[\Delta Q_t]$, $[\Delta P_t]$ are, respectively, the three-phase power variation vectors. The form of the Sensitivity matrices in (3.31) is identical to which reported in (3.27) and (3.30); however the term $-1/E_n$ must be substituted with $-1/V_n$, where V_n is the network line-to-line rated voltage. The three phase form of the Sensitivity matrices can be used in Chapter 2, where the RQV local voltage regulation technique will be presented.

3.4 THE "BEST GENERATOR" CHOICE

The BG is the generator that has the greatest influence on node i, which is the node where the voltage exceeds the threshold.

Thus, after analyzing (3.25), we can say that the BG is the generator that maximizes the following product, which we call the *"Sensitivity product"*:

$$\frac{\partial E_i}{\partial Q_j} \Delta Q_j \tag{3.32}$$

For example, if the node with a voltage that exceeds V_{max} is $i = 2$ and the BG is connected to node $j = 4$, the Sensitivity product $(\partial E_2 / \partial Q_4) \Delta Q_4$ is the highest compared to the other products contained in row 2 of the Sensitivity Matrix. In addition, in order to choose the BG, it is necessary to evaluate the single products (3.32) of the row that represents node i. Thus, the value ΔQ_j is needed and is acquired as the VCS polls the UPGs, as stated previously. Another possibility is that each generator it is able to exchange to the network a "guaranteed" reactive power Q_g^*, for every generated active power. In this case:

$$\Delta Q_j = Q_g^* \tag{3.33}$$

This last hypothesis is taken into account in this work. In particular, we can say that a generator is able to guarantee a minimum (inductive or capacitive) power factor $\cos\varphi_g^* = 0.9$ at every generated active power. Then if A_n is the (three-phase) nominal apparent power, the guaranteed (three-phase) reactive power is:

$$Q_g^* = A_n \sin \varphi_g^* \tag{3.34}$$

which can be inductive or capacitive in function of the power factor type (inductive or capacitive). When the VCS choose a BG, send to it the reactive power set-point Q_g^*, which can be inductive in case of "high voltage" or capacitive in case of "low voltage".

The procedure above described suggests a way of defining the "*reactive power Sensitivity Table*" $\left[T_{SQ} \right]$ that contains the single Sensitivity products and which is necessary to choose the BG.

For the MVDN represented in Fig. 3.3-2, $\left[T_{SQ} \right]$ takes the following form:

$$\begin{bmatrix} \dfrac{\partial E_1}{\partial Q_1} \Delta Q_1 & \dfrac{\partial E_1}{\partial Q_2} \Delta Q_2 & \dfrac{\partial E_1}{\partial Q_3} \Delta Q_3 & \dfrac{\partial E_1}{\partial Q_4} \Delta Q_4 \\[2ex] \dfrac{\partial E_2}{\partial Q_1} \Delta Q_1 & \dfrac{\partial E_2}{\partial Q_2} \Delta Q_2 & \dfrac{\partial E_2}{\partial Q_3} \Delta Q_3 & \dfrac{\partial E_2}{\partial Q_4} \Delta Q_4 \\[2ex] \dfrac{\partial E_3}{\partial Q_1} \Delta Q_1 & \dfrac{\partial E_3}{\partial Q_2} \Delta Q_2 & \dfrac{\partial E_3}{\partial Q_3} \Delta Q_3 & \dfrac{\partial E_3}{\partial Q_4} \Delta Q_4 \\[2ex] \dfrac{\partial E_4}{\partial Q_1} \Delta Q_1 & \dfrac{\partial E_4}{\partial Q_2} \Delta Q_2 & \dfrac{\partial E_4}{\partial Q_3} \Delta Q_3 & \dfrac{\partial E_4}{\partial Q_4} \Delta Q_4 \end{bmatrix} \tag{3.35}$$

Row i represents the node in which we want to control the voltage (the OTG node), and column j represents the nodes in which we can control the reactive power. The BG is the generator connected to node j that has the maximum absolute value of the Sensitivity product in position i, j. By finding the maximum (in absolute value) Sensitivity product in row i, we automatically choose the BG because the location corresponds to column j of the maximum Sensitivity product. The automatic "BG finder algorithm", implemented in the VCS, is explained in Paragraph 3.4.1.

It is clear that, for a general network with N nodes, the Sensitivity Table takes the following form:

$$\begin{bmatrix} \dfrac{\partial E_1}{\partial Q_1} \Delta Q_1 & \dfrac{\partial E_1}{\partial Q_2} \Delta Q_2 & \dots & \dfrac{\partial E_1}{\partial Q_N} \Delta Q_N \\[2ex] \dfrac{\partial E_2}{\partial Q_1} \Delta Q_1 & \dots & \dots & \dots \\[2ex] \dots & \dots & \dots & \dots \\[2ex] \dfrac{\partial E_N}{\partial Q_1} \Delta Q_1 & \dots & \dots & \dfrac{\partial E_N}{\partial Q_N} \Delta Q_N \end{bmatrix} \tag{3.36}$$

It is important to note that, if it is not possible to regulate the reactive power (e.g., if in that node there is a load or a non-controllable generator) in a node j, then $\Delta Q_j = 0$ and, consequently, the Sensitivity product in the position i, j of the Sensitivity Table is 0.

Comparing (3.35) with (3.25), we can say that each element i, j of $\left[T_{SQ} \right]$ represents the line-to-ground voltage variation in node i when a reactive power variation occurs in node j.

It is clear that also the "*active power Sensitivity Table*" $\left[T_{SP} \right]$ can be defined. The elements of this table are $\left(\partial E_i / \partial P_j \right) \Delta P_j$.

3.4.1 The "Best Generator" choice flow-chart

The BG finding algorithm, implemented in the VCS, can be described using the flow-chart depicted in Fig. 3.4-1. Let us suppose we have the highest voltage on the OTG (*i*-th node sent VFLS = 1 to the VCS). The Centralized Voltage Control must be activated: as said before, by finding the maximum (in absolute value) Sensitivity product in the reactive power Sensitivity Table row i, we automatically choose the BG (*j*-th node). When the BG is found, the VCS:

- send to it the reactive power set-point (3.34)
- "locks" the BG because no others reactive power requests can be sent to it
- repeats the cycle if VFLS is still present, in order to chose the successive BG

This procedure is also represented in Fig. 3.4-2, where the OTG is on the node 2 while the BG is connected to the node 3. It is important to note that also multiple OTGs can be present. In this case the above described procedure will be applied on more than one reactive power Sensitivity Table rows.

When the VFLS signal becomes 0 the Centralized Voltage Control must be deactivated: the above described procedure will be inverted by the VCS. In particular it:

- deactivates the reactive power set-point to the BG
- "unlocks" the BG
- repeats the cycle

If during the Centralized Voltage Regulation deactivation a new VFLS incomes, the later BG will be "recalled" again, sending to it the set-point (3.34).

In case of VFLI the BG finding procedure is similar to the previous one. However, in this case a capacitive reactive power is needed. Then the reactive power set-point sent to the BG will be:
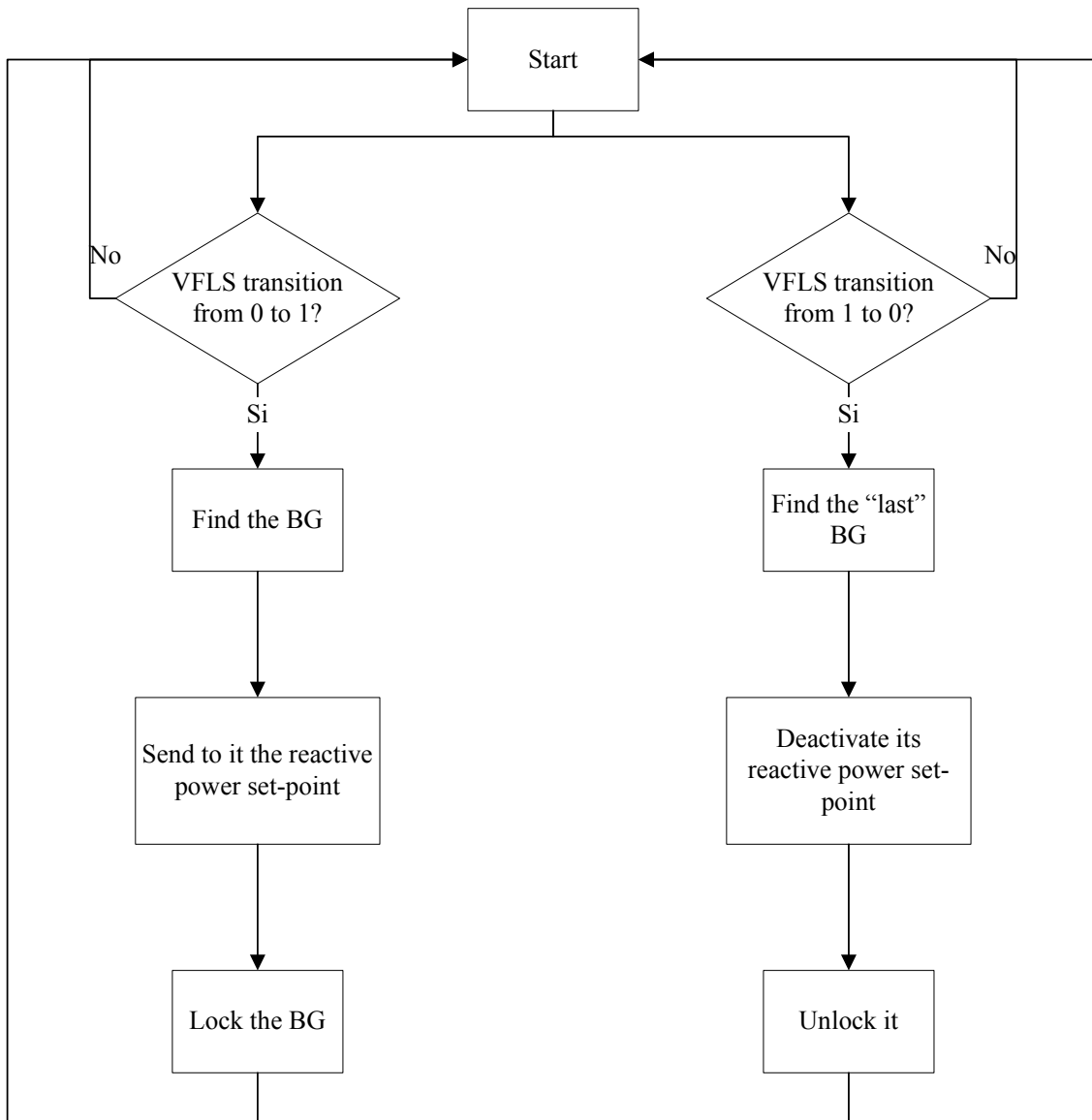
$$Q_g^* = -A_n \sin \varphi_g^* \tag{3.37}$$

Fig. 3.4-1. The "Best Generator" choice flow-chart

$$i = 2 \xrightarrow{\hspace{2cm}} \begin{bmatrix} T_{SQ} \end{bmatrix} = \begin{bmatrix} \dfrac{\partial E_1}{\partial Q_1}\Delta Q_1 & \dfrac{\partial E_1}{\partial Q_2}\Delta Q_2 & \dfrac{\partial E_1}{\partial Q_3}\Delta Q_3 & \dfrac{\partial E_1}{\partial Q_4}\Delta Q_4 \\[2mm] \dfrac{\partial E_2}{\partial Q_1}\Delta Q_1 & \dfrac{\partial E_2}{\partial Q_2}\Delta Q_2 & \dfrac{\partial E_2}{\partial Q_3}\Delta Q_3 & \dfrac{\partial E_2}{\partial Q_4}\Delta Q_4 \\[2mm] \dfrac{\partial E_3}{\partial Q_1}\Delta Q_1 & \dfrac{\partial E_3}{\partial Q_2}\Delta Q_2 & \dfrac{\partial E_3}{\partial Q_3}\Delta Q_3 & \dfrac{\partial E_3}{\partial Q_4}\Delta Q_4 \\[2mm] \dfrac{\partial E_4}{\partial Q_1}\Delta Q_1 & \dfrac{\partial E_4}{\partial Q_2}\Delta Q_2 & \dfrac{\partial E_4}{\partial Q_3}\Delta Q_3 & \dfrac{\partial E_4}{\partial Q_4}\Delta Q_4 \end{bmatrix}$$
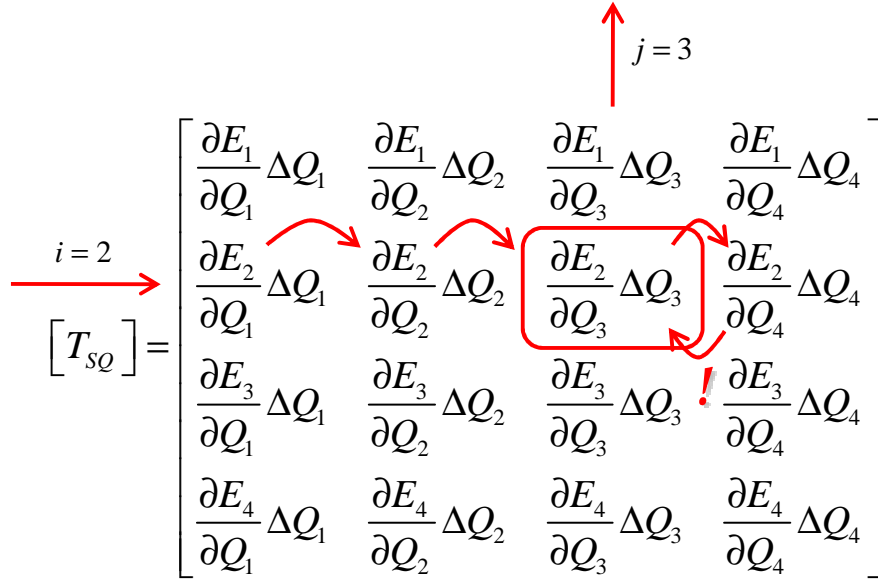
$j = 3$

Fig. 3.4-2. The "Best Generator" choice in terms of reactive power Sensitivity Table

3.5 REFERENCES

[1] R. Marconato, "Electric Power Systems Vol. II" CEI, Milano, 2008.

[2] M. Brenna, E. De Berardinis, L. Delli Carpini, F. Foiadelli Member, P. Paulon, P. Petroni, G. Sapienza, G. Scrosati, D. Zaninelli, " Automatic Distributed Voltage Control Algorithm in Smart Grids applications", IEEE Transaction on Smart Grids, in publication.

[3] M. Brenna, E. De Berardinis, F. Foiadelli, G. Sapienza, D. Zaninelli, "Voltage Control in Smart Grids: an Approach Based On Sensitivity Theory", J. Electromagnetic Analysis & Applications, 2010.

[4] F. Cottignoli, A. Baccarini, "Elettrotecnica Generale", Edizioni Calderini, Bologna.

[5] F. Cottignoli, A. Baccarini, "Macchine Elettriche", Edizioni Calderini, Bologna.

[6] F. Cottignoli, A. Baccarini, "Misure elettriche ed elettrotecniche", 3 voll., Edizioni Calderini, Bologna, 1970.

[7] F. Cottignoli, A. Baccarini, "Guida al laboratorio di misure elettriche", 2 voll., E-dizioni Calderini, Bologna, 1971.

[8] S. Conti, S. A. Rizzo, "Voltages Sensitivity Analysis in Radial Active Distribution Networks using Novel Closed-Form Approximate Equations", International Review of Electrical Engineering (I.R.E.E.).

[9] S. Conti, S. Raiti, G. Vagliasindi, "A Simplified Approach to Voltage Sensitivity Analysis in Radial MV Distribution Networks with Constant Current Models for Loads and Generators", Industrial Electronics (ISIE), 2010 IEEE International Symposium on, Issue Date: 4-7 July 2010, On page(s): 2548 - 2554.

[10]   P. Kundur, "Power System Stability and Control" McGraw-Hill, 1994.

[11]   Y. Rosales Hernandez, T. Hiyama, "Distance Measure Based Rules for Voltage Regulation with Loss Reduction"

[12]   F. Saccomanno, "Electric Power Systems" Wiley-Interscience IEEE Press, Piscataway, NJ, 2003.

[13]   G. Andersson, "Modeling and Analysis of Electric Power Systems" Lecture 227-0526-00, ITET ETH Zürich, 2008, Zürich.

[14]   Y. Abdel-Rady I. Mohamed E. F. El-Saadany "A Control Scheme for PWM Voltage-Source Distributed-Generation Inverters for Fast Load-Voltage Regulation and Effective Mitigation of Unbalanced Voltage Disturbances" IEEE Transactions on Industrial Electronics, Vol. 55, N. 5, May 2008 Page(s): 2072 – 2084.

[15]   P. M. S. Carvalho, P. F. Correia, L. A. F. M. Ferreira, "Distributed Reactive Power Generation Control for Voltage Rise Mitigation in Distribution Networks," Power Systems, IEEE Transactions on Volume: 23 , Issue: 2, 2008 , Page(s): 766 – 772.

[16]   P. N. Vovos, A. E. Kiprakis, A. R. Wallace, G. P. Harrison, "Centralized and Distributed Voltage Control: Impact on Distributed Generation Penetration," Power Systems, IEEE Transactions on Volume: 22, Issue: 1, 2007 , Page(s): 476 – 483.

[17]   P.M. Anderson, "Power System Protection," IEEE Press, Piscataway, NJ, 1999.

[18]   N. Mohan, T. M. Undeland, W. P. Robbins, "Power electronics: converters, applications, and design", Wiley, 1995.

[19]   M. H. Rashid, "Power Electronics Handbook", Academic Press-Elsevier, 2007.

[20]   L. L. Grigsby, "Electric Power Generation, Transmission and Distribution", CRC Press-Taylor & Francis Group, Boca Raton, 2006.

[21]   F. A. Viawan, D. Karlsson, "Coordinated Voltage and Reactive Power Control in the Presence of Distributed Generation," PES General Meeting - Conversion and Delivery of Electrical Energy in the 21st Century, 2008 IEEE.

[22]   S. Corsi, "Wide Area Voltage Regulation & Protection" Paper accepted for presentation at 2009 IEEE Bucharest Power Tech Conference, June 28th - July 2nd, Bucharest, Romania.

[23]   A. Gandelli, S. Leva, A. P. Morando, "Topological Considerations on the Symmetrical Components Transformation, "Circuits and Systems I: Fundamental Theory and Applications, IEEE Transactions on Vol. 47, Issue 8, Aug. 2000 Page(s): 1202 – 1211.

[24]   Radial Distribution Test Feeders, Distribution System Analysis Subcommittee Report.

[25]   H. M. Ayres, L. C. P. da Silva, W. Freitas, M. C. de Almeida V. F. da Costa, "Evaluation of the Impact of Distributed Generation on Power Losses by Using a Sensitivity-Based Method," PES General Meeting, 2009 IEEE.

[26]   A. Kishore, E. F. Hill, "Static optimization of Reactive Power Sources by use of Sensitivity Parameters", Power Apparatus and Systems, IEEE Transactions on, Volume: PAS-90, Issue: 3, 1971, Page(s): 1166 – 1173.

Chapter 4

Real-Time Digital Simulator model for the Proposed Voltage Control

4.1 INTRODUCTION TO CHAPTER 4

In this chapter the Real-Time Digital Simulator (RTDS) model for the proposed voltage control is presented. The proposed voltage control model is implemented on the "Ciccalento" MV line[7] which is installed in the Puglia region, in the south of Italy. The Ciccalento MV line is fed by the "San Giovanni Rotondo" primary substation.

The power system modeled in the RTDS is composed by:

- the entire primary substation model, which contains
    - HV grid equivalent circuit.
    - HV/MV transformer equipped by the on-load tap changer (OLTC)
    - automatic voltage regulator (AVR) of the MV busbar
- the entire MV line model, which contains
    - MV line pi-sections model
    - PQ loads which represent
        - MV/LV secondary substations
        - MV customers
    - distributed generators, based on renewable energy
    - generators local voltage controllers
        - UPG regulation function model
        - RQV regulation function model
    - centralized voltage control system (VCS), based on the sensitivity approach

In the following paragraphs the RTDS simulator and the power system model will be described.

4.2 RTDS SIMULATOR DESCRIPTION

The Real-Time Digital simulator is a digital machine which allows to perform numerical simulations in real-time. Moreover the RTDS is equipped by analog and digital signals interface

---

[7] This 20 kV MV line has been analyzed for the POI-P3 pilot project on Smart Grids.

cards which allow to connect the RTDS to real devices, like protection, regulation and control systems. The RTDS simulates the power system but interconnected devices are real devices.

The RTDS installed by Enel Distribuzione in the "Enel Test Center[8]" of Milan (Italy), is a four-rack (two-cubicles) machine, as reported in Fig. 4.2-1.

Each rack allows to simulate a grid composed by 54 single-phase nodes. Then the nodes capability of the entire RTDS is $54 \times 4 = 216$ single-phase nodes (72 three-phase busbars). The nominal simulation time-step is $50\,\mu s$ and $2\,\mu s$ for the "small-dt" components, like power electronics devices.

Fig. 4.2-1. The RTDS (on the right side), with the amplifiers bank (on the left side), installed in the Enel Distribuzione Test Center (Milan, Italy)

The processor cards, which allow to perform the numerical simulations, contained in the racks are:

- 3PC Triple Processor Card (40 MHz 40 bit, 3 processors)
- GPC Giga Processor Card (1 GHz 64 bit, 2 processors)

A WIF (Workstation InterFace) card synchronize the racks and allows the human-machine interface, using a personal computer.

The analog and digital interface cards are:

- GTAO (Gigabit Transceiver Analogue Output card). This card is necessary to carry-out analog signals (± 10 V) from the RTDS
- GTAI (Gigabit Transceiver Analogue Input card). This card allow to read analog signal using the RTDS

---

[8] "Centro Prove Enel (Enel Test Center), Via Rubattino 84, Milano, 20134, Italy"

- GTDO (Gigabit Transceiver Digital Output card). This card is necessary to carry-out digital signals from the RTDS
- GTDI (Gigabit Transceiver Digital Input card). This card allow to read digital signal using the RTDS
- GTFPI (Gigabit Transceiver Front Panel Interface card). This card allow to read and carry-out digital signal using the RTDS. The interface is installed on the front panel of the RTDS and is equipped by plugs.

Carried-out signals can be amplified using the voltage/current amplifier bank of the RTDS (see Fig. 4.2-1).
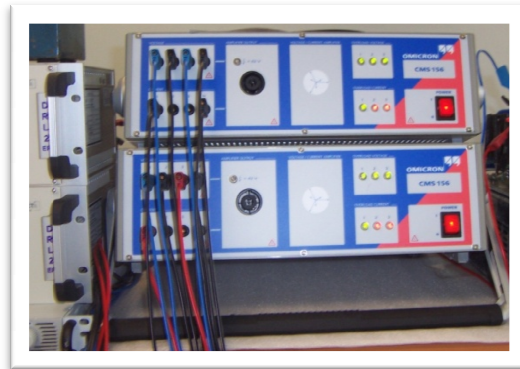
Fig. 4.2-2. Voltage and current amplifier

4.3 ANALYZED MV NETWORK

4.3.1 Network reduction procedure

The proposed voltage control has been applied to the "Ciccalento" MV line. The grid has been implemented in the RTDS, including the "San Giovanni Rotondo" primary substation. As said before, the RTDS is able to simulate a 216 nodes grid. Unfortunately, the considered grid is bigger than 216 nodes. Then a "network reduction" has been applied. It is clear that the consequence of this simplification is a change of the line topology. Hence the topology simplification can be performed only if the consecutive error, in terms of voltage, is negligible.

The distribution lines operate in radial topology. Hence two load structures can be present:

- cluster loads
- successive loads

Fig. 4.3-1 represents the two load structures above mentioned.
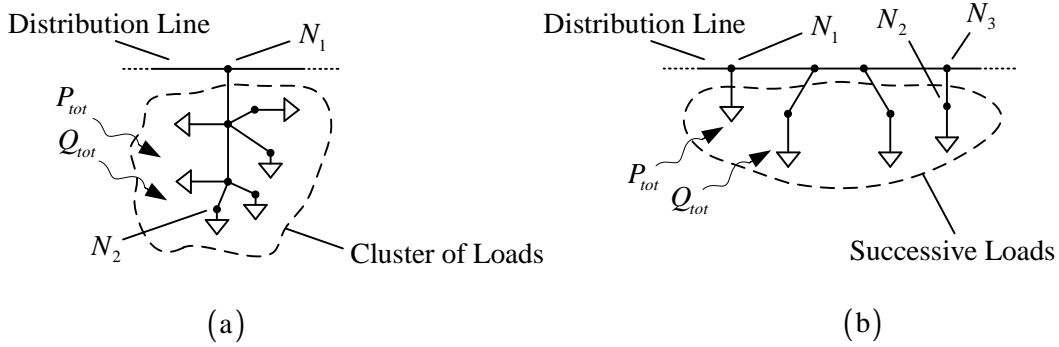
Fig. 4.3-1. Example of cluster loads (a) and successive loads (b).

In the following sections the methods to simplify a network with cluster loads and successive loads are presented. In the following treatment loads have been considered as constant (active/reactive) power devices.

4.3.1.1 Cluster loads simplification

Let us suppose that the entire active and reactive powers absorbed by the cluster are P_{tot} and Q_{tot} (see Fig. 4.3-1-a). There powers include the losses along all of the branches of the cluster and can be calculated using a load-flow software. Knowing P_{tot} and Q_{tot} it is possible to substitute the cluster with an equivalent load that absorbs these powers (see Fig. 4.3-2).

It is important to note that the power losses of the branches of the cluster are dependant from the nodal voltages, and then from the load condition. Using the equivalent load with P_{tot} and Q_{tot} we lost this dependence causing an error. However, due to the low value of the power losses, this error can be neglected.

This procedure can be applied only if the voltage error between the main node (N_1) and the of node which have the lowest voltage (N_2) is less than the maximum admissible voltage error $errV_{max}$ [9], i.e.:

$$\frac{\left|V_{N_1} - V_{N_2}\right|}{V_{N_2}} \leq errV_{max} \tag{4.1}$$

---

[9] The maximum admissible voltage error is 0,25 %. This value represents the half of the error committed by the voltage measuring equipments used in this pilot project.
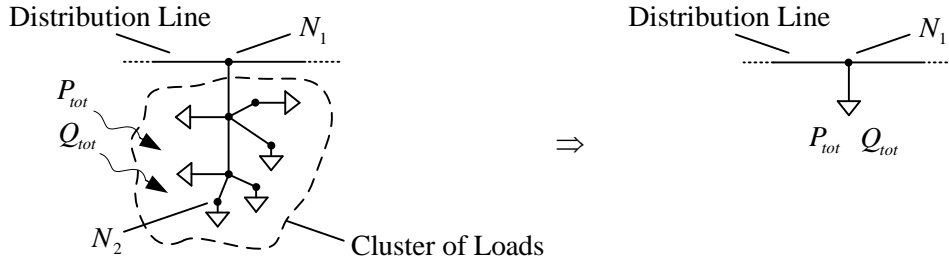
Fig. 4.3-2. Equivalent load for the cluster structure.

It is important to note that this procedure allow to reduce the node number request to the RTDS. For example, if a cluster has N three-phase nodes, the equivalent load need only one three-phase node (three single-phase nodes).

4.3.1.2 Successive loads simplification

Let us now consider a group of loads which are topologically in succession, as reported in Fig. 4.3-1-b. The boundaries of the group are represented by the node N_1 and N_3. The purpose of the simplification is to substitute the group with a single equivalent load (P_{eq}, Q_{eq}). In this case the concept of equivalent load is related to the voltages at the boundary nodes. Let us consider Fig. 4.3-3-a. To the successive loads of the feeder it is associated the voltage profile V_{p_1}. The voltages at the boundary nodes are V_{N_1} and V_{N_3}. When the successive loads are substituted with the equivalent load, the voltage profile becomes V_{p_1}' and the voltages at the boundary nodes V_{N_1}' and V_{N_3}'.

The equivalent load must be chosen in order to guarantee the same voltage, of the original feeder, at the boundary nodes. In other words the condition:

$$\begin{cases} V_{N_1} = V_{N_1}' \\ V_{N_3} = V_{N_3}' \end{cases} \tag{4.2}$$

must be verified. If the condition (4.2) is verified, all of the voltages along the line remain unchanged after the substitution of the successive load group with the equivalent load. It is important to note that the voltage profile between the boundary nodes cannot remains equal to the original, but this is not a problem because the equivalence is based on the boundary nodes.

It is now necessary to explain the method to choose the equivalent load which satisfy the condition (4.2).

Let us consider Fig. 4.3-3-b. The group of successive loads is delimited by the sections S_i (initial) and S_f (final).
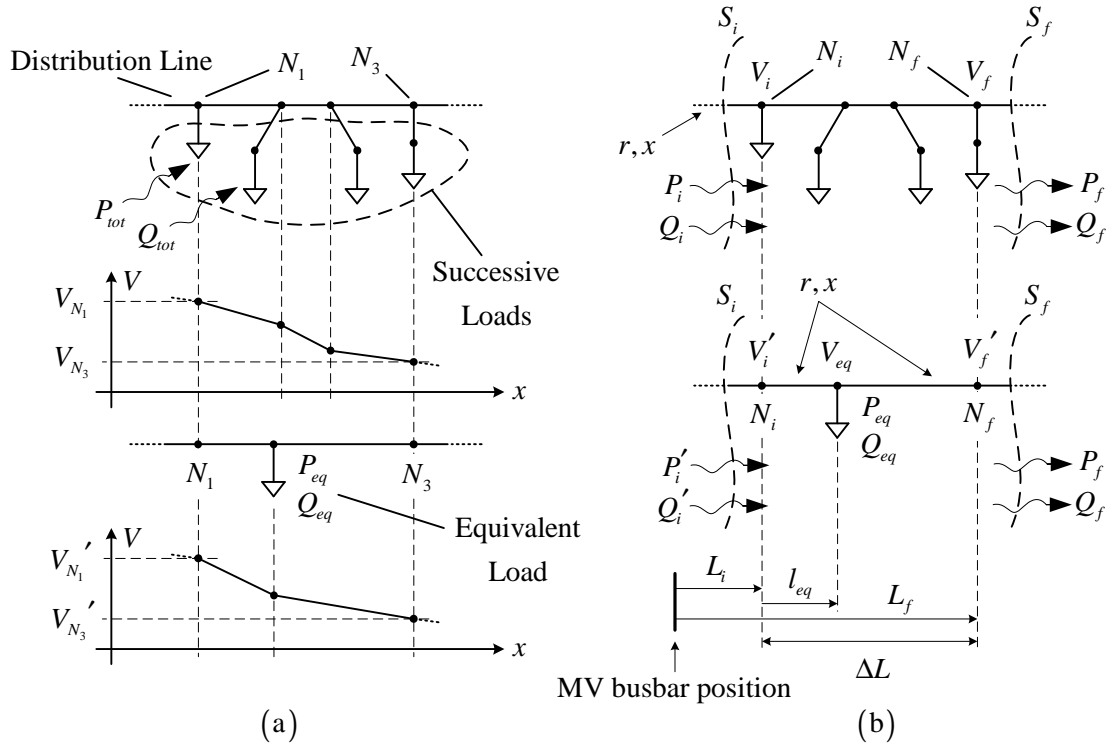
Fig. 4.3-3.   The concept of equivalent load for successive loads (a). Electrical circuit for the equivalent calculation (b).

If we neglect the power losses with respect to the powers which interest the group of load, we can calculate (for the top figure) the powers which fed the initial section:

$$P_i = P_{tot} + P_f \tag{4.3}$$

$$Q_i = Q_{tot} + Q_f \tag{4.4}$$

where P_i and Q_i are the total active and reactive powers respectively absorbed by the group of loads. The voltage V_i at the initial node N_i depends on these powers. In the bottom figure the equivalent load is installed. Hence, if we want the same voltage of the original network in the at the initial section, i.e. $V_i' = V_i$, we must define the equivalent load as:

$$P_{eq} \triangleq P_{tot} \tag{4.5}$$

$$Q_{eq} \triangleq Q_{tot} \tag{4.6}$$

If (4.5) and (4.6) are satisfied $P_i' = P_i$, $Q_i' = Q_i$ and then $V_i' = V_i$. In other words the equivalence at the beginning of the section is satisfied.

69

It is now necessary to verify the equivalence at the end of the section, at the node N_f. In other words we want $V_f{'} = V_f$. This condition can be reached positioning the equivalent load in the correct position, as reported in Fig. 4.3-4, i.e. calculating the correct distance l_{eq} (see Fig. 4.3-3-b).
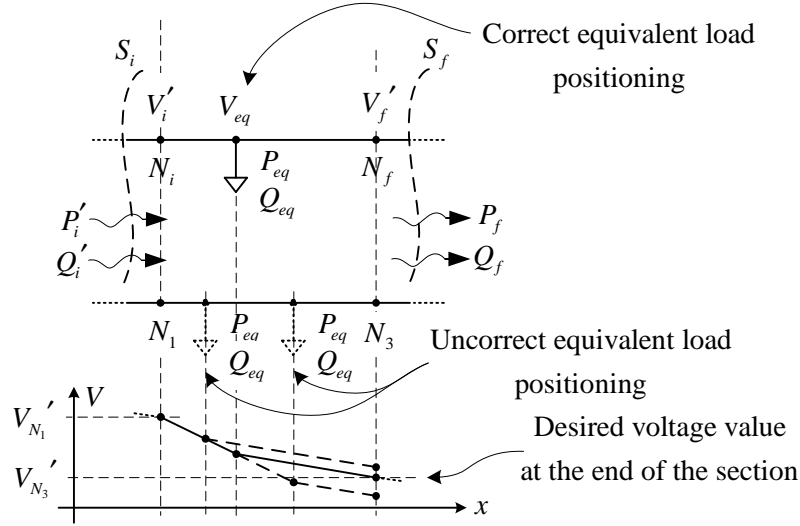

Fig. 4.3-4. Equivalent load positioning along the feeder.

For this purpose the *calculation of the voltage drop* can be used. In particular, if r and x are the per-kilometer resistance and reactance respectively of the feeder (which is considered as a constant section line), we can calculate the voltage drop between the initial section and the equivalent load connection point:

$$V_i - V_{eq} = \frac{l_{eq}\left[\left(P_{eq} + P_f\right) \cdot r + \left(Q_{eq} + Q_f\right) \cdot x\right]}{V_{eq}} \Rightarrow \left(V_i - V_{eq}\right)V_{eq} = l_{eq} \cdot K_1 \tag{4.7}$$

where:

$$K_1 \triangleq \left[\left(P_{eq} + P_f\right) \cdot r + \left(Q_{eq} + Q_f\right) \cdot x\right] \tag{4.8}$$

Similarly we can calculate the voltage drop between the equivalent load connection point and the final section:

$$V_{eq} - V_f = \frac{\left(\Delta L - l_{eq}\right)\left[P_f \cdot r + Q_f \cdot x\right]}{V_f} \Rightarrow \left(V_{eq} - V_f\right)V_f = \left(\Delta L - l_{eq}\right) \cdot K_2 \tag{4.9}$$

where:

$$\Delta L \triangleq L_f - L_i \tag{4.10}$$

and:

$$K_2 \triangleq \left[P_f \cdot r + Q_f \cdot x \right] \tag{4.11}$$

From (4.9) we can derive V_{eq}:

$$V_{eq} = K_3 - K_2 \cdot l_{eq} \tag{4.12}$$

where:

$$K_3 \triangleq \frac{K_2 \cdot \Delta L + V_f^{\ 2}}{V_f} \tag{4.13}$$

Substituting (4.13) in (4.7) we can calculate the distance l_{eq}, solving the following second order equation:

$$K_2^2 \cdot l_{eq}^{\ 2} + \left(K_1 + V_i \cdot K_2 - 2 \cdot K_2 \cdot K_3 \right) l_{eq} + \left(K_3^{\ 2} - V_i \cdot K_3 \right) = 0 \tag{4.14}$$

Normally only one solution is positive and have physical meaning.

Summarizing we can say that the equivalent load (of a group of successive loads) must have the power indicated by (4.5) and (4.6), and must be placed at the distance l_{eq} derived by (4.14).

The voltages V_i and V_f, necessary in (4.14) can be calculated, starting from the original network, using a load-flow software.

It is important to note that the proposed approach works correctly also when the direction of the active and reactive powers is inverted (this condition occurs when distributed generators are installed along the feeder, after the final section) because the power balance it is also satisfied in this case. In other words the powers represented in Fig. 4.3-3-b must be considered with its signs.

In order to define the group of successive loads the following rule has been used: "a group of load can be reduced in a single equivalent load if the difference between all load voltages is less than $errV_{max}$ ".

It is important to note that, from (4.14), the distance l_{eq} is a function of the active and reactive powers. In other words the positioning of the equivalent load should be varied during the time, because the powers are typically time-variant. It is clear that is impossible to move the load during the network operation. So l_{eq} will be calculated in a particular load condition, evaluating the consequent error.

4.3.2 Grid topology and characteristics

The reduced grid is represented in Canvas 1, Canvas 2 and Canvas 3, attached at the end of this chapter. In the follow of this chapter, the grid characteristics are presented, in terms of lines parameters, sensitivity table, generators and regulators characteristics etc.

4.3.2.1 Primary substation parameters

In this paragraph the primary substation components are described. In particular Table I summarizes the HV grid Thévenin equivalent circuit parameters and Table II summarizes HV/MV transformer parameters. The transformer is equipped by an on-load tap changer which allows to vary the voltage by ±15 % of the nominal voltage using ±10 taps. The tap changer is controlled by an automatic voltage regulator (ARV) which follows the MV busbar voltage set-point.

TABLE I. HV GRID THÉVENIN EQUIVALENT CIRCUIT PARAMETERS

Thévenin generator		*Thévenin impedance*		*Short-circuit power*
Nom. voltage [kV]	f [Hz]	R [Ω]	L [H]	S_{cc} [MVA]
150	50	1.216	0.02176	2500

TABLE II. HV/MV TRANSFORMER PARAMETERS

Nom. power [MVA]	Nom. voltage [kV]		Windings connection		P_0 [kW]	P_{cc} [kW]	v_{cc} [%] (on central tap)	i_0 [%]	f [Hz]
	HV	MV	HV	MV					
25	150	20	Y	Y	16	122	14.6	1	50

4.3.2.2 Lines pi-section parameters

The "Ciccalento" MV line pi-sections parameters are summarized in Table III, where:
- "SPIRA[10] Code" is the section ID code
- "R1" is the pi-section positive sequence series resistance
- "X1" is the pi-section positive sequence series inductive reactance
- "Xc1" is the pi-section positive sequence shunt capacitive reactance
- "R0" is the pi-section zero-sequence series resistance
- "Xc0" is the pi-section zero-sequence shunt capacitive reactance
- "l" is the pi-section length
- "Material" is the pi-section material (CU = copper, AL = aluminum)
- "S" is the pi-section section
- "% of cable" is the pi-section cable percentage length

---

[10] SPIRA is the CESI S.p.A. load-flow software, used to reduce the network, as described in this chapter.

- "% of overhead line" is the pi-section overhead line percentage length
- "% of overhead cable" is the pi-section overhead cable percentage length

It is important to note that pi-sections characterized by a "m", as last character of the "SPIRA code", are the modified section necessary to reduce the original MV grid. In these sections, fields "Material", "S", "% of cable", "% of overhead line" and "% of overhead cable" are not present.

TABLE III. "CICCALENTO" MV LINE PI-SECTIONS PARAMETERS

SPIRA Code	R1 (ohm)	X1 (ohm)	Xc1 (Mohm)	R0 (ohm)	X0 (ohm)	Xc0 (Mohm)	l (km)	Material	S (mm2)	% of cable	% overhead line	% overhead cable
MM678	2,22	1,38	0,026850	3	5,952	0,031505	3,795	CU	35	0	92,095	7,905

SPIRA Code	R1 (ohm)	X1 (ohm)	Xc1 (Mohm)	R0 (ohm)	X0 (ohm)	Xc0 (Mohm)	l (km)	Material	S (mm2)	% of cable	% overhead line	% overhead cable
MM679	0,252	0,116	1,175877	0,296	0,484	2,665912	0,3	AL	40	0	100	0

SPIRA Code	R_1 (ohm)	X_1 (ohm)	Xc_1 (Mohm)	R_0 (ohm)	X_0 (ohm)	Xc_0 (Mohm)	l (km)	Material	S (mm^2)	% of cable	% overhead line	% overhead cable
MM6208	1,312	0,492	0,338808	1,484	1,936	0,908678	1,172	CU	16	0	100	0

SPIRA Code	R_1 (ohm)	X_1 (ohm)	Xc_1 (Mohm)	R_0 (ohm)	X_0 (ohm)	Xc_0 (Mohm)	l (km)
MM680m	1,2124	0,5478	0,245050	1,4258	2,3402	0,551492	1,445

SPIRA Code	R1 (ohm)	X1 (ohm)	Xc1 (Mohm)	R0 (ohm)	X0 (ohm)	Xc0 (Mohm)	l (km)	Material	S (mm2)	% of cable	% overhead line	% overhead cable
AA6002	0,1596	0,0722	1,829998	0,1862	0,3078	4,209335	0,19	AL	40	0	100	0

SPIRA Code	R1 (ohm)	X1 (ohm)	Xc1 (Mohm)	R0 (ohm)	X0 (ohm)	Xc0 (Mohm)	l (km)	Material	S (mm2)	% of cable	% overhead line	% overhead cable
MM684	1,512	0,86	0,189481	1,824	3,416	0,506057	2,1	CU	25	0	100	0

SPIRA Code	R1 (ohm)	X1 (ohm)	Xc1 (Mohm)	R0 (ohm)	X0 (ohm)	Xc0 (Mohm)	l (km)	Material	S (mm2)	% of cable	% overhead line	% overhead cable
MM685	1,152	0,656	0,248330	1,388	2,6	0,666338	1,6	CU	25	0	100	0

SPIRA Code	R1 (ohm)	X1 (ohm)	Xc1 (Mohm)	R0 (ohm)	X0 (ohm)	Xc0 (Mohm)	l (km)	Material	S (mm2)	% of cable	% overhead line	% overhead cable
MM6196	0,144	0,084	1,999434	0,172	0,324	4,997015	0,2	CU	25	0	100	0

SPIRA Code	R1 (ohm)	X1 (ohm)	Xc1 (Mohm)	R0 (ohm)	X0 (ohm)	Xc0 (Mohm)	l (km)	Material	S (mm2)	% of cable	% overhead line	% overhead cable
MM686	0,072	0,04	3,998868	0,088	0,164	10,009745	0,1	CU	25	0	100	0

SPIRA Code	R1 (ohm)	X1 (ohm)	Xc1 (Mohm)	R0 (ohm)	X0 (ohm)	Xc0 (Mohm)	l (km)
MM687m	1,9048	1,4544	0,076764439	13,224	4,3472	0,118349291	3,74

SPIRA Code	R1 (ohm)	X1 (ohm)	Xc1 (Mohm)	R0 (ohm)	X0 (ohm)	Xc0 (Mohm)	l (km)
AB6002m	1,4032	0,5256	0,267955659	1,608	2,0648	0,56950885	1,26

SPIRA Code	R1 (ohm)	X1 (ohm)	Xc1 (Mohm)	R0 (ohm)	X0 (ohm)	Xc0 (Mohm)	l (km)	Material	S (mm2)	% of cable	% overhead line	% overhead cable
MM691	0,112	0,04	3,998868	0,128	0,164	10,009745	0,1	CU	16	0	100	0

SPIRA Code	R1 (ohm)	X1 (ohm)	Xc1 (Mohm)	R0 (ohm)	X0 (ohm)	Xc0 (Mohm)	l (km)
MM692m	1,676	0,628	0,264772822	1,9	2,48	0,701432098	1,5

SPIRA Code	R1 (ohm)	X1 (ohm)	Xc1 (Mohm)	R0 (ohm)	X0 (ohm)	Xc0 (Mohm)	l (km)	Material	S (mm2)	% of cable	% overhead line	% overhead cable
MM6150	0,06	0,012	0,214944	0,192	0,008	0,214944	0,08	AL	50	100	0	0

SPIRA Code	R1 (ohm)	X1 (ohm)	Xc1 (Mohm)	R0 (ohm)	X0 (ohm)	Xc0 (Mohm)	l (km)	Material	S (mm2)	% of cable	% overhead line	% overhead cable
MM6151	0,112	0,04	3,998868	0,128	0,164	10,009745	0,1	CU	16	0	100	0

SPIRA Code	R1 (ohm)	X1 (ohm)	Xc1 (Mohm)	R0 (ohm)	X0 (ohm)	Xc0 (Mohm)	l (km)
MM6152m	0,9728	0,3639	0,023642713	2,2273	1,0998	0,024206554	1,34

SPIRA Code	R1 (ohm)	X1 (ohm)	Xc1 (Mohm)	R0 (ohm)	X0 (ohm)	Xc0 (Mohm)	l (km)
AC6002m	0,3912	0,2081	0,634639697	0,4727	0,9042	1,460405057	0,55

SPIRA Code	R1 (ohm)	X1 (ohm)	Xc1 (Mohm)	R0 (ohm)	X0 (ohm)	Xc0 (Mohm)	l (km)	Material	S (mm2)	% of cable	% overhead line	% overhead cable
AD6001	0,0112	0,004	39,988679	0,0128	0,0168	100,097448	0,01	CU	16	0	100	0

SPIRA Code	R1 (ohm)	X1 (ohm)	Xc1 (Mohm)	R0 (ohm)	X0 (ohm)	Xc0 (Mohm)	l (km)
AD6002m	0,1808	0,068	2,499684987	0,2072	0,2712	6,060736599	0,123

SPIRA Code	R1 (ohm)	X1 (ohm)	Xc1 (Mohm)	R0 (ohm)	X0 (ohm)	Xc0 (Mohm)	l (km)
MM6167m	2,088	1,188	0,136919256	2,516	4,712	0,36345043	2,9

SPIRA Code	R1 (ohm)	X1 (ohm)	Xc1 (Mohm)	R0 (ohm)	X0 (ohm)	Xc0 (Mohm)	l (km)	Material	S (mm2)	% of cable	% overhead line	% overhead cable
MM6175	0,36	0,204	0,799573	0,436	0,812	2,103833	0,5	CU	25	0	100	0

SPIRA Code	R1 (ohm)	X1 (ohm)	Xc1 (Mohm)	R0 (ohm)	X0 (ohm)	Xc0 (Mohm)	l (km)
MM6173m	0,664	0,28	0,493580224	0,772	1,172	1,110641613	0,724

SPIRA Code	R1 (ohm)	X1 (ohm)	Xc1 (Mohm)	R0 (ohm)	X0 (ohm)	Xc0 (Mohm)	l (km)
MM6169m	0,54	0,232	0,016258467	1,212	1,124	0,016425506	0,951

SPIRA Code	R1 (ohm)	X1 (ohm)	Xc1 (Mohm)	R0 (ohm)	X0 (ohm)	Xc0 (Mohm)	l (km)
MM6171m	0,22	0,112	0,016445789	0,852	0,652	0,016500093	0,666

SPIRA Code	R1 (ohm)	X1 (ohm)	Xc1 (Mohm)	R0 (ohm)	X0 (ohm)	Xc0 (Mohm)	l (km)	Material	S (mm2)	% of cable	% overhead line	% overhead cable
MM694	0,632	0,344	0,112936	0,848	1,396	0,131511	0,9	CU	25	11,111	88,889	0

SPIRA Code	R1 (ohm)	X1 (ohm)	Xc1 (Mohm)	R0 (ohm)	X0 (ohm)	Xc0 (Mohm)	l (km)	Material	S (mm2)	% of cable	% overhead line	% overhead cable
MM695	0,488	0,26	0,119701	0,676	1,072	0,134615	0,7	CU	25	14,286	85,714	0

SPIRA Code	R1 (ohm)	X1 (ohm)	Xc1 (Mohm)	R0 (ohm)	X0 (ohm)	Xc0 (Mohm)	l (km)	Material	S (mm2)	% of cable	% overhead line	% overhead cable
MM696	0,152	0,084	0,470316	0,2	0,344	0,547677	0,22	CU	25	0	90,909	9,091

SPIRA Code	R1 (ohm)	X1 (ohm)	Xc1 (Mohm)	R0 (ohm)	X0 (ohm)	Xc0 (Mohm)	l (km)
MM6105m	0,0487	0,0284	0,65428548	0,0729	0,1136	0,700968699	0,076

SPIRA Code	R1 (ohm)	X1 (ohm)	Xc1 (Mohm)	R0 (ohm)	X0 (ohm)	Xc0 (Mohm)	l (km)
AE6002m	0,9633	0,5516	0,29637792	1,1631	2,1784	0,784400902	1,339

SPIRA Code	R1 (ohm)	X1 (ohm)	Xc1 (Mohm)	R0 (ohm)	X0 (ohm)	Xc0 (Mohm)	l (km)	Material	S (mm2)	% of cable	% overhead line	% overhead cable

SPIRA Code	R1 (ohm)	X1 (ohm)	Xc1 (Mohm)	R0 (ohm)	X0 (ohm)	Xc0 (Mohm)	l (km)	Material	S (mm2)	% of cable	% overhead line	% overhead cable
MM6109	1,08	0,616	0,264773	1,304	2,44	0,701432	1,5	CU	25	0	100	0
SPIRA Code	R1 (ohm)	X1 (ohm)	Xc1 (Mohm)	R0 (ohm)	X0 (ohm)	Xc0 (Mohm)	l (km)	Material	S (mm2)	% of cable	% overhead line	% overhead cable
MM6123	0,612	0,348	0,470316	0,74	1,384	1,249254	0,85	CU	25	0	100	0

SPIRA Code	R1 (ohm)	X1 (ohm)	Xc1 (Mohm)	R0 (ohm)	X0 (ohm)	Xc0 (Mohm)	l (km)
MM6124m	1,6761	0,628	0,264755204	1,9001	2,4802	0,701385731	1,5001

SPIRA Code	R1 (ohm)	X1 (ohm)	Xc1 (Mohm)	R0 (ohm)	X0 (ohm)	Xc0 (Mohm)	l (km)	Material	S (mm2)	% of cable	% overhead line	% overhead cable
AF6002	0,0559	0,02	8,013844	0,0639	0,0838	20,057334	0,0499	CU	16	0	100	0

SPIRA Code	R1 (ohm)	X1 (ohm)	Xc1 (Mohm)	R0 (ohm)	X0 (ohm)	Xc0 (Mohm)	l (km)
MM6129m	0,3931	0,1484	1,138854691	0,4453	0,5817	3,065978484	0,351

SPIRA Code	R1 (ohm)	X1 (ohm)	Xc1 (Mohm)	R0 (ohm)	X0 (ohm)	Xc0 (Mohm)	l (km)
AG6002m	1,6713	0,832	0,188594553	3,5753	3,232	0,399796385	2,087

SPIRA Code	R1 (ohm)	X1 (ohm)	Xc1 (Mohm)	R0 (ohm)	X0 (ohm)	Xc0 (Mohm)	l (km)	Material	S (mm2)	% of cable	% overhead line	% overhead cable
AH6002	0,4116	0,3596	0,454793	0,5594	1,7463	0,800377	0,999	AA	60	0	100	0

SPIRA Code	R1 (ohm)	X1 (ohm)	Xc1 (Mohm)	R0 (ohm)	X0 (ohm)	Xc0 (Mohm)	l (km)	Material	S (mm2)	% of cable	% overhead line	% overhead cable
MM6137	0,692	0,26	0,644874	0,784	1,024	1,738448	0,62	CU	16	0	100	0

SPIRA Code	R1 (ohm)	X1 (ohm)	Xc1 (Mohm)	R0 (ohm)	X0 (ohm)	Xc0 (Mohm)	l (km)
MM6138m	1,788	1,252	0,112939926	2,264	5,188	0,261316711	3,205

4.3.3 Line sensitivity matrices and line sensitivity tables

The "Ciccalento" MV line sensitivity matrices and tables are presented in this paragraph. In particular:

- Table IV represents the line reactive power sensitivity matrix
- Table V represents the line active power sensitivity matrix
- Table VI represents the line reactive power sensitivity table, calculated considering a single-phase reactive power variation and phase voltage variation. The sensitivity table is calculated considering the reactive power variation which corresponds to the power factor $\cos\varphi_g^* = 0.9$ (see Chapter 3) applied to the generator rated apparent power (for generator characteristics see Paragraph 4.3.4).

The reactive power sensitivity table is implemented in the Voltage Control System (VCS), described in Chapter 3, in order to perform the centralized voltage control.

TABLE IV. "CICCALENTO" MV LINE REACTIVE POWER SENSITIVITY MATRIX (UNITS [V/VAR])

	Nodes	1	2	3	4	5	6	7	8	9	10	11	12	13	14	15	G1 16	G2 17	G3 18	G4 19	20	21	22	23	24	25	26	27	28	29	30	G5 31
	1	0	0	0	0	0	0	0	0	0	0	0	0	0	0	0	-0,00011951	-0,00011951	-0,00011951	-0,00011951	0	0	0	0	0	0	0	0	0	0	0	-0,00011951
	2	0	0	0	0	0	0	0	0	0	0	0	0	0	0	0	-0,00012956	-0,00012956	-0,00012956	-0,00012956	0	0	0	0	0	0	0	0	0	0	0	-0,00012956
	3	0	0	0	0	0	0	0	0	0	0	0	0	0	0	0	-0,00017700	-0,00017700	-0,00017700	-0,00017700	0	0	0	0	0	0	0	0	0	0	0	-0,00017700
	4	0	0	0	0	0	0	0	0	0	0	0	0	0	0	0	-0,00018325	-0,00018325	-0,00018325	-0,00018325	0	0	0	0	0	0	0	0	0	0	0	-0,00018325
	5	0	0	0	0	0	0	0	0	0	0	0	0	0	0	0	-0,00025773	-0,00025773	-0,00025773	-0,00025773	0	0	0	0	0	0	0	0	0	0	0	-0,00025773
	6	0	0	0	0	0	0	0	0	0	0	0	0	0	0	0	-0,00031454	-0,00031454	-0,00031454	-0,00031454	0	0	0	0	0	0	0	0	0	0	0	-0,00031454
	7	0	0	0	0	0	0	0	0	0	0	0	0	0	0	0	-0,00031800	-0,00031800	-0,00031800	-0,00031800	0	0	0	0	0	0	0	0	0	0	0	-0,00031800
	8	0	0	0	0	0	0	0	0	0	0	0	0	0	0	0	-0,00044396	-0,00044396	-0,00044396	-0,00044396	0	0	0	0	0	0	0	0	0	0	0	-0,00044396
	9	0	0	0	0	0	0	0	0	0	0	0	0	0	0	0	-0,00048948	-0,00048948	-0,00048948	-0,00048948	0	0	0	0	0	0	0	0	0	0	0	-0,00048948
	10	0	0	0	0	0	0	0	0	0	0	0	0	0	0	0	-0,00054386	-0,00054386	-0,00054386	-0,00054386	0	0	0	0	0	0	0	0	0	0	0	-0,00054386
	11	0	0	0	0	0	0	0	0	0	0	0	0	0	0	0	-0,00054490	-0,00054490	-0,00054490	-0,00054386	0	0	0	0	0	0	0	0	0	0	0	-0,00054386
	12	0	0	0	0	0	0	0	0	0	0	0	0	0	0	0	-0,00057642	-0,00057642	-0,00057642	-0,00054386	0	0	0	0	0	0	0	0	0	0	0	-0,00054386
	13	0	0	0	0	0	0	0	0	0	0	0	0	0	0	0	-0,00059444	-0,00059444	-0,00059444	-0,00054386	0	0	0	0	0	0	0	0	0	0	0	-0,00054386
	14	0	0	0	0	0	0	0	0	0	0	0	0	0	0	0	-0,00059479	-0,00059479	-0,00059479	-0,00054386	0	0	0	0	0	0	0	0	0	0	0	-0,00054386
	15	0	0	0	0	0	0	0	0	0	0	0	0	0	0	0	-0,00060068	-0,00060068	-0,00060068	-0,00054386	0	0	0	0	0	0	0	0	0	0	0	-0,00054386
G1	16	0	0	0	0	0	0	0	0	0	0	0	0	0	0	0	-0,00070356	-0,00060068	-0,00060068	-0,00054386	0	0	0	0	0	0	0	0	0	0	0	-0,00054386
G2	17	0	0	0	0	0	0	0	0	0	0	0	0	0	0	0	-0,00060068	-0,00061834	-0,00060068	-0,00054386	0	0	0	0	0	0	0	0	0	0	0	-0,00054386
G3	18	0	0	0	0	0	0	0	0	0	0	0	0	0	0	0	-0,00060068	-0,00060068	-0,00062077	-0,00054386	0	0	0	0	0	0	0	0	0	0	0	-0,00054386
G4	19	0	0	0	0	0	0	0	0	0	0	0	0	0	0	0	-0,00054386	-0,00054386	-0,00054386	-0,00057366	0	0	0	0	0	0	0	0	0	0	0	-0,00057366
	20	0	0	0	0	0	0	0	0	0	0	0	0	0	0	0	-0,00054386	-0,00054386	-0,00054386	-0,00057366	0	0	0	0	0	0	0	0	0	0	0	-0,00059617
	21	0	0	0	0	0	0	0	0	0	0	0	0	0	0	0	-0,00054386	-0,00054386	-0,00054386	-0,00057366	0	0	0	0	0	0	0	0	0	0	0	-0,00060345
	22	0	0	0	0	0	0	0	0	0	0	0	0	0	0	0	-0,00054386	-0,00054386	-0,00054386	-0,00057366	0	0	0	0	0	0	0	0	0	0	0	-0,00060591
	23	0	0	0	0	0	0	0	0	0	0	0	0	0	0	0	-0,00054386	-0,00054386	-0,00054386	-0,00057366	0	0	0	0	0	0	0	0	0	0	0	-0,00065368
	24	0	0	0	0	0	0	0	0	0	0	0	0	0	0	0	-0,00054386	-0,00054386	-0,00054386	-0,00057366	0	0	0	0	0	0	0	0	0	0	0	-0,00070702
	25	0	0	0	0	0	0	0	0	0	0	0	0	0	0	0	-0,00054386	-0,00054386	-0,00054386	-0,00057366	0	0	0	0	0	0	0	0	0	0	0	-0,00073716
	26	0	0	0	0	0	0	0	0	0	0	0	0	0	0	0	-0,00054386	-0,00054386	-0,00054386	-0,00057366	0	0	0	0	0	0	0	0	0	0	0	-0,00079155
	27	0	0	0	0	0	0	0	0	0	0	0	0	0	0	0	-0,00054386	-0,00054386	-0,00054386	-0,00057366	0	0	0	0	0	0	0	0	0	0	0	-0,00079328
	28	0	0	0	0	0	0	0	0	0	0	0	0	0	0	0	-0,00054386	-0,00054386	-0,00054386	-0,00057366	0	0	0	0	0	0	0	0	0	0	0	-0,00080613
	29	0	0	0	0	0	0	0	0	0	0	0	0	0	0	0	-0,00054386	-0,00054386	-0,00054386	-0,00057366	0	0	0	0	0	0	0	0	0	0	0	-0,00087818
	30	0	0	0	0	0	0	0	0	0	0	0	0	0	0	0	-0,00054386	-0,00054386	-0,00054386	-0,00057366	0	0	0	0	0	0	0	0	0	0	0	-0,00090933
G5	31	0	0	0	0	0	0	0	0	0	0	0	0	0	0	0	-0,00054386	-0,00054386	-0,00054386	-0,00057366	0	0	0	0	0	0	0	0	0	0	0	-0,00101775

TABLE V. "CICCALENTO" MV LINE ACTIVE POWER SENSITIVITY MATRIX (UNITS [V/W])

Nodes	1	2	3	4	5	6	7	8	9	10	11	12	13	14	15	G1 16	G2 17	G3 18	G4 19	20	21	22	23	24	25	26	27	28	29	30	G5 31
1	0	0	0	0	0	0	0	0	0	0	0	0	0	0	0	-0,00019226	-0,00019226	-0,00019226	-0,00019226	0	0	0	0	0	0	0	0	0	0	0	-0,00019226
2	0	0	0	0	0	0	0	0	0	0	0	0	0	0	0	-0,00021408	-0,00021408	-0,00021408	-0,00021408	0	0	0	0	0	0	0	0	0	0	0	-0,00021408
3	0	0	0	0	0	0	0	0	0	0	0	0	0	0	0	-0,00031908	-0,00031908	-0,00031908	-0,00031908	0	0	0	0	0	0	0	0	0	0	0	-0,00031908
4	0	0	0	0	0	0	0	0	0	0	0	0	0	0	0	-0,00033290	-0,00033290	-0,00033290	-0,00033290	0	0	0	0	0	0	0	0	0	0	0	-0,00033290
5	0	0	0	0	0	0	0	0	0	0	0	0	0	0	0	-0,00046384	-0,00046384	-0,00046384	-0,00046384	0	0	0	0	0	0	0	0	0	0	0	-0,00046384
6	0	0	0	0	0	0	0	0	0	0	0	0	0	0	0	-0,00056361	-0,00056361	-0,00056361	-0,00056361	0	0	0	0	0	0	0	0	0	0	0	-0,00056361
7	0	0	0	0	0	0	0	0	0	0	0	0	0	0	0	-0,00056984	-0,00056984	-0,00056984	-0,00056984	0	0	0	0	0	0	0	0	0	0	0	-0,00056984
8	0	0	0	0	0	0	0	0	0	0	0	0	0	0	0	-0,00073481	-0,00073481	-0,00073481	-0,00073481	0	0	0	0	0	0	0	0	0	0	0	-0,00073481
9	0	0	0	0	0	0	0	0	0	0	0	0	0	0	0	-0,00085633	-0,00085633	-0,00085633	-0,00085633	0	0	0	0	0	0	0	0	0	0	0	-0,00085633
10	0	0	0	0	0	0	0	0	0	0	0	0	0	0	0	-0,00100147	-0,00100147	-0,00100147	-0,00100147	0	0	0	0	0	0	0	0	0	0	0	-0,00100147
11	0	0	0	0	0	0	0	0	0	0	0	0	0	0	0	-0,00100667	-0,00100667	-0,00100667	-0,00100147	0	0	0	0	0	0	0	0	0	0	0	-0,00100147
12	0	0	0	0	0	0	0	0	0	0	0	0	0	0	0	-0,00109091	-0,00109091	-0,00109091	-0,00100147	0	0	0	0	0	0	0	0	0	0	0	-0,00100147
13	0	0	0	0	0	0	0	0	0	0	0	0	0	0	0	-0,00112479	-0,00112479	-0,00112479	-0,00100147	0	0	0	0	0	0	0	0	0	0	0	-0,00100147
14	0	0	0	0	0	0	0	0	0	0	0	0	0	0	0	-0,00112576	-0,00112576	-0,00112576	-0,00100147	0	0	0	0	0	0	0	0	0	0	0	-0,00100147
15	0	0	0	0	0	0	0	0	0	0	0	0	0	0	0	-0,00114142	-0,00114142	-0,00114142	-0,00100147	0	0	0	0	0	0	0	0	0	0	0	-0,00100147
G1 16	0	0	0	0	0	0	0	0	0	0	0	0	0	0	0	-0,00132225	-0,00114142	-0,00114142	-0,00100147	0	0	0	0	0	0	0	0	0	0	0	-0,00100147
G2 17	0	0	0	0	0	0	0	0	0	0	0	0	0	0	0	-0,00114142	-0,00117260	-0,00114142	-0,00100147	0	0	0	0	0	0	0	0	0	0	0	-0,00100147
G3 18	0	0	0	0	0	0	0	0	0	0	0	0	0	0	0	-0,00114142	-0,00114142	-0,00118819	-0,00100147	0	0	0	0	0	0	0	0	0	0	0	-0,00100147
G4 19	0	0	0	0	0	0	0	0	0	0	0	0	0	0	0	-0,00100147	-0,00100147	-0,00100147	-0,00105620	0	0	0	0	0	0	0	0	0	0	0	-0,00105620
20	0	0	0	0	0	0	0	0	0	0	0	0	0	0	0	-0,00100147	-0,00100147	-0,00100147	-0,00105620	0	0	0	0	0	0	0	0	0	0	0	-0,00109847
21	0	0	0	0	0	0	0	0	0	0	0	0	0	0	0	-0,00100147	-0,00100147	-0,00100147	-0,00105620	0	0	0	0	0	0	0	0	0	0	0	-0,00111163
22	0	0	0	0	0	0	0	0	0	0	0	0	0	0	0	-0,00100147	-0,00100147	-0,00100147	-0,00105620	0	0	0	0	0	0	0	0	0	0	0	-0,00111585
23	0	0	0	0	0	0	0	0	0	0	0	0	0	0	0	-0,00100147	-0,00100147	-0,00100147	-0,00105620	0	0	0	0	0	0	0	0	0	0	0	-0,00119927
24	0	0	0	0	0	0	0	0	0	0	0	0	0	0	0	-0,00100147	-0,00100147	-0,00100147	-0,00105620	0	0	0	0	0	0	0	0	0	0	0	-0,00129280
25	0	0	0	0	0	0	0	0	0	0	0	0	0	0	0	-0,00100147	-0,00100147	-0,00100147	-0,00105620	0	0	0	0	0	0	0	0	0	0	0	-0,00134580
26	0	0	0	0	0	0	0	0	0	0	0	0	0	0	0	-0,00100147	-0,00100147	-0,00100147	-0,00105620	0	0	0	0	0	0	0	0	0	0	0	-0,00149096
27	0	0	0	0	0	0	0	0	0	0	0	0	0	0	0	-0,00100147	-0,00100147	-0,00100147	-0,00105620	0	0	0	0	0	0	0	0	0	0	0	-0,00149580
28	0	0	0	0	0	0	0	0	0	0	0	0	0	0	0	-0,00100147	-0,00100147	-0,00100147	-0,00105620	0	0	0	0	0	0	0	0	0	0	0	-0,00152984
29	0	0	0	0	0	0	0	0	0	0	0	0	0	0	0	-0,00100147	-0,00100147	-0,00100147	-0,00105620	0	0	0	0	0	0	0	0	0	0	0	-0,00167458
30	0	0	0	0	0	0	0	0	0	0	0	0	0	0	0	-0,00100147	-0,00100147	-0,00100147	-0,00105620	0	0	0	0	0	0	0	0	0	0	0	-0,00171023
G5 31	0	0	0	0	0	0	0	0	0	0	0	0	0	0	0	-0,00100147	-0,00100147	-0,00100147	-0,00105620	0	0	0	0	0	0	0	0	0	0	0	-0,00186507

TABLE VI. **"CICCALENTO" MV LINE REACTIVE POWER SENSITIVITY TABLE (GENERATORS MINIMUM POWER FACTOR = 0.9, TABLE UNITS [V])**

	Nodes	1	2	3	4	5	6	7	8	9	10	11	12	13	14	15	G1 16	G2 17	G3 18	G4 19	20	21	22	23	24	25	26	27	28	29	30	G5 31
	1	0	0	0	0	0	0	0	0	0	0	0	0	0	0	0	-24,6963	-24,6963	-24,6963	-3,9360	0	0	0	0	0	0	0	0	0	0	0	-20,0851
	2	0	0	0	0	0	0	0	0	0	0	0	0	0	0	0	-26,7723	-26,7723	-26,7723	-4,2668	0	0	0	0	0	0	0	0	0	0	0	-21,7734
	3	0	0	0	0	0	0	0	0	0	0	0	0	0	0	0	-36,5756	-36,5756	-36,5756	-5,8292	0	0	0	0	0	0	0	0	0	0	0	-29,7463
	4	0	0	0	0	0	0	0	0	0	0	0	0	0	0	0	-37,8677	-37,8677	-37,8677	-6,0352	0	0	0	0	0	0	0	0	0	0	0	-30,7971
	5	0	0	0	0	0	0	0	0	0	0	0	0	0	0	0	-53,2582	-53,2582	-53,2582	-8,4880	0	0	0	0	0	0	0	0	0	0	0	-43,3139
	6	0	0	0	0	0	0	0	0	0	0	0	0	0	0	0	-64,9979	-64,9979	-64,9979	-10,3590	0	0	0	0	0	0	0	0	0	0	0	-52,8616
	7	0	0	0	0	0	0	0	0	0	0	0	0	0	0	0	-65,7138	-65,7138	-65,7138	-10,4731	0	0	0	0	0	0	0	0	0	0	0	-53,4438
	8	0	0	0	0	0	0	0	0	0	0	0	0	0	0	0	-91,7416	-91,7416	-91,7416	-14,6213	0	0	0	0	0	0	0	0	0	0	0	-74,6117
	9	0	0	0	0	0	0	0	0	0	0	0	0	0	0	0	-101,1476	-101,1476	-101,1476	-16,1204	0	0	0	0	0	0	0	0	0	0	0	-82,2615
	10	0	0	0	0	0	0	0	0	0	0	0	0	0	0	0	-112,3863	-112,3863	-112,3863	-17,9116	0	0	0	0	0	0	0	0	0	0	0	-91,4017
	11	0	0	0	0	0	0	0	0	0	0	0	0	0	0	0	-112,6010	-112,6010	-112,6010	-17,9116	0	0	0	0	0	0	0	0	0	0	0	-91,4017
	12	0	0	0	0	0	0	0	0	0	0	0	0	0	0	0	-119,1133	-119,1133	-119,1133	-17,9116	0	0	0	0	0	0	0	0	0	0	0	-91,4017
	13	0	0	0	0	0	0	0	0	0	0	0	0	0	0	0	-122,8375	-122,8375	-122,8375	-17,9116	0	0	0	0	0	0	0	0	0	0	0	-91,4017
	14	0	0	0	0	0	0	0	0	0	0	0	0	0	0	0	-122,9091	-122,9091	-122,9091	-17,9116	0	0	0	0	0	0	0	0	0	0	0	-91,4017
	15	0	0	0	0	0	0	0	0	0	0	0	0	0	0	0	-124,1260	-124,1260	-124,1260	-17,9116	0	0	0	0	0	0	0	0	0	0	0	-91,4017
G1	16	0	0	0	0	0	0	0	0	0	0	0	0	0	0	0	-145,3863	-124,1260	-124,1260	-17,9116	0	0	0	0	0	0	0	0	0	0	0	-91,4017
G2	17	0	0	0	0	0	0	0	0	0	0	0	0	0	0	0	-124,1260	-127,7768	-124,1260	-17,9116	0	0	0	0	0	0	0	0	0	0	0	-91,4017
G3	18	0	0	0	0	0	0	0	0	0	0	0	0	0	0	0	-124,1260	-124,1260	-128,2778	-17,9116	0	0	0	0	0	0	0	0	0	0	0	-91,4017
G4	19	0	0	0	0	0	0	0	0	0	0	0	0	0	0	0	-112,3863	-112,3863	-112,3863	-18,8927	0	0	0	0	0	0	0	0	0	0	0	-96,4084
	20	0	0	0	0	0	0	0	0	0	0	0	0	0	0	0	-112,3863	-112,3863	-112,3863	-18,8927	0	0	0	0	0	0	0	0	0	0	0	-100,1925
	21	0	0	0	0	0	0	0	0	0	0	0	0	0	0	0	-112,3863	-112,3863	-112,3863	-18,8927	0	0	0	0	0	0	0	0	0	0	0	-101,4151
	22	0	0	0	0	0	0	0	0	0	0	0	0	0	0	0	-112,3863	-112,3863	-112,3863	-18,8927	0	0	0	0	0	0	0	0	0	0	0	-101,8284
	23	0	0	0	0	0	0	0	0	0	0	0	0	0	0	0	-112,3863	-112,3863	-112,3863	-18,8927	0	0	0	0	0	0	0	0	0	0	0	-109,8566
	24	0	0	0	0	0	0	0	0	0	0	0	0	0	0	0	-112,3863	-112,3863	-112,3863	-18,8927	0	0	0	0	0	0	0	0	0	0	0	-118,8221
	25	0	0	0	0	0	0	0	0	0	0	0	0	0	0	0	-112,3863	-112,3863	-112,3863	-18,8927	0	0	0	0	0	0	0	0	0	0	0	-123,8871
	26	0	0	0	0	0	0	0	0	0	0	0	0	0	0	0	-112,3863	-112,3863	-112,3863	-18,8927	0	0	0	0	0	0	0	0	0	0	0	-133,0272
	27	0	0	0	0	0	0	0	0	0	0	0	0	0	0	0	-112,3863	-112,3863	-112,3863	-18,8927	0	0	0	0	0	0	0	0	0	0	0	-133,3183
	28	0	0	0	0	0	0	0	0	0	0	0	0	0	0	0	-112,3863	-112,3863	-112,3863	-18,8927	0	0	0	0	0	0	0	0	0	0	0	-135,4782
	29	0	0	0	0	0	0	0	0	0	0	0	0	0	0	0	-112,3863	-112,3863	-112,3863	-18,8927	0	0	0	0	0	0	0	0	0	0	0	-147,5875
	30	0	0	0	0	0	0	0	0	0	0	0	0	0	0	0	-112,3863	-112,3863	-112,3863	-18,8927	0	0	0	0	0	0	0	0	0	0	0	-152,8212
G5	31	0	0	0	0	0	0	0	0	0	0	0	0	0	0	0	-112,3863	-112,3863	-112,3863	-18,8927	0	0	0	0	0	0	0	0	0	0	0	-171,0433

TABLE VII. "CICCALENTO" MV LINE REACTIVE POWER SENSITIVITY TABLE (GENERATORS MINIMUM POWER FACTOR = 0.9, TABLE UNITS [VOLTAGE P.U.])

	Nodes	1	2	3	4	5	6	7	8	9	10	11	12	13	14	15	G1 16	G2 17	G3 18	G4 19	20	21	22	23	24	25	26	27	28	29	30	G5 31
	1	0	0	0	0	0	0	0	0	0	0	0	0	0	0	0	-0,0021	-0,0021	-0,0021	-0,0003	0	0	0	0	0	0	0	0	0	0	0	-0,0017
	2	0	0	0	0	0	0	0	0	0	0	0	0	0	0	0	-0,0023	-0,0023	-0,0023	-0,0004	0	0	0	0	0	0	0	0	0	0	0	-0,0019
	3	0	0	0	0	0	0	0	0	0	0	0	0	0	0	0	-0,0032	-0,0032	-0,0032	-0,0005	0	0	0	0	0	0	0	0	0	0	0	-0,0026
	4	0	0	0	0	0	0	0	0	0	0	0	0	0	0	0	-0,0033	-0,0033	-0,0033	-0,0005	0	0	0	0	0	0	0	0	0	0	0	-0,0027
	5	0	0	0	0	0	0	0	0	0	0	0	0	0	0	0	-0,0046	-0,0046	-0,0046	-0,0007	0	0	0	0	0	0	0	0	0	0	0	-0,0038
	6	0	0	0	0	0	0	0	0	0	0	0	0	0	0	0	-0,0056	-0,0056	-0,0056	-0,0009	0	0	0	0	0	0	0	0	0	0	0	-0,0046
	7	0	0	0	0	0	0	0	0	0	0	0	0	0	0	0	-0,0057	-0,0057	-0,0057	-0,0009	0	0	0	0	0	0	0	0	0	0	0	-0,0046
	8	0	0	0	0	0	0	0	0	0	0	0	0	0	0	0	-0,0079	-0,0079	-0,0079	-0,0013	0	0	0	0	0	0	0	0	0	0	0	-0,0065
	9	0	0	0	0	0	0	0	0	0	0	0	0	0	0	0	-0,0088	-0,0088	-0,0088	-0,0014	0	0	0	0	0	0	0	0	0	0	0	-0,0071
	10	0	0	0	0	0	0	0	0	0	0	0	0	0	0	0	-0,0097	-0,0097	-0,0097	-0,0016	0	0	0	0	0	0	0	0	0	0	0	-0,0079
	11	0	0	0	0	0	0	0	0	0	0	0	0	0	0	0	-0,0098	-0,0098	-0,0098	-0,0016	0	0	0	0	0	0	0	0	0	0	0	-0,0079
	12	0	0	0	0	0	0	0	0	0	0	0	0	0	0	0	-0,0103	-0,0103	-0,0103	-0,0016	0	0	0	0	0	0	0	0	0	0	0	-0,0079
	13	0	0	0	0	0	0	0	0	0	0	0	0	0	0	0	-0,0106	-0,0106	-0,0106	-0,0016	0	0	0	0	0	0	0	0	0	0	0	-0,0079
	14	0	0	0	0	0	0	0	0	0	0	0	0	0	0	0	-0,0106	-0,0106	-0,0106	-0,0016	0	0	0	0	0	0	0	0	0	0	0	-0,0079
	15	0	0	0	0	0	0	0	0	0	0	0	0	0	0	0	-0,0107	-0,0107	-0,0107	-0,0016	0	0	0	0	0	0	0	0	0	0	0	-0,0079
G1	16	0	0	0	0	0	0	0	0	0	0	0	0	0	0	0	-0,0126	-0,0107	-0,0107	-0,0016	0	0	0	0	0	0	0	0	0	0	0	-0,0079
G2	17	0	0	0	0	0	0	0	0	0	0	0	0	0	0	0	-0,0107	-0,0111	-0,0107	-0,0016	0	0	0	0	0	0	0	0	0	0	0	-0,0079
G3	18	0	0	0	0	0	0	0	0	0	0	0	0	0	0	0	-0,0107	-0,0107	-0,0111	-0,0016	0	0	0	0	0	0	0	0	0	0	0	-0,0079
G4	19	0	0	0	0	0	0	0	0	0	0	0	0	0	0	0	-0,0097	-0,0097	-0,0097	-0,0016	0	0	0	0	0	0	0	0	0	0	0	-0,0083
	20	0	0	0	0	0	0	0	0	0	0	0	0	0	0	0	-0,0097	-0,0097	-0,0097	-0,0016	0	0	0	0	0	0	0	0	0	0	0	-0,0087
	21	0	0	0	0	0	0	0	0	0	0	0	0	0	0	0	-0,0097	-0,0097	-0,0097	-0,0016	0	0	0	0	0	0	0	0	0	0	0	-0,0088
	22	0	0	0	0	0	0	0	0	0	0	0	0	0	0	0	-0,0097	-0,0097	-0,0097	-0,0016	0	0	0	0	0	0	0	0	0	0	0	-0,0088
	23	0	0	0	0	0	0	0	0	0	0	0	0	0	0	0	-0,0097	-0,0097	-0,0097	-0,0016	0	0	0	0	0	0	0	0	0	0	0	-0,0095
	24	0	0	0	0	0	0	0	0	0	0	0	0	0	0	0	-0,0097	-0,0097	-0,0097	-0,0016	0	0	0	0	0	0	0	0	0	0	0	-0,0103
	25	0	0	0	0	0	0	0	0	0	0	0	0	0	0	0	-0,0097	-0,0097	-0,0097	-0,0016	0	0	0	0	0	0	0	0	0	0	0	-0,0107
	26	0	0	0	0	0	0	0	0	0	0	0	0	0	0	0	-0,0097	-0,0097	-0,0097	-0,0016	0	0	0	0	0	0	0	0	0	0	0	-0,0115
	27	0	0	0	0	0	0	0	0	0	0	0	0	0	0	0	-0,0097	-0,0097	-0,0097	-0,0016	0	0	0	0	0	0	0	0	0	0	0	-0,0115
	28	0	0	0	0	0	0	0	0	0	0	0	0	0	0	0	-0,0097	-0,0097	-0,0097	-0,0016	0	0	0	0	0	0	0	0	0	0	0	-0,0117
	29	0	0	0	0	0	0	0	0	0	0	0	0	0	0	0	-0,0097	-0,0097	-0,0097	-0,0016	0	0	0	0	0	0	0	0	0	0	0	-0,0128
	30	0	0	0	0	0	0	0	0	0	0	0	0	0	0	0	-0,0097	-0,0097	-0,0097	-0,0016	0	0	0	0	0	0	0	0	0	0	0	-0,0132
G5	31	0	0	0	0	0	0	0	0	0	0	0	0	0	0	0	-0,0097	-0,0097	-0,0097	-0,0016	0	0	0	0	0	0	0	0	0	0	0	-0,0148

4.3.4 Generators characteristics

In this paragraph generators characteristics will be presented. Table VIII summarizes the generators characteristics.

In terms of active power, each generator follows a daily profile. In particular:

- for solar generators, the active power profile is like a Gaussian curve
- for the wind generator, the active power profile is periodically modulated. The modulation period is 30 minutes, and the modulation amplitude is $0 \div -40$ % of the nominal power.

Daily profiles curves will be presented in Chapter 5.

Generators PQ regulators, in RTDS, are contained in the block "P, Q reg." (see Canvas 2 and 3 at the end of this chapter).

TABLE VIII.   GENERATORS CHARACTERISTICS

Generator name	Nominal active power [kW]	Primary energy type	Minimum power factor	Regulation type
G1	1000	Solar	0.9 (ind/cap)	PQ
G2	1000	Solar	0.9 (ind/cap)	PQ
G3	1000	Solar	0.9 (ind/cap)	PQ
G4	160	Solar	0.9 (ind/cap)	PQ
G5	814	Wind	0.9 (ind/cap)	PQ

4.3.5 Generators UPG and RQV local voltage regulation settings

All generators are equipped with both UPG and RQV local voltage regulation system (see Chapter 2. UPG settings are presented in Table IX and RQV settings are summarized in Table X.

The RTDS UPG and RQV models are contained, respectively, in the blocks "UPG" and "Q(V)" (see Canvas 2 and 3 at the end of this chapter).

TABLE IX.   UPG SETTINGS

Parameter name	Units	Value
$V_{1S\text{-}UPG}$	p.u.	1.04
$T_{1S\text{-}UPG}$	s	30
$V_{2S\text{-}UPG}$	p.u.	1.07
$T_{2S\text{-}UPG}$	s	30
$V_{1S\text{-}VCS}$	p.u.	1.06
$T_{1S\text{-}VCS}$	s	30
$V_{2S\text{-}VCS}$	p.u.	1.09
$T_{2S\text{-}VCS}$	s	30
$V_{1I\text{-}UPG}$	p.u.	0.96
$T_{1I\text{-}UPG}$	s	30
$V_{2I\text{-}UPG}$	p.u.	0.93
$T_{2I\text{-}UPG}$	s	30
$V_{1I\text{-}VCS}$	p.u.	0.94
$T_{1I\text{-}VCS}$	s	30
$V_{2I\text{-}VCS}$	p.u.	0.91
$T_{2I\text{-}VCS}$	s	30
Inductive power factor in RAM	-	0.9
Inductive power factor in RGM	-	0.9
Lock-in active power	% of A_n	5
Lock-out active power	% of A_n	4.5

<div align="center">**TABLE X. RQV SETTINGS**</div>

Parameter name	Units	Value
V_{1S}	p.u.	1.04
Q_{1S}	kVAr	0
V_{2S}	p.u.	1.09
Q_{2S}	kVAr	$+A_n \sin \varphi_g^*$
V_{1I}	p.u.	0.96
Q_{1I}	kVAr	0
V_{2I}	p.u.	0.91
Q_{2I}	kVAr	$-A_n \sin \varphi_g^*$
Voltage hysteresis ε_{V_MT}	% of V_n	1
Time period T_{cycle}	ms	200
Lock-in active power	% of A_n	5
Lock-out active power	% of A_n	4.5

4.3.6 Loads characteristics

Load (P and Q) daily profiles have been extracted by the Enel Distribuzione Distribution Management System (DMS) database. These curves are built using the Enel Automatic Metering Management (AMM) system which read electronic power meters installed at the customers delivery point. The active and reactive power daily profile is generated using a "load profiler", programmed for this PhD work, which reads the DMS database curves and reproduces them in the RTDS software environment. The load profiler, represented in Fig. 4.3-5, is contained in the "Load Profiler" block.

In order to show the loads daily profile, avoiding the presentation of each load daily profile, the active power at some line section is presented. In particular:

- Fig. 4.3-6 represents the active power a the "Fornovecchio" section
- Fig. 4.3-7 represents the active power a the "Caccavelli" section
- Fig. 4.3-8 represents the active power a the "MM694" section
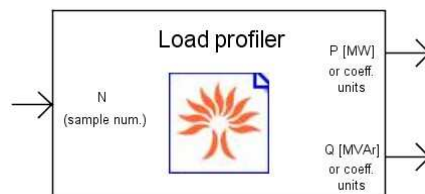
Fig. 4.3-5.   Load profiler RTDS block.
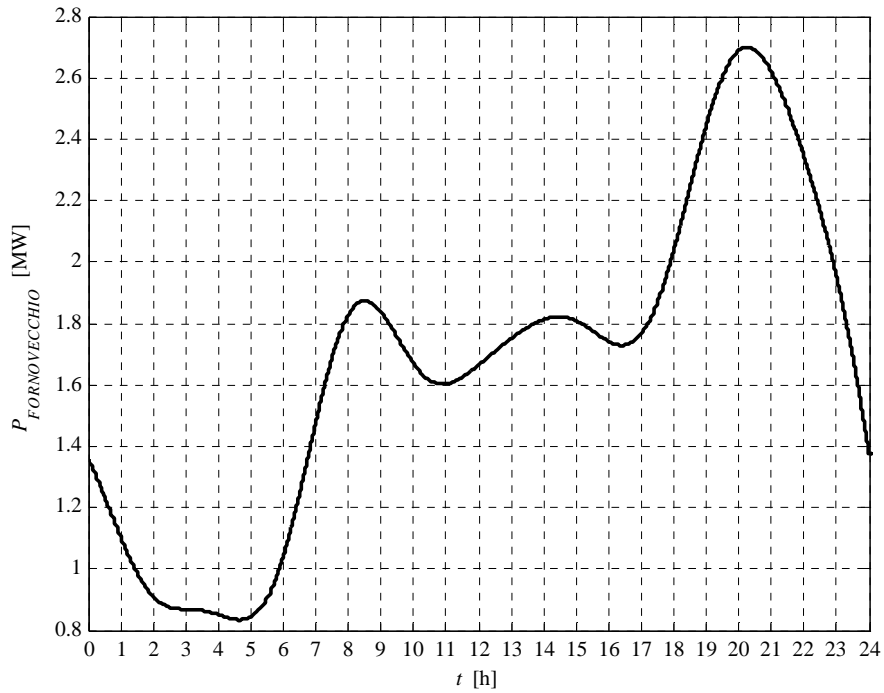
Fig. 4.3-6. **"Fornovecchio" section active power daily profile.**
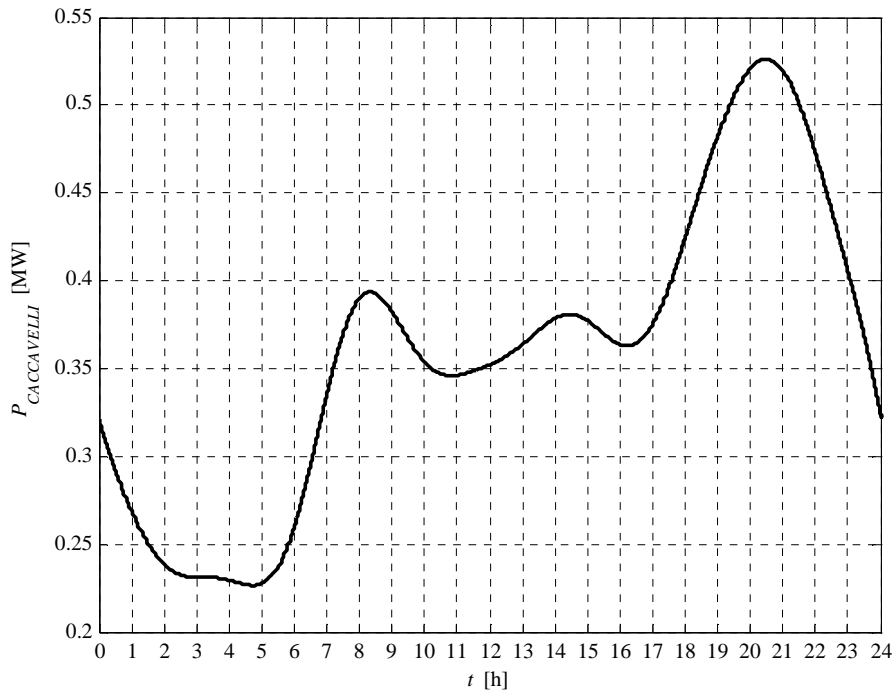
Fig. 4.3-7. **"Caccavelli" section active power daily profile.**
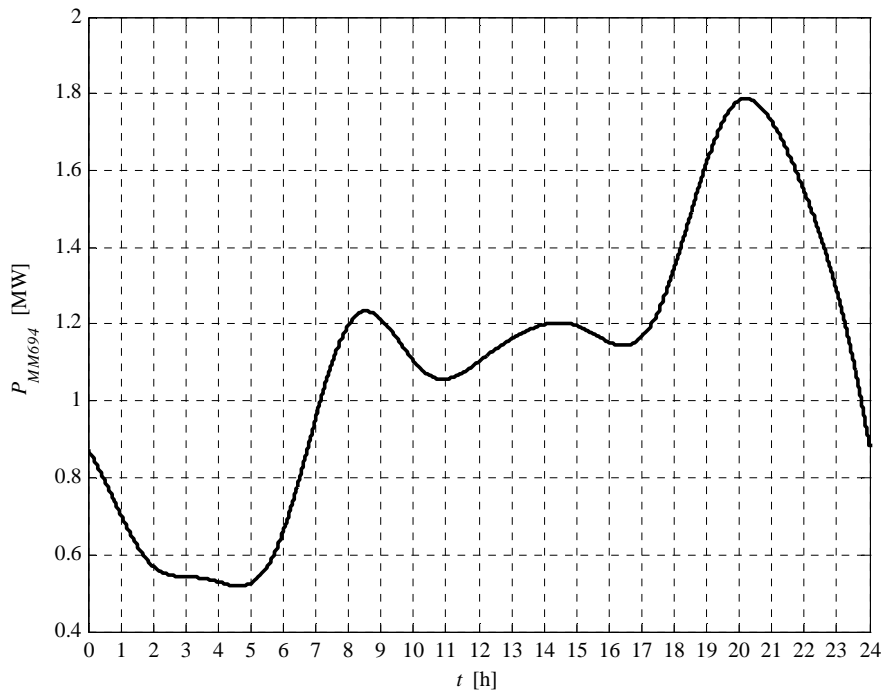
Fig. 4.3-8. "MM694" section active power daily profile.

Load reactive power daily profiles are very similar, in terms of shape, to the active power because loads can be represented using a constant power factor.

4.4 REFERENCES

[1] T. Maguire, J. Giesbrecht "Small Time-step ($< 2\mu Sec$) VSC Model for the Real Time Digital Simulator," presented at Int. Conf. on Power Systems Transients (IPST'05) in Montreal, Canada 2005.

[2] M. Brenna, E. De Berardinis, L. Delli Carpini, P. Paulon, P. Petroni, G. Sapienza, G. Scrosati, D. Zaninelli, "Petersen Coil Regulators Analysis using a Real-Time Digital Simulator", Power Delivery, IEEE Transactions on, Issue Date: July 2011, Volume: 26 Issue: 3, On page(s): 1479 – 1488.

[3] M. Brenna, E. De Berardinis, L. Delli Carpini, P. Paulon, P. Petroni, G. Sapienza, G. Scrosati, D. Zaninelli, "Real Time Simulation of Smart Grids for Interface Protection Test and Analysis", Harmonics and Quality of Power (ICHQP), 2010 14th International Conference on, Issue Date: 26-29 Sept. 2010, On page(s): 1 – 6.

[4] C. Noce, E. De Berardinis, G. Sapienza, G. Scrosati, L. Delli Carpini, P. Paulon, R. Calone "Smart grids: preliminary MV network model using real time digital simulator and real devices in a closed loop control," presented at 20th Int. Conf. on Electricity Distribution CIRED, Prague, Czech Republic, 2009.

[5] X. Mamo, M. McGranaghan, R. Dugan, J. Maire, O. Devaux, "A roadmap for developing real time distribution system simulation tools for the smart grid," SmartGrids for Distribution, 2008. IET-CIRED. Year: 2008 , Page(s): 1 – 7.

[6] A. Saran, S.K. Palla, A.K. Srivastava, N.N. Schulz, "Real time power system simulation using RTDS and NI PXI," Power Symposium, 2008. NAPS '08. 40th North American, 2008, Page(s): 1 – 6.

[7] C.H. Jung, H.S. Jung, J.O. Kim, "Dynamic characteristic test of protective relay for double circuit using real time digital simulator (RTDS)," Power System Technology, 2000, Page(s): 1461 - 1464 vol.3.

[8] L.H. Tsoukalas, R. Gao, "From smart grids to an energy internet: Assumptions, architectures and requirements," Electric Utility Deregulation and Restructuring and Power Technologies, 2008. Publication Year: 2008 , Page(s): 94 – 98.

[9] A. Chuang, M. McGranaghan, "Functions of a local controller to coordinate distributed resources in a smart grid," Power and Energy Society General Meeting - Conversion and Delivery of Electrical Energy in the 21st Century, 2008 IEEE, Publication Year: 2008 , Page(s): 1 – 6.

[10] P.M. Anderson, "Power System Protection," IEEE Press, Piscataway, NJ, 1999.

[11] B. Ceresoli, A. Cerretti, E. De Berardinis, A. Gallerani, P. Perna, G. Valtorta, "Neutral connection to earth in medium voltage networks: operation experience in Enel," presented at 16th Int. Conf. on Electricity Distribution CIRED, 2001, (IEE Conf. Publ. No. 482) Volume Summaries, 2001 Page(s):192 – 192.

[12] *IEEE Guide for Power System Protection Testing*, IEEE Standard C37.233-2009.

[13] R. Marconato, "Electric Power Systems Vol. II" CEI, Milano, 2008.

[14] ENEL (Italian Distributor) document DK4451 "Protection criteria for MV distribution networks", 2005.

[15] D. Griffel, V. Leitloff, Y. Harmand, J. Bergeal, "A New Deal for Safety and Quality on MV Networks", Power Delivery, IEEE Transactions on Volume: 12, Issue: 4, Oct. 1997, Pages: 1428 – 1433.

[16] L. Hongbo, T. Weipu, L. Wenfeng, Y. Yihan, "Research on a New Compensation Mode in MV Power Network", presented at Power Systems Conf. and Exposition, 2004.

[17] A. Cerretti, F.M. Gatta, A. Geri, S. Lauria, M. Maccioni, G. Valtorta, "Temporary overvoltages due to ground faults in MV networks," *2009 IEEE Bucharest Power Tech Conf.,* Bucharest, Romania.

[18] *IEEE Guide for the Application of Neutral Grounding in Electrical Utility Systems, Part I – Introduction*, IEEE Standard C62.92.1-2000, Sept. 2000.

[19] *IEEE Guide for the Application of Neutral Grounding in Electrical Utility Systems, Part IV – Distribution*, IEEE Standard C62.92.4-1991, Dec. 1992.

[20] E. Clarke, Circuit Analysis of AC Power Systems, vol. I, II. New York: Wiley, 1950.

[21] S. Conti, L. Raffa, U. Vagliasindi, "Innovative solutions for protection schemes in autonomous MV micro-grids", International Conference on Clean Electrical Power, ICCEP 2009, Pages: 647 – 654.

[22] G. Druml, A. Kugi, B. Parr, "Control of Petersen Coils," XI. International Symposium on Theoretical Electrical Engineering August / 2001.

RTDS Technologies

File: CP SG Rotondo
Created: Dec 20, 2010 (aedd513)
Last Modified: Feb 12, 2012 (Gianlu)
Printed On: Feb 12, 2012

Enel Distribuzione

Ciccalento MV Line

Canvas N°1: Line part N°1
Subsystem #1 of 3

RTDS Technologies

Enel Distribuzione

File: CP SG Rotondo
Created: Dec 20, 2010 (aedd513)
Last Modified: Feb 12, 2012 (Gianlu)
Printed On: Feb 12, 2012

Ciccalento MV Line

Canvas N°2: Line part N°2
Subsystem #2 of 3

From SS 3 Ciccalento Line

Enel Distribuzione
Centro Prove Enel
Milano

Sensitivity Matrix/Table
node number
19

Positive sequence
line capacity at the line terminal

Total power and
losses calculation

Reactor bank used to completely
compensate the line capacity increased
in order to force
Tsteout Time = Time Step
The L calculation is at Time Step =100us
See the .map file to know the
increased line capacity

Generator G4: TERENZIO M

Profiler
Load

RISC
Dynamic Load (R/L)
TERENZIOM

| P, Q reg. G4 | LPG G4 | Q(V) G4 |

Sensitivity Matrix/Table
node number
20

Load Profiler

Sensitivity Matrix/Table
node number
21

Load Profiler

Load Profiler

CS VILLANOVA

Sensitivity Matrix/Table
node number
22

Load Profiler

CS SERRILLI2

Load Profiler

SERRILIUM
Dynamic Load (R/L)
RISC

Sensitivity Matrix/Table
node number
23

RISC
End #1   End #2
PI
SECTION
Name = AE60G2m

Sensitivity Matrix/Table
node number
24

RISC
Dynamic Load (R/L)
SERRILIUM

Load Profiler

Sensitivity Matrix/Table
node number
25

RISC
Dynamic Load (R/L)
VILLANOVA

Load Profiler

Sensitivity Matrix/Table
node number
26

RISC
Dynamic Load (R/L)
EO2

Load Profiler

Sensitivity Matrix/Table
node number
27

IMS PESCOROS

Sensitivity Matrix/Table
node number
28

RISC
Dynamic Load (R/L)
EO039

Load Profiler

Sensitivity Matrix/Table
node number
29

RISC
Dynamic Load (R/L)
EO2

Load Profiler

Sensitivity Matrix/Table
node number
30

RISC
PI
SECTION
Name = MM6127

RISC
Dynamic Load (R/L)
PAULITELLI2

Load Profiler

Sensitivity Matrix/Table
node number
31

RISC
Dynamic Load (R/L)
MARTESSERV

Generator G5: 238M1

| P, Q reg. G5 | LPG G5 | Q(V) G5 |

RTDS Technologies

Enel Distribuzione

File: CP SG Rotondo
Created: Dec 20, 2010 (aedd513)
Last Modified: Feb 12, 2012 (Gianlu)
Printed On: Feb 12, 2012

Ciccalento MV Line

Canvas N°3: Line part N°3
Subsystem #3 of 3

Chapter 5

Real-Time Digital Simulator Tests Results

5.1 INTRODUCTION TO CHAPTER 5

In this chapter tests results, performed using the Real-Time Digital Simulator (RTDS)[11] are presented. Tests are performed in order to:

- analyze the voltage regulation efficiency
- calculate the MV grid hosting capacity increment
- evaluate the active energy losses

In order to satisfy this concepts, tests are arranged in this order:

1. base case
   a. no distributed generation and MV busbar voltage fixed to 1.06 p.u., which is the voltage that guarantee the correct voltage in the critical node in the maximum load time
   b. distributed generation enabled, without local and centralized voltage regulation[12]. MV busbar voltage fixed to 1.06 p.u., which is the voltage that guarantee the correct voltage in the critical node in the maximum load time
2. "UPG" local voltage regulation tests: distributed generation enabled, with "UPG" local voltage regulation. MV busbar voltage fixed to 1.06 p.u., which is the voltage that guarantee the correct voltage in the critical node in the maximum load time
3. "RQV" local voltage regulation tests: distributed generation enabled, with "RQV" local voltage regulation. MV busbar voltage fixed to 1.06 p.u., which is the voltage that guarantee the correct voltage in the critical node in the maximum load time
4. hosting capacity increment tests with local voltage control only:
   a. with "UPG" local voltage regulation. MV busbar voltage fixed to 1.06 p.u., which is the voltage that guarantee the correct voltage in the critical node in the maximum load time
   b. with "RQV" local voltage regulation. MV busbar voltage fixed to 1.06 p.u., which is the voltage that guarantee the correct voltage in the critical node in the maximum load time

---

[11] The RTDS is installed in the "Centro Prove Enel (Enel Test Center), Via Rubattino 84, Milano, 20134, Italy"

[12] The DG power profiles has been described in Chapter 4

5. hosting capacity increment tests with both local and MV busbar voltage control:
   a. with "UPG" local voltage regulation. MV busbar voltage regulated in order to daily guarantee the correct voltage in the critical node
   b. with "RQV" local voltage regulation. MV busbar voltage regulated in order to daily guarantee the correct voltage in the critical node
6. Centralized Voltage Control tests

Electrical quantities plotted for the study cases[13] are summarized in Table XI.

TABLE XI. ELECTRICAL QUANTITIES PLOTTED FOR THE STUDY CASES

Electrical quantity	Description	Notes
V_{Gi}	Generator voltage	i is the generator number; p.u. are referred to the rated voltage
$P_{m,Gi}$	Generator active power	Positive when generated; i is the generator number
$Q_{m,Gi}$	Generator reactive power	Positive when generated; i is the generator number
P_{TR}	HV/MV transformer active power	Positive when power flows to the MV grid
Q_{TR}	HV/MV transformer reactive power	Positive when power flows to the MV grid
P_{pMV}	MV grid lost power	-

For each study case the test report will be presented. Table XII summarizes the report structure.

TABLE XII. REPORT STRUCTURE SUMMARIZATION

Report quantity	Description
Maximum VGi value	Maximum generator voltage; i is the generator number
Loads power daily peak	Is the peak of the loads sum active power (daily profile)
Generators power daily peak	Is the peak of the generators sum active power (daily profile)
Loads daily active energy (absorbed)	Is the daily energy absorbed by the loads
Generators daily active energy (generated)	Is the daily generated energy
Daily active energy absorbed from the HV grid	Is the daily energy absorbed from the HV grid

---

[13] For each study, only electrical quantities which are taken into account in the study will be plotted.

Daily lost active energy	Is the daily MV grid lost energy
Daily lost active energy (percentual)	Is the daily MV grid lost percentual energy. Is calculated dividing energy losses by the total absorbed energy, which is the sum of the "daily energy absorbed from the HV grid" and the "daily generated energy"

5.2 CASE 1.A RESULTS

This is the base case without distributed generation and MV busbar voltage fixed to 1.06 p.u. This set-point value guarantees the correct voltage in the critical node in the maximum load condition.
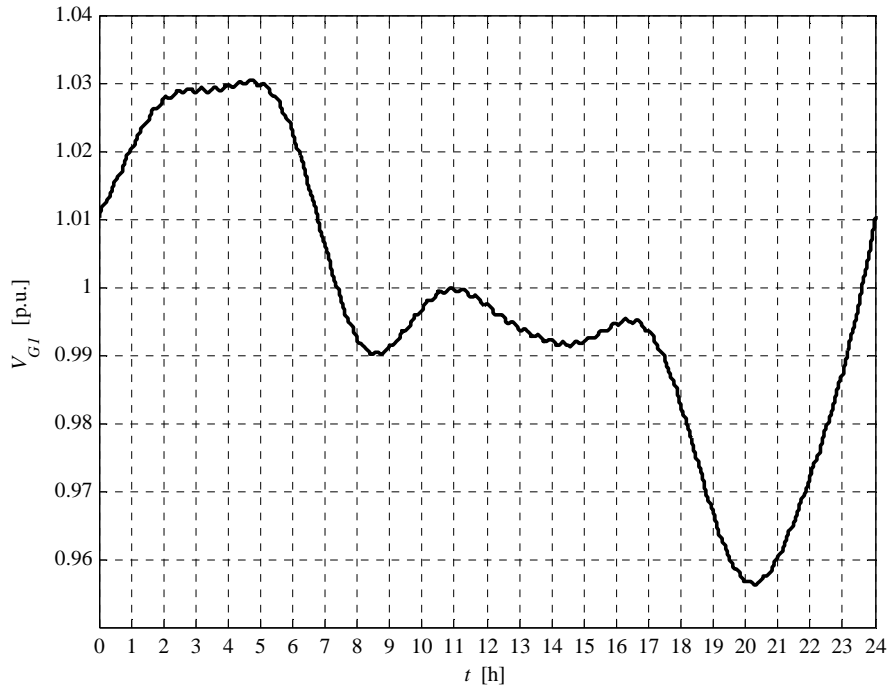
Fig. 5.2-1. G1 voltage daily profile
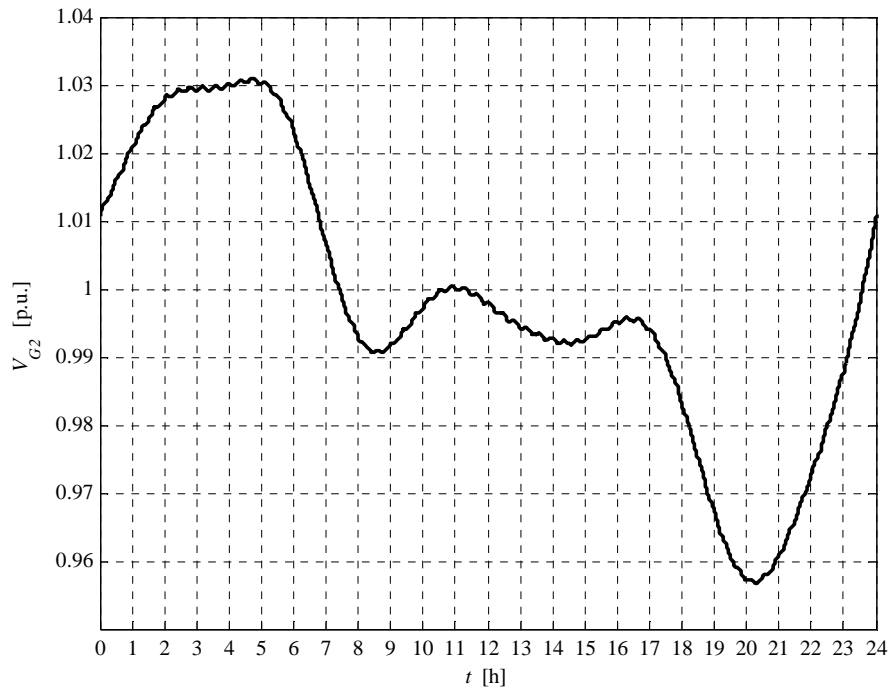
Fig. 5.2-2. G2 voltage daily profile
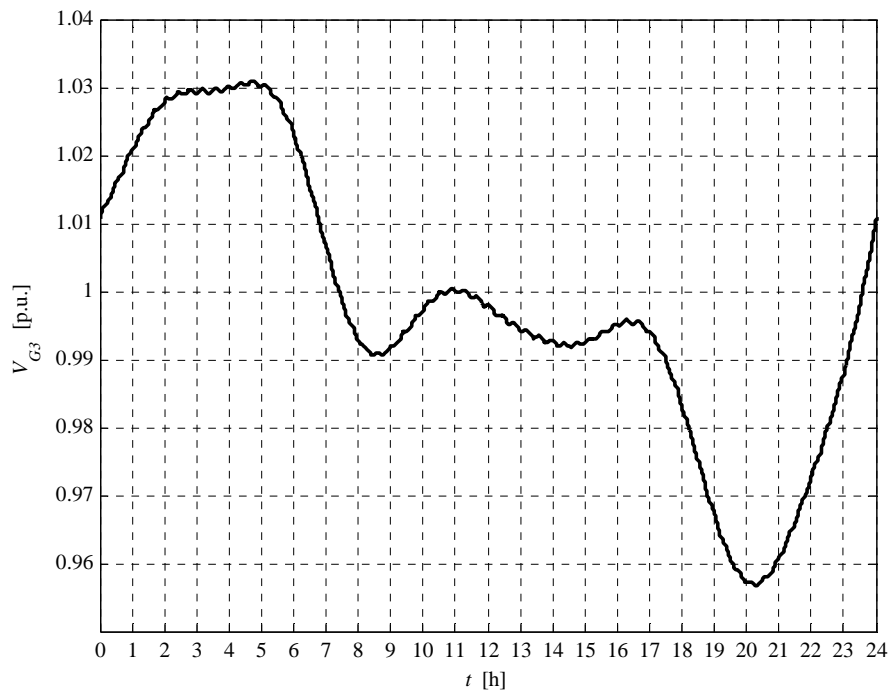
Fig. 5.2-3. G3 voltage daily profile
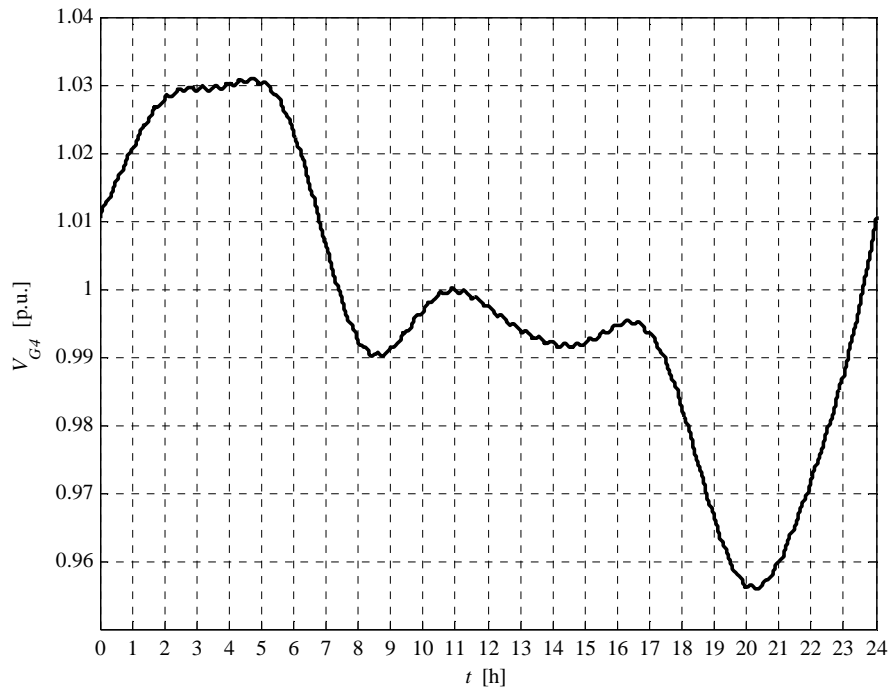
Fig. 5.2-4. G4 voltage daily profile
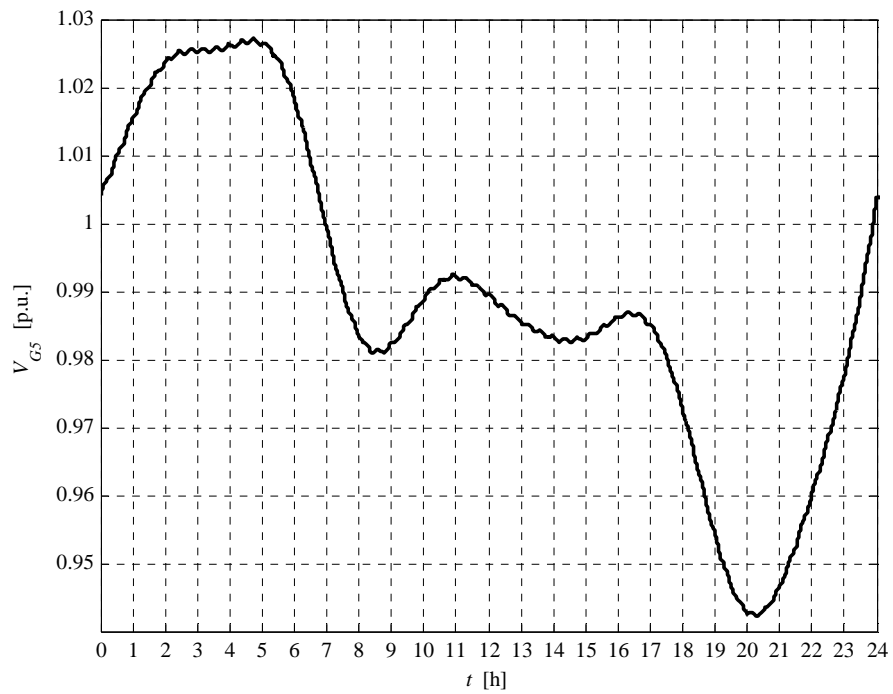
Fig. 5.2-5. G5 voltage daily profile

90
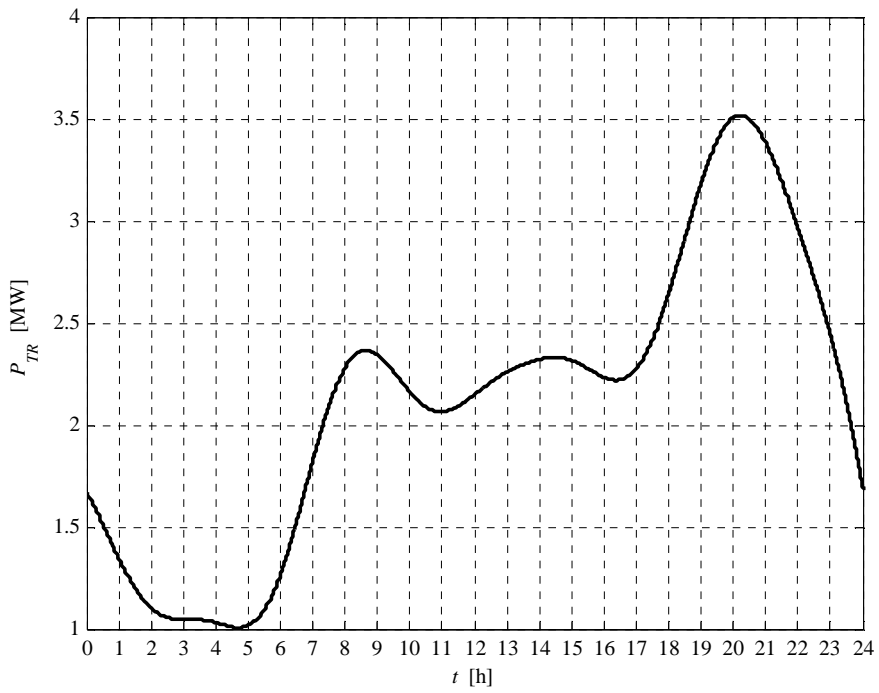
Fig. 5.2-6. HV/MV transformer daily active power profile
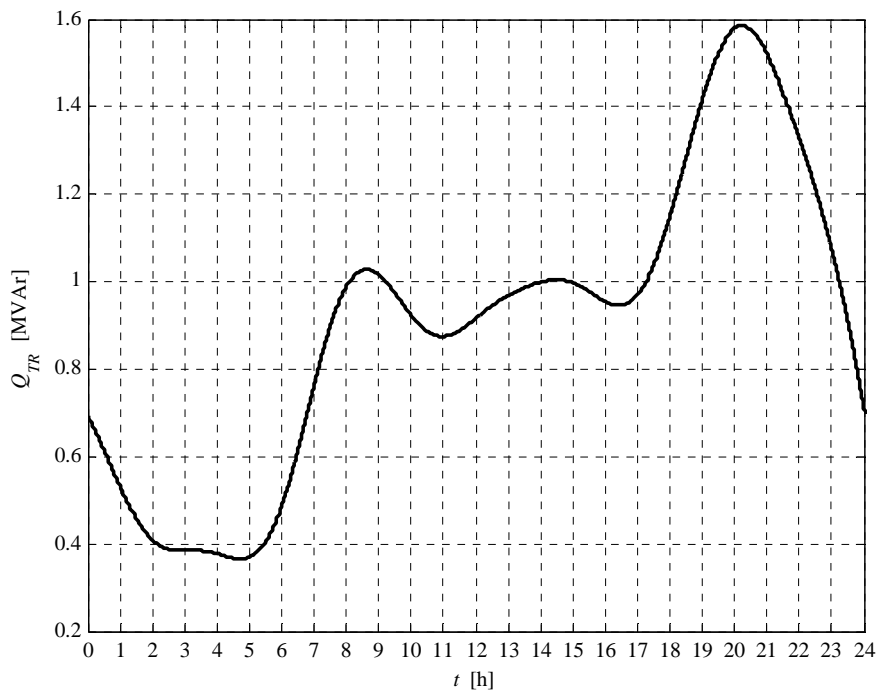
Fig. 5.2-7. HV/MV transformer daily reactive power profile
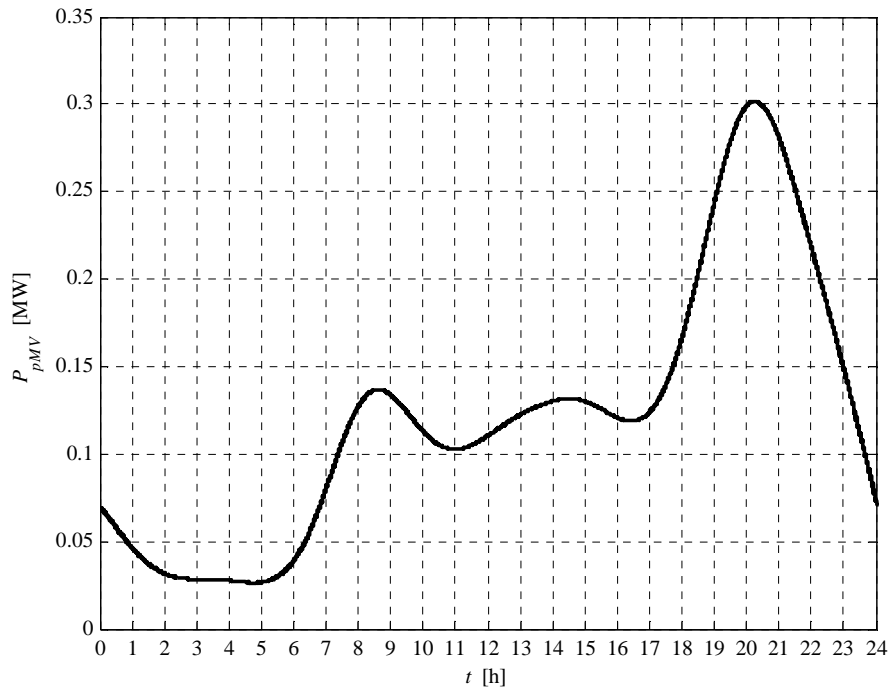
Fig. 5.2-8. MV grid daily active power losses profile

All of the voltage daily profiles are good. The active power trough the HV/MV transformer is correctly always positive, as well as the reactive one. The power losses peak corresponds to the load power peak.

The report, referred to this case, is:

```
Report case: 1.a

Maximum VG1 value = 1.0305 [p.u.]
Maximum VG2 value = 1.0310 [p.u.]
Maximum VG3 value = 1.0310 [p.u.]
Maximum VG4 value = 1.0310 [p.u.]
Maximum VG5 value = 1.0272 [p.u.]

Loads power daily peak = 3.2157 [MW]
Generators power daily peak = 0.0000 [MW]

Loads daily active energy (absorbed) = 49.2306 [MWh]
Generators daily active energy (generated) = 0.0000 [MWh]
Daily active energy absorbed from the HV grid = 52.2159 [MWh]
Daily lost active energy = 2.9853 [MWh]
Daily lost active energy (percentual) = 5.7172 [%]
```

5.3 CASE 1.B RESULTS

This is the base case with distributed generation. The MV busbar voltage is fixed to 1.06 p.u. This set-point value guarantees the correct voltage in the critical node in the maximum load condition, when the generation is de-activated.
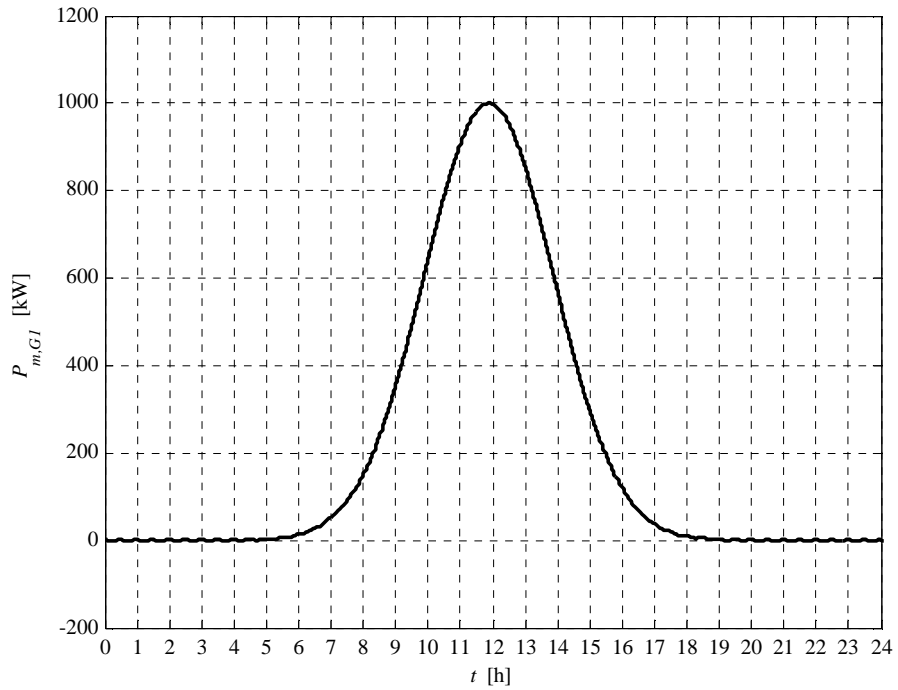
Fig. 5.3-1. G1 active power daily profile
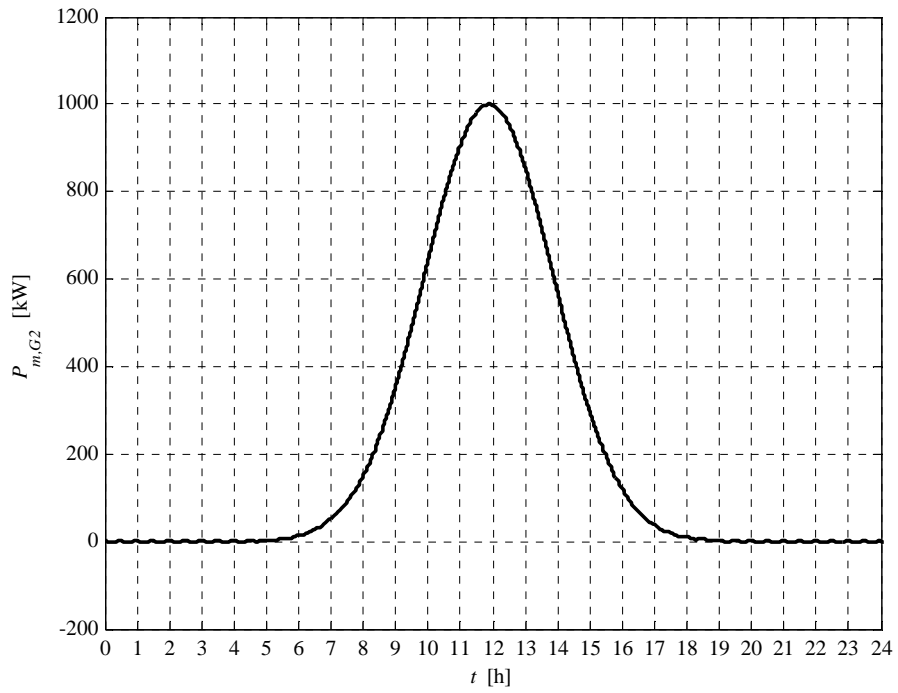
Fig. 5.3-2. G2 active power daily profile
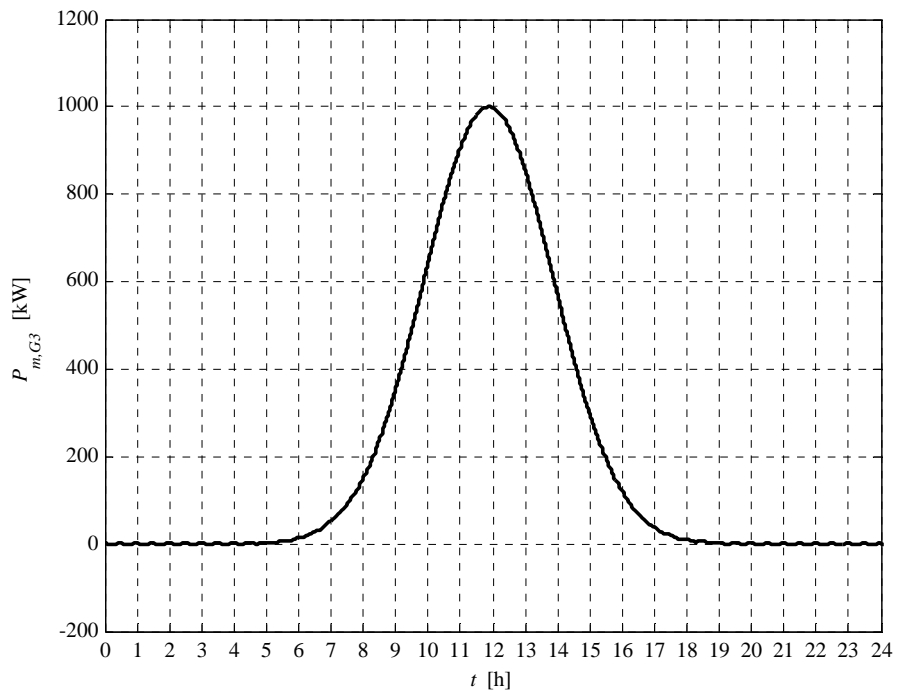
Fig. 5.3-3. G3 active power daily profile

94
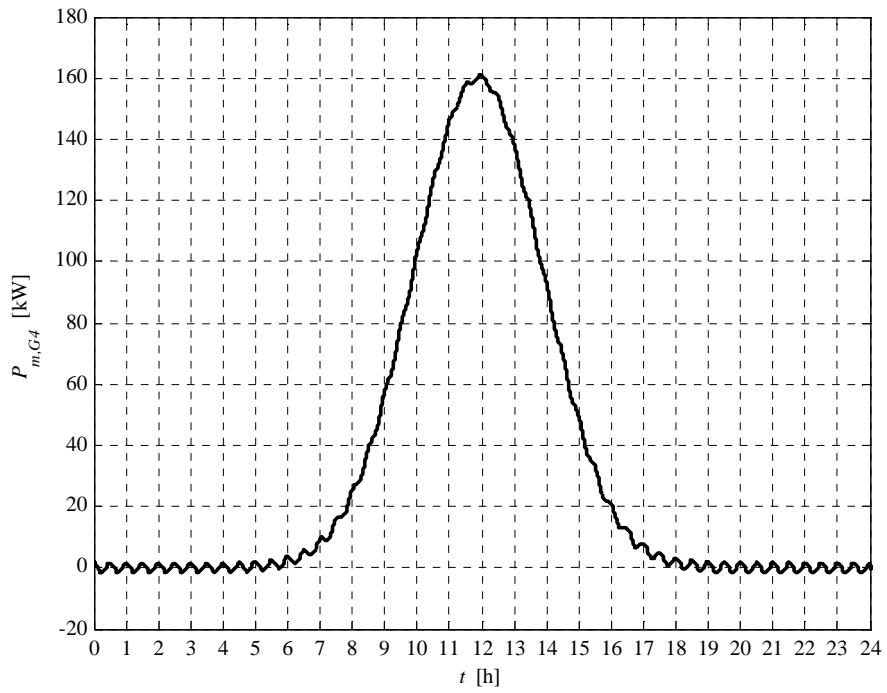
Fig. 5.3-4. G4 active power daily profile
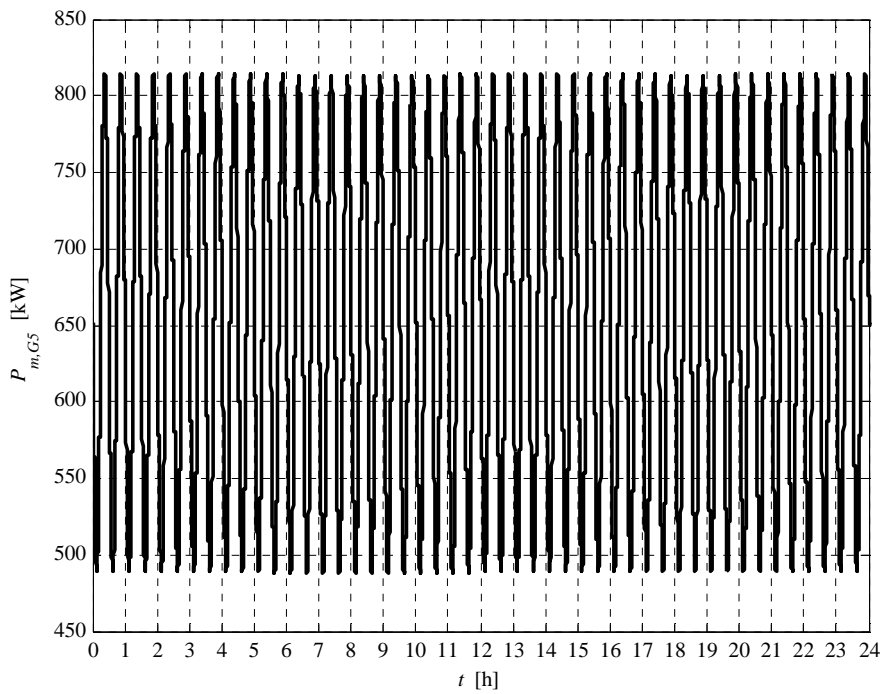
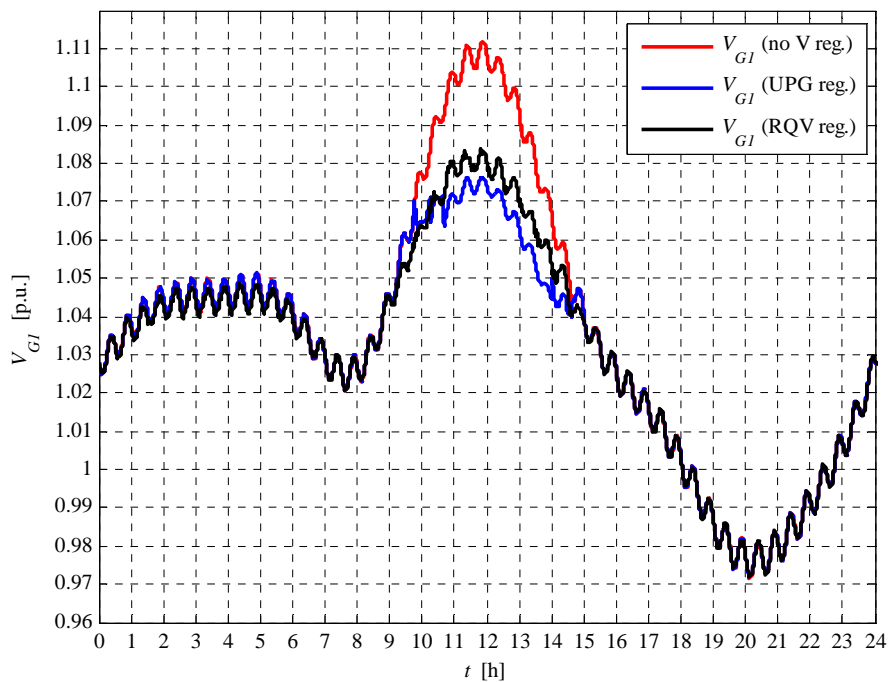**Fig. 5.3-5. G5 active power daily profile**
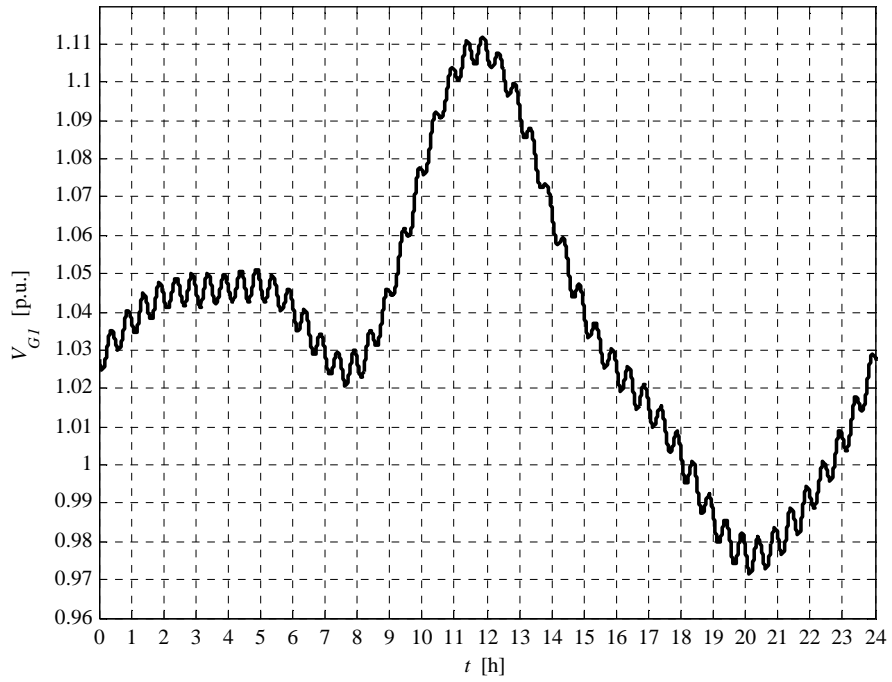
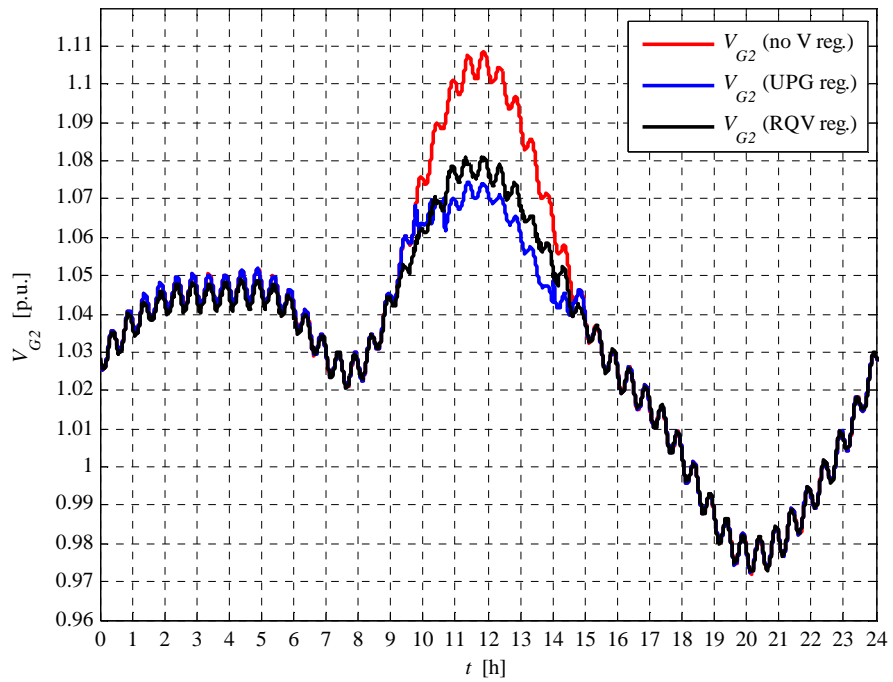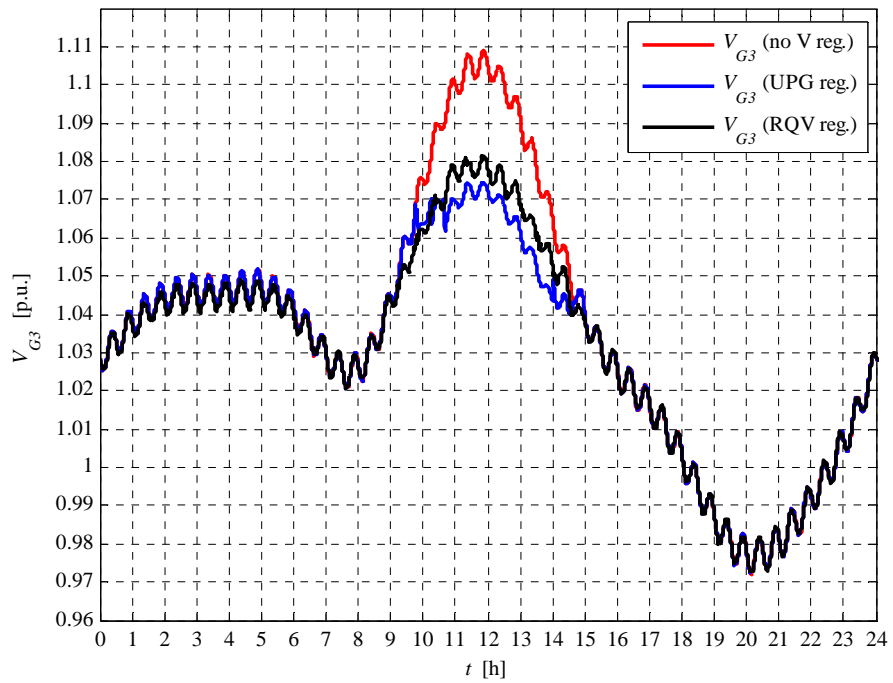**Fig. 5.3-6. G1 voltage daily profile**
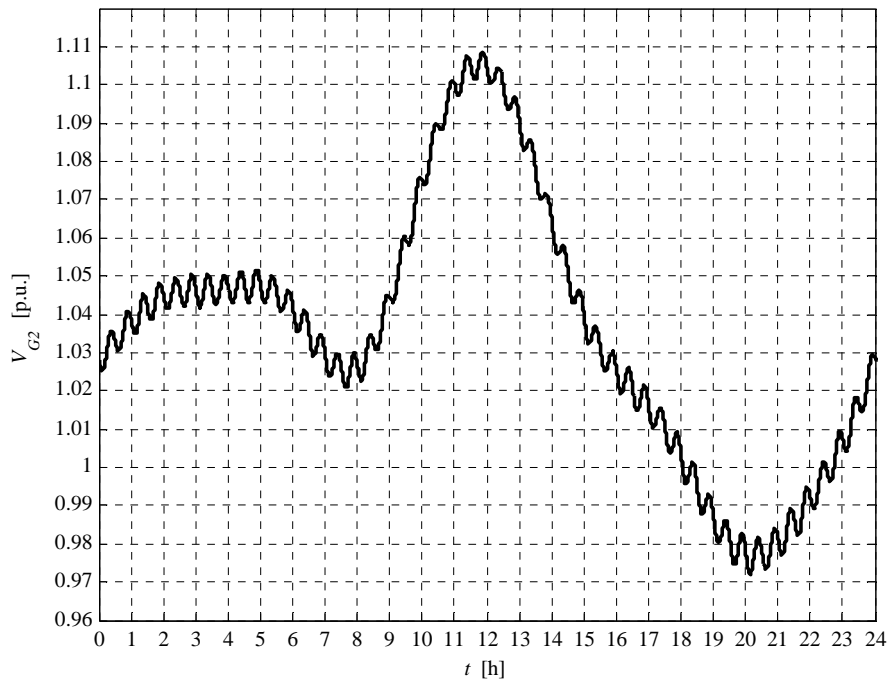
Fig. 5.3-7. G2 voltage daily profile
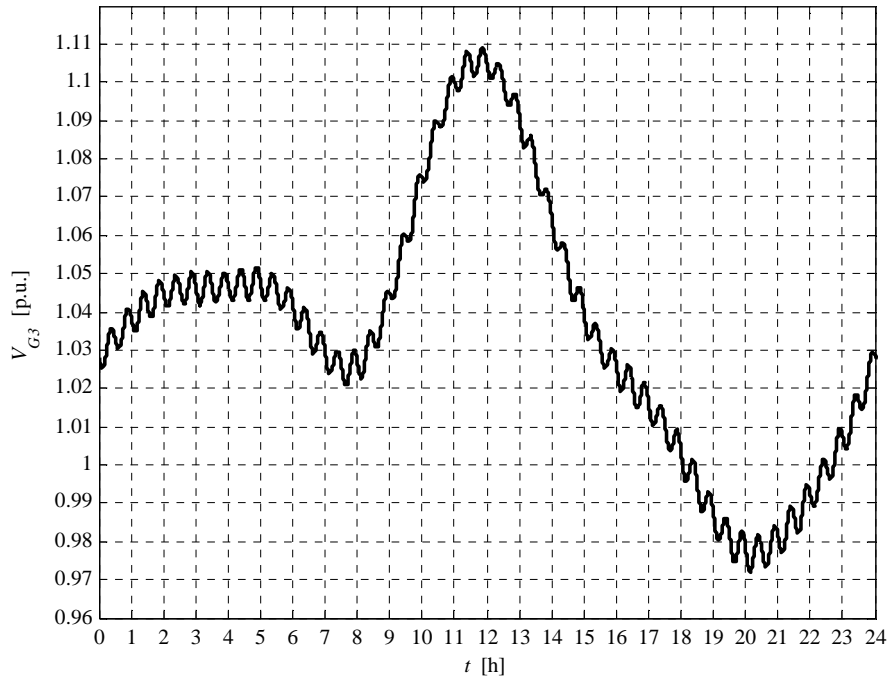
Fig. 5.3-8. G3 voltage daily profile
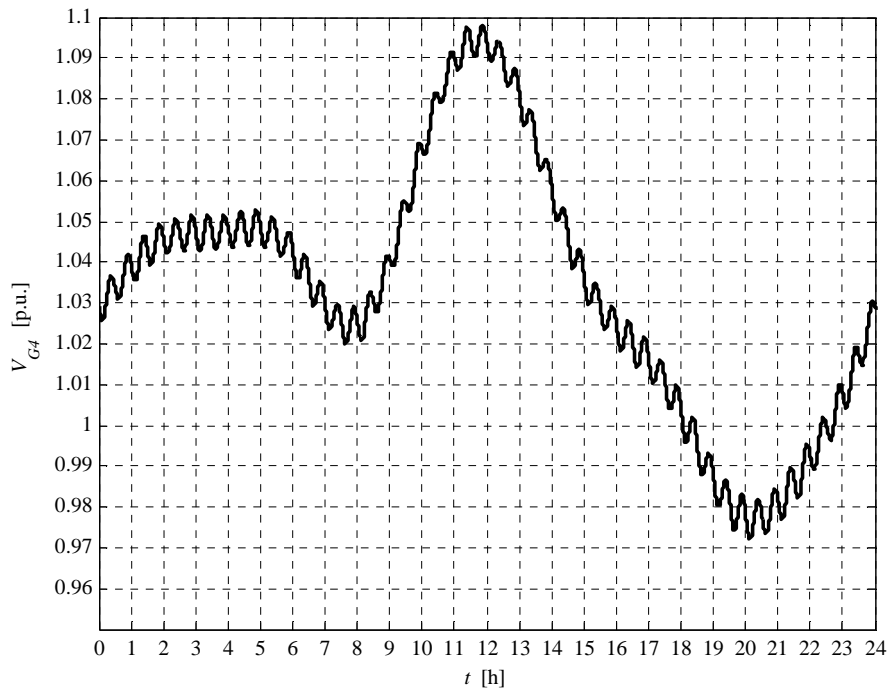
Fig. 5.3-9. G4 voltage daily profile

97
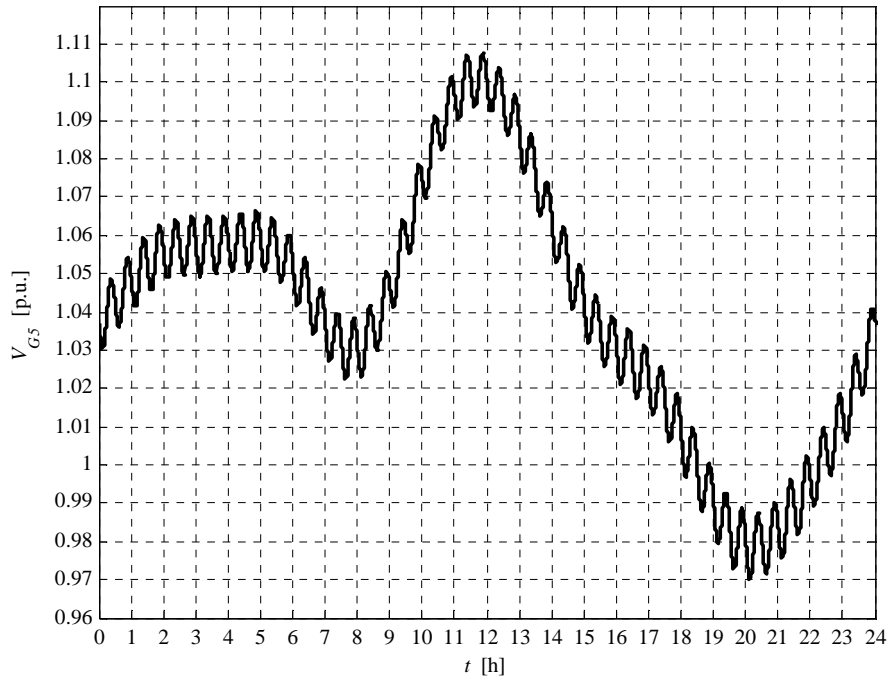
Fig. 5.3-10. G5 voltage daily profile
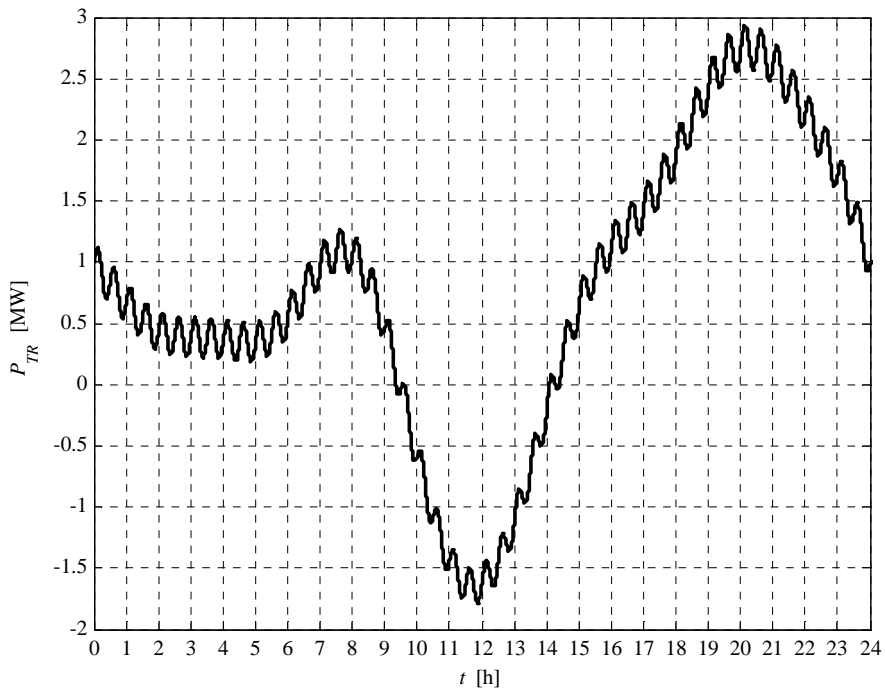
Fig. 5.3-11. HV/MV transformer daily active power profile

98
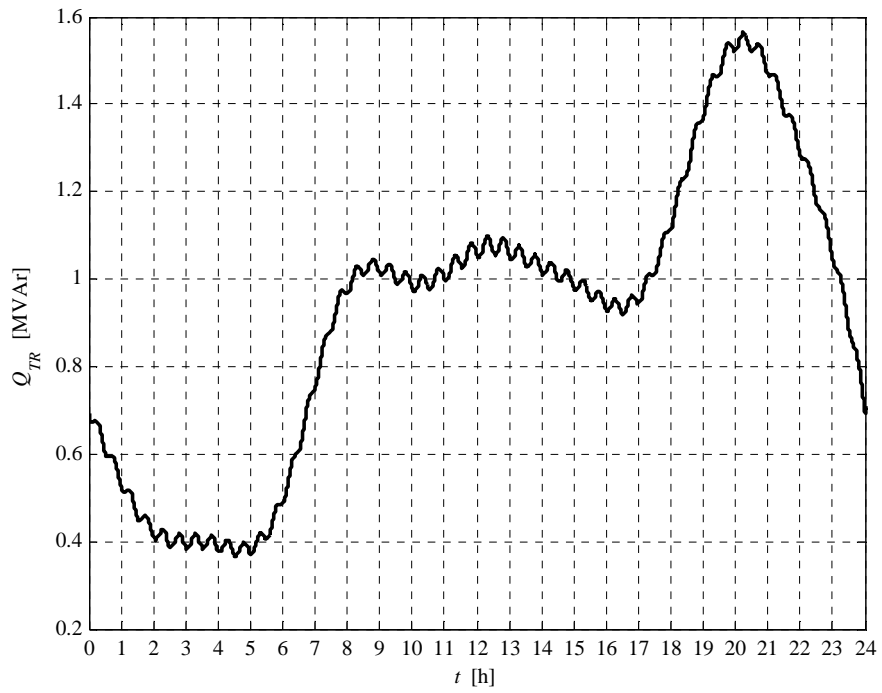
Fig. 5.3-12. HV/MV transformer daily reactive power profile
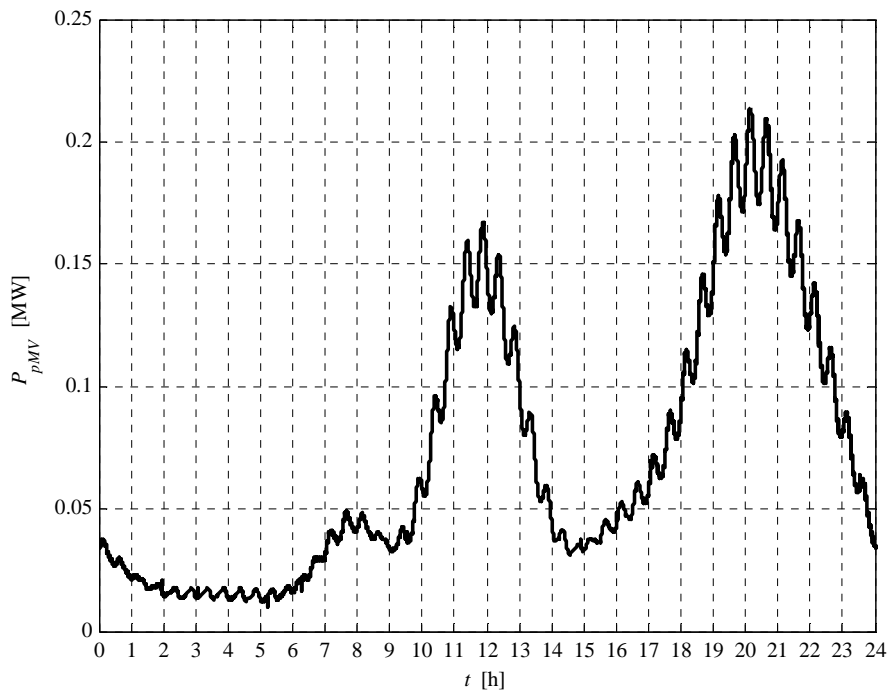
Fig. 5.3-13. MV network daily lost power profile

We can observe that the voltage daily profiles peak is very high. If no voltage regulation is active, the interface protection relay risk to trip (maximum voltage threshold trip). We can also observe the HV/MV transformer active power inversion, due to the DG presence. The power losses profile is characterized by two peaks. The first peak is related to the generated power, the second one is due to the loads power.

The report, referred to this case, is:

```
Report case: 1.b

Maximum VG1 value = 1.1120 [p.u.]
Maximum VG2 value = 1.1087 [p.u.]
Maximum VG3 value = 1.1091 [p.u.]
Maximum VG4 value = 1.0981 [p.u.]
Maximum VG5 value = 1.1077 [p.u.]

Loads power daily peak = 3.2157 [MW]
Generators power daily peak = 3.9746 [MW]

Loads daily active energy (absorbed) = 49.2306 [MWh]
Generators daily active energy (generated) = 31.9846 [MWh]
Daily active energy absorbed from the HV grid = 18.9825 [MWh]
Daily lost active energy = 1.7365 [MWh]
Daily lost active energy (percentual) = 3.4070 [%]
```

We can observe a daily energy losses decaying, if compared to the case 1.a, due to the DG presence.

5.4 COMPARISON BETWEEN CASES 1.A AND 1.B

In order to graphically compare cases 1.a and 1.b, the following plots are presented. They represent generators voltage, HV/MV transformer powers and network losses of cases 1.a and 1.b.
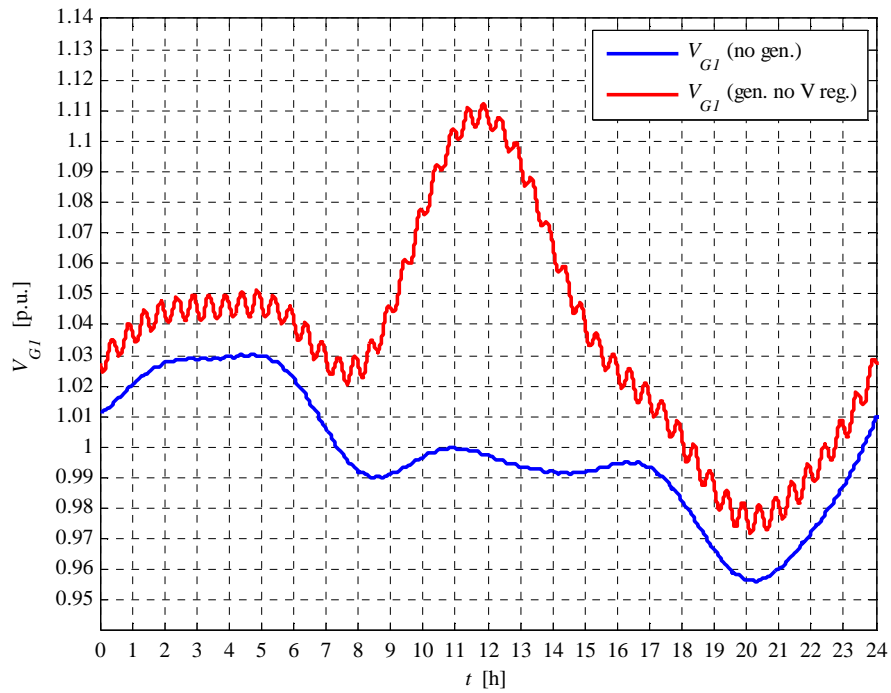
Fig. 5.4-1. G1 voltage daily profile
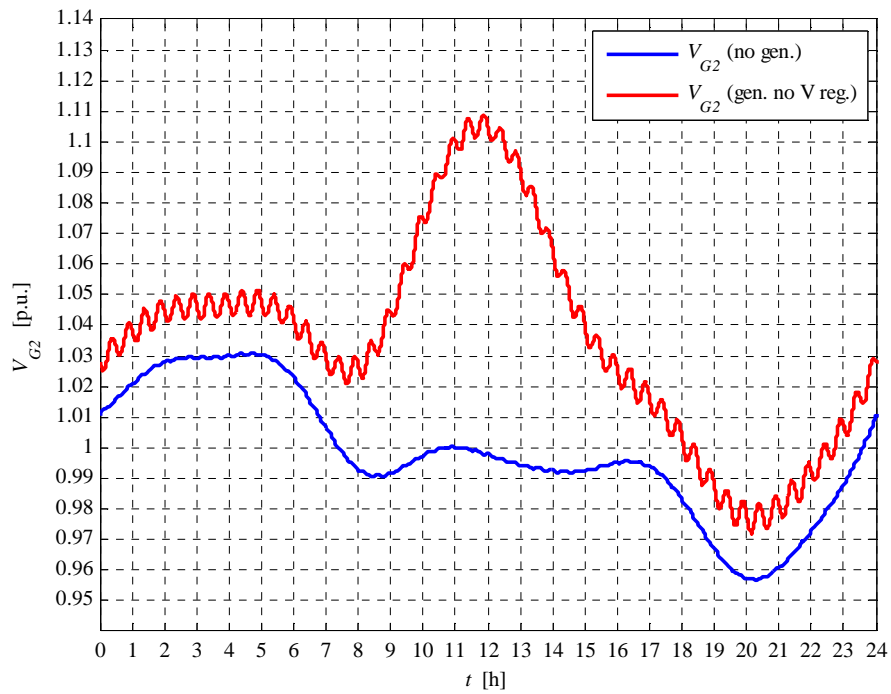
Fig. 5.4-2. G2 voltage daily profile

101
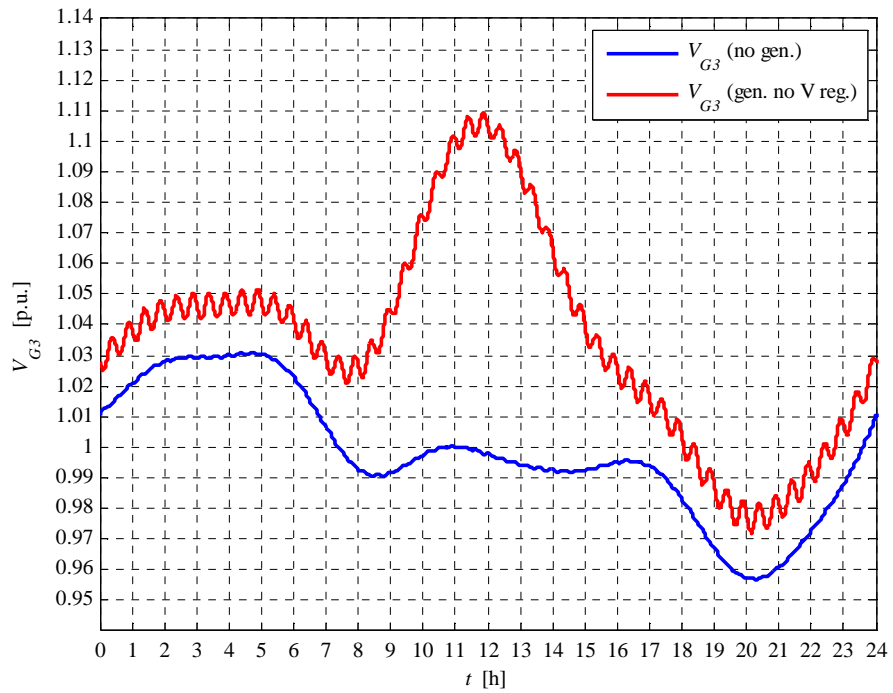
Fig. 5.4-3. G3 voltage daily profile
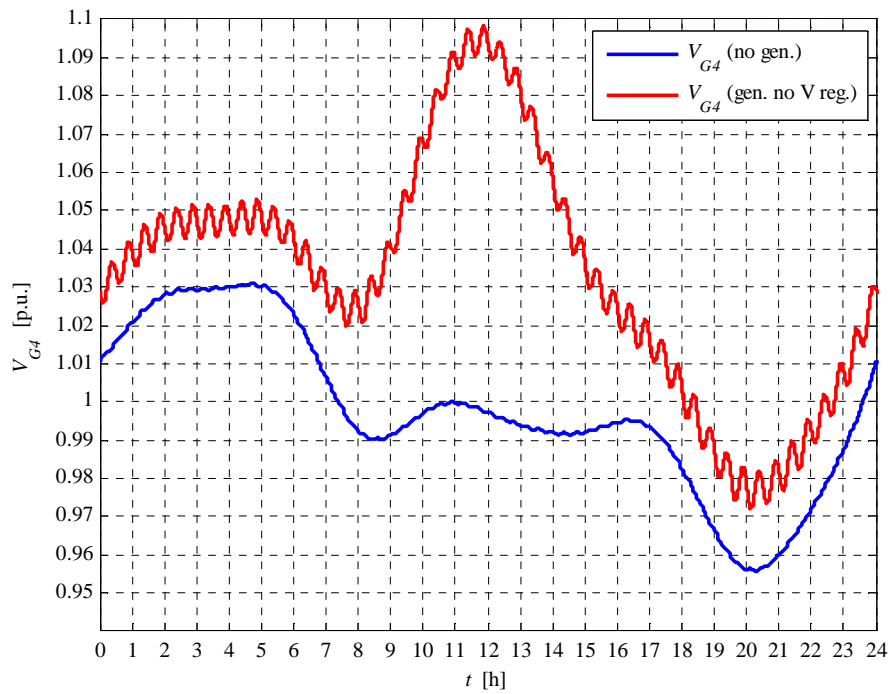
Fig. 5.4-4. G4 voltage daily profile
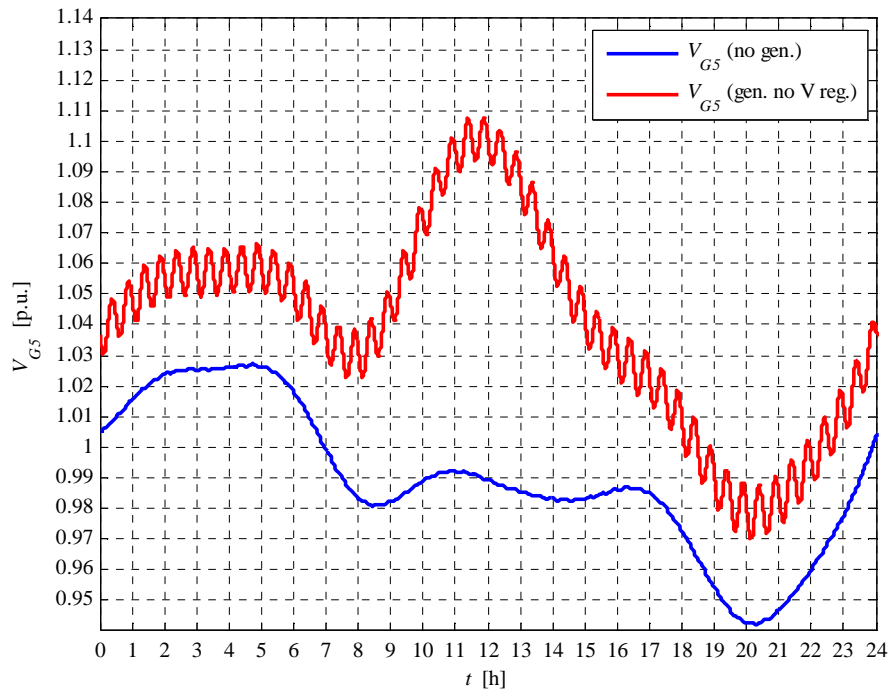
Fig. 5.4-5. G5 voltage daily profile
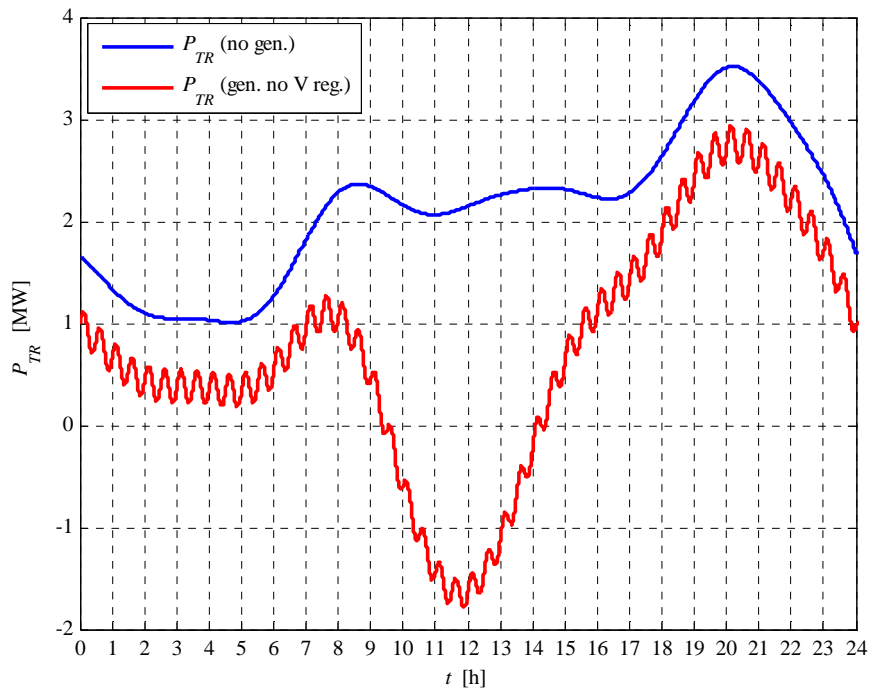
Fig. 5.4-6. HV/MV transformer daily active power profile
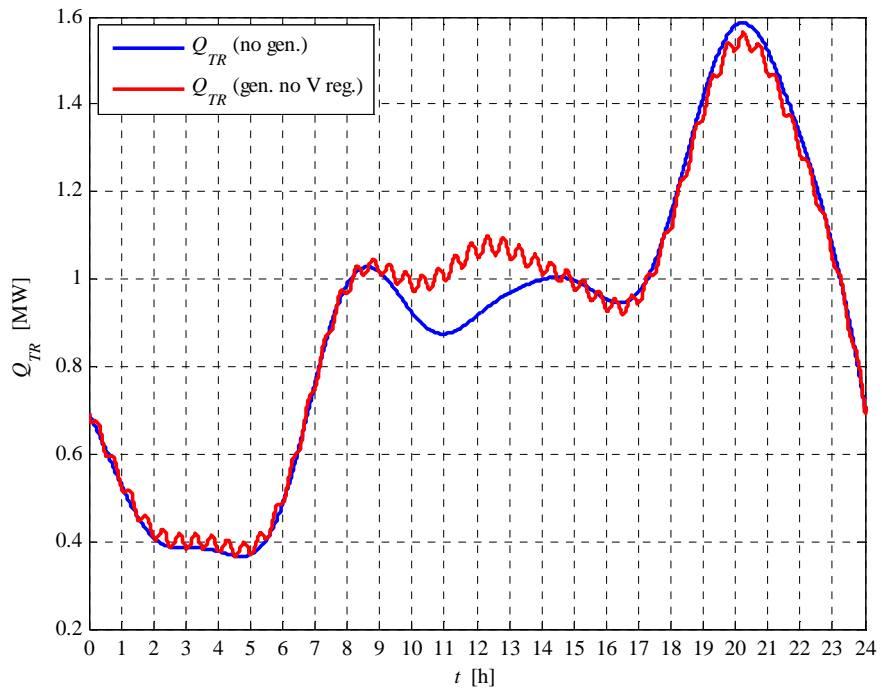
Fig. 5.4-7. HV/MV transformer daily reactive power profile
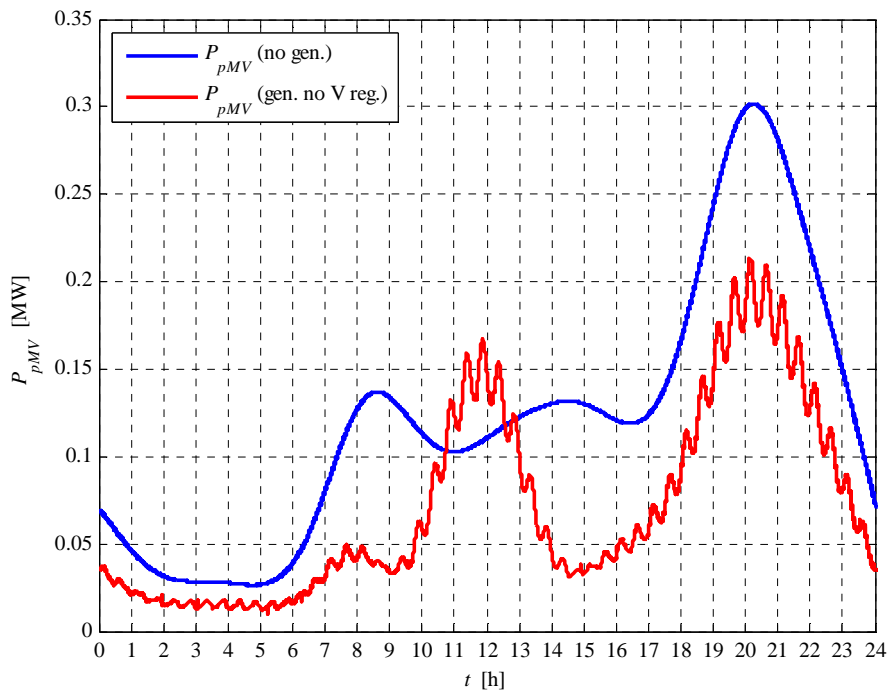
Fig. 5.4-8. MV network daily lost power profile

5.5 CASE 2 RESULTS

In this case the "UPG" local voltage regulation is activated. The MV busbar voltage is fixed to 1.06 p.u. This set-point value guarantees the correct voltage in the critical node in the maximum load condition, when the generation is de-activated.
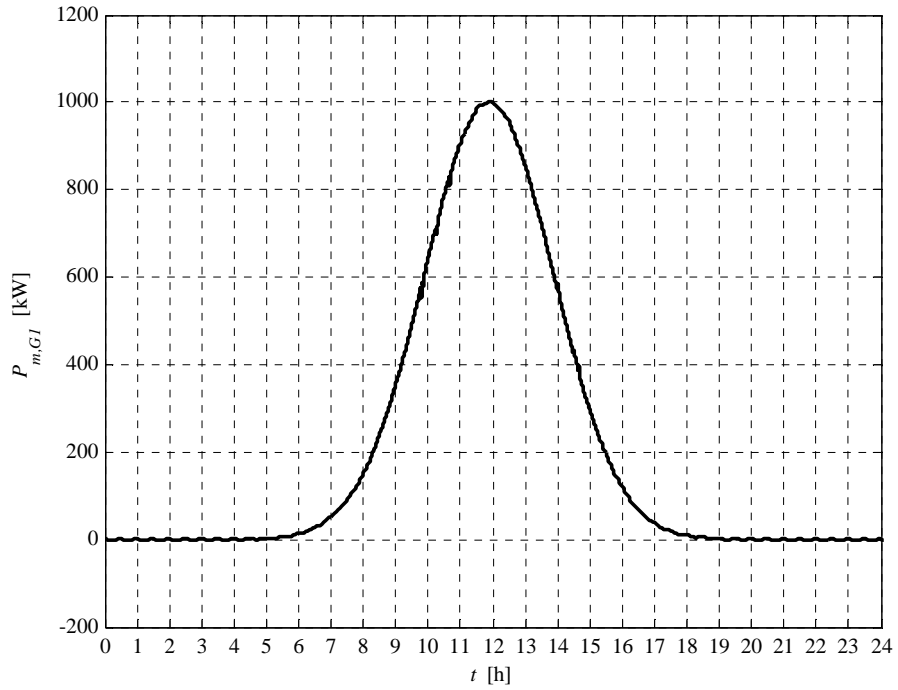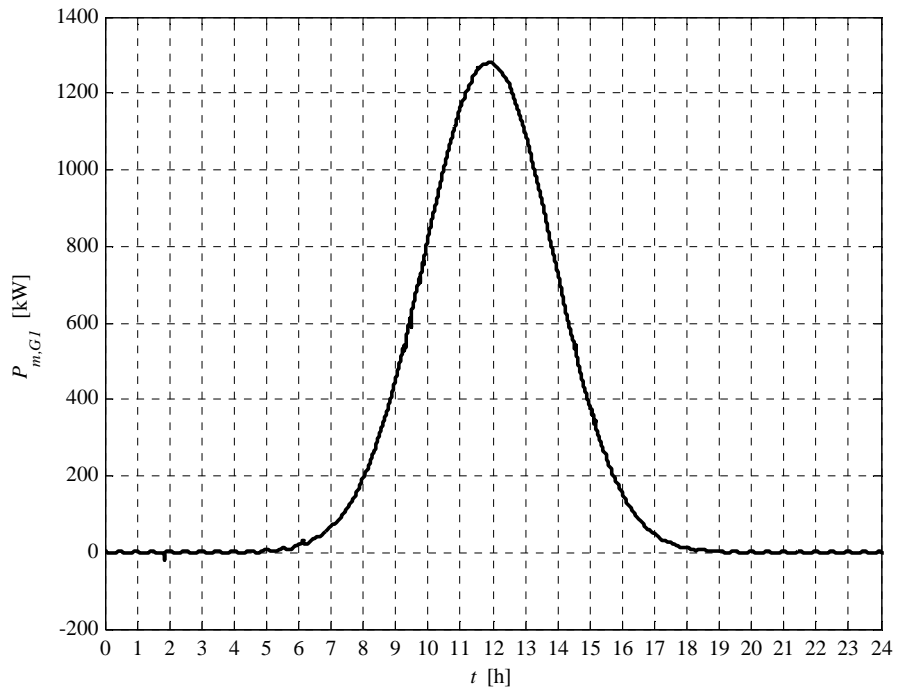

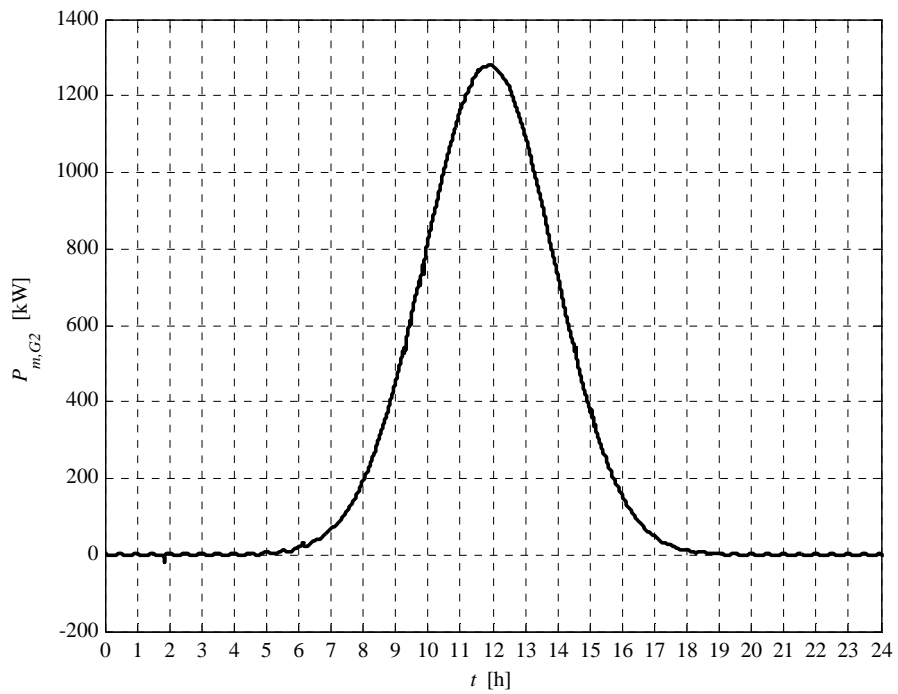**Fig. 5.5-1. G1 active power daily profile**
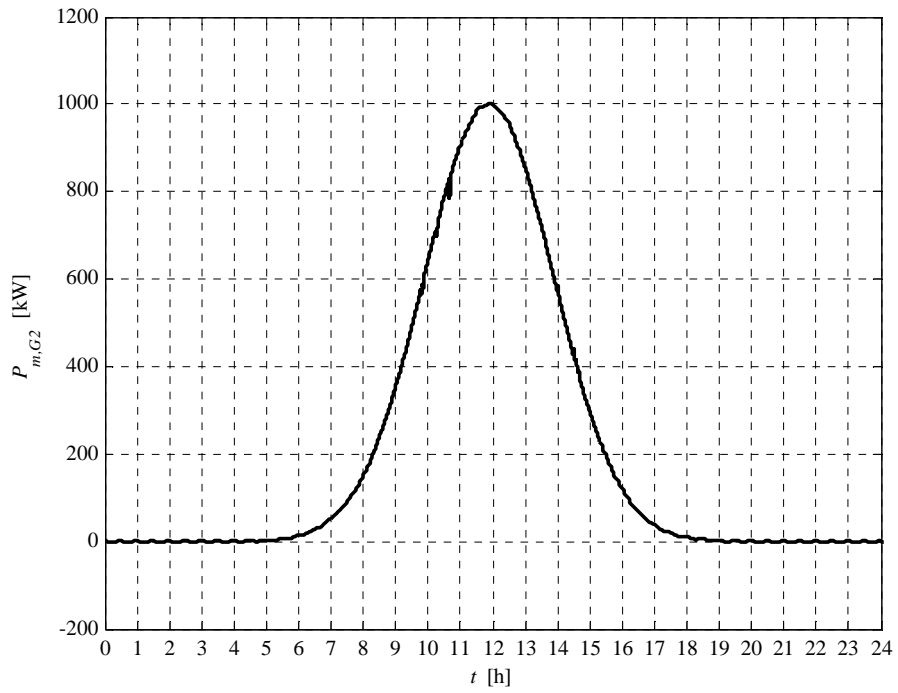
Fig. 5.5-2. G2 active power daily profile
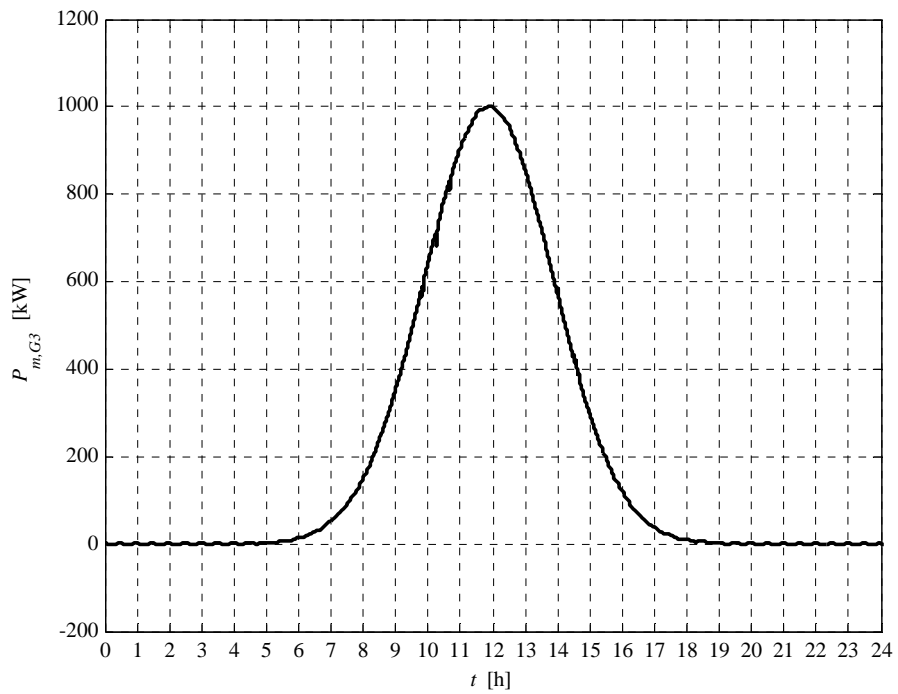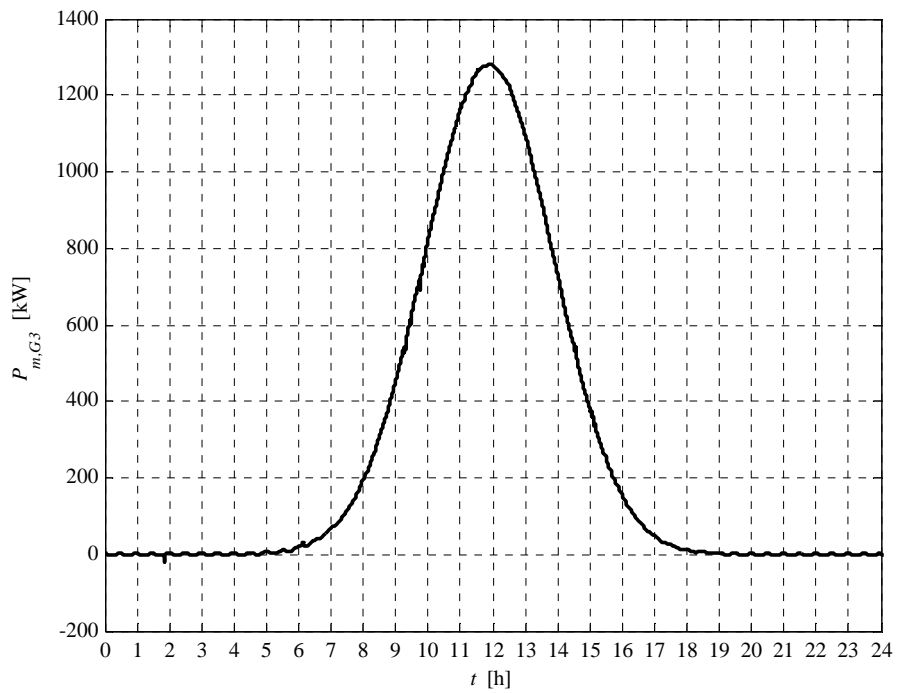

Fig. 5.5-3. G3 active power daily profile
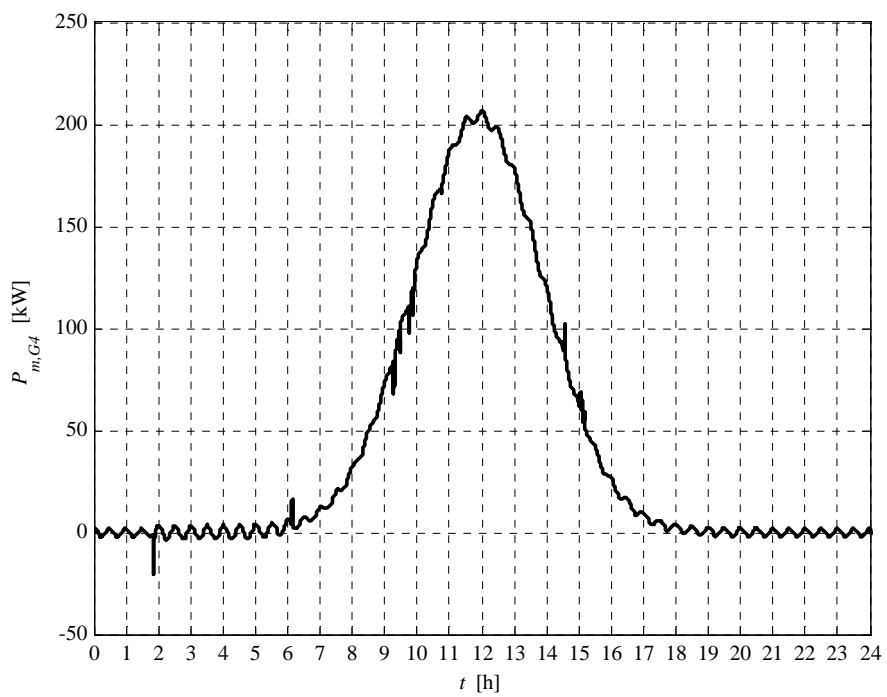
106
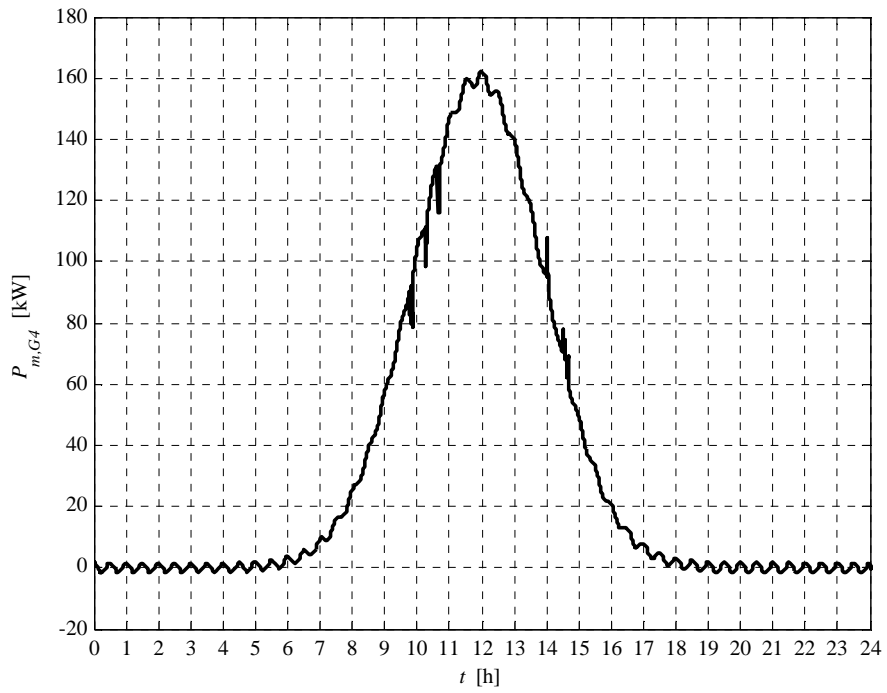
Fig. 5.5-4. G4 active power daily profile
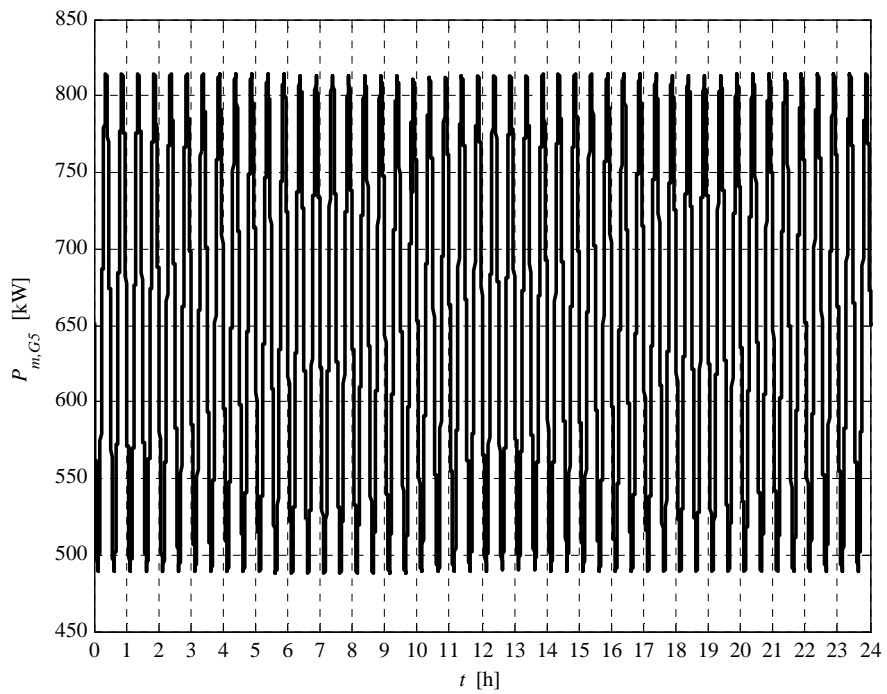
Fig. 5.5-5. G5 active power daily profile

107
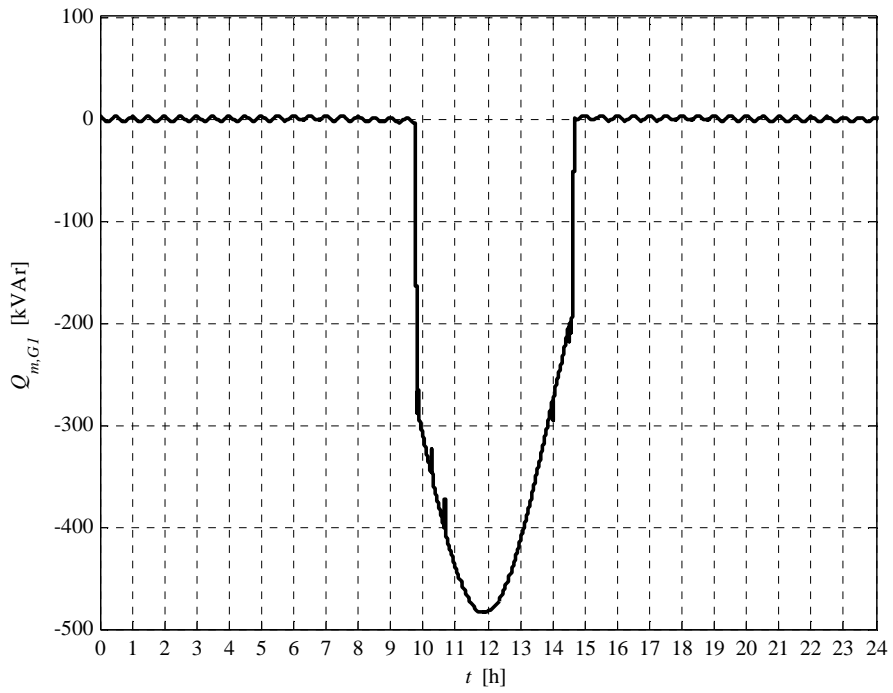
Fig. 5.5-6. G1 reactive power daily profile
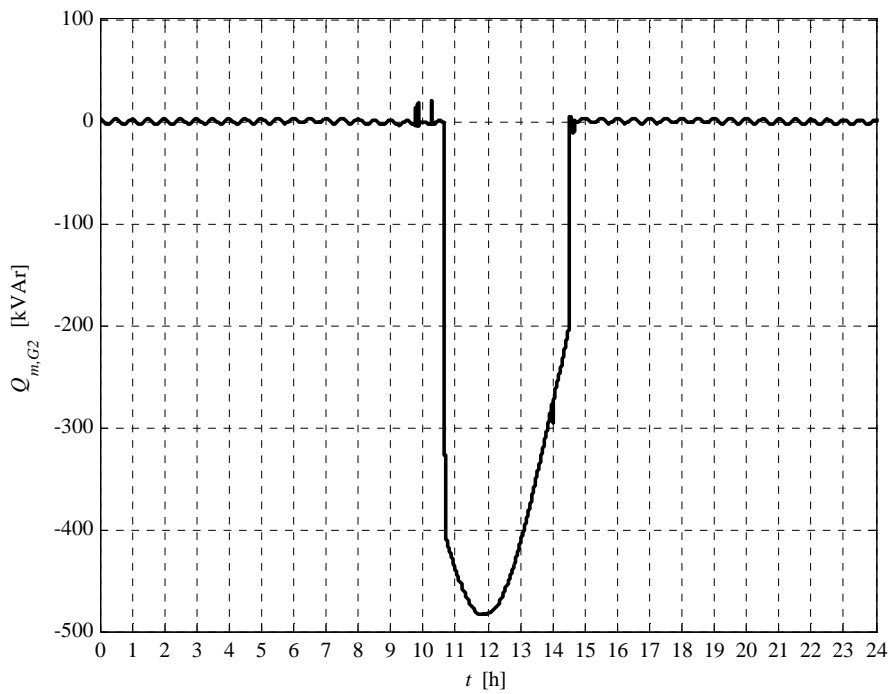
Fig. 5.5-7. G2 reactive power daily profile
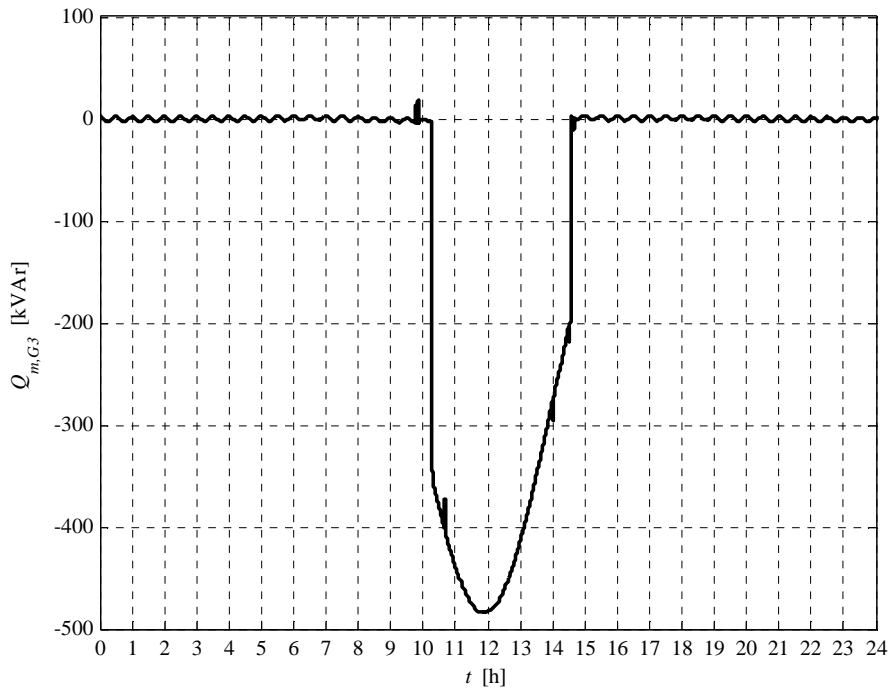
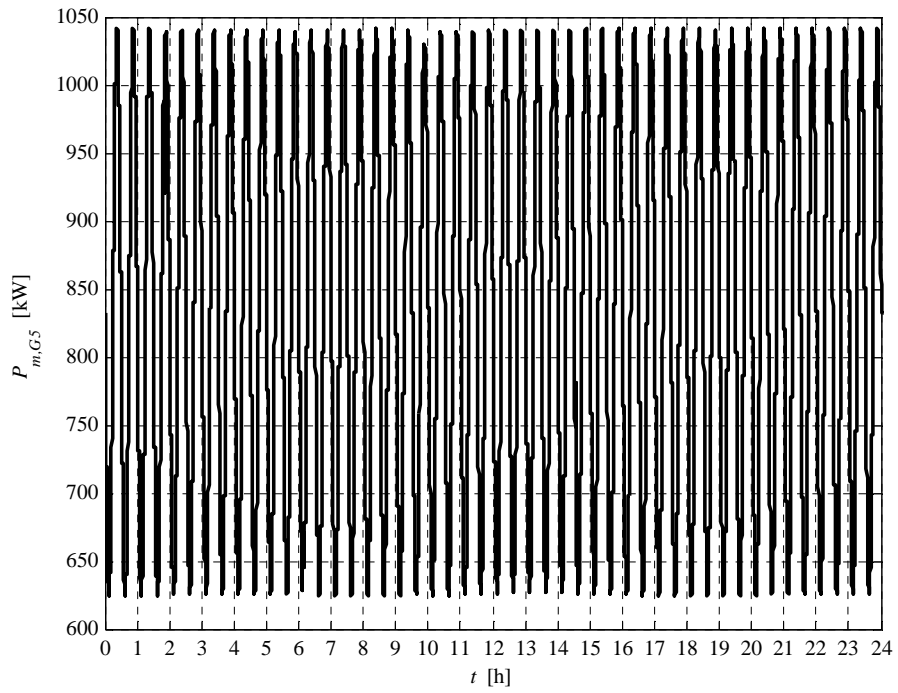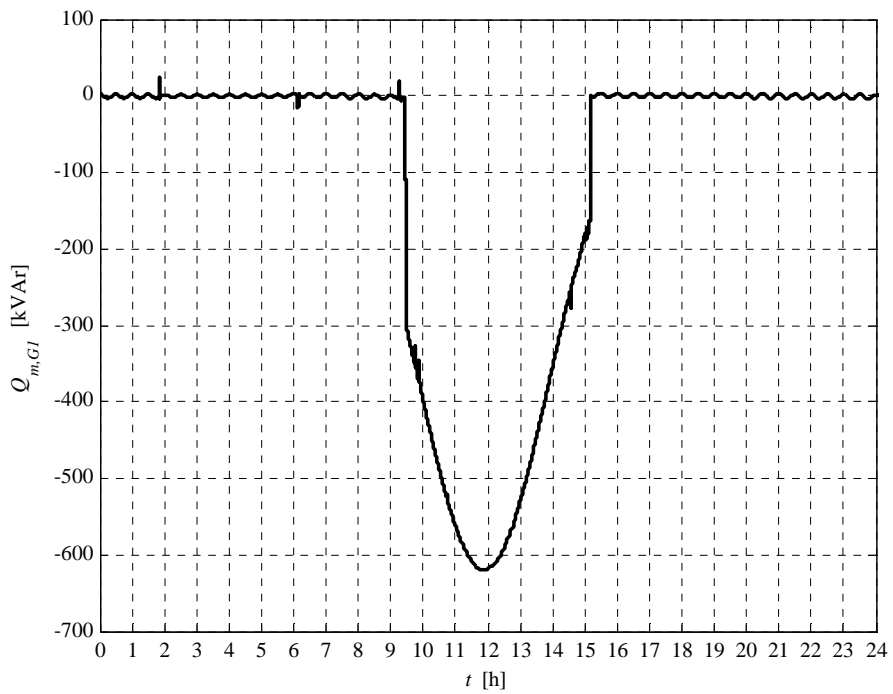**Fig. 5.5-8. G3 reactive power daily profile**
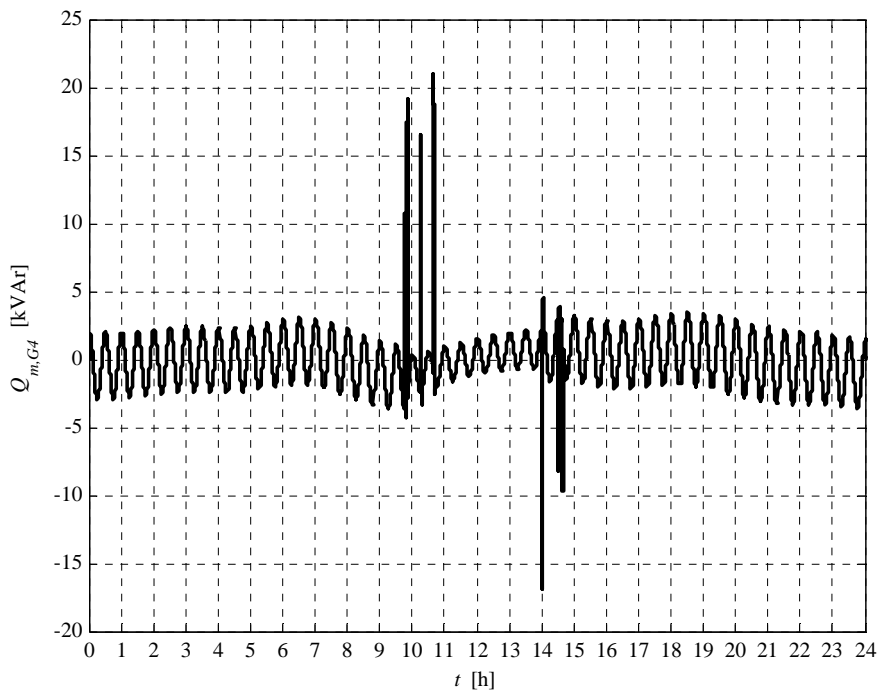
Fig. 5.5-9. G4 reactive power daily profile
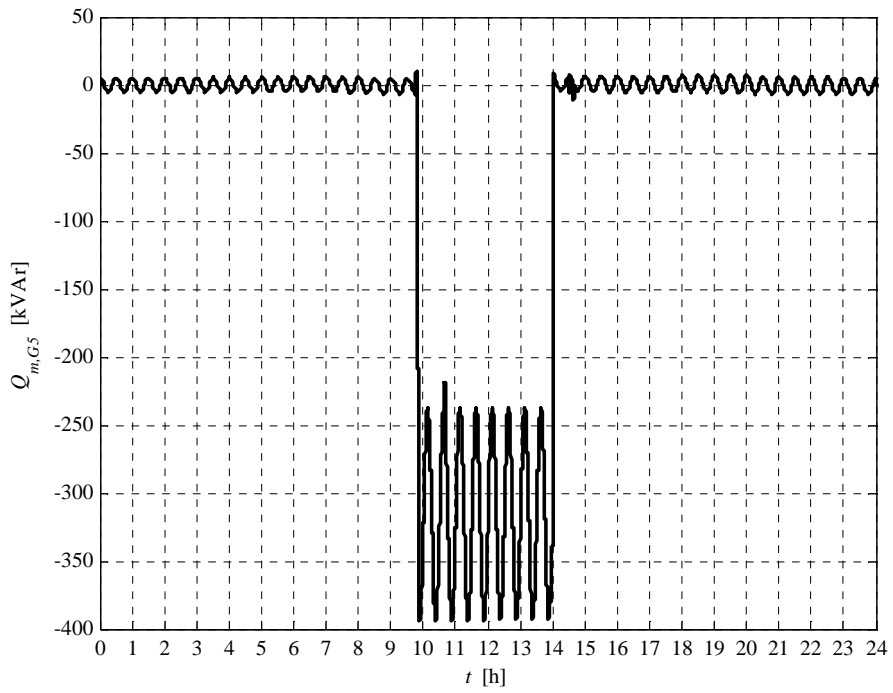
Fig. 5.5-10. G5 reactive power daily profile
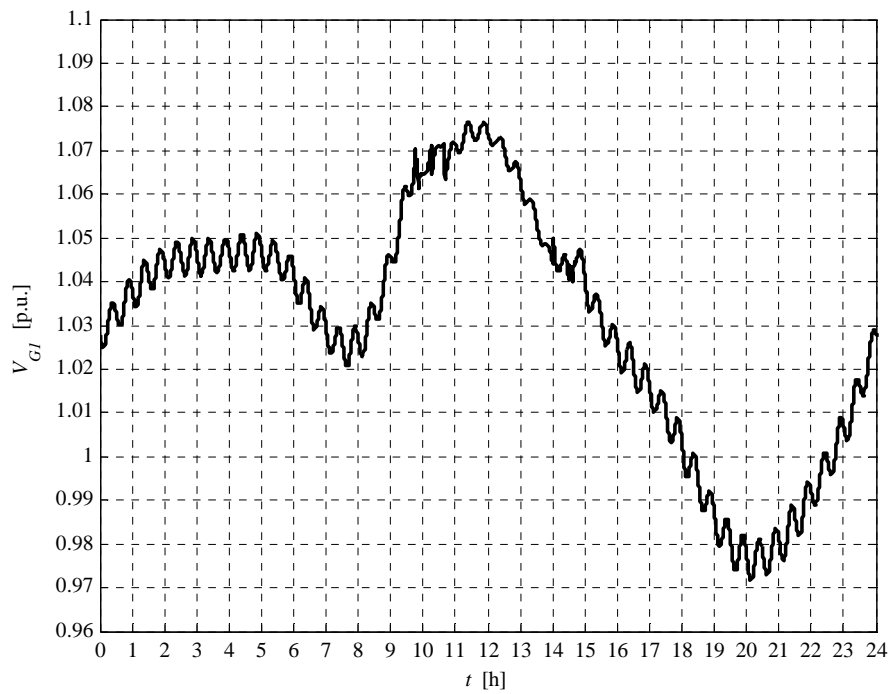
Fig. 5.5-11. G1 voltage daily profile

110
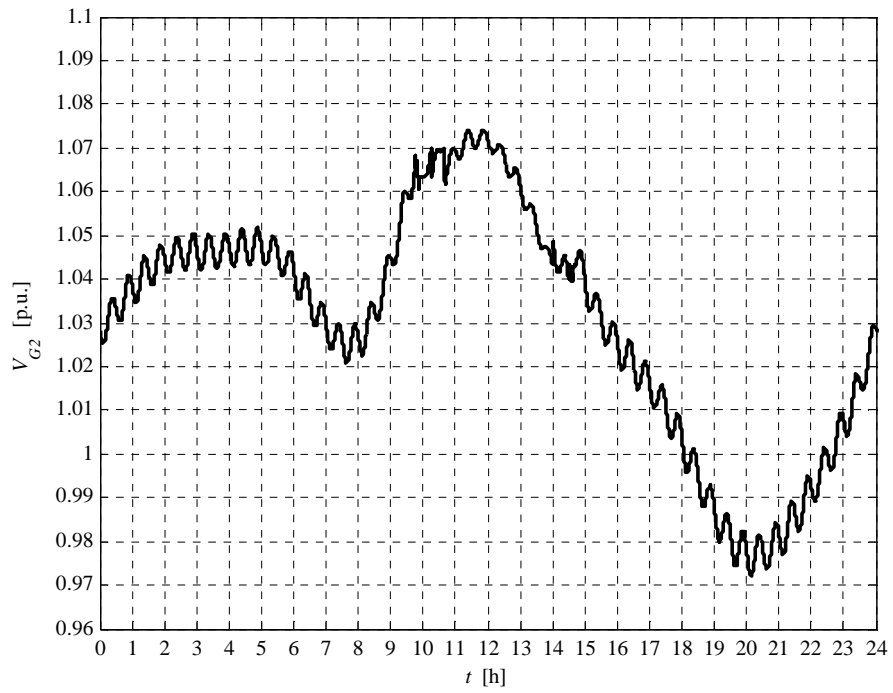
Fig. 5.5-12. G2 voltage daily profile
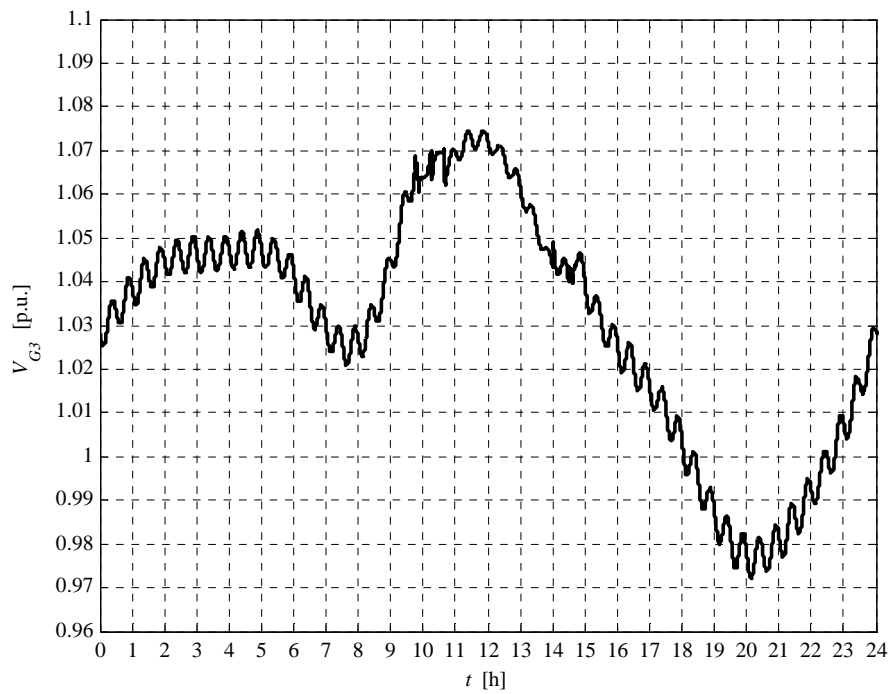
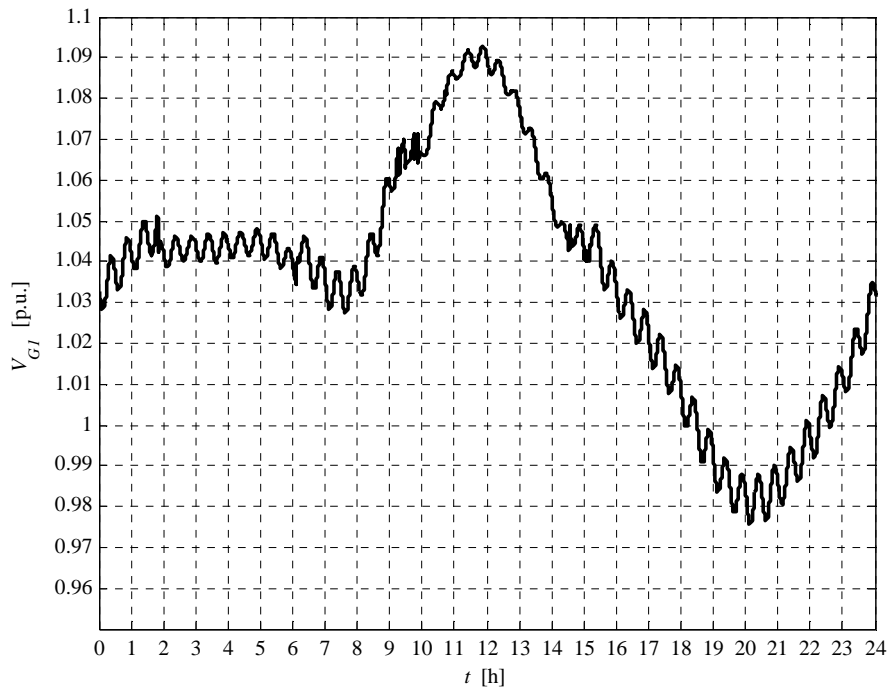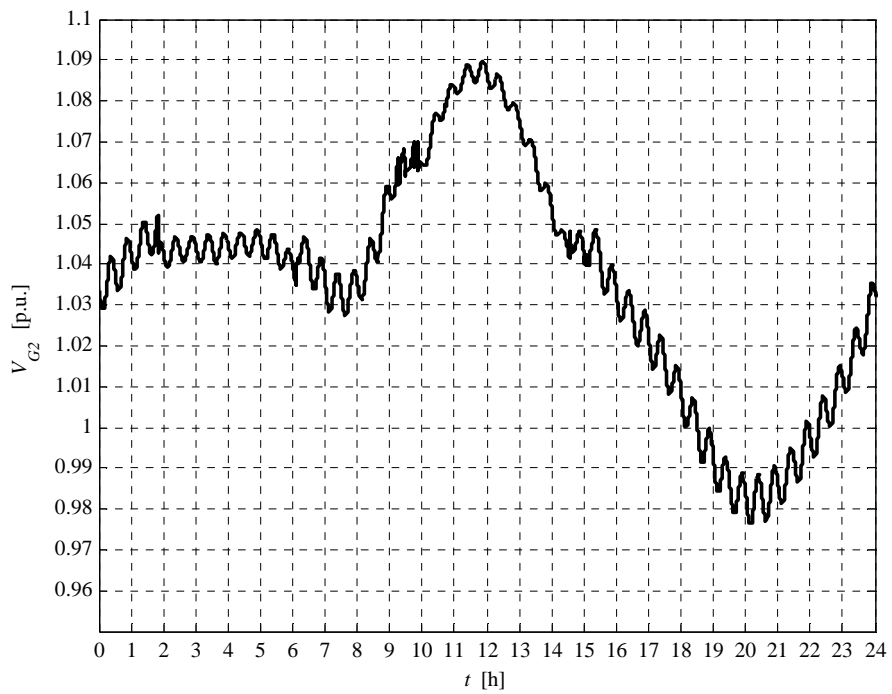**Fig. 5.5-13. G3 voltage daily profile**

111
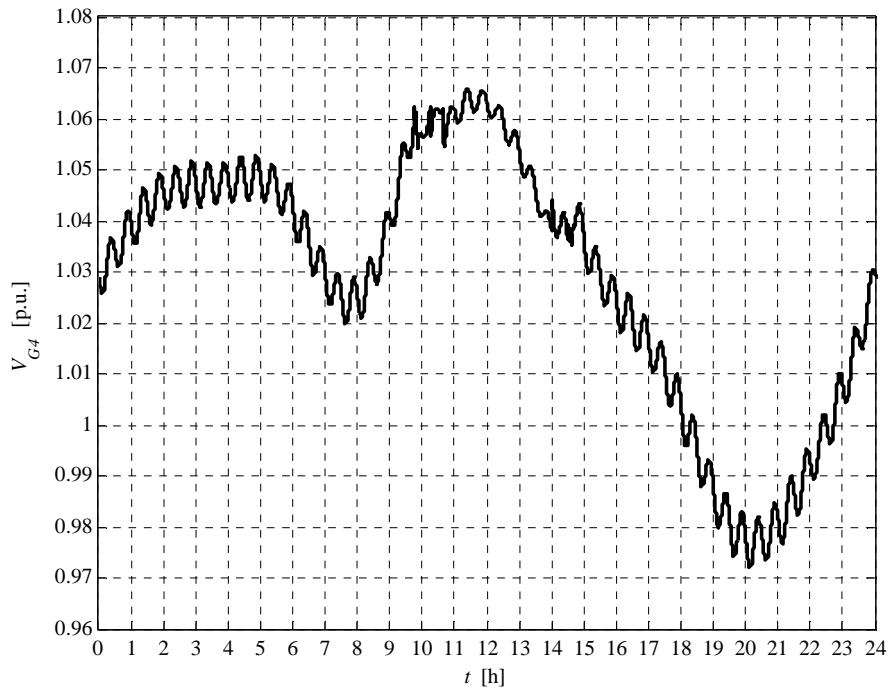
Fig. 5.5-14. G4 voltage daily profile
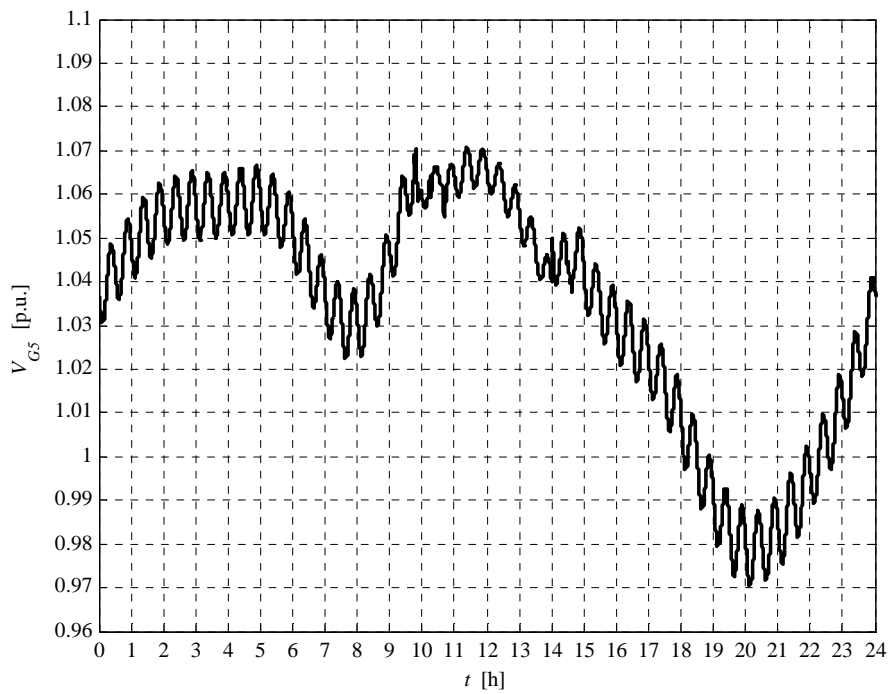
Fig. 5.5-15. G5 voltage daily profile

112
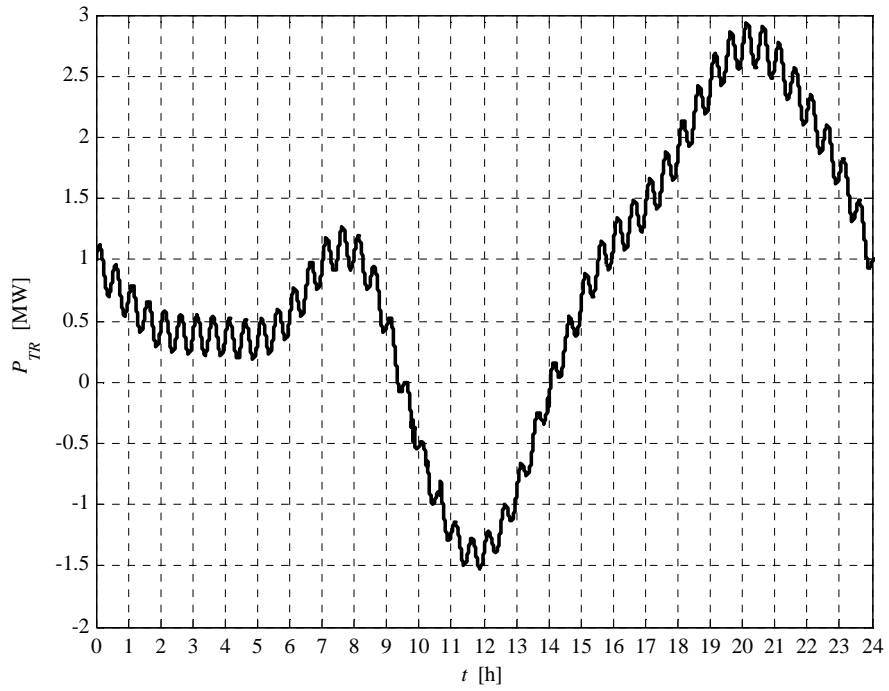
Fig. 5.5-16. HV/MV transformer daily active power profile
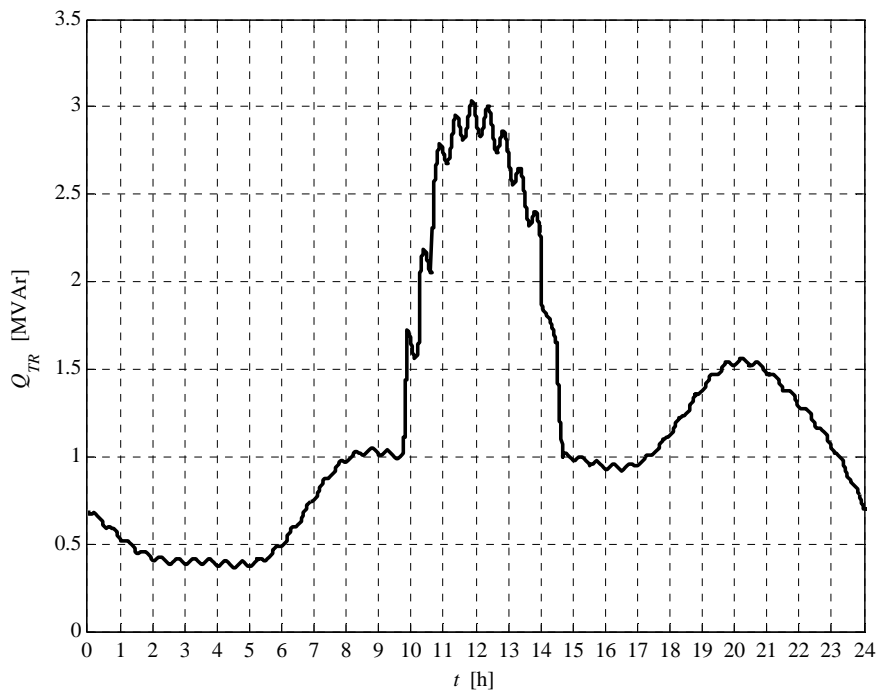
Fig. 5.5-17. HV/MV transformer daily reactive power profile

113
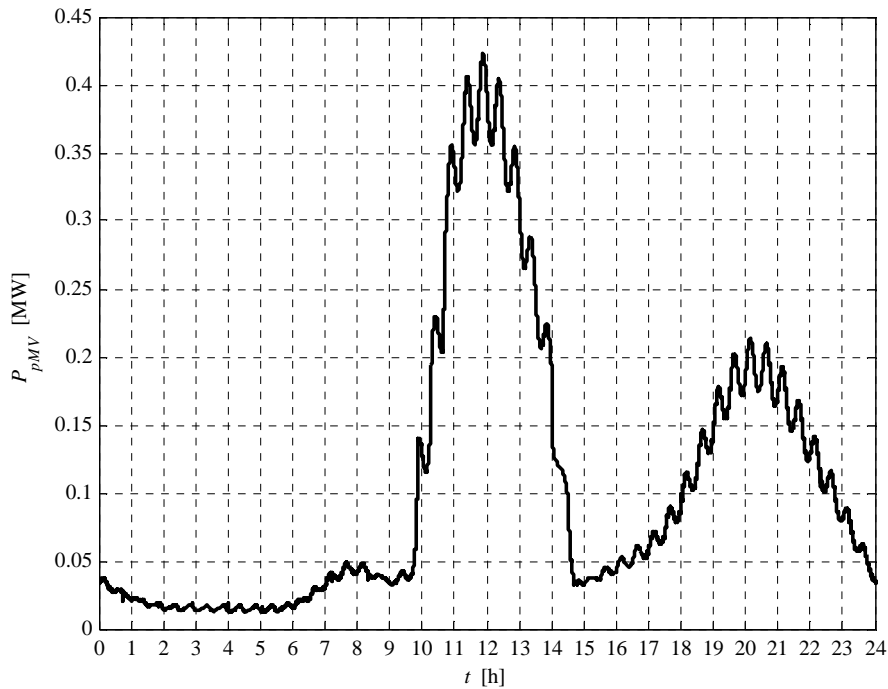
Fig. 5.5-18. MV network daily lost power profile

We can observe that the voltage daily profiles peak is limited by the local "UPG" voltage regulation action. The interface protection relay trip is impossible. We can also observe the HV/MV transformer active power inversion, due to the DG presence. The HV/MV transformer reactive power is characterized by an high peak, requested from the HV grid, due to the "UPG" local voltage regulation. In fact the reactive power requested from each generator must be supplied by the HV grid. The generators requested reactive power curve shape is similar to the active power (when the "UPG" is active) because the "UPG" regulation is a "constant power factor regulation". No reactive power is requested to generator G4 because its voltage remains less top the "UPG" activation threshold.

The power losses profile is characterized by two peaks. The first peak, which is the highest peak, is related to the generated power, the second one is due to the loads power.

The report, referred to this case, is:

```
Report case: 2

Maximum VG1 value = 1.0763 [p.u.]
Maximum VG2 value = 1.0742 [p.u.]
Maximum VG3 value = 1.0745 [p.u.]
Maximum VG4 value = 1.0660 [p.u.]
Maximum VG5 value = 1.0709 [p.u.]

Loads power daily peak = 3.2157 [MW]
```

114

```
Generators power daily peak = 3.9721 [MW]

Loads daily active energy (absorbed) = 49.2306 [MWh]
Generators daily active energy (generated) = 31.9846 [MWh]
Daily active energy absorbed from the HV grid = 19.8162 [MWh]
Daily lost active energy = 2.5702 [MWh]
Daily lost active energy (percentual) = 4.9616 [%]
```

We can observe a daily energy losses increment, if compared to the case 1.b, due to the DG reactive power request, in order to act the local "UPG" voltage regulation control. However the energy losses are less than the base case 1.a.

5.6 CASE 3 RESULTS

This case is necessary to test the "RQV" local voltage regulation modality. Then the "RQV" local voltage regulation is activated. The MV busbar voltage is fixed to 1.06 p.u. This set-point value guarantees the correct voltage in the critical node in the maximum load condition, when the generation is de-activated.
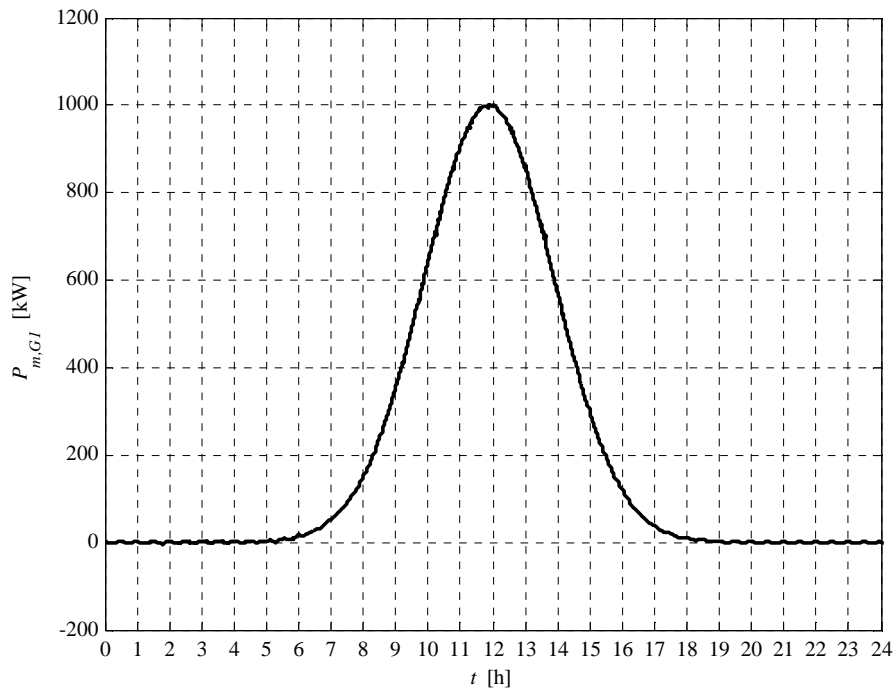
Fig. 5.6-1. G1 active power daily profile
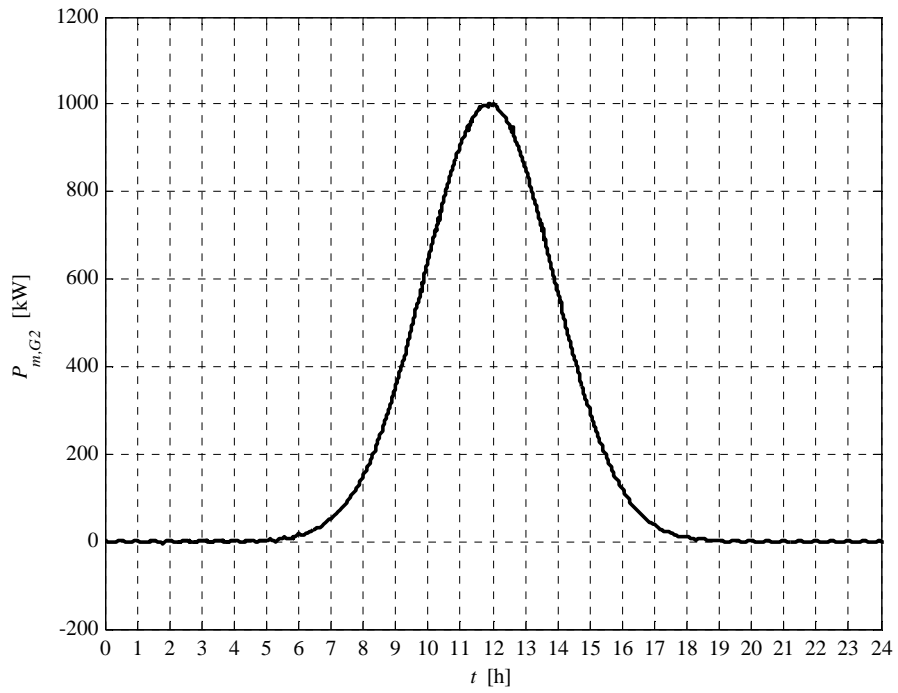
Fig. 5.6-2. G2 active power daily profile
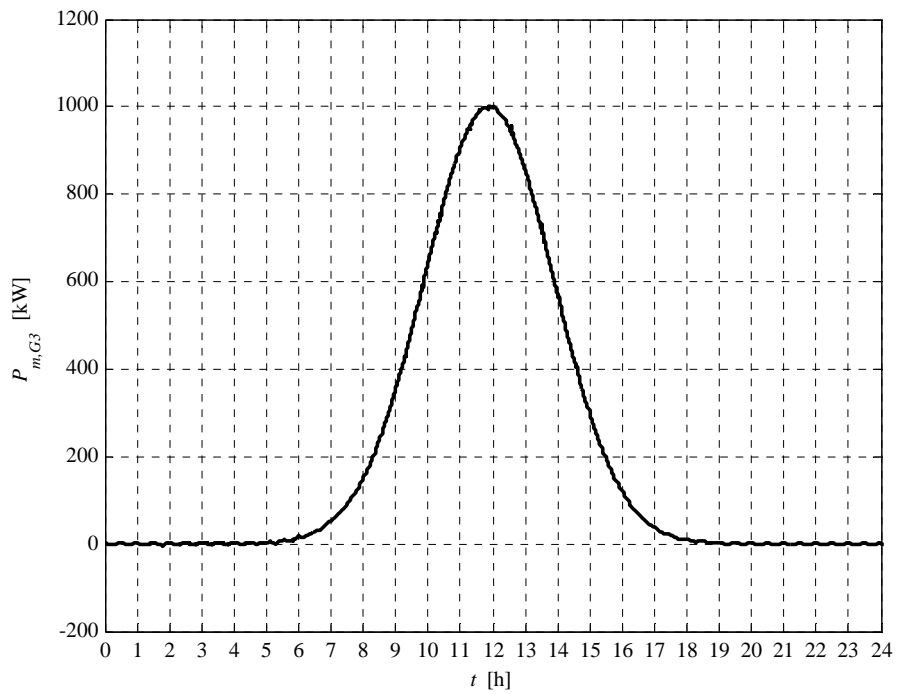
Fig. 5.6-3. G3 active power daily profile

116
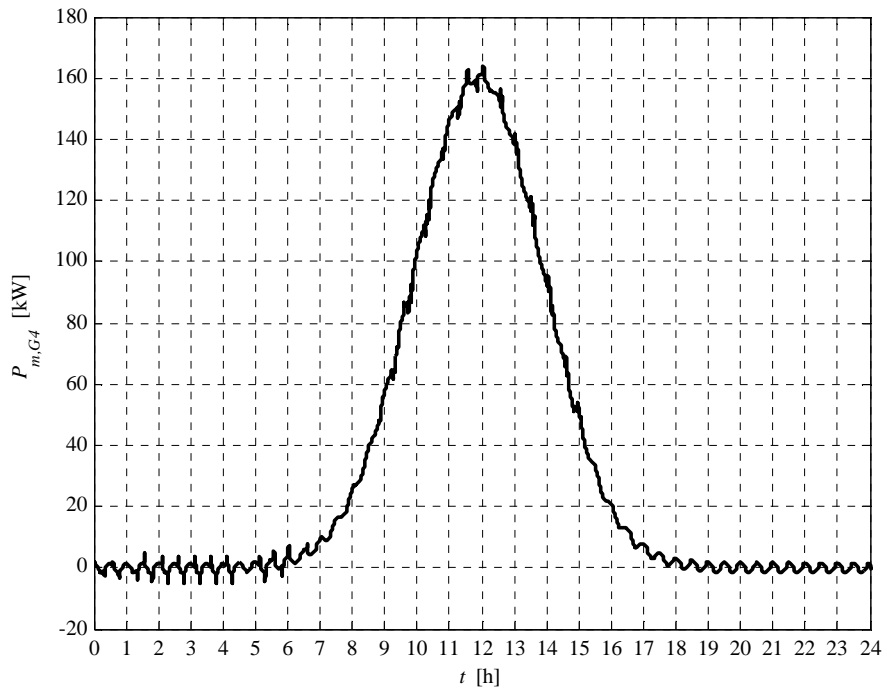
Fig. 5.6-4. G4 active power daily profile
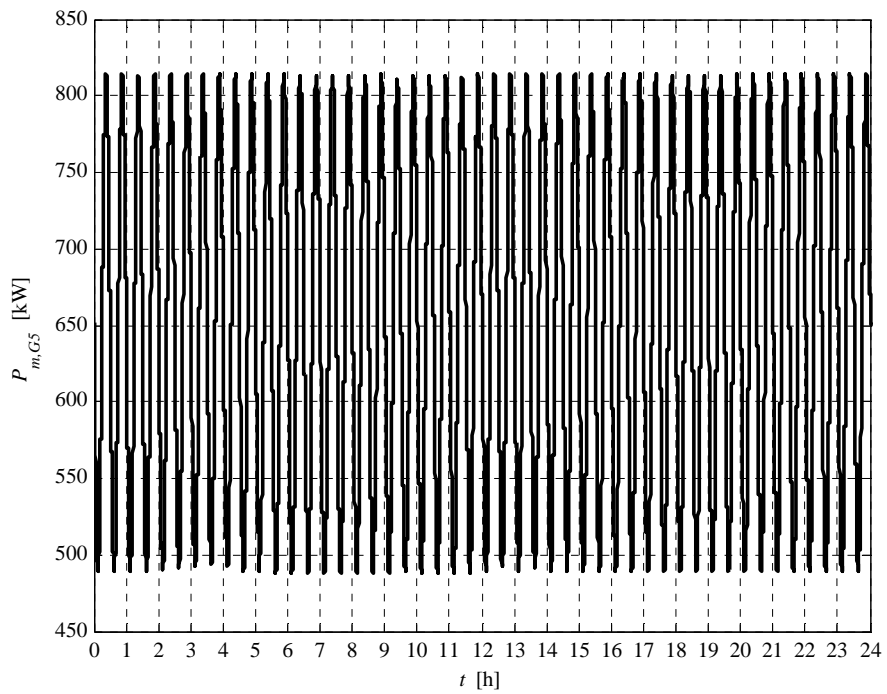
Fig. 5.6-5. G5 active power daily profile

117
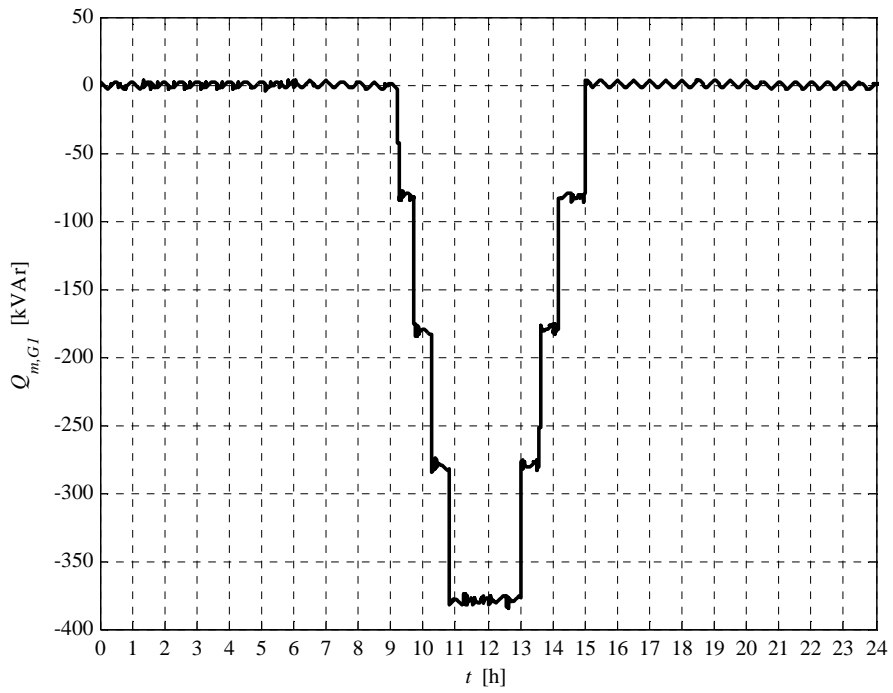
Fig. 5.6-6. G1 reactive power daily profile
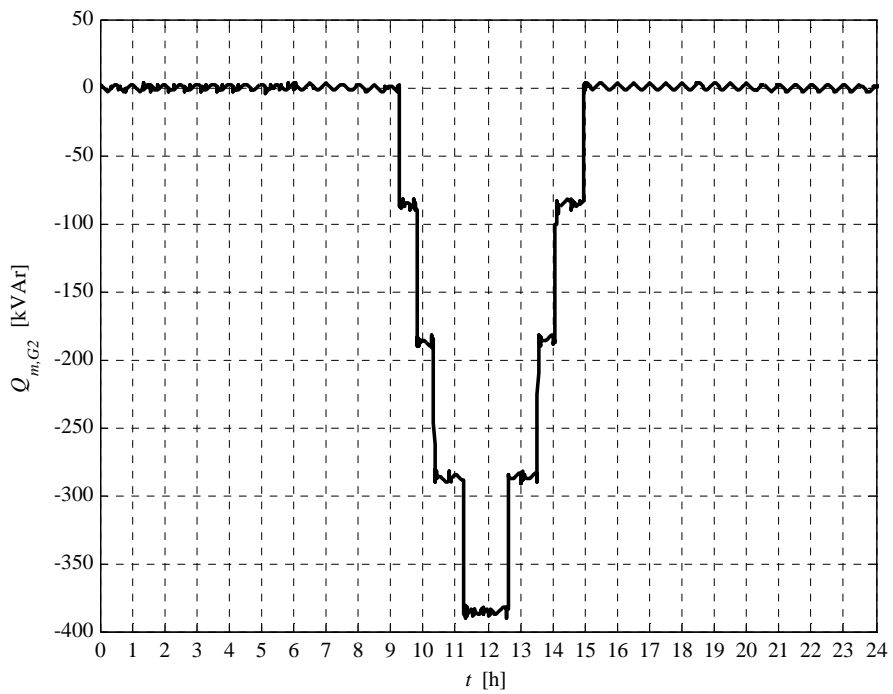
Fig. 5.6-7. G2 reactive power daily profile
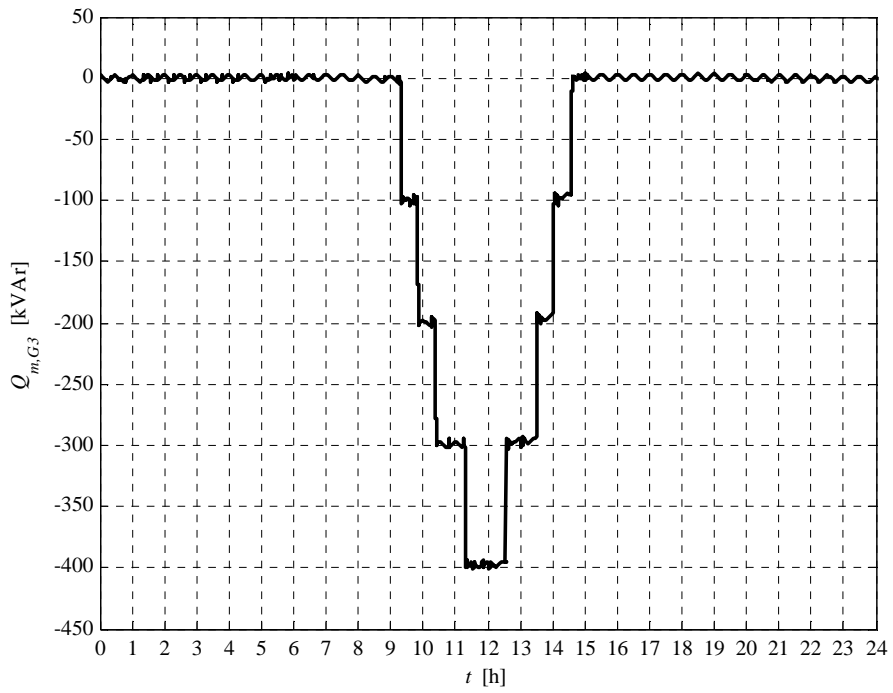
Fig. 5.6-8. G3 reactive power daily profile
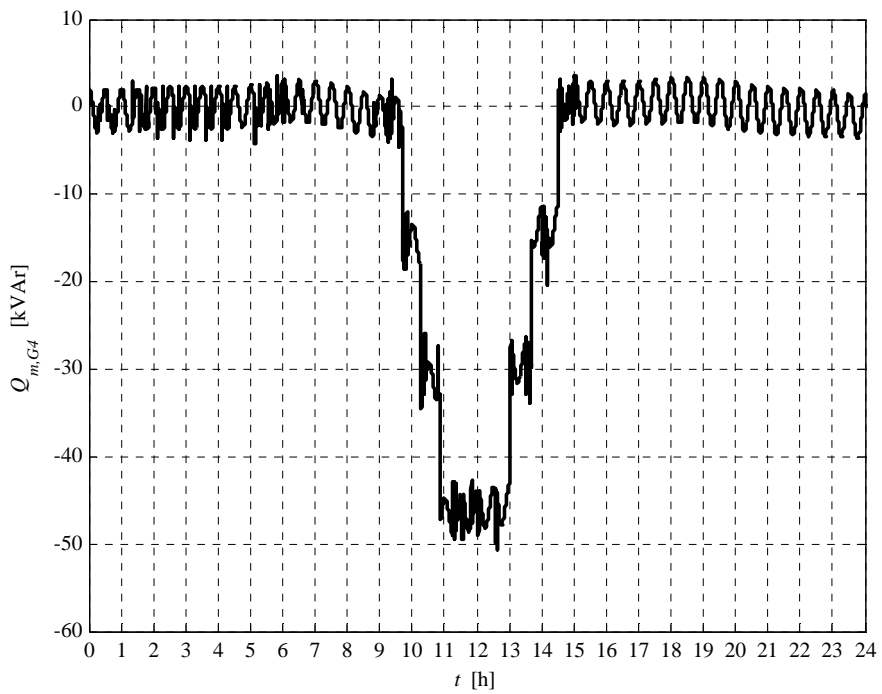
Fig. 5.6-9. G4 reactive power daily profile

119
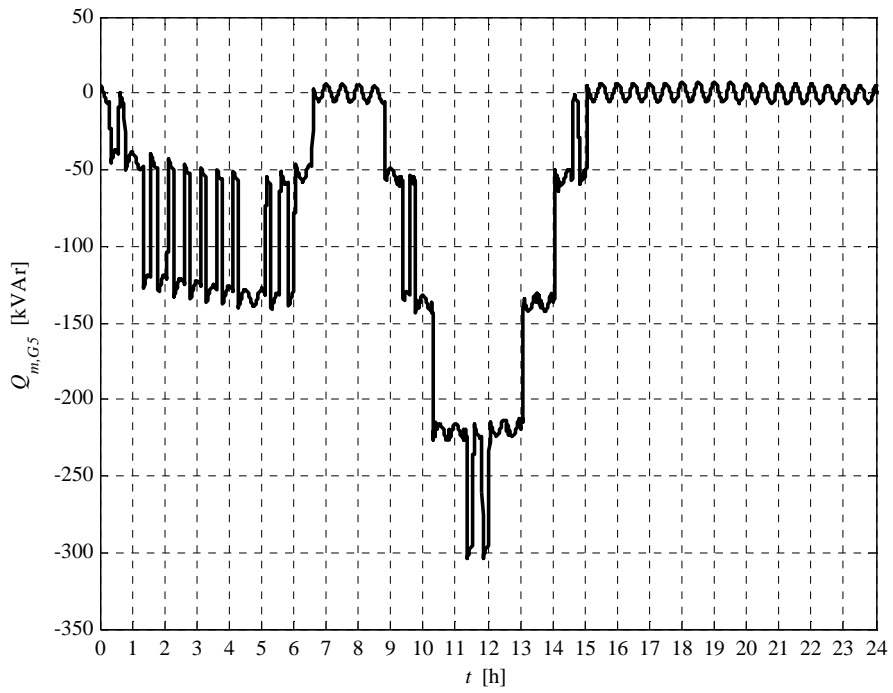
Fig. 5.6-10. G5 reactive power daily profile
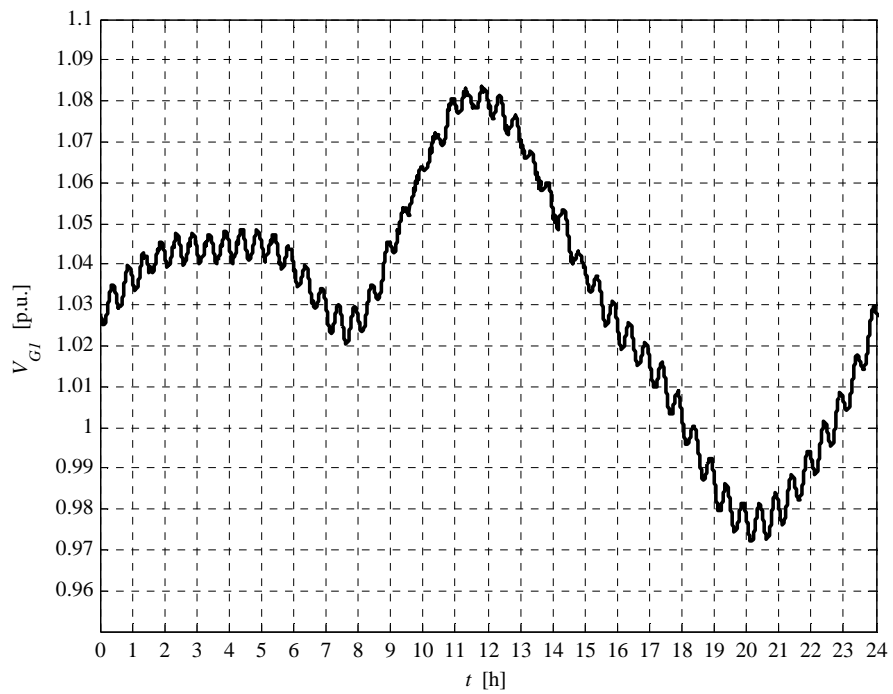
Fig. 5.6-11. G1 voltage daily profile

120
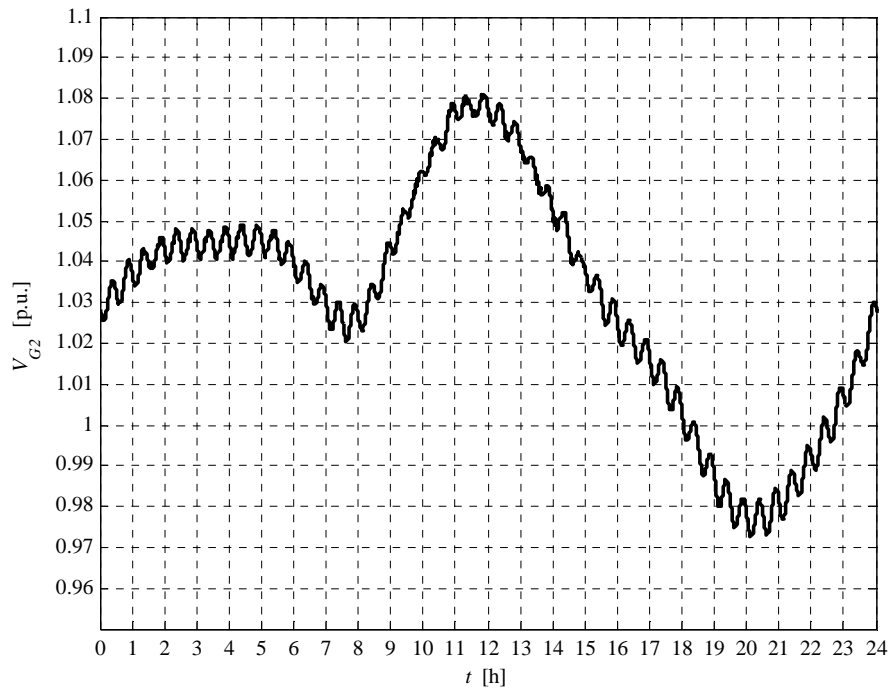
Fig. 5.6-12. G2 voltage daily profile
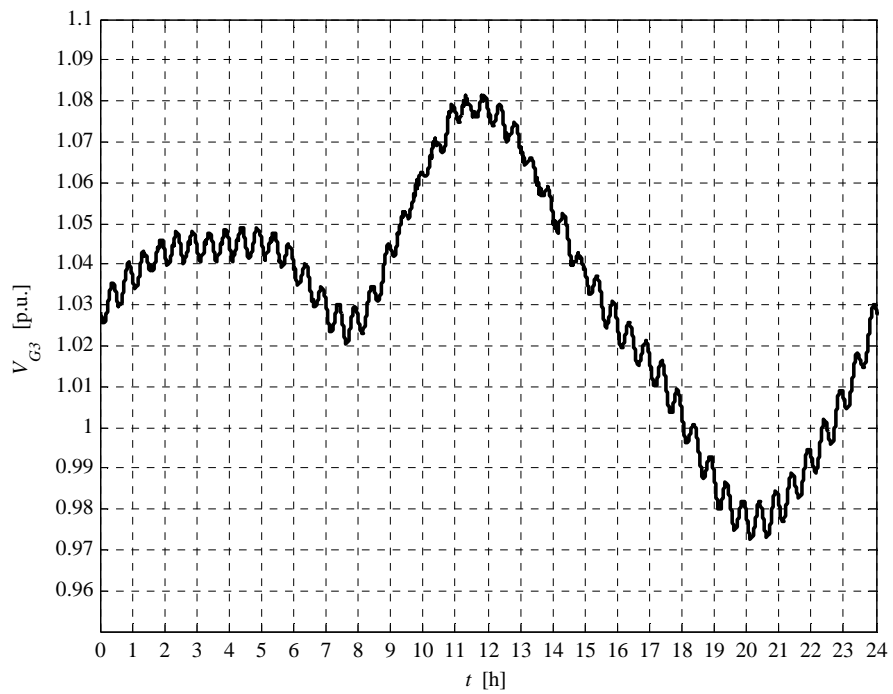
Fig. 5.6-13. G3 voltage daily profile

121
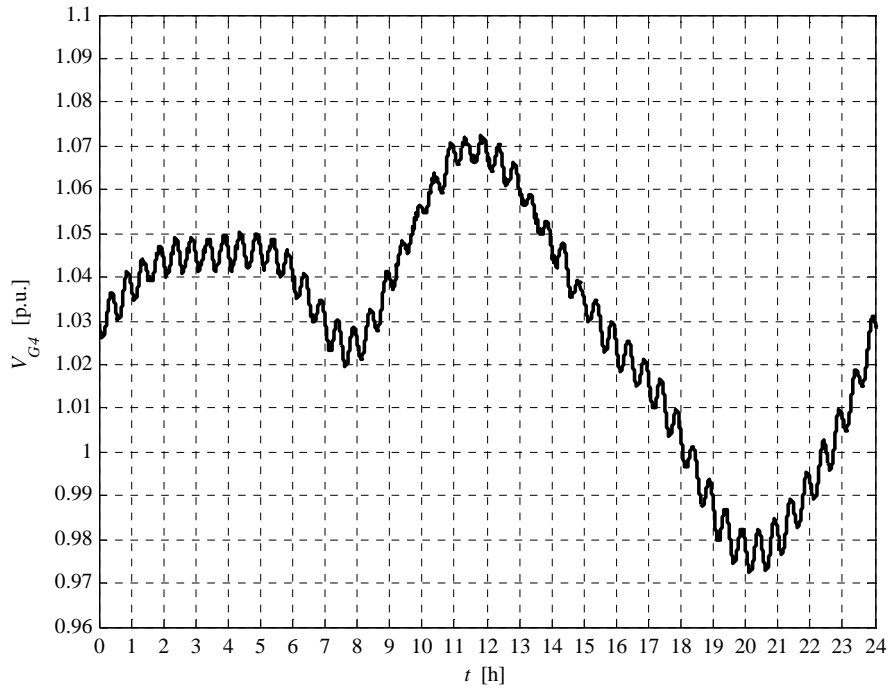
Fig. 5.6-14. G4 voltage daily profile
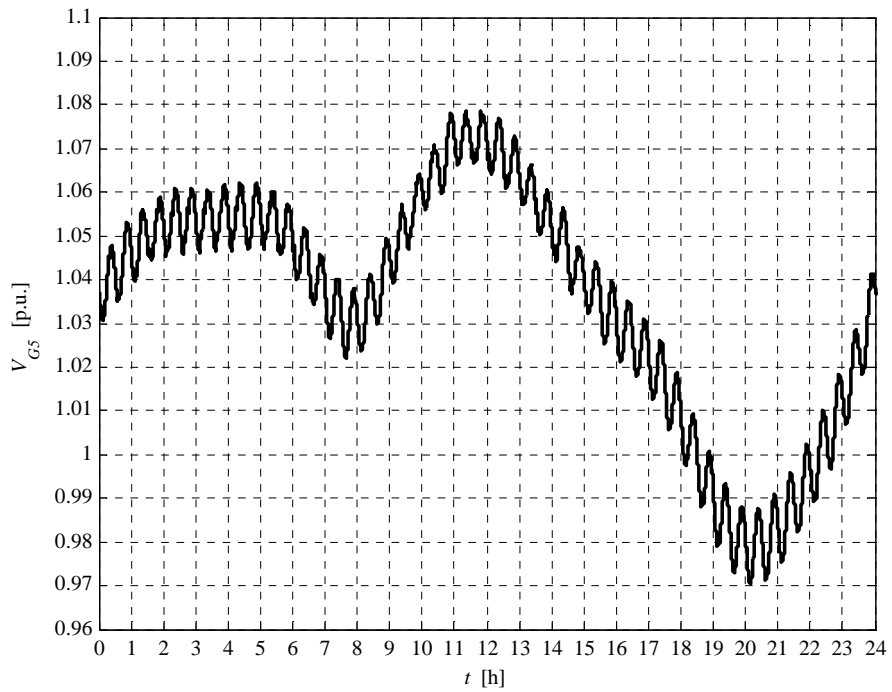
Fig. 5.6-15. G5 voltage daily profile

122
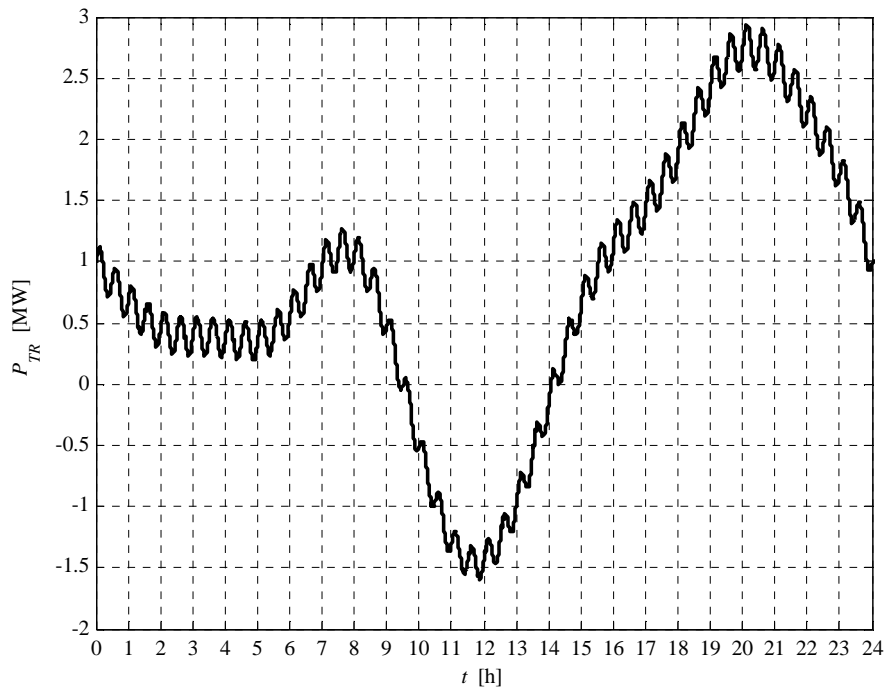
Fig. 5.6-16. HV/MV transformer daily active power profile
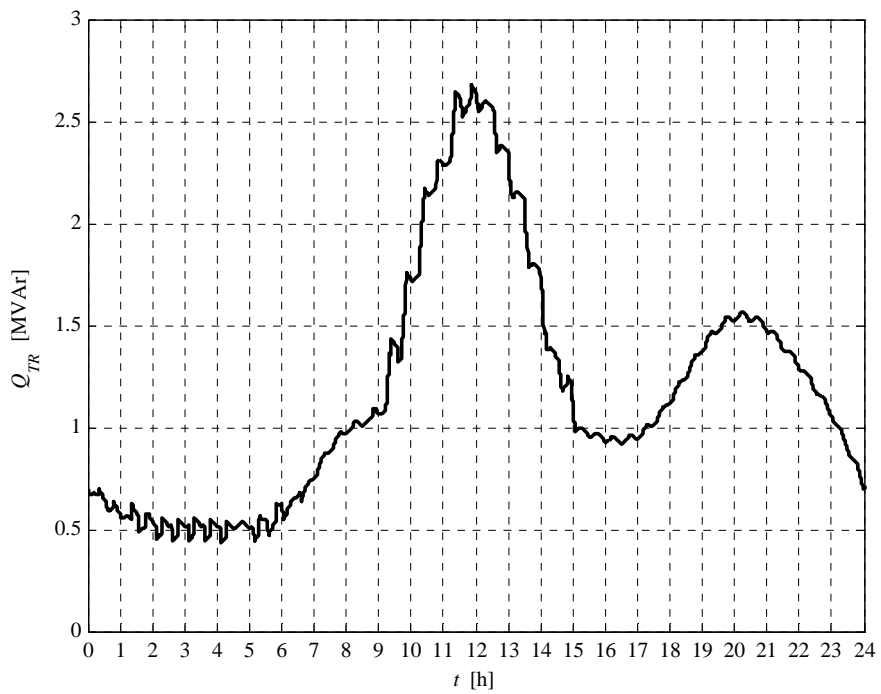
Fig. 5.6-17. HV/MV transformer daily reactive power profile
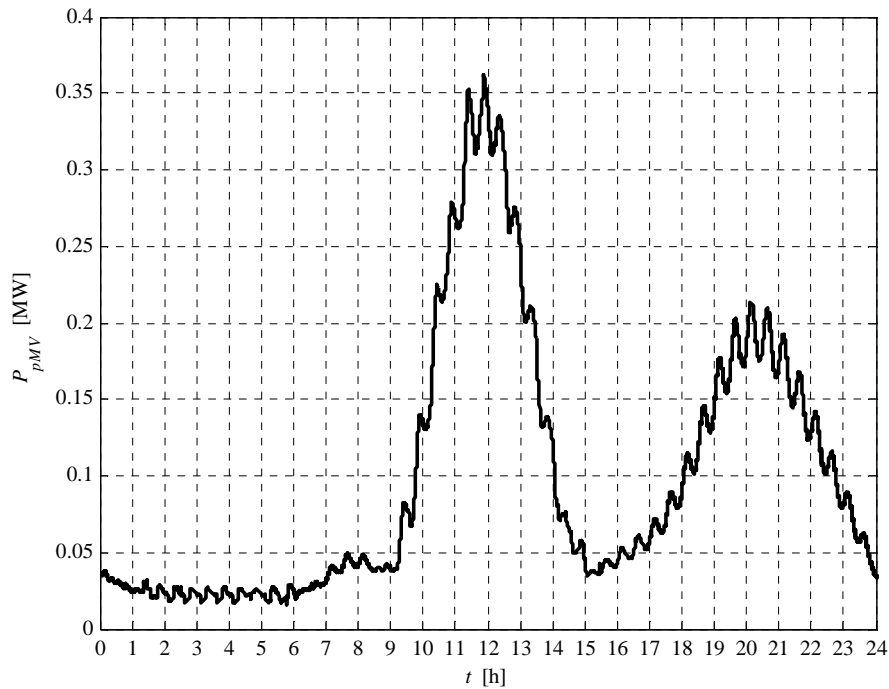
Fig. 5.6-18. MV network daily lost power profile

We can observe that the voltage daily profiles peak is limited by the local "RQV" voltage regulation action. The interface protection relay trip is impossible. However the "UPG" voltage regulation effect is better than the "RQV" one. In fact the node voltages in "RQV" regulation mode is slightly high then the "UPG" regulation case (0.01 p.u. difference). However the losses in "UPG" mode are greater that the "RQV" regulation case (0.3 % difference).

We can observe the HV/MV transformer active power inversion, due to the DG presence. The HV/MV transformer reactive power is characterized by an high peak, requested from the HV grid, due to the "RQV" local voltage regulation. In fact the reactive power requested from each generator must be supplied by the HV grid. The generators requested reactive power curve shape is "stepped" (when the "RQV" is active) because the "RQV" regulation is characterized by the voltage hysteresis. In this case reactive power is requested to generator G4 and G5 absorbs reactive power more than one time in the day. This phenomena occurs because the RQV voltage dead-band (1.04 p.u.) is less than the "UPG" activation voltage threshold (1.07 p.u.).

The power losses profile is characterized by two peaks. The first peak, which is the highest peak, is related to the generated power, the second one is due to the loads power.

The report, referred to this case, is:

```
Report case: 3

Maximum VG1 value = 1.0836 [p.u.]
Maximum VG2 value = 1.0811 [p.u.]
```

```
Maximum VG3 value = 1.0815 [p.u.]
Maximum VG4 value = 1.0722 [p.u.]
Maximum VG5 value = 1.0783 [p.u.]

Loads power daily peak = 3.2157 [MW]
Generators power daily peak = 3.9755 [MW]

Loads daily active energy (absorbed) = 49.2306 [MWh]
Generators daily active energy (generated) = 31.9846 [MWh]
Daily active energy absorbed from the HV grid = 19.6516 [MWh]
Daily lost active energy = 2.4056 [MWh]
Daily lost active energy (percentual) = 4.6587 [%]
```

We can observe a daily energy losses increment, if compared to the case 1.b, due to the DG reactive power request, in order to act the local "UPG" voltage regulation control. However the energy losses are less than the base case 1.a.

5.7 COMPARISON BETWEEN CASES 1.B, 2 AND 3

In order to graphically compare cases 1.b, 2 and 3, in terms of generators voltages and reactive powers, the following plots are presented.

Fig. 5.7-1. G1 voltage daily profile

Fig. 5.7-2. G2 voltage daily profile

Fig. 5.7-3. G3 voltage daily profile

126
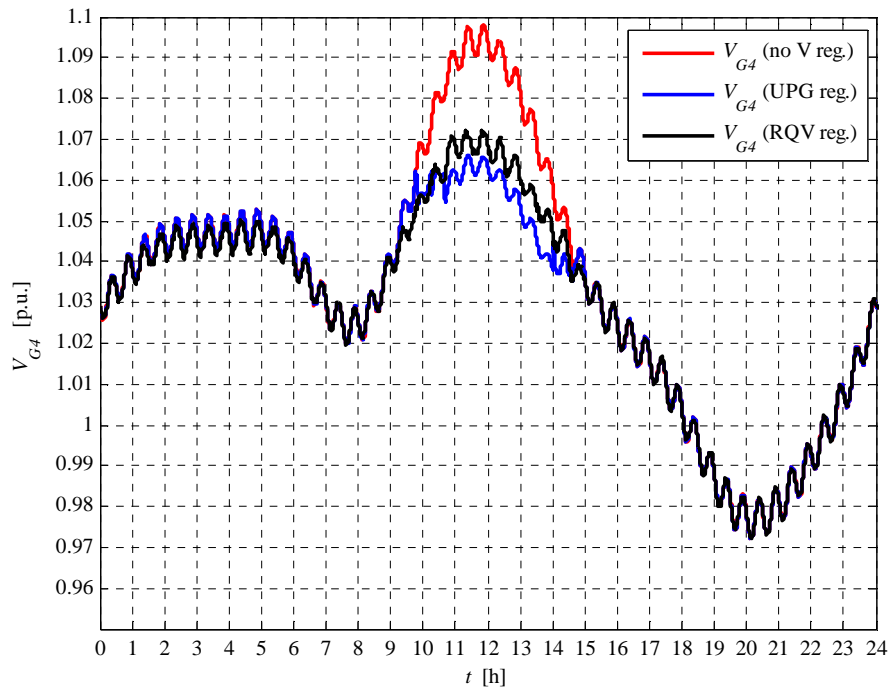
Fig. 5.7-4. G4 voltage daily profile
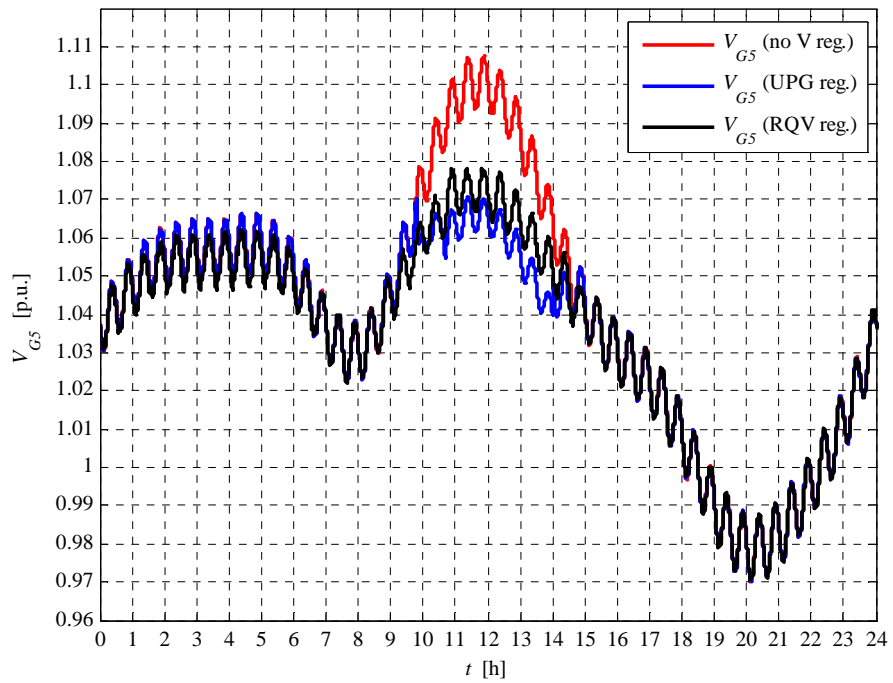
Fig. 5.7-5. G5 voltage daily profile
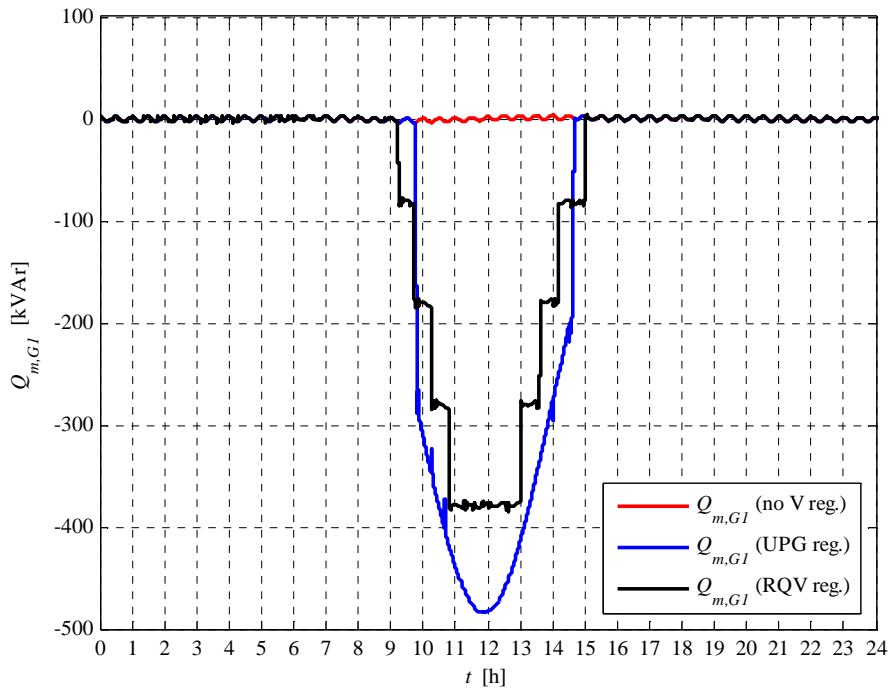
Fig. 5.7-6. G1 reactive power daily profile
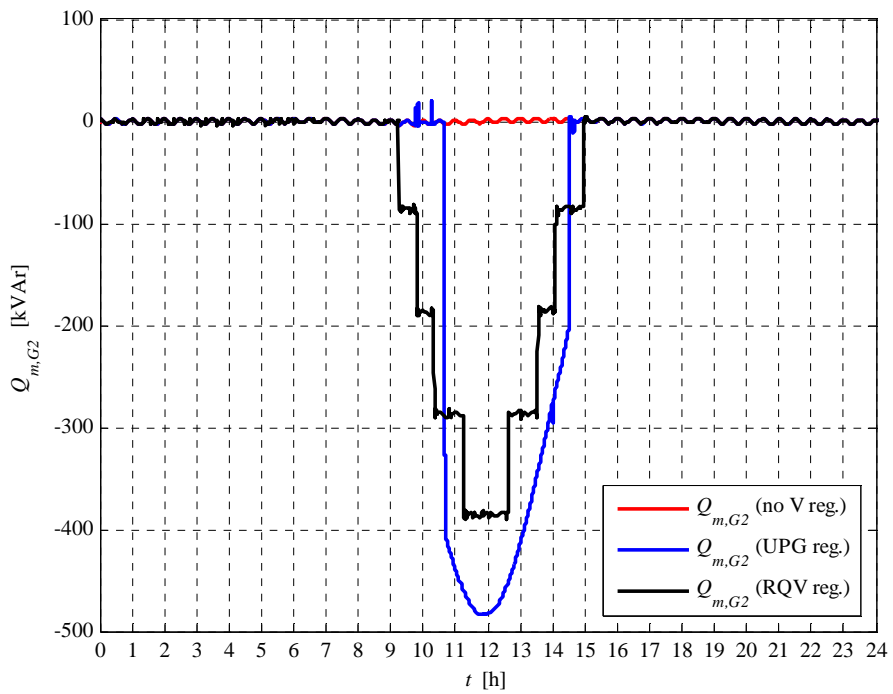
Fig. 5.7-7. G2 reactive power daily profile
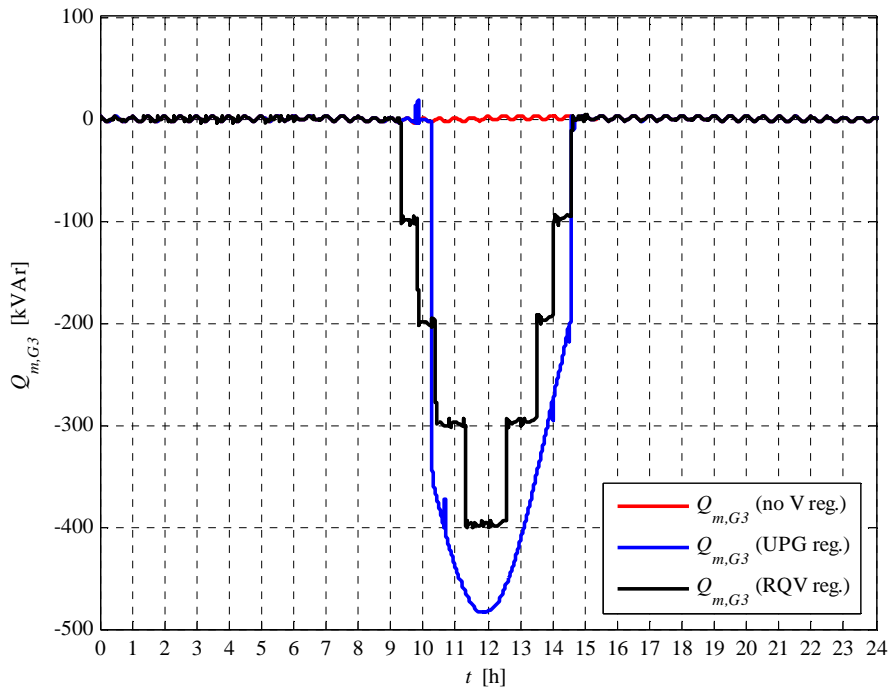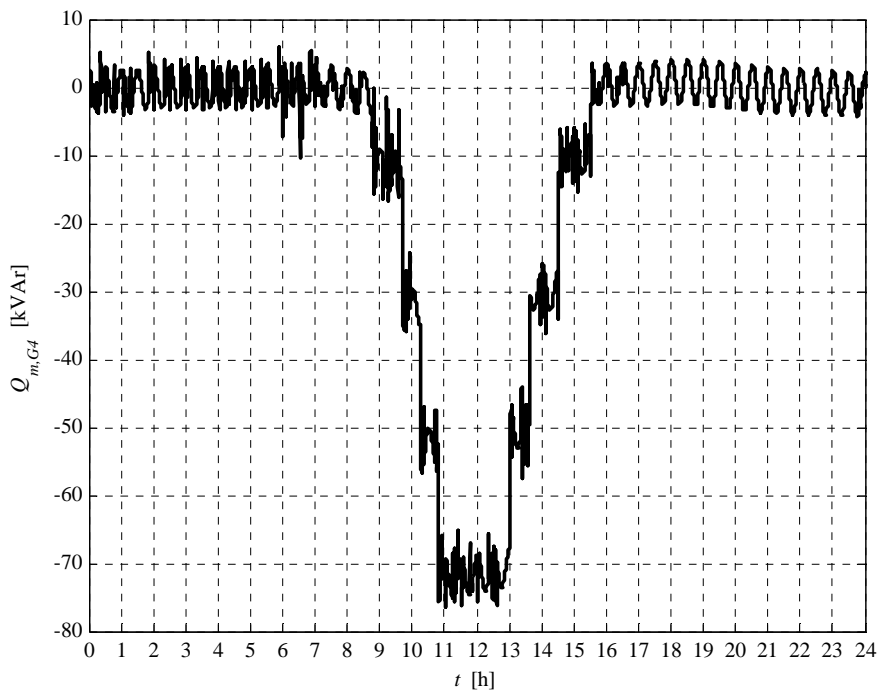
Fig. 5.7-8. G3 reactive power daily profile
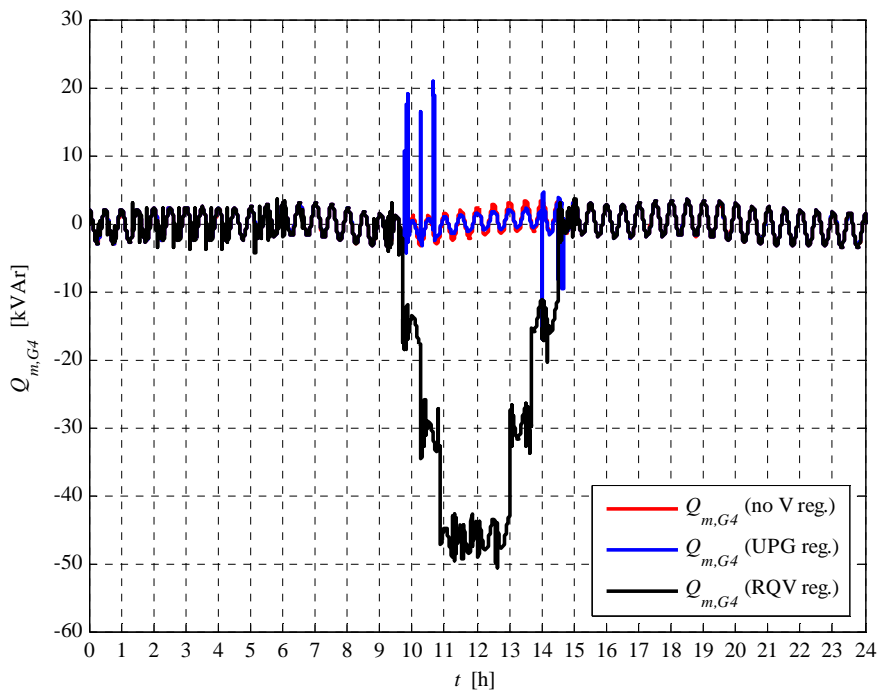
Fig. 5.7-9. G4 reactive power daily profile

129
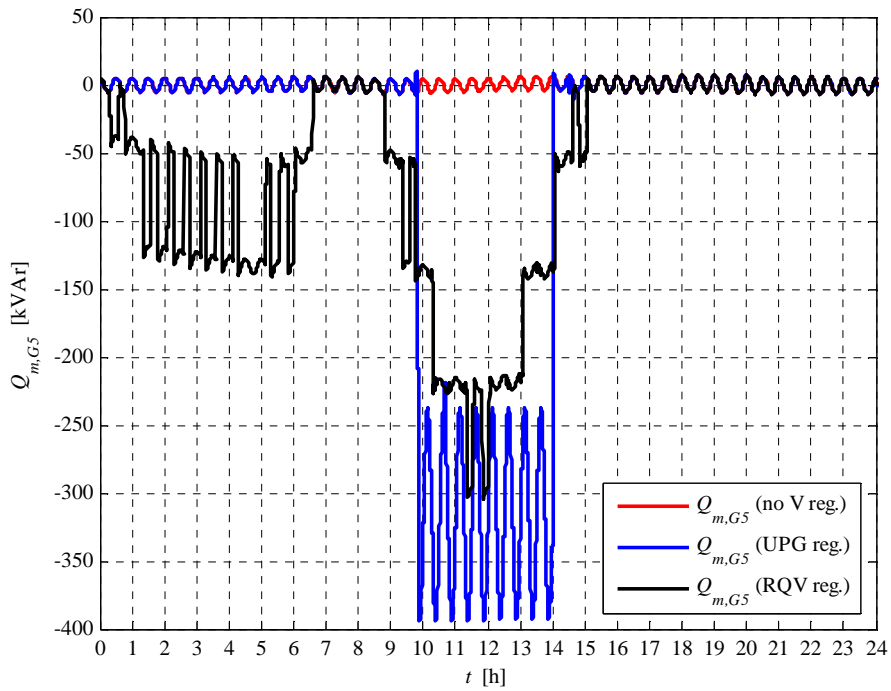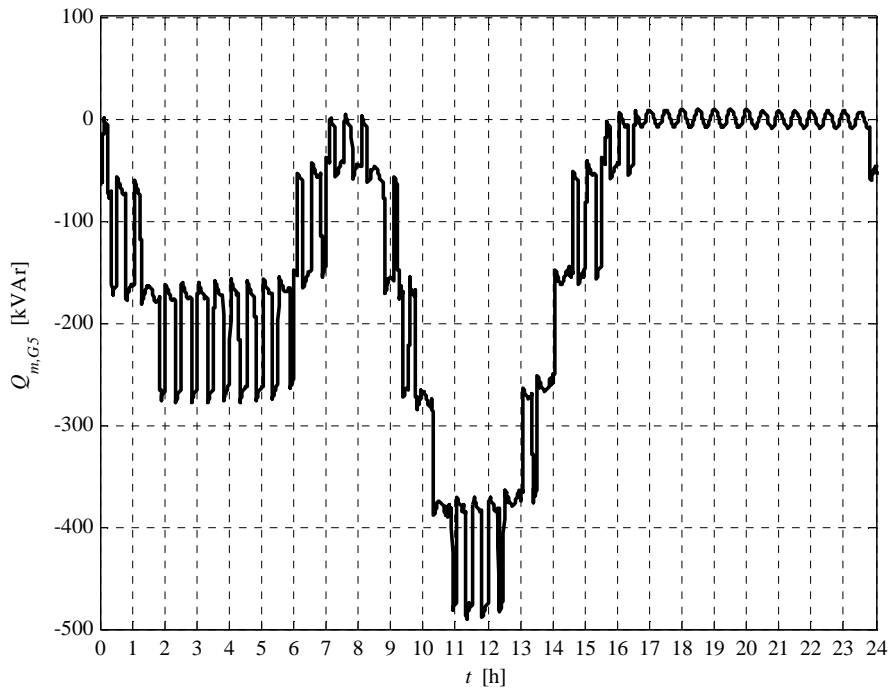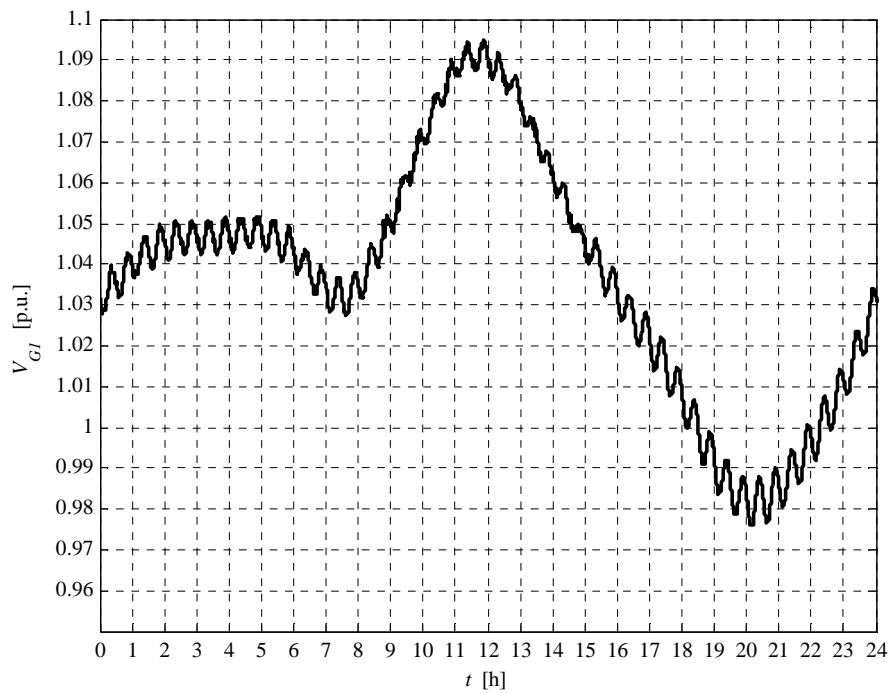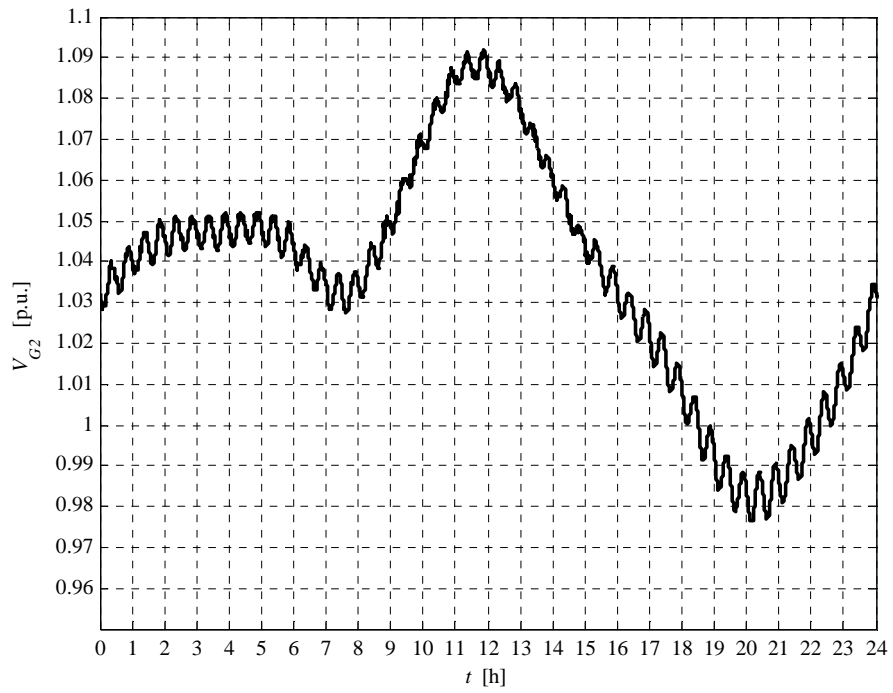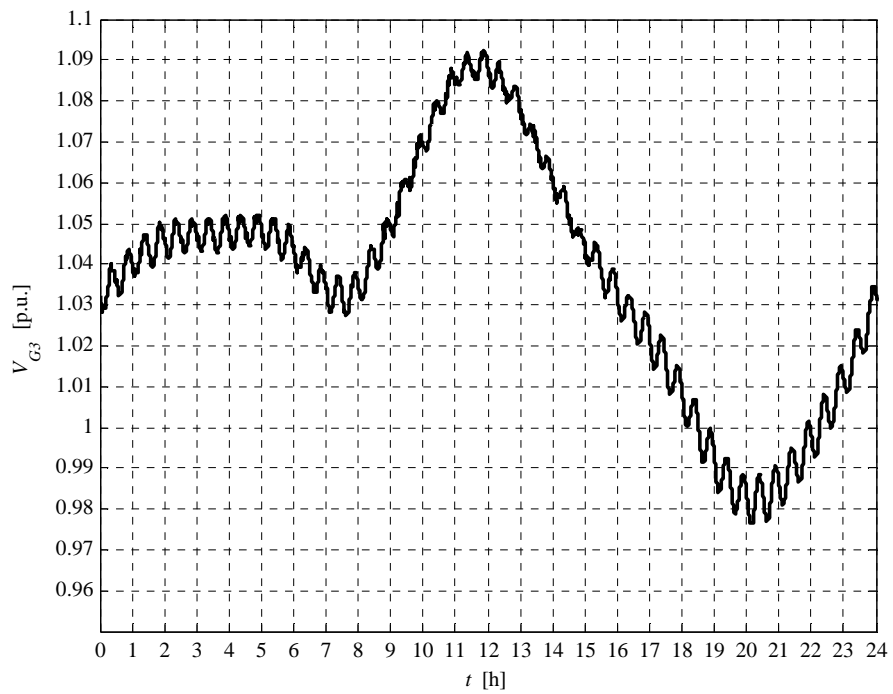
Fig. 5.7-10. G5 reactive power daily profile

5.8 CASE 4.A RESULTS

This case is necessary to define the hosting capacity increment when the "UPG" local voltage control is activated. The MV busbar voltage is fixed to 1.06 p.u. This set-point value guarantees the correct voltage in the critical node in the maximum load condition, when the generation is de-activated. The generated active power has been incremented (on each generator) in order to reach, in the highest voltage node, the value 1.09 p.u.

Fig. 5.8-1. G1 active power daily profile

Fig. 5.8-2. G2 active power daily profile

131

Fig. 5.8-3. G3 active power daily profile

Fig. 5.8-4. G4 active power daily profile

Fig. 5.8-5. G5 active power daily profile

Fig. 5.8-6. G1 reactive power daily profile
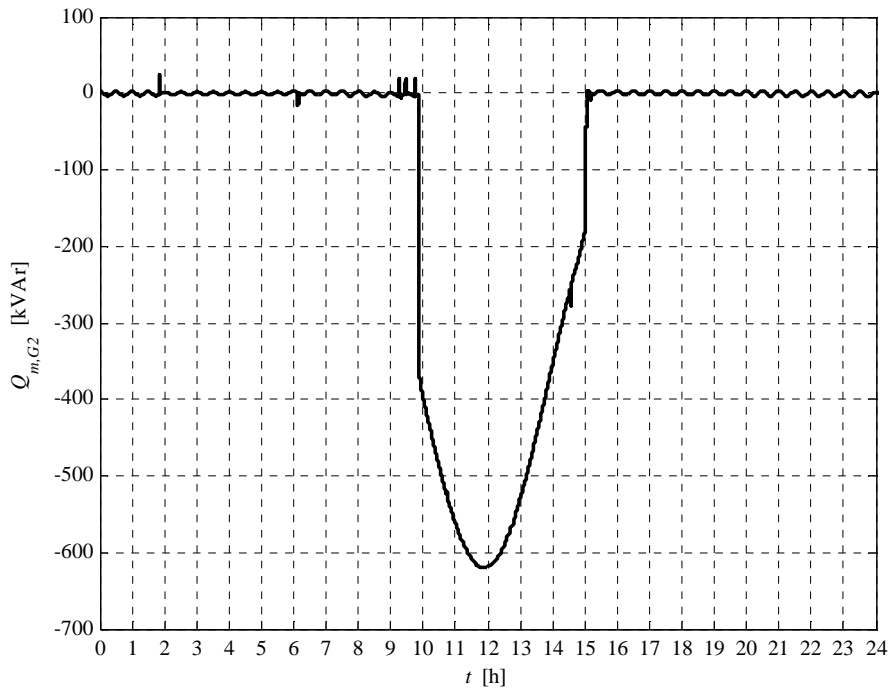
Fig. 5.8-7. G2 reactive power daily profile
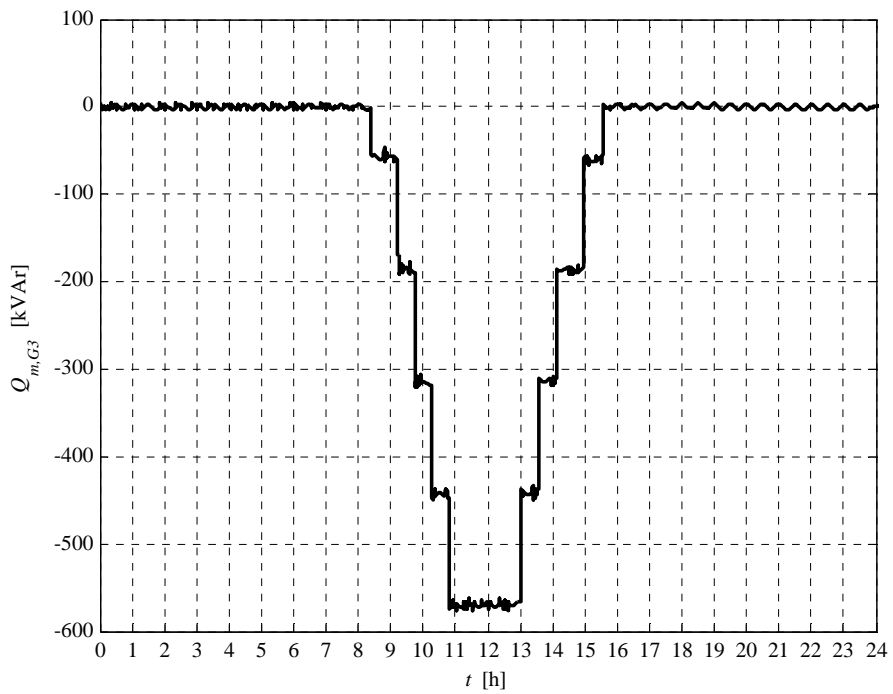
Fig. 5.8-8. G3 reactive power daily profile

134
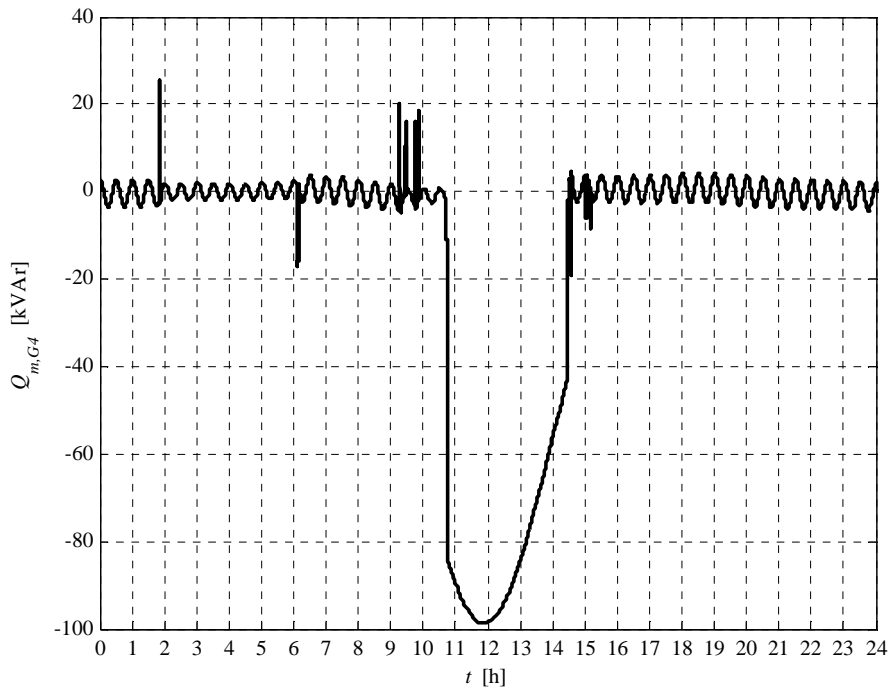
Fig. 5.8-9. G4 reactive power daily profile
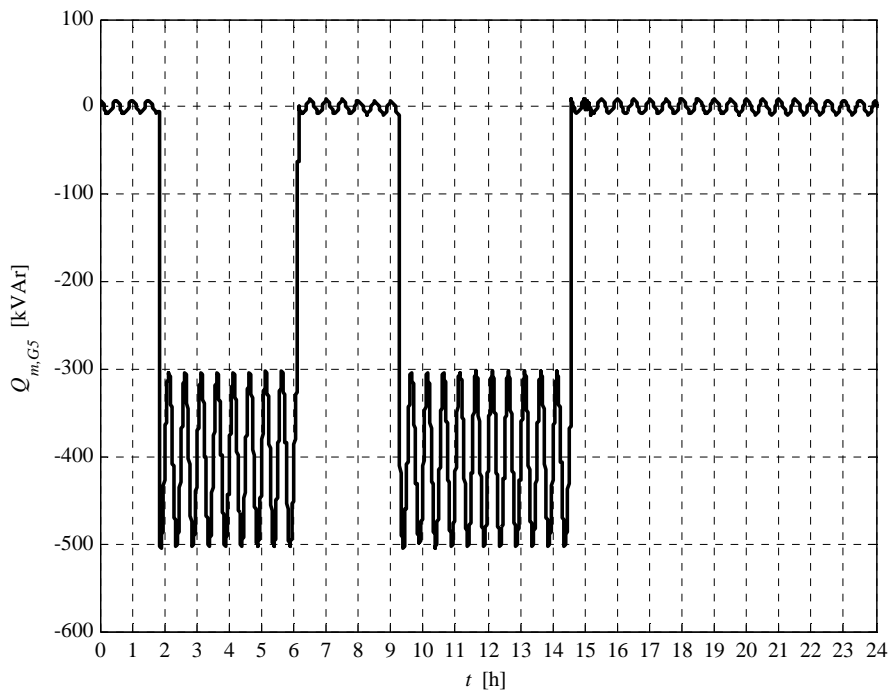
Fig. 5.8-10. G5 reactive power daily profile

135

Fig. 5.8-11. G1 voltage daily profile

Fig. 5.8-12. G2 voltage daily profile
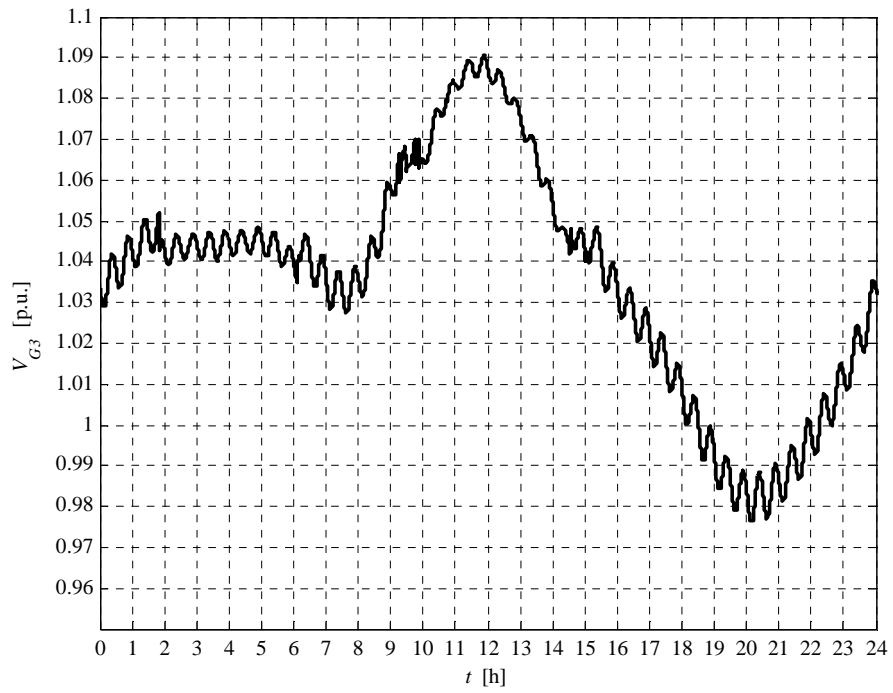
Fig. 5.8-13. G3 voltage daily profile
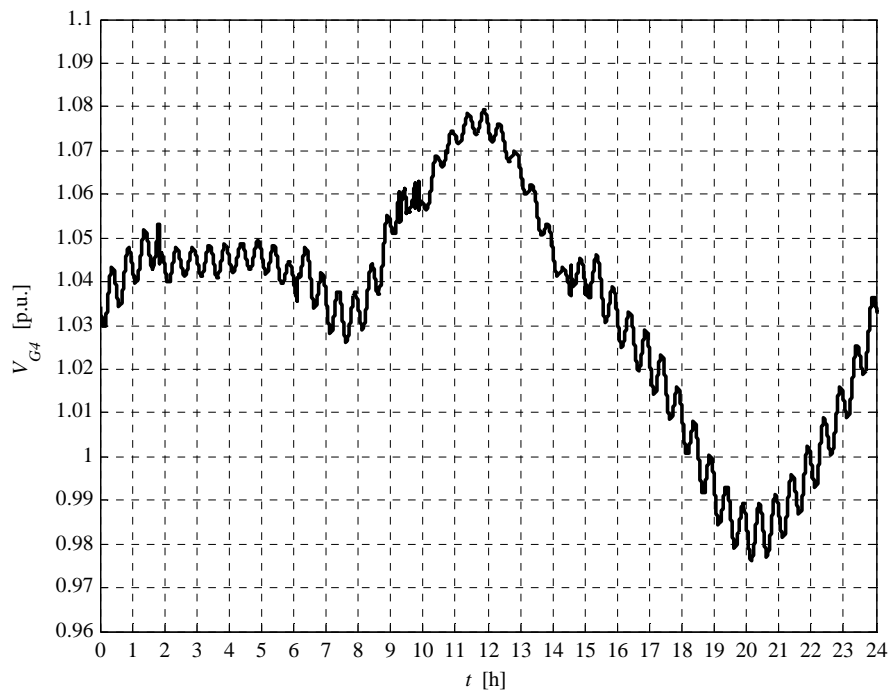
Fig. 5.8-14. G4 voltage daily profile

137
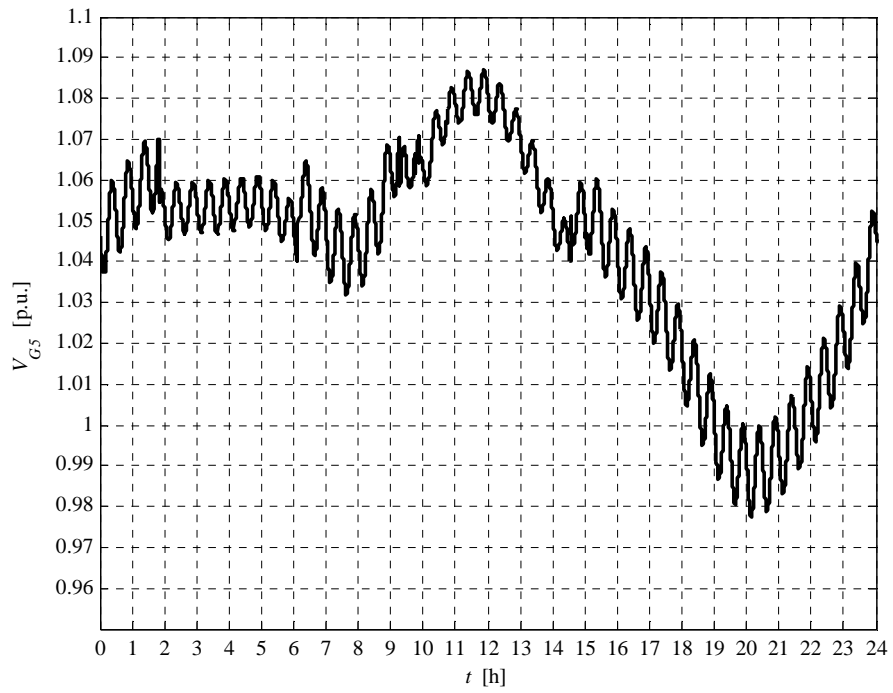
Fig. 5.8-15. G5 voltage daily profile
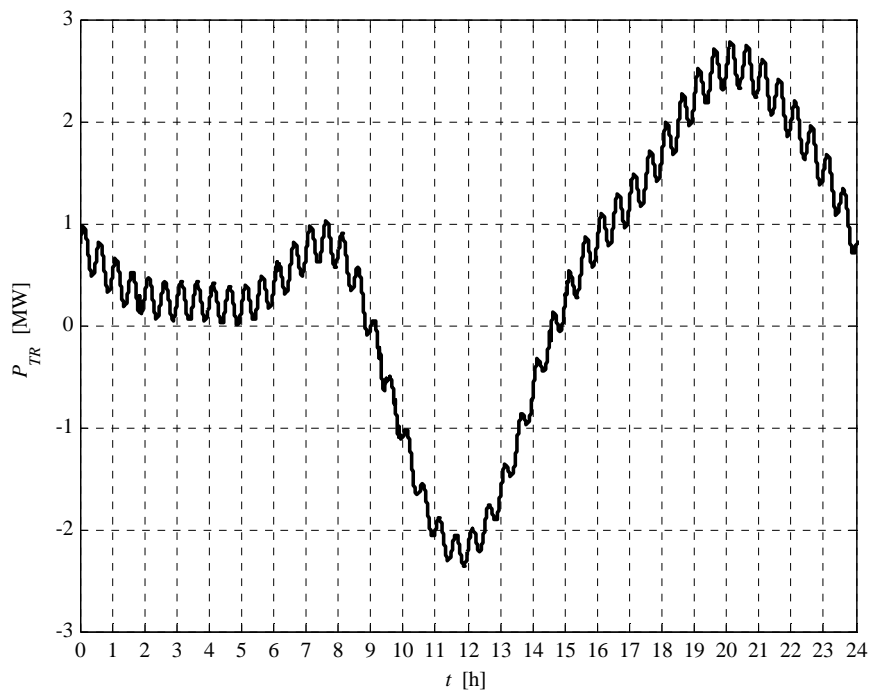
Fig. 5.8-16. HV/MV transformer daily active power profile
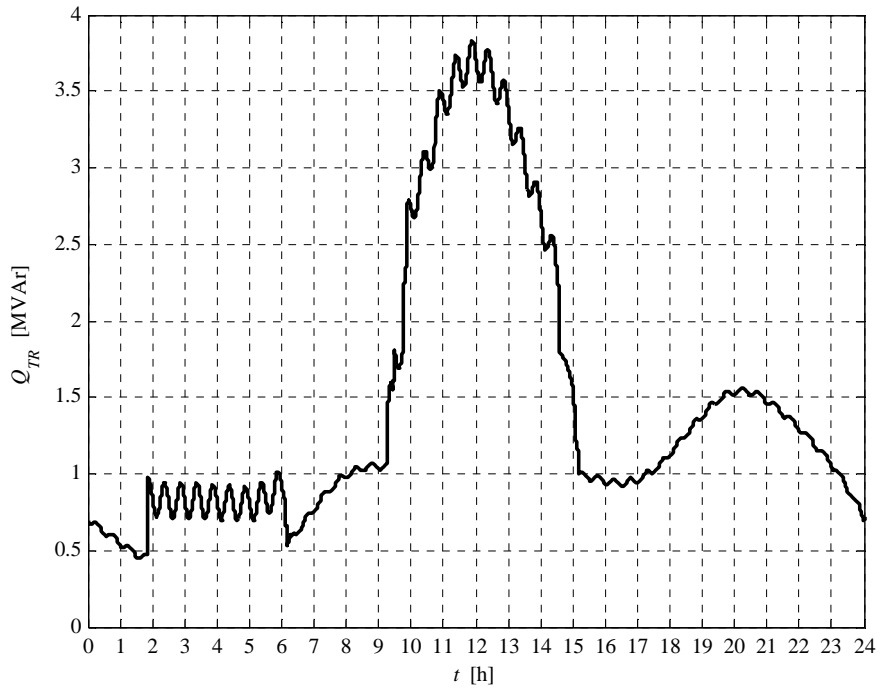
Fig. 5.8-17. HV/MV transformer daily reactive power profile
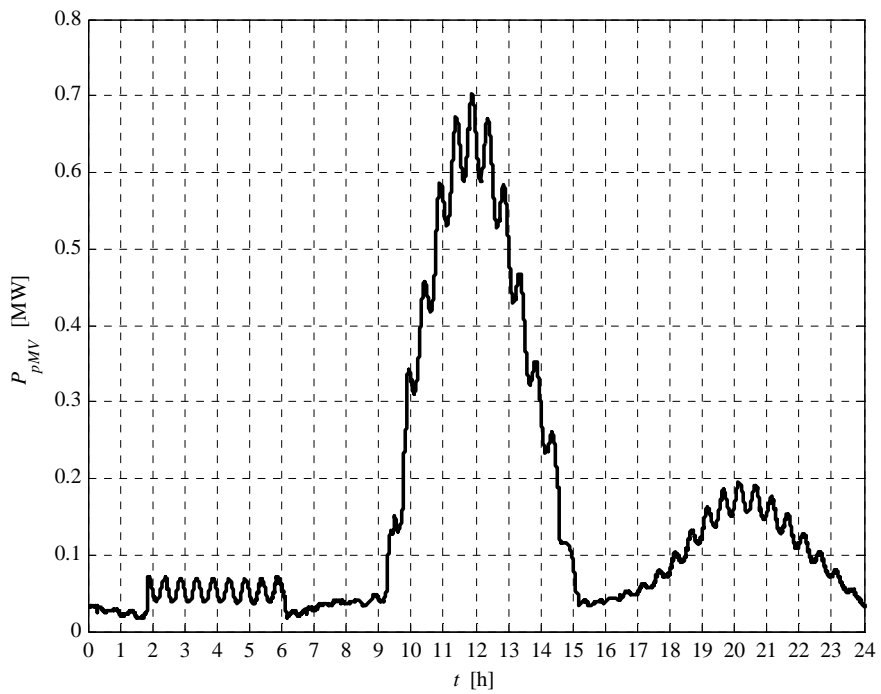
Fig. 5.8-18. MV network daily lost power profile

We can observe that the voltage rising, due to the generated active power increment, is compensated by the "UPG" local voltage regulation. This phenomenon increments the line hosting capacity. This hosting capacity increment is 28 %.

The report, referred to this case, is:

```
Report case: 4.a

Maximum VG1 value = 1.0929 [p.u.]
Maximum VG2 value = 1.0899 [p.u.]
Maximum VG3 value = 1.0904 [p.u.]
Maximum VG4 value = 1.0792 [p.u.]
Maximum VG5 value = 1.0871 [p.u.]


Loads power daily peak = 3.2157 [MW]
Generators power daily peak = 5.0826 [MW]


Loads daily active energy (absorbed) = 49.2306 [MWh]
Generators daily active energy (generated) = 40.9181 [MWh]
Daily active energy absorbed from the HV grid = 11.9779 [MWh]
Daily lost active energy = 3.6654 [MWh]
Daily lost active energy (percentual) = 6.9294 [%]
```

It is important to note the losses increment, if compared to the case 2. This phenomenon is due to the increment of both generated active power and requested reactive power, necessary to the "UPG" voltage regulation. We can also observe a losses increment due to the generated power growth.

5.9 CASE 4.B RESULTS

This case is necessary to define the hosting capacity increment when the "RQV" local voltage control is activated. The MV busbar voltage is fixed to 1.06 p.u. This set-point value guarantees the correct voltage in the critical node in the maximum load condition, when the generation is de-activated. The generated active power has been incremented (on each generator) in order to reach, in the highest voltage node, the value 1.09 p.u.

As reported in the following report, the hosting capacity with the "RQV" regulation is similar to which can be obtained with the "UPG" case (case 4.a). Then the generators active power curves will not be plotted (see case 4.a).
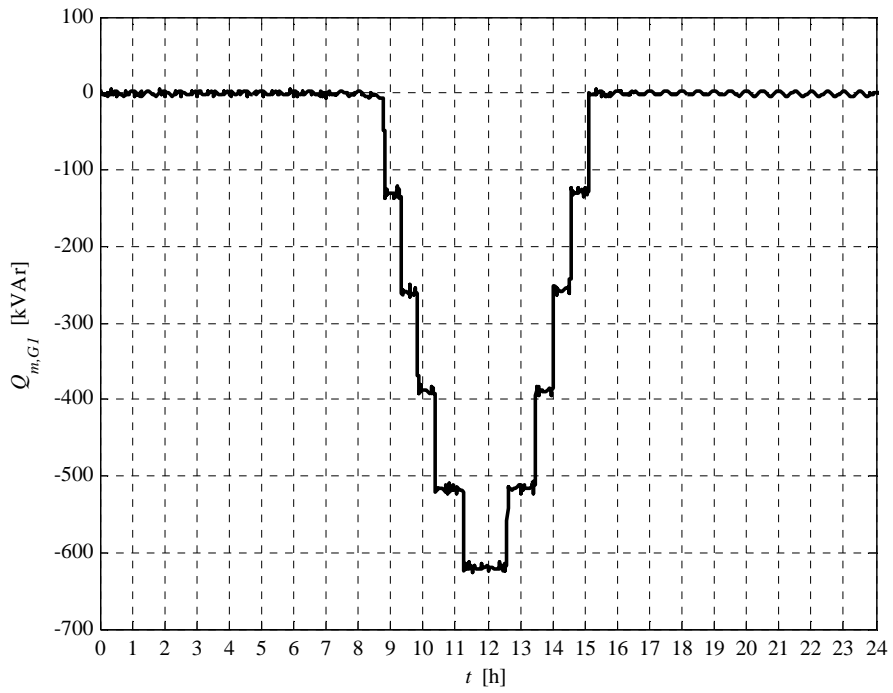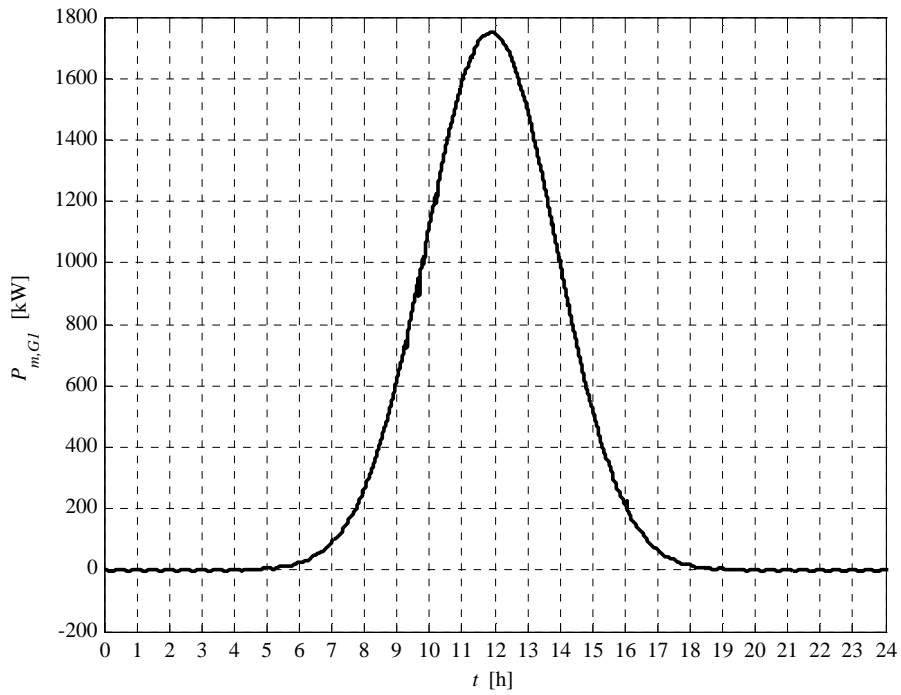
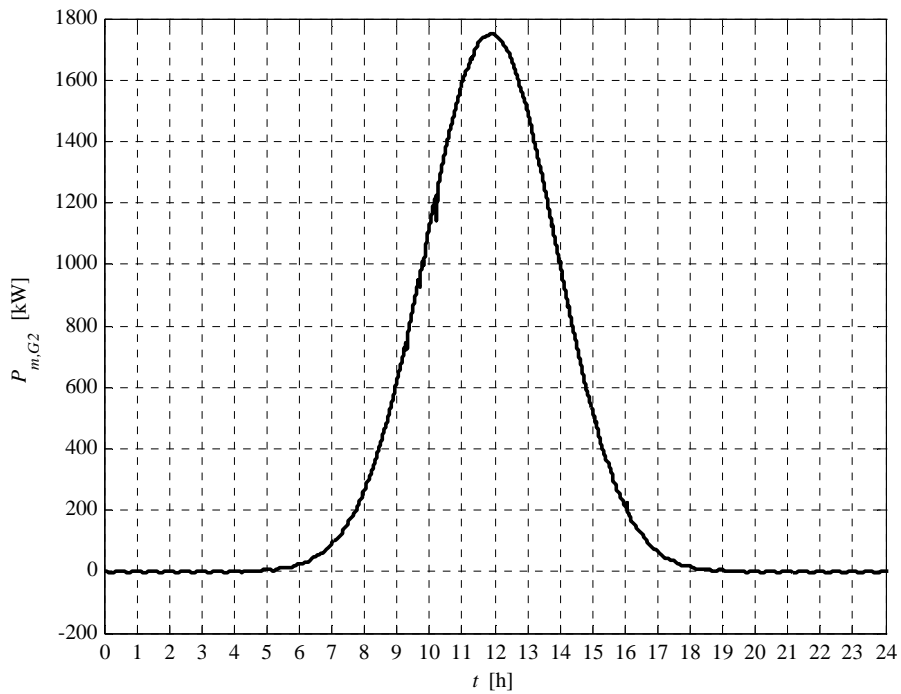**Fig. 5.9-1. G1 reactive power daily profile**
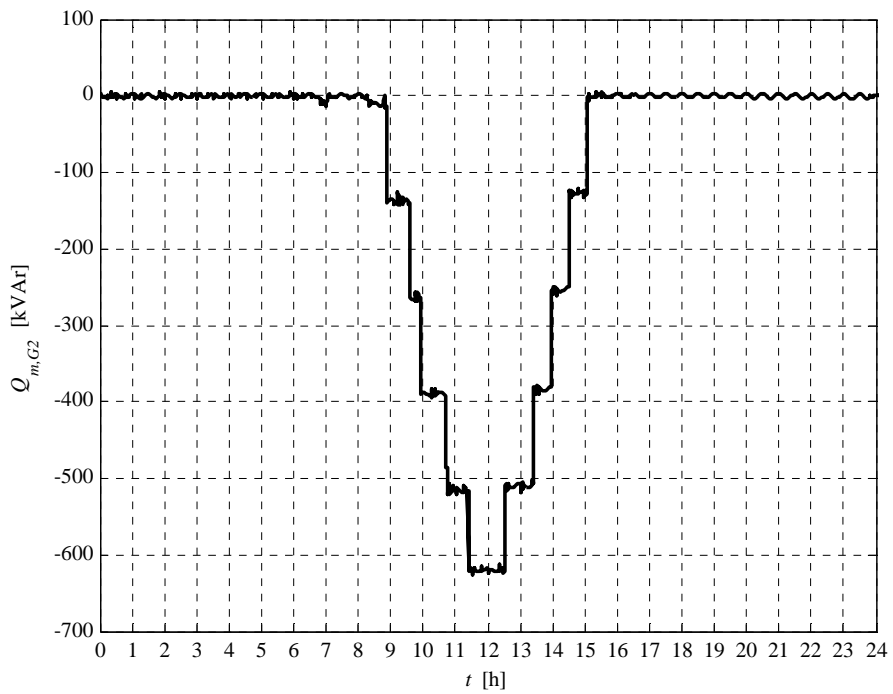
Fig. 5.9-2. G2 reactive power daily profile
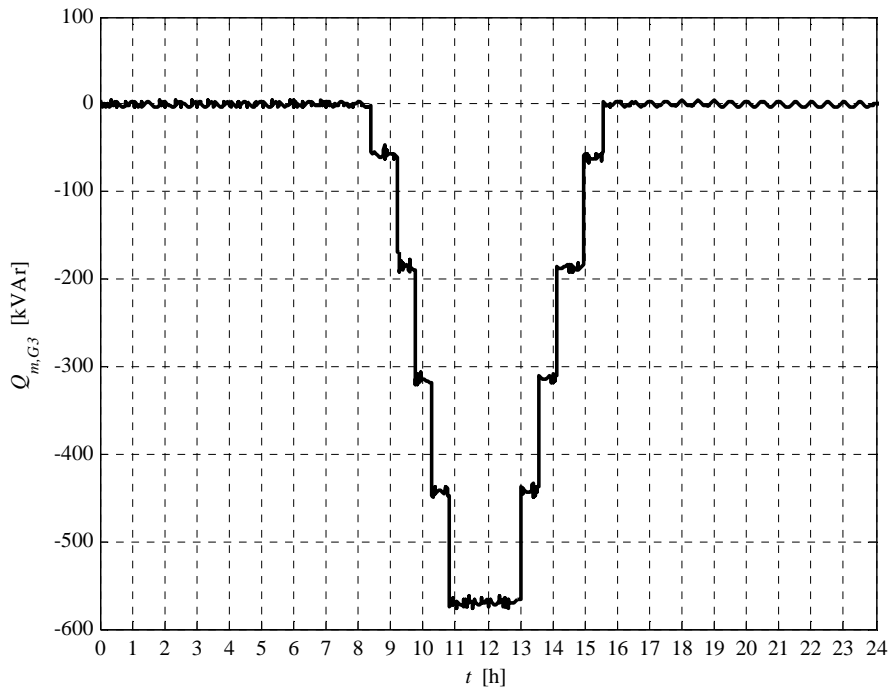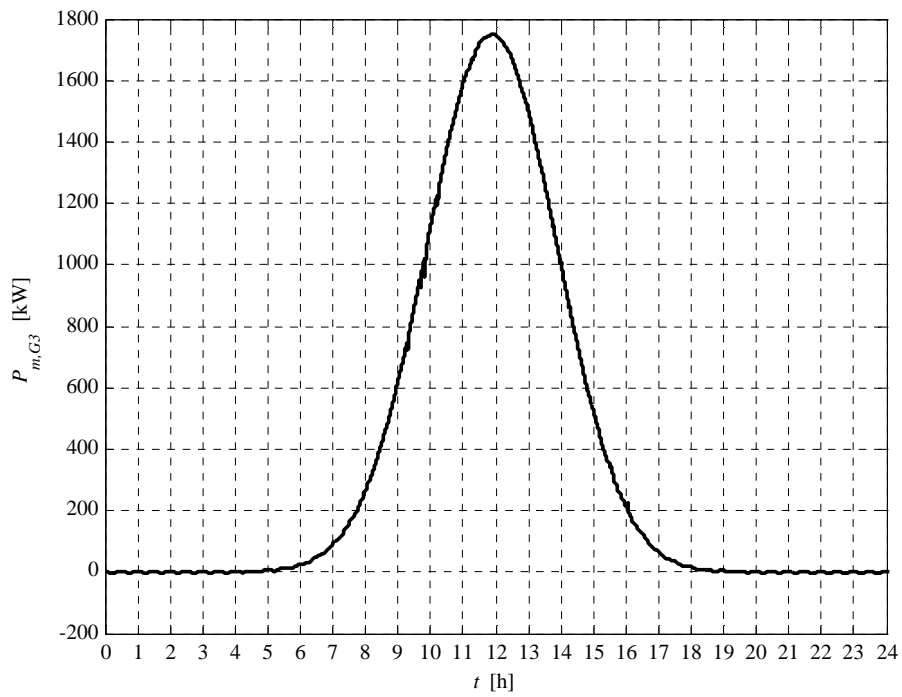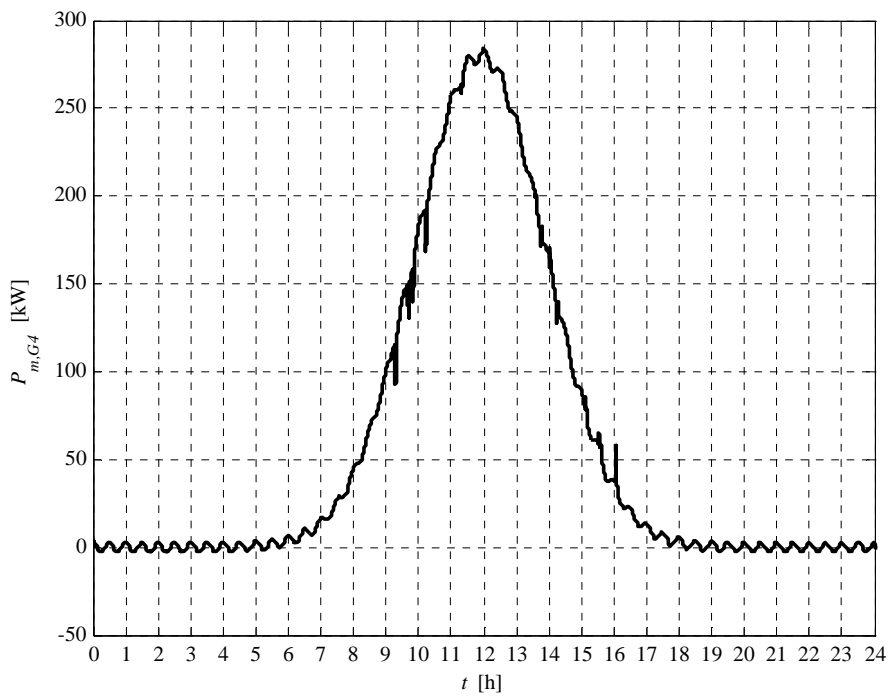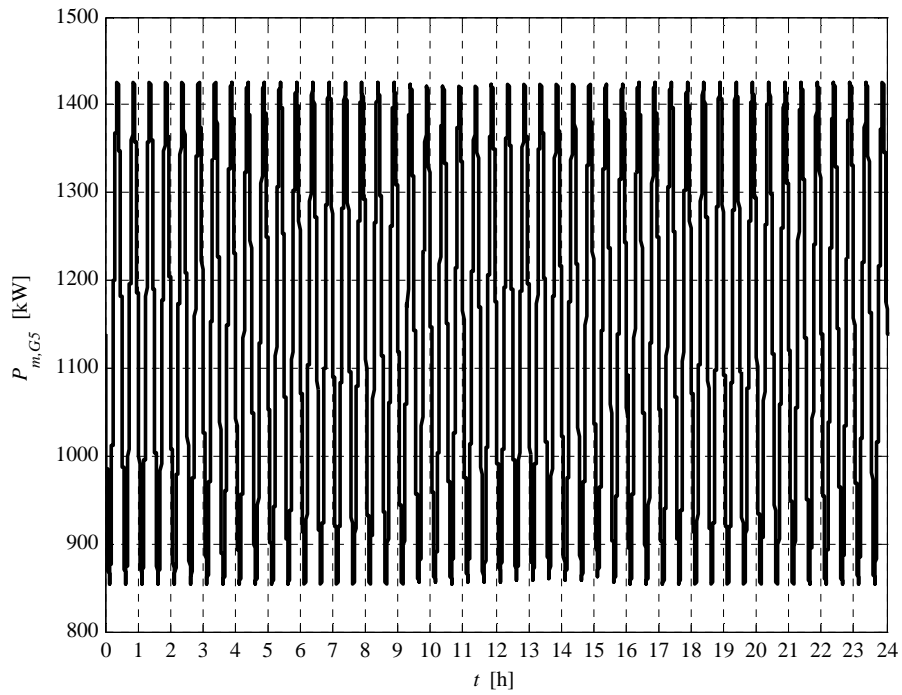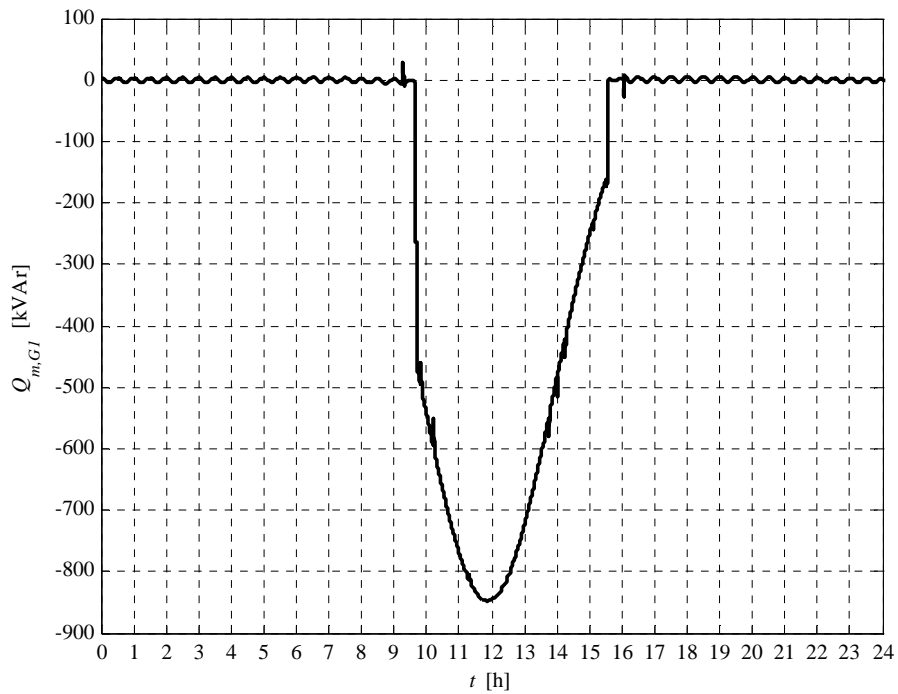
Fig. 5.9-3. G3 reactive power daily profile

Fig. 5.9-4. G4 reactive power daily profile

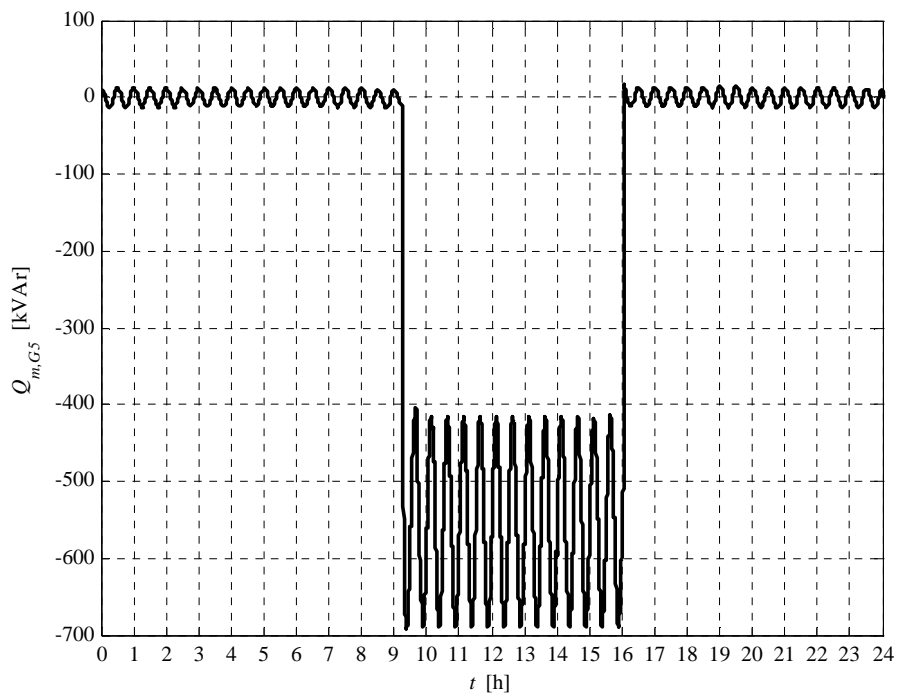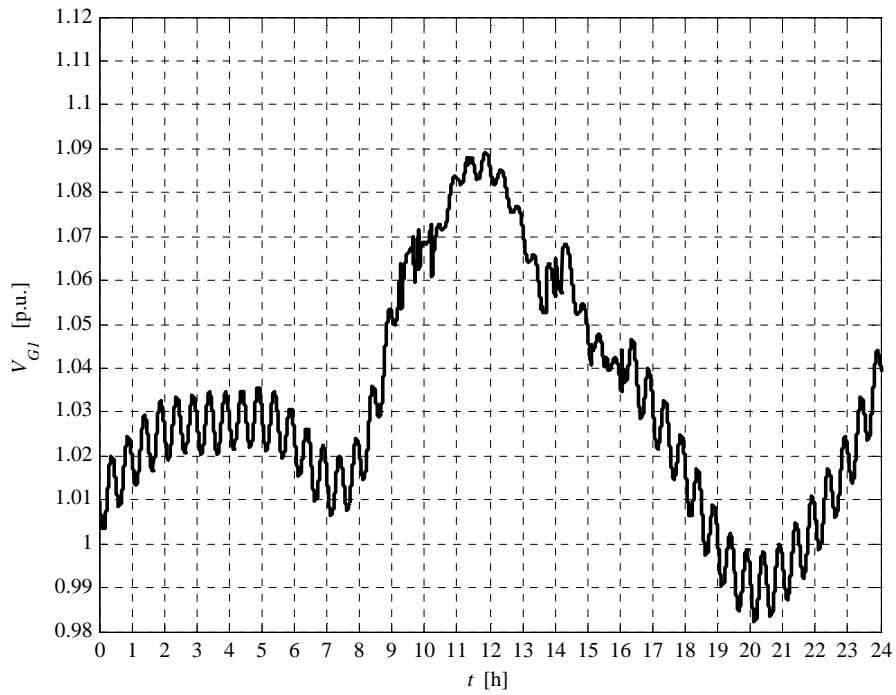**Fig. 5.9-5. G5 reactive power daily profile**

Fig. 5.9-6. G1 voltage daily profile

Fig. 5.9-7. G2 voltage daily profile

Fig. 5.9-8. G3 voltage daily profile
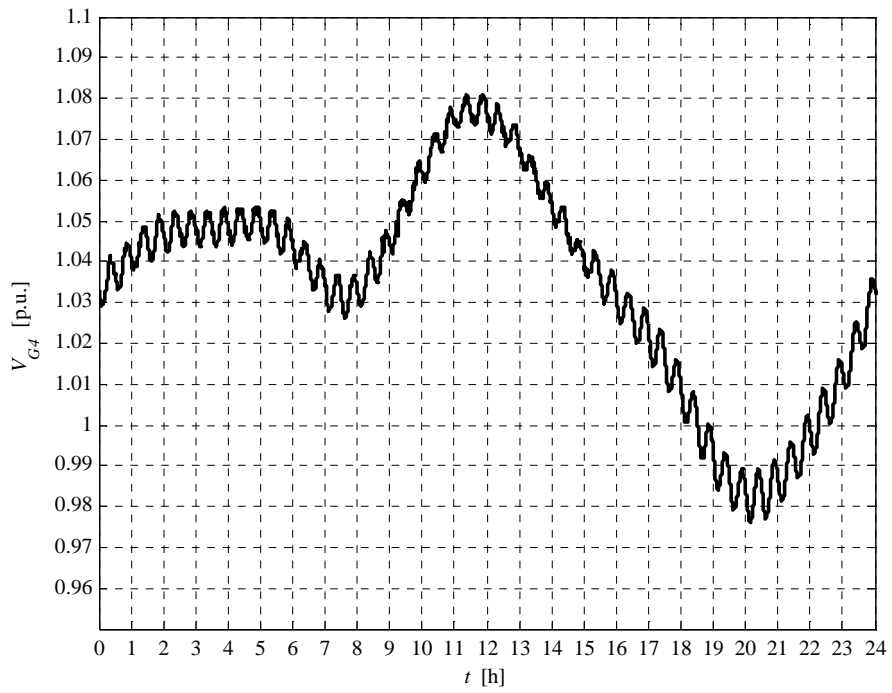
Fig. 5.9-9. G4 voltage daily profile
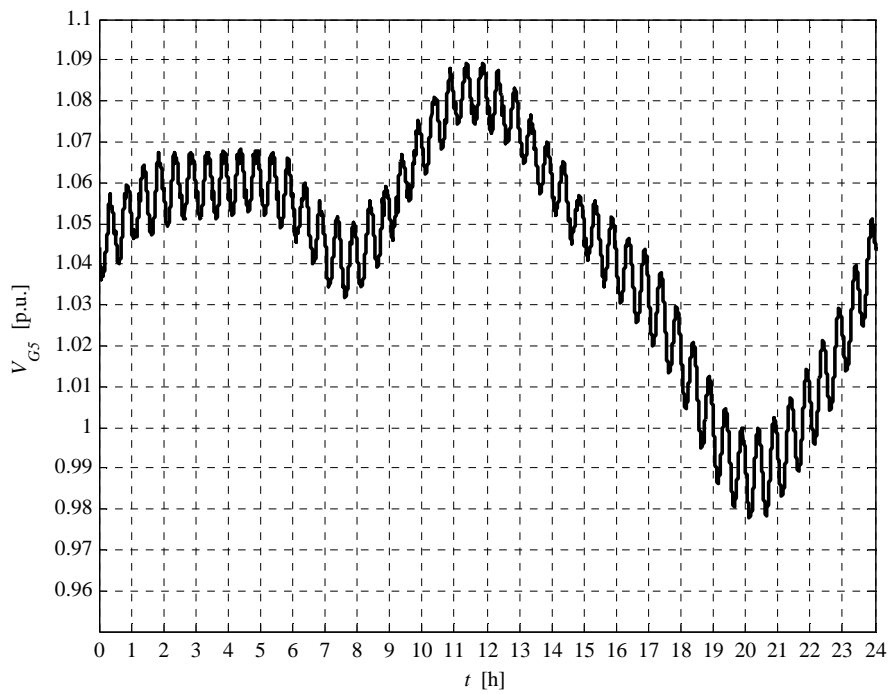
Fig. 5.9-10. G5 voltage daily profile
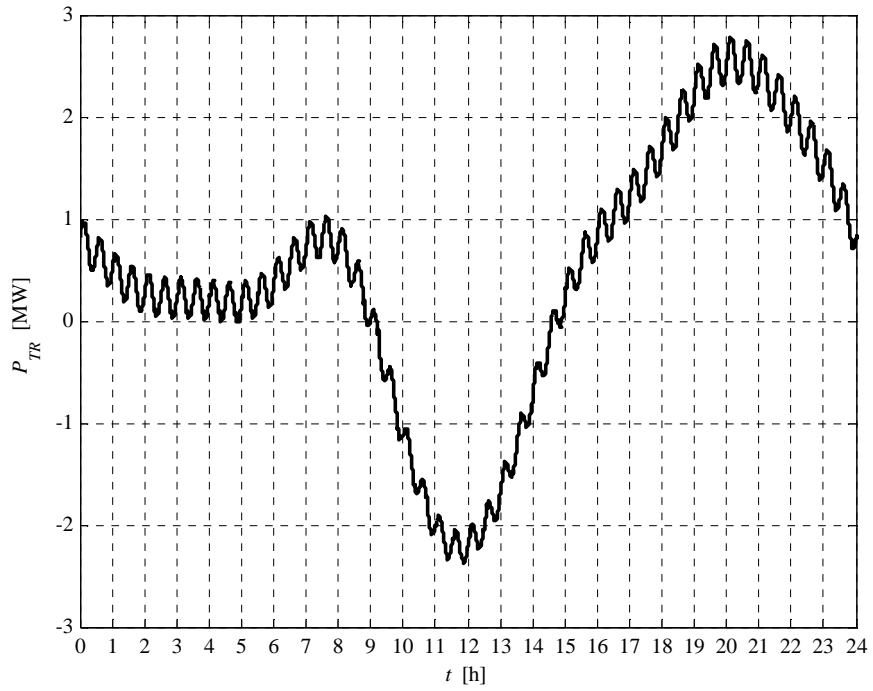
Fig. 5.9-11. HV/MV transformer daily active power profile
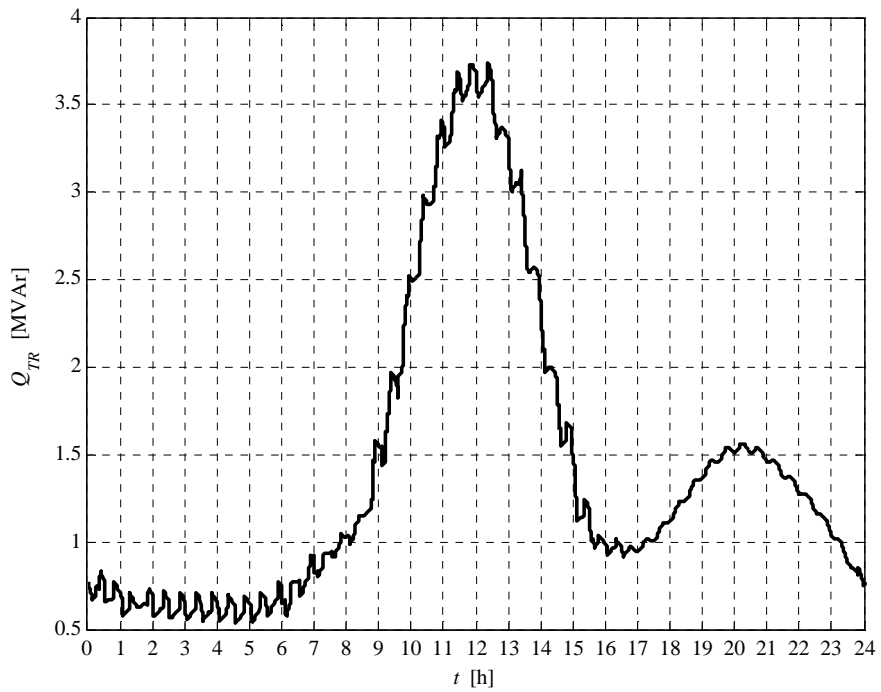
Fig. 5.9-12. HV/MV transformer daily reactive power profile
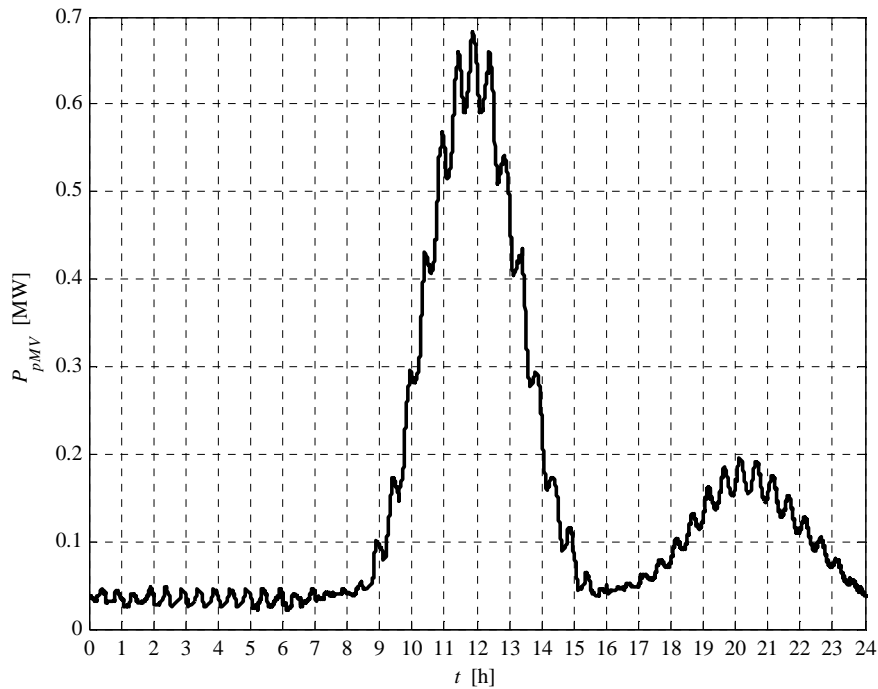
Fig. 5.9-13. MV network daily lost power profile

We can observe that the voltage rising, due to the generated active power increment, is compensated by the "RQV" local voltage regulation. This phenomenon increments the line hosting capacity. This hosting capacity increment is 28 %.

The report, referred to this case, is:

```
Report case: 4.b


Maximum VG1 value = 1.0947 [p.u.]
Maximum VG2 value = 1.0918 [p.u.]
Maximum VG3 value = 1.0923 [p.u.]
Maximum VG4 value = 1.0811 [p.u.]
Maximum VG5 value = 1.0895 [p.u.]


Loads power daily peak = 3.2157 [MW]
Generators power daily peak = 5.0879 [MW]


Loads daily active energy (absorbed) = 49.2306 [MWh]
Generators daily active energy (generated) = 40.9182 [MWh]
Daily active energy absorbed from the HV grid = 11.8305 [MWh]
Daily lost active energy = 3.5180 [MWh]
Daily lost active energy (percentual) = 6.6694 [%]
```

It is important to note the losses increment, if compared to the case 3. This phenomenon is due to the increment of both generated active power and requested reactive power, necessary to

the "UPG" voltage regulation. The hosting capacity increment using the "RQV" is similar[14] to which obtainable using the "UPG" regulation because the reactive power requested when the voltage is 1.09 p.u. corresponds to a 0.9 inductive power factor, which is identical to the "UPG" regulation power factor. We can observe a losses increment due to the generated power growth.

5.10 CASE 5.A RESULTS

This case is necessary to define the hosting capacity increment when the "UPG" local voltage control is activated and the MV busbar is regulated in order to guarantee (without distributed generation), in the critical node, the voltage 0.95 p.u. in each time instant (as described in Chapter 1). In order to reach this goal, the MV busbar set-point daily profile is (see Fig. 5.10-1):

- from 0 to 13:45 h = 1.04 p.u.
- from 13:45 h to 14:15 h = 1.05 p.u.
- from 14:15 h to 24:00 h = 1.06 p.u.
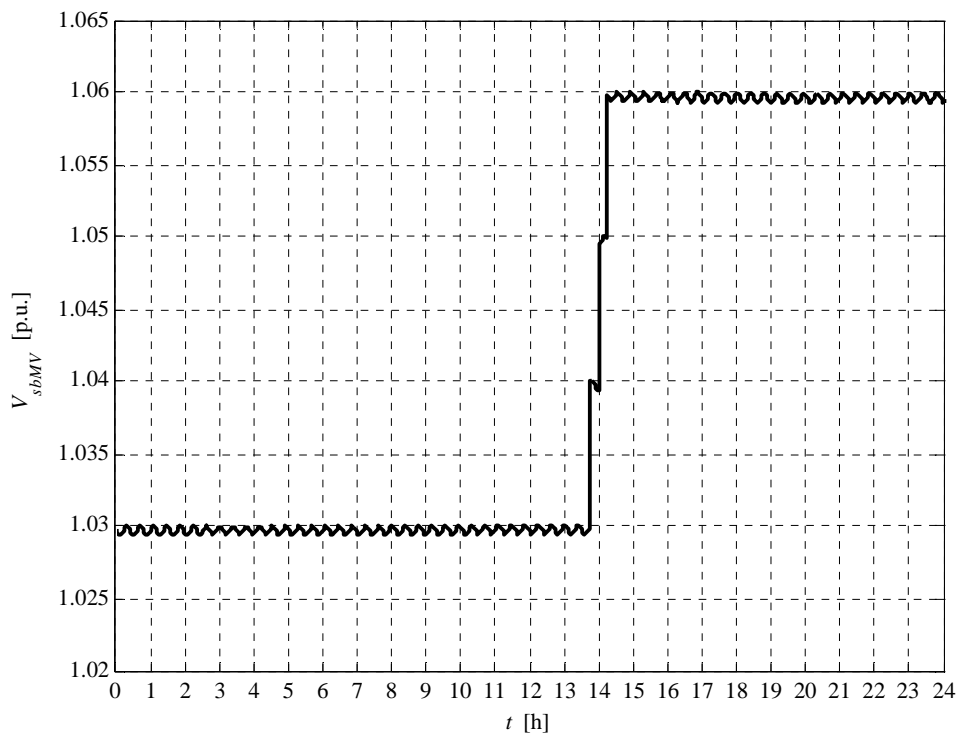
Fig. 5.10-1. MV busbar voltage daily profile

---

[14] Really the hosting capacity in the "RQV" case is slightly less than the hosting capacity of the "UPG" case.

Fig. 5.10-2. G1 active power daily profile

Fig. 5.10-3. G2 active power daily profile

149

Fig. 5.10-4. G3 active power daily profile

Fig. 5.10-5. G4 active power daily profile

Fig. 5.10-6. G5 active power daily profile

Fig. 5.10-7. G1 reactive power daily profile

151
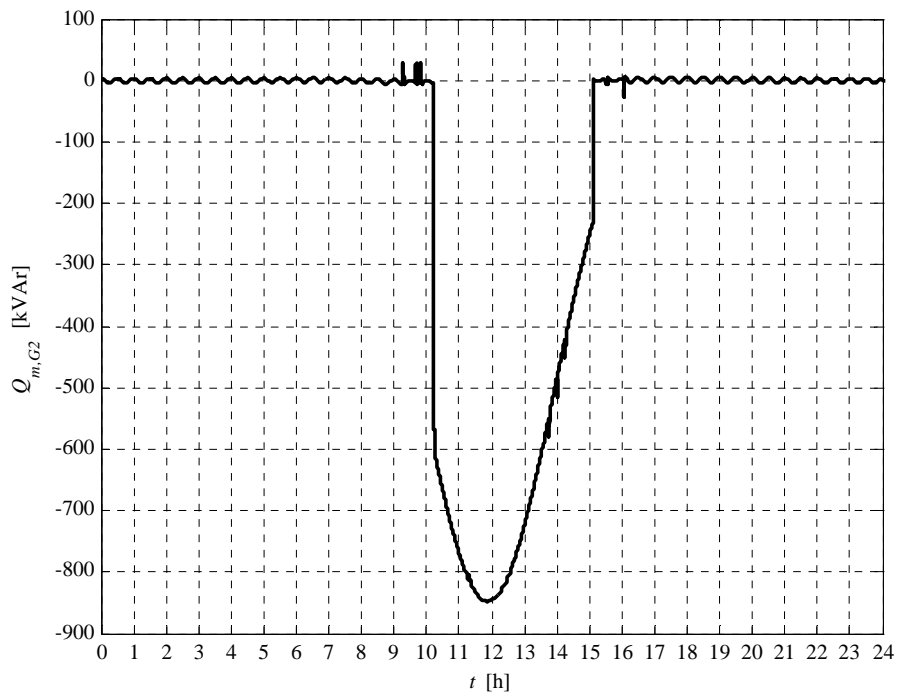
Fig. 5.10-8. G2 reactive power daily profile
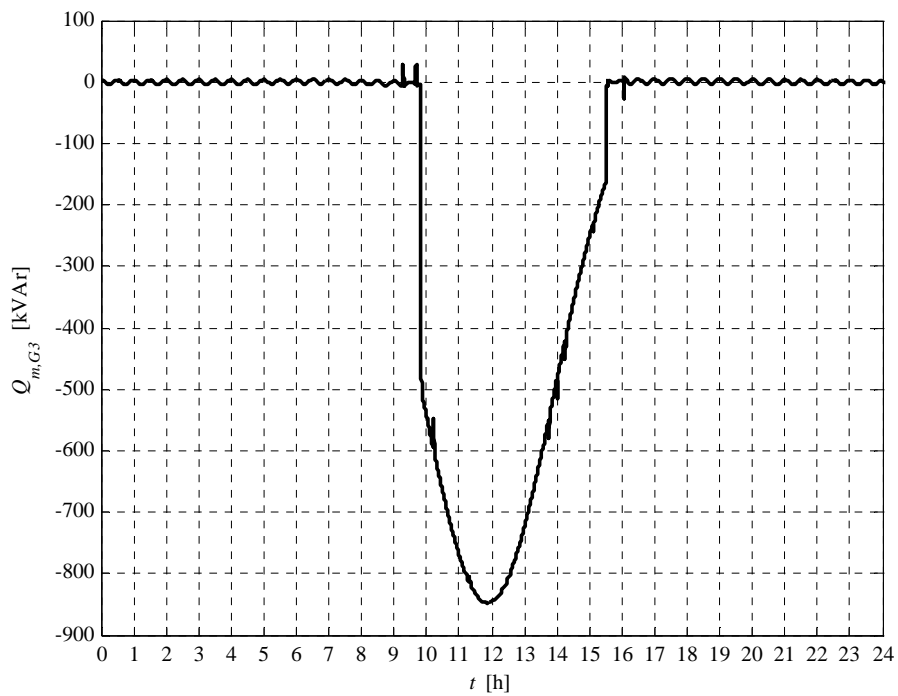
Fig. 5.10-9. G3 reactive power daily profile
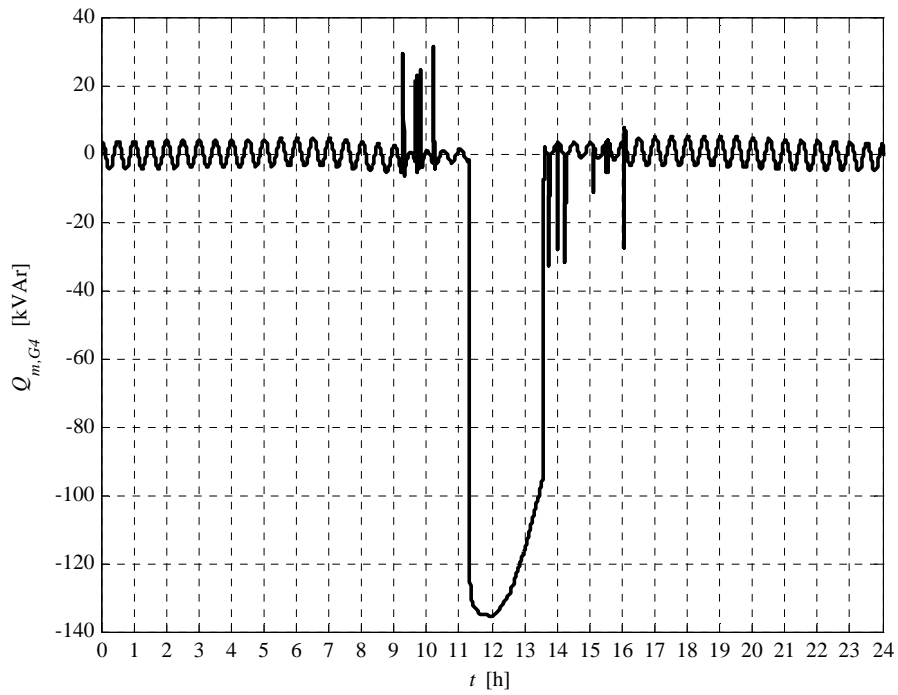
Fig. 5.10-10. G4 reactive power daily profile

Fig. 5.10-11. G5 reactive power daily profile

153

Fig. 5.10-12. G1 voltage daily profile
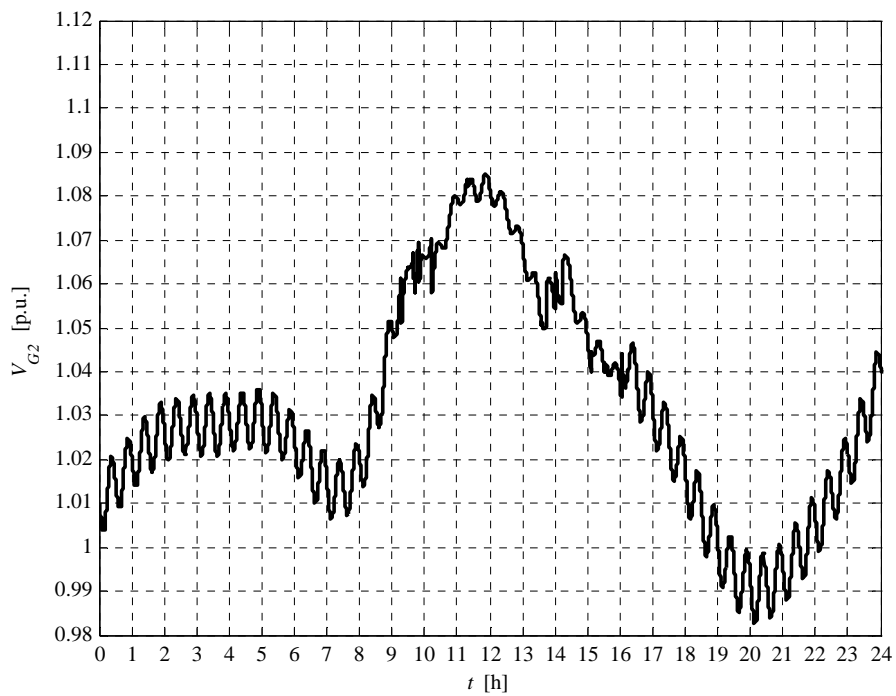
Fig. 5.10-13. G2 voltage daily profile

154
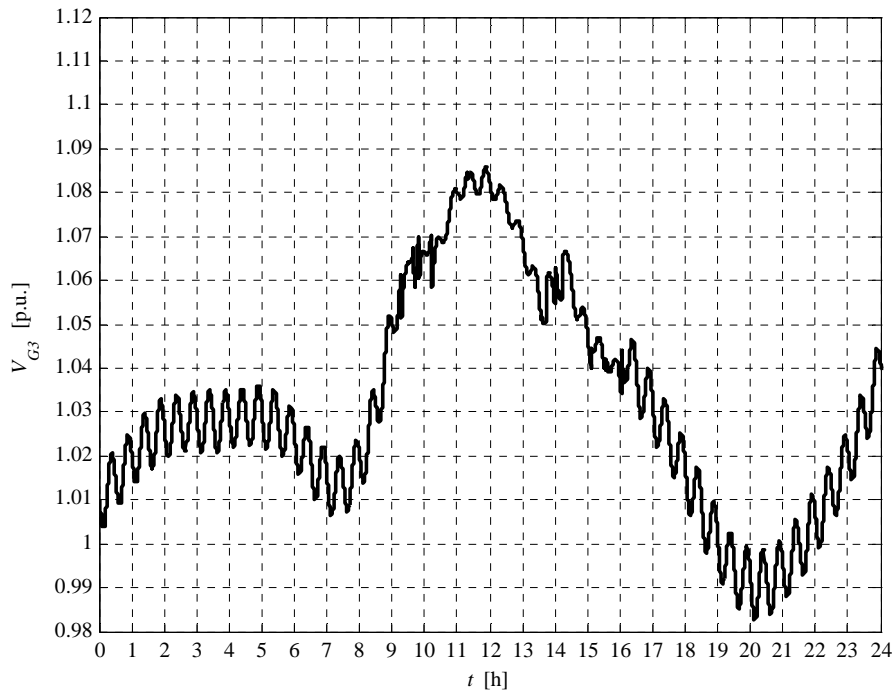
Fig. 5.10-14. G3 voltage daily profile
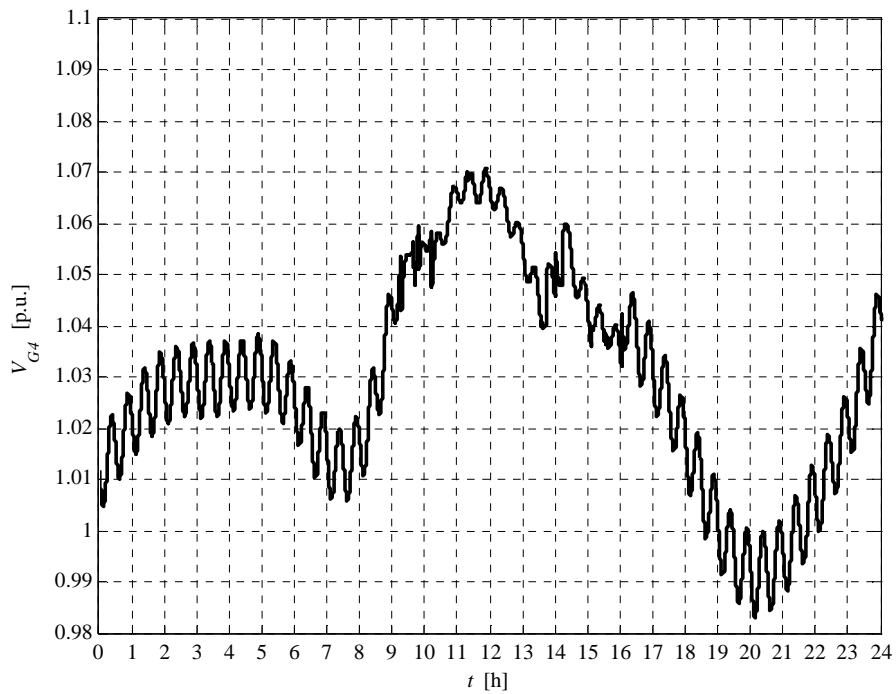
Fig. 5.10-15. G4 voltage daily profile

155
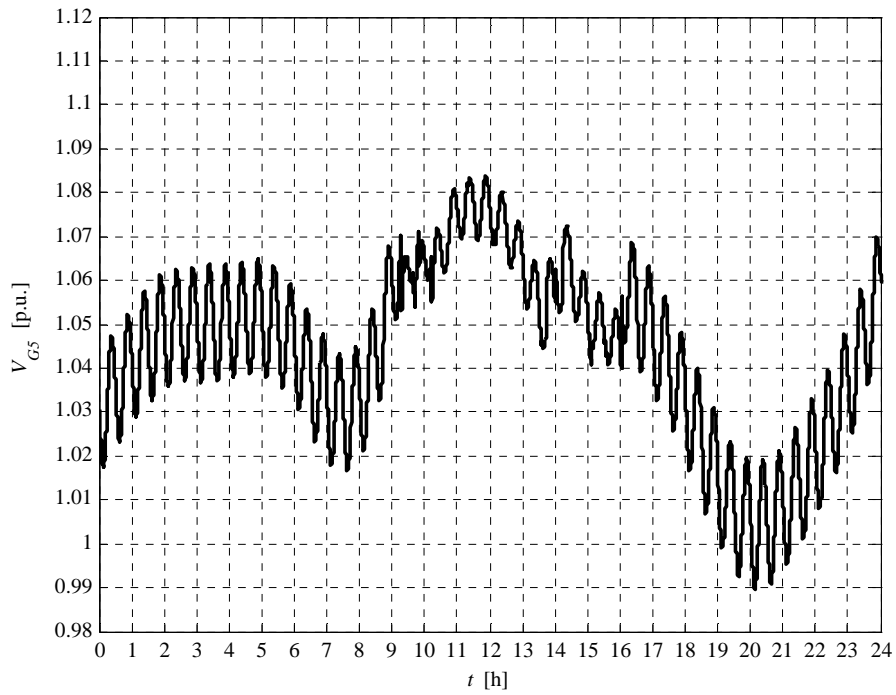
Fig. 5.10-16. G5 voltage daily profile
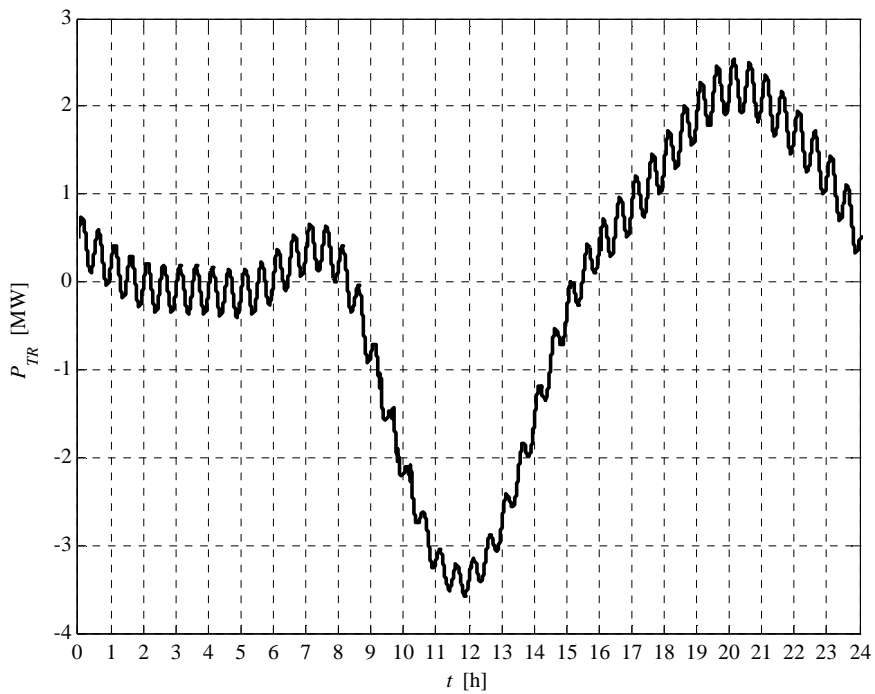
Fig. 5.10-17. HV/MV transformer daily active power profile
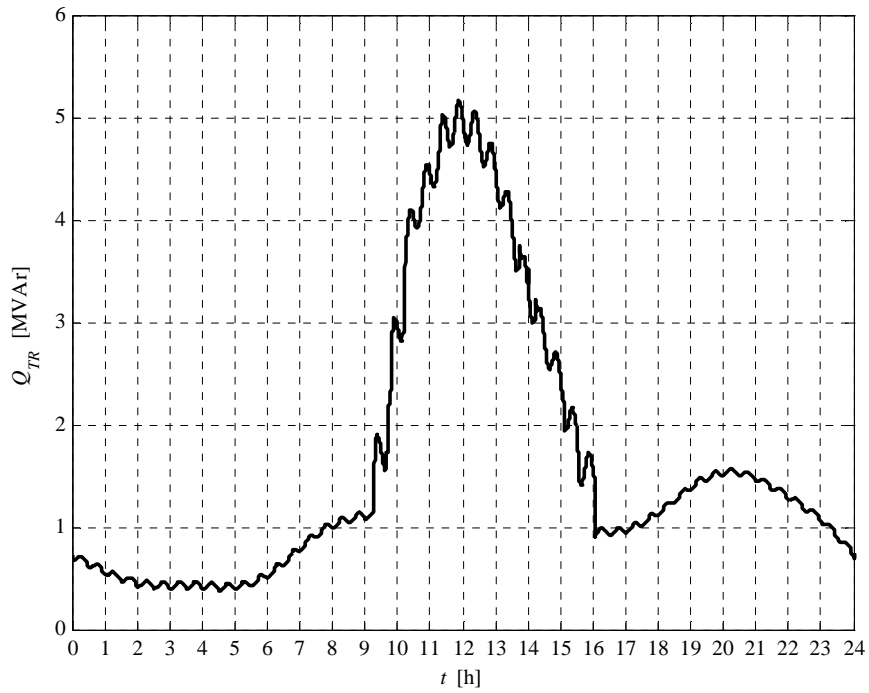
Fig. 5.10-18. HV/MV transformer daily reactive power profile
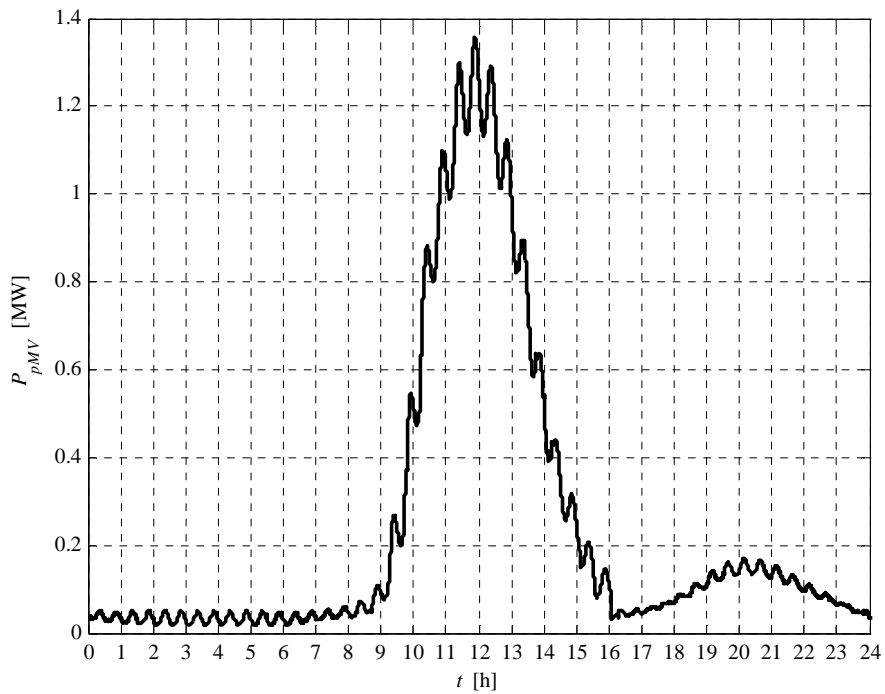
Fig. 5.10-19. MV network daily lost power profile

We can observe that the voltage rising, due to the generated active power increment, is compensated by the "UPG" local voltage regulation. Moreover, the "MV busbar intelligent set-point calculation" (see Chapter 1) allows to connect more generation because it maintains the lowest possible voltage level, on the MV busbar, for each load condition (the DG is de-activated in the calculation); the lowest voltage level allows increments the line hosting capacity. In particular the line hosting capacity increment is 75 %. It is clear that we can observe a losses increment.

The report, referred to this case, is:

```
Report case: 5.a

Maximum VG1 value = 1.0893 [p.u.]
Maximum VG2 value = 1.0851 [p.u.]
Maximum VG3 value = 1.0857 [p.u.]
Maximum VG4 value = 1.0706 [p.u.]
Maximum VG5 value = 1.0840 [p.u.]

Loads power daily peak = 3.2158 [MW]
Generators power daily peak = 6.9511 [MW]

Loads daily active energy (absorbed) = 49.2307 [MWh]
Generators daily active energy (generated) = 55.9738 [MWh]
Daily active energy absorbed from the HV grid = -0.9750 [MWh]
Daily lost active energy = 5.7681 [MWh]
Daily lost active energy (percentual) = 10.4877 [%]
```

It is important to note the losses increment, if compared to the case 3. This phenomenon is due to the increment of both generated active power and requested reactive power, necessary to the "UPG" voltage regulation.

5.11 CASE 5.B RESULTS

This case is necessary to define the hosting capacity increment when the "RQV" local voltage control is activated. Moreover the MV busbar is regulated in order to guarantee (without distributed generation), in the critical node, the voltage 0.95 p.u. in each time instant (as described in Chapter 1). The MV busbar voltage set-point is described in Paragraph 5.a. Generators active power plots are similar to which explained in Paragraph 5.a then will not be presented in this Pharagraph.

As reported in the following report, the hosting capacity with the "RQV" regulation is similar to which can be obtained with the "UPG" case (case 5.a). Then the generators active power curves will not be plotted (see case 5.a).
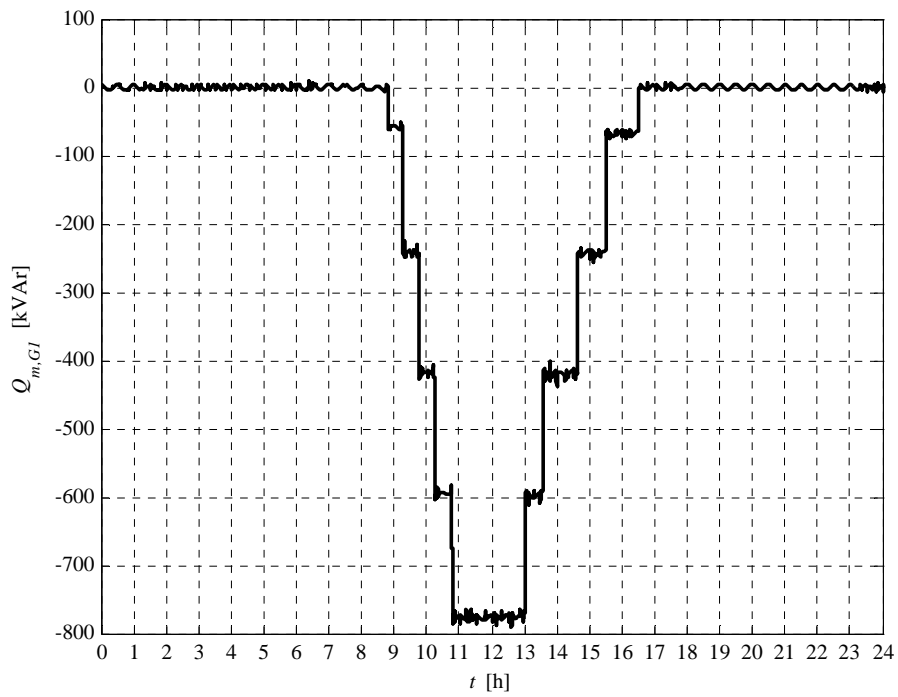
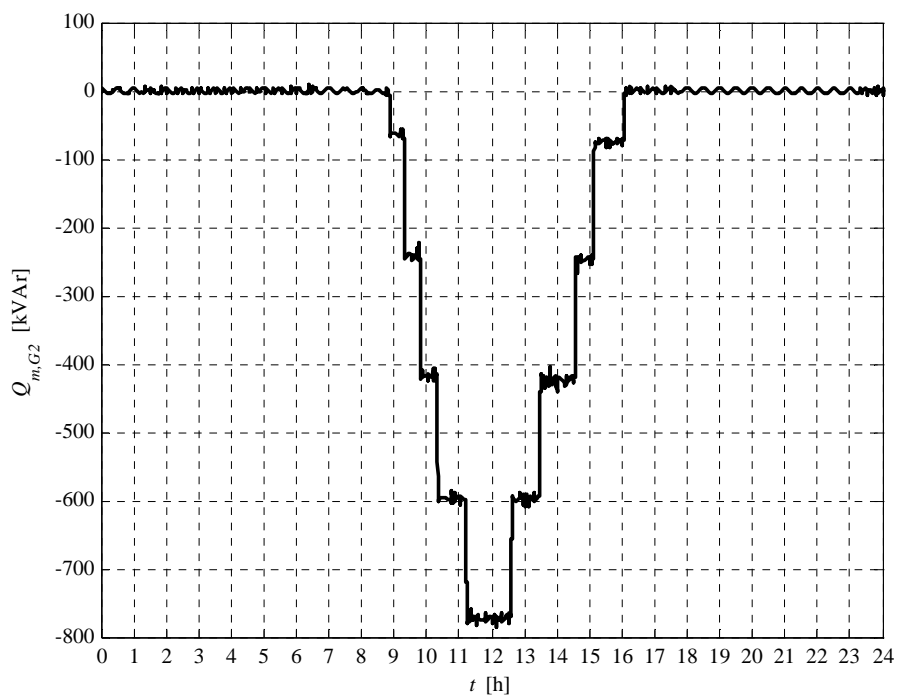**Fig. 5.11-1. G1 reactive power daily profile**

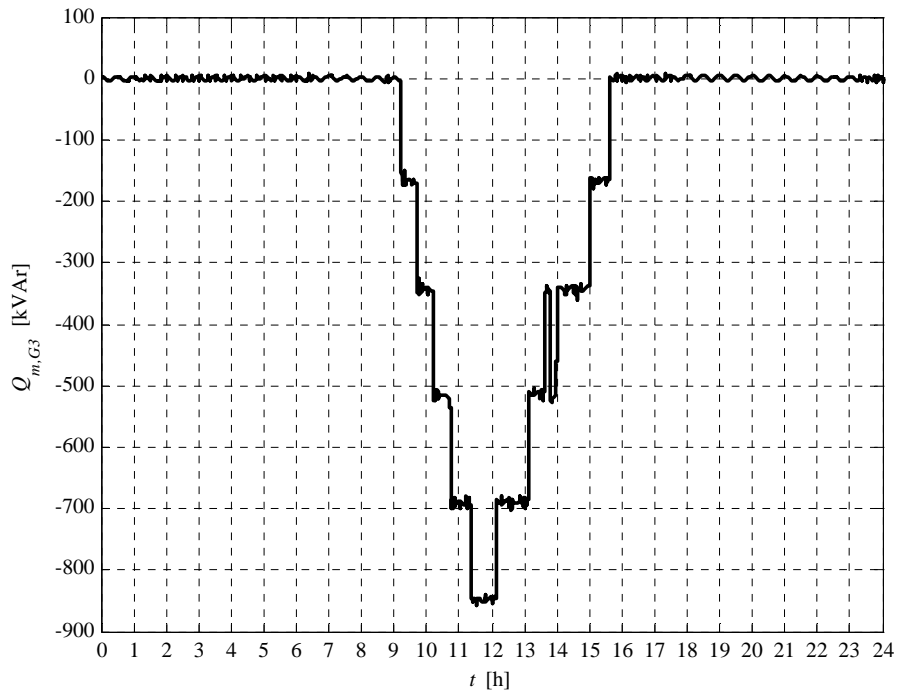**Fig. 5.11-2. G2 reactive power daily profile**

159

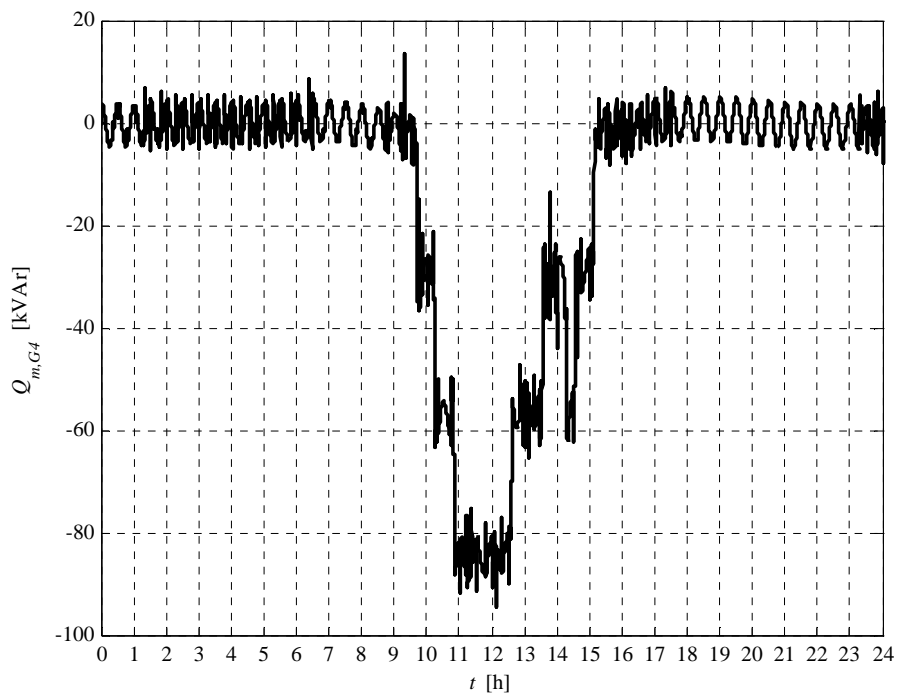**Fig. 5.11-3. G3 reactive power daily profile**
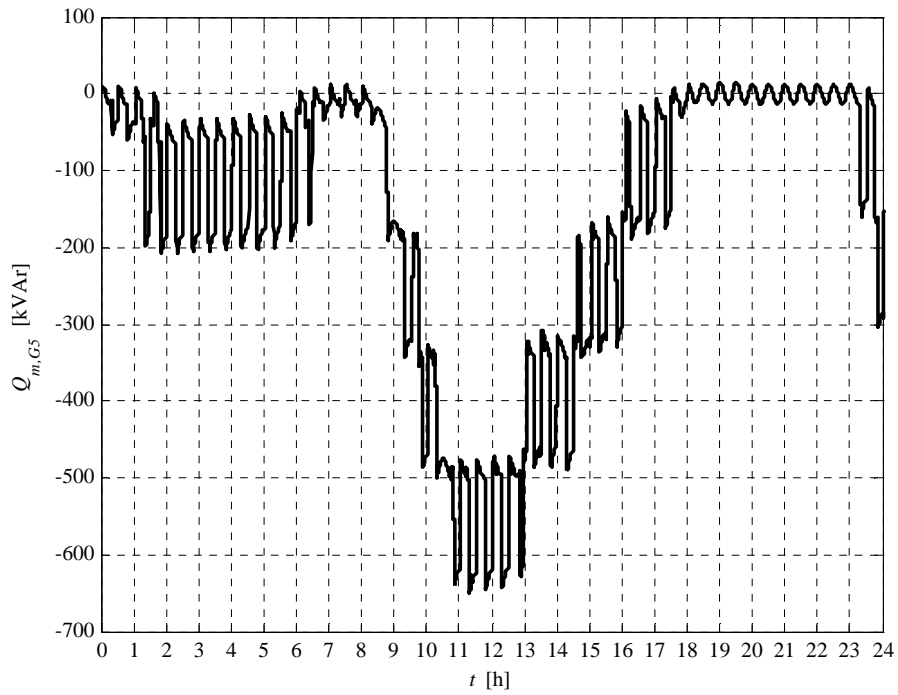

Fig. 5.11-4. G4 reactive power daily profile
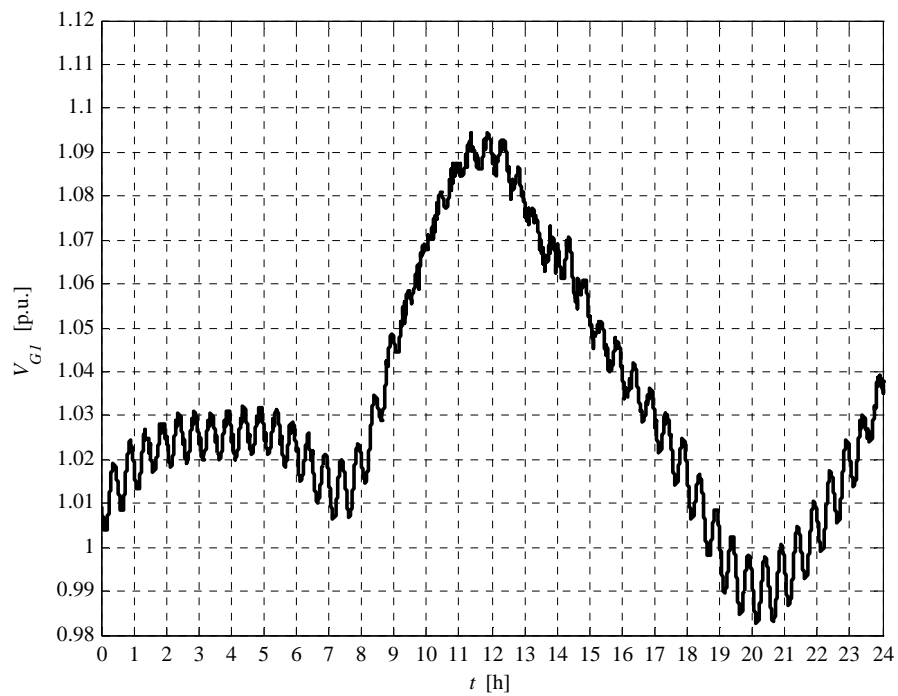
Fig. 5.11-5. G5 reactive power daily profile

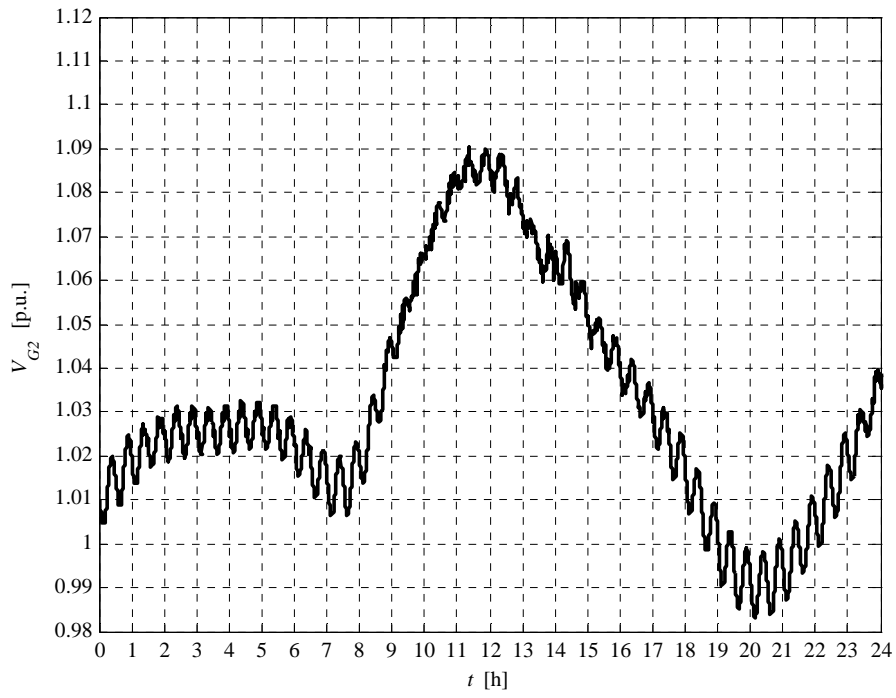**Fig. 5.11-6. G1 voltage daily profile**

161

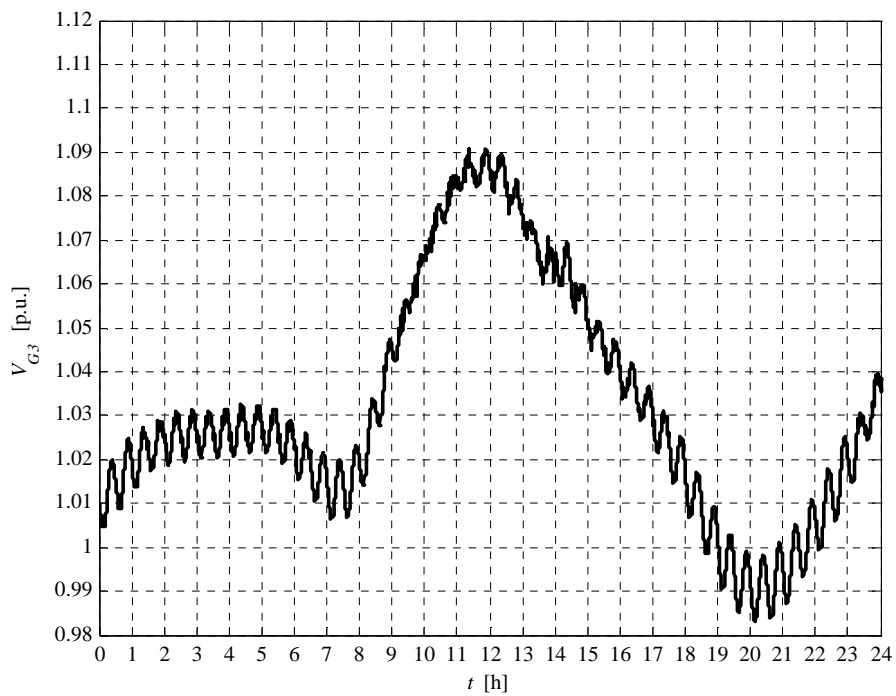**Fig. 5.11-7. G2 voltage daily profile**

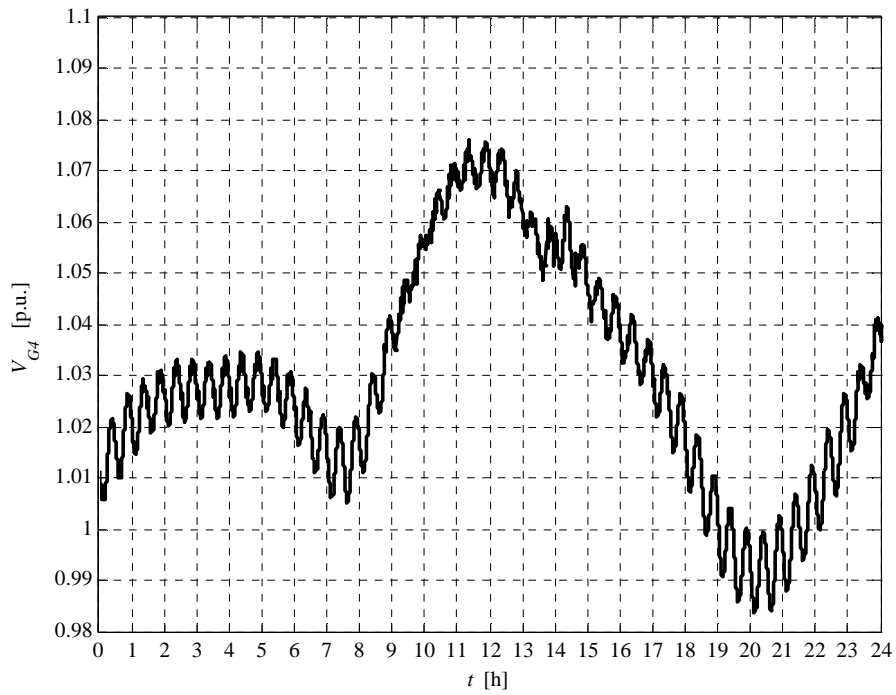

Fig. 5.11-8. G3 voltage daily profile

162

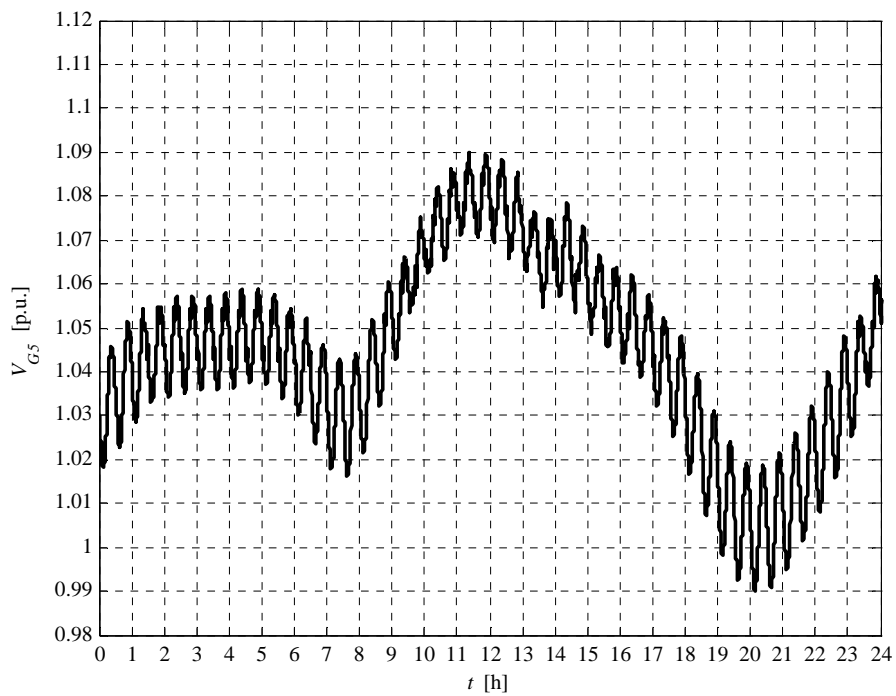**Fig. 5.11-9. G4 voltage daily profile**

Fig. 5.11-10. G5 voltage daily profile
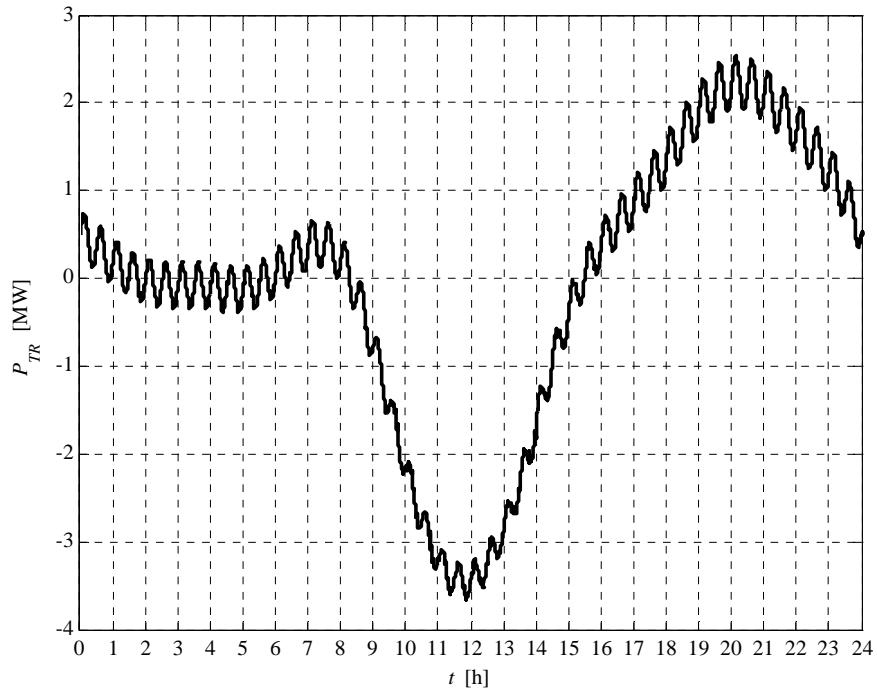
163

Fig. 5.11-11. HV/MV transformer daily active power profile
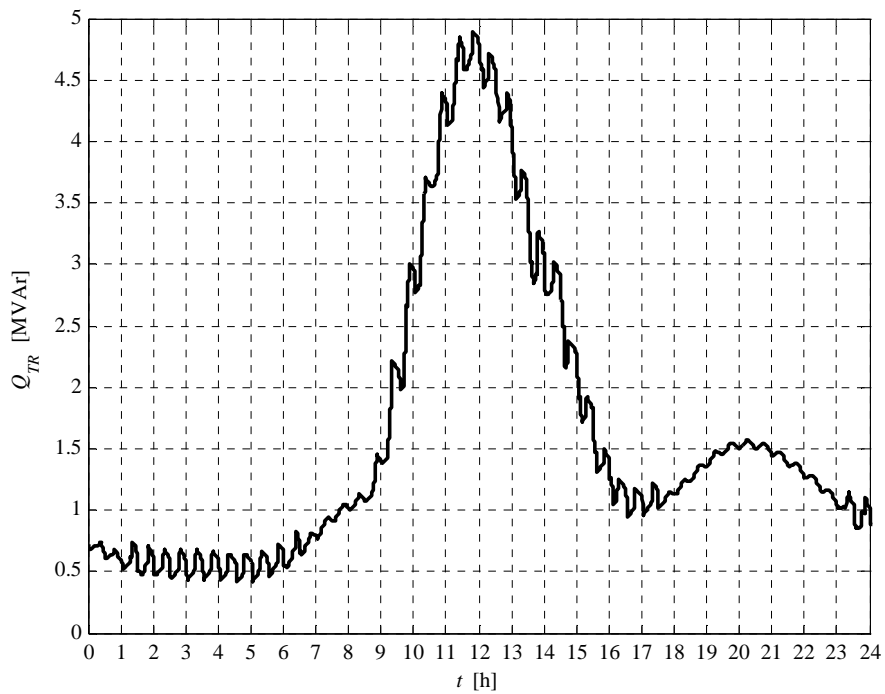

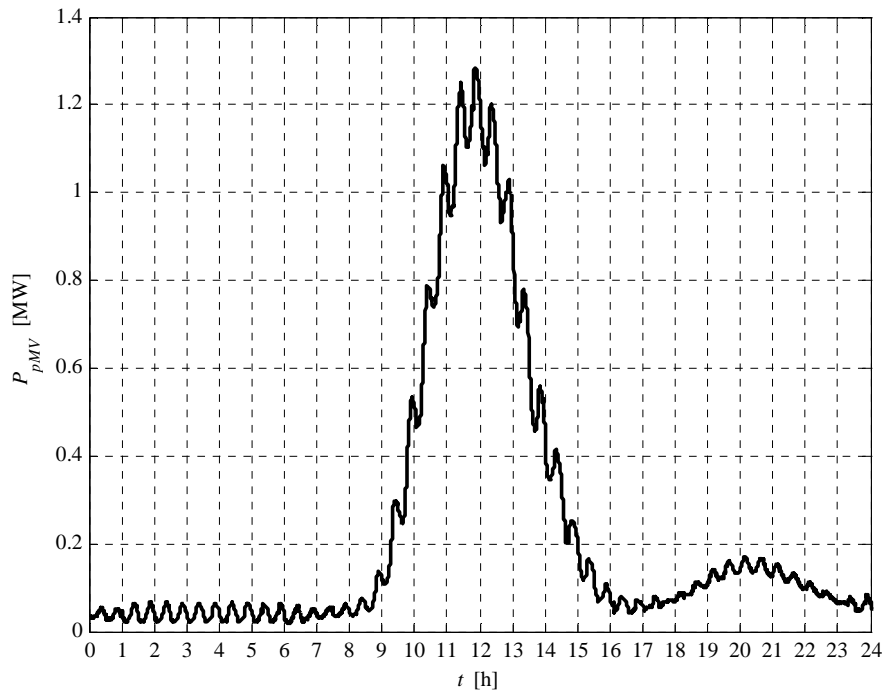**Fig. 5.11-12. HV/MV transformer daily reactive power profile**

Fig. 5.11-13. MV network daily lost power profile

We can observe that the voltage rising, due to the generated active power increment, is compensated by the "RQV" local voltage regulation. Moreover, the "MV busbar intelligent set-point calculation" (see Chapter 1) allows to connect more generation because it maintains the lowest possible voltage level, on the MV busbar, for each load condition (the DG is de-activated in the calculation); the lowest voltage level allows increments the line hosting capacity. Also in this case the line hosting capacity increment is close to 75 % and we can observe a losses increment.

The hosting capacity increasing using the UPG function is very similar to the hosting capacity obtainable adopting the RQV regulation modality. This phenomenon is due to the UPG and RQV settings; the inductive power factor of the UPG function is 0.9 and the reactive power set-point, commanded by the RQV in correspondence of the voltage threshold V_{2S} (1.09 p.u.), corresponds to same power factor (see Chapter 4). Then UPG and RQV command to generators the similar reactive power absorption in case of "high" voltage.

The report, referred to this case, is:

```
Report case: 5.b

Maximum VG1 value = 1.0944 [p.u.]
Maximum VG2 value = 1.0902 [p.u.]
Maximum VG3 value = 1.0909 [p.u.]
Maximum VG4 value = 1.0760 [p.u.]
Maximum VG5 value = 1.0901 [p.u.]
```

165

```
Loads power daily peak = 3.2158 [MW]
Generators power daily peak = 6.9579 [MW]

Loads daily active energy (absorbed) = 49.2307 [MWh]
Generators daily active energy (generated) = 55.9725 [MWh]
Daily active energy absorbed from the HV grid = -1.2322 [MWh]
Daily lost active energy = 5.5096 [MWh]
Daily lost active energy (percentual) = 10.0651 [%]
```

5.12 CASE 6 RESULTS

In this last case the Voltage Control System (VCS), based on the Sensitivity approach presented in Chapter 3, has been analyzed in order to test the Centralized Voltage Control.

In this case:

- G1, G2, G3 and G4 power profile is identical to which explained in Paragraph 4.a;
- G5 power profile is reported in Fig. 5.12-5. We can observe that wind power decreases along the day.

All generators can be "called" by the VCS but UPG is activated only on G1, G2 and G3. The calling time interval is 1 min.
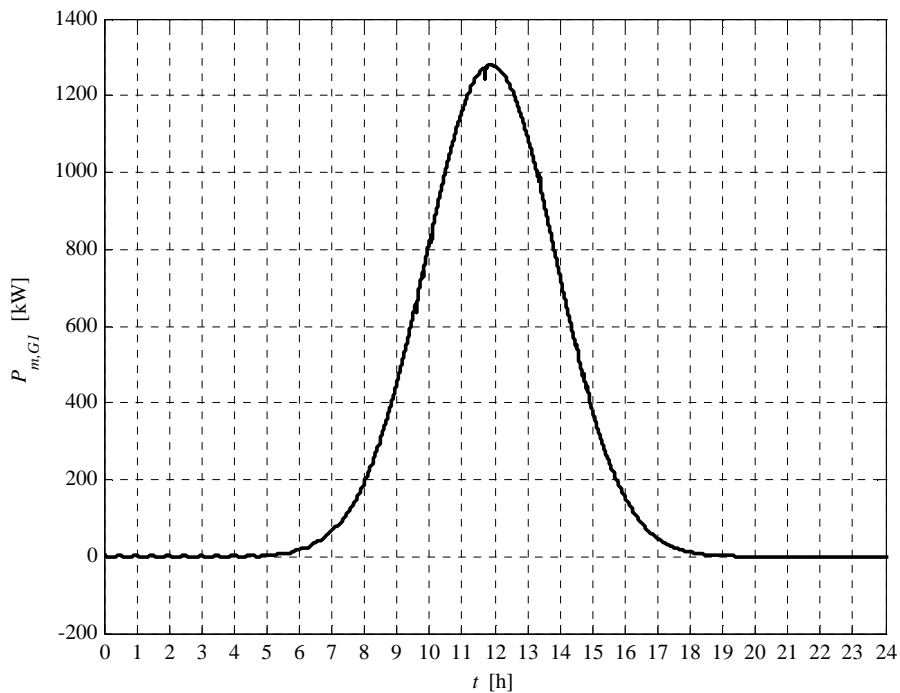
Fig. 5.12-1. G1 active power daily profile
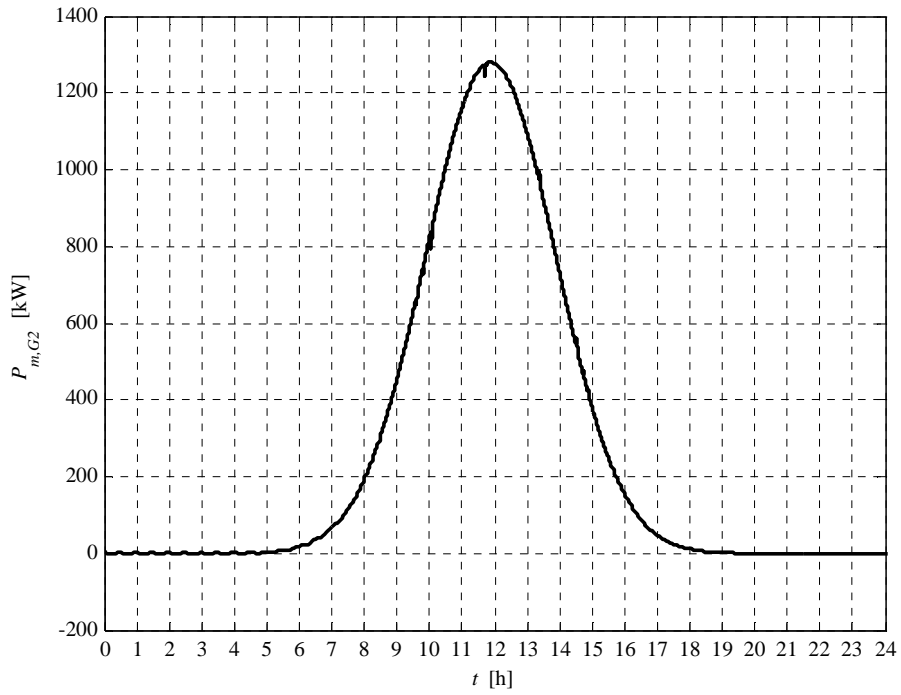
Fig. 5.12-2. G2 active power daily profile
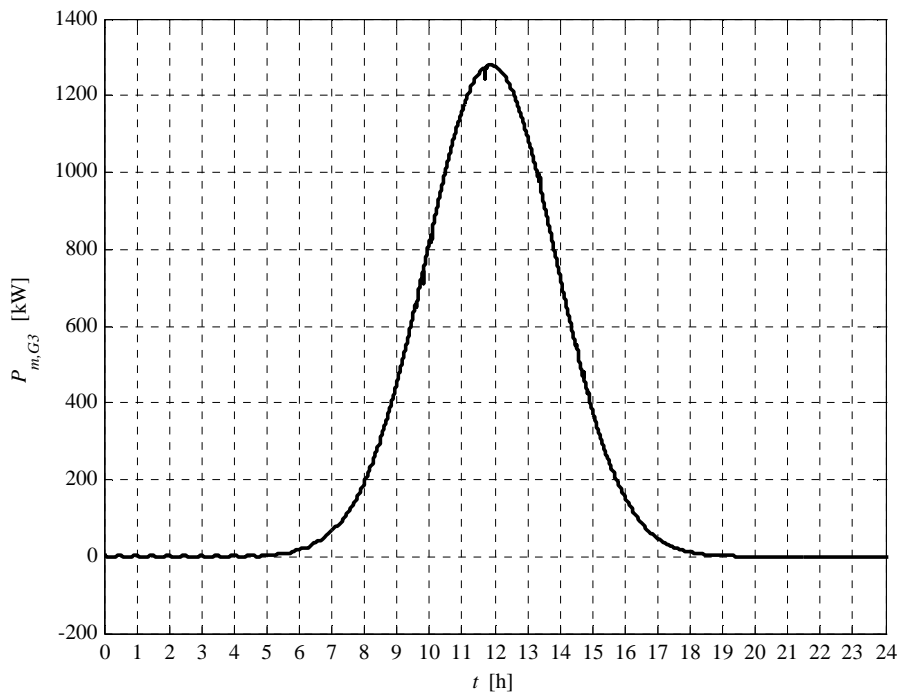
Fig. 5.12-3. G3 active power daily profile

167
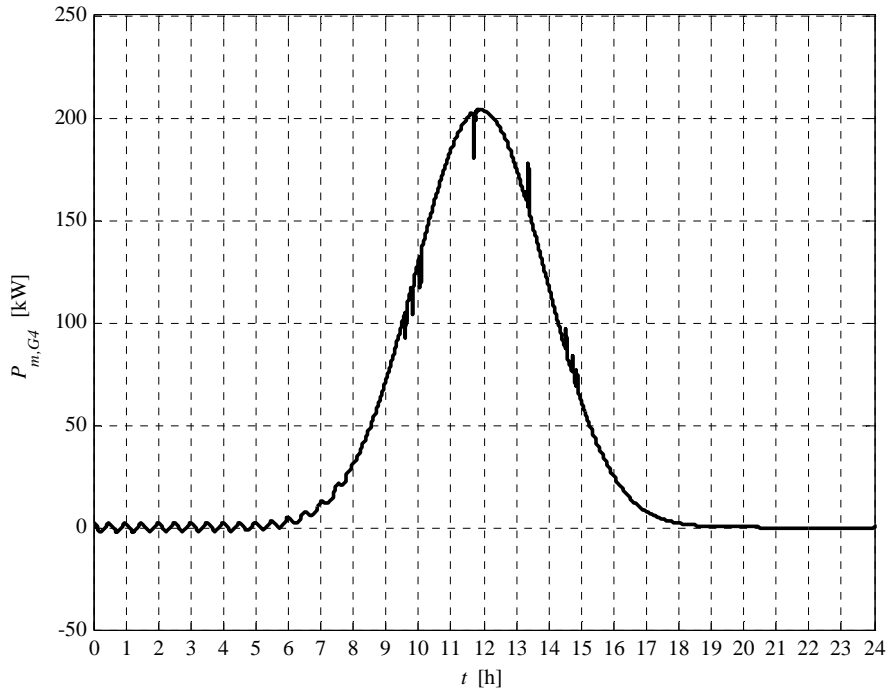
Fig. 5.12-4. G4 active power daily profile
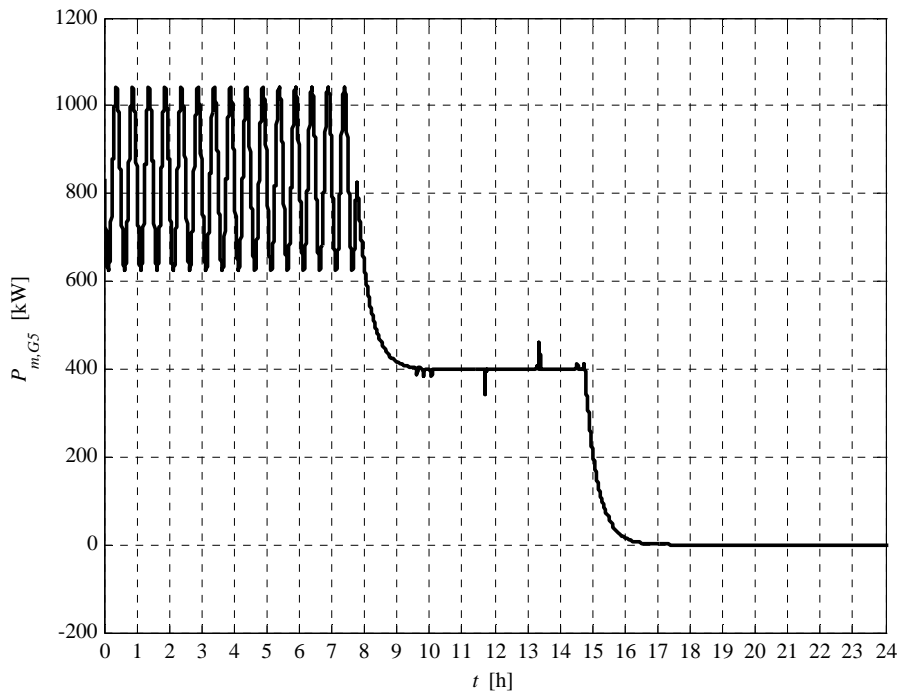
Fig. 5.12-5. G5 active power daily profile

168
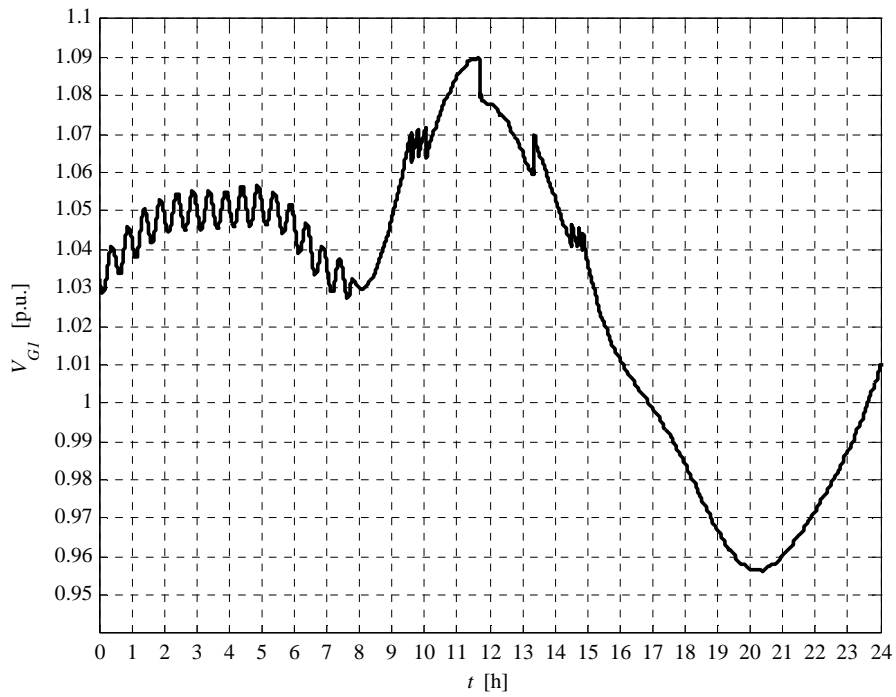
Fig. 5.12-6. G1 voltage daily profile
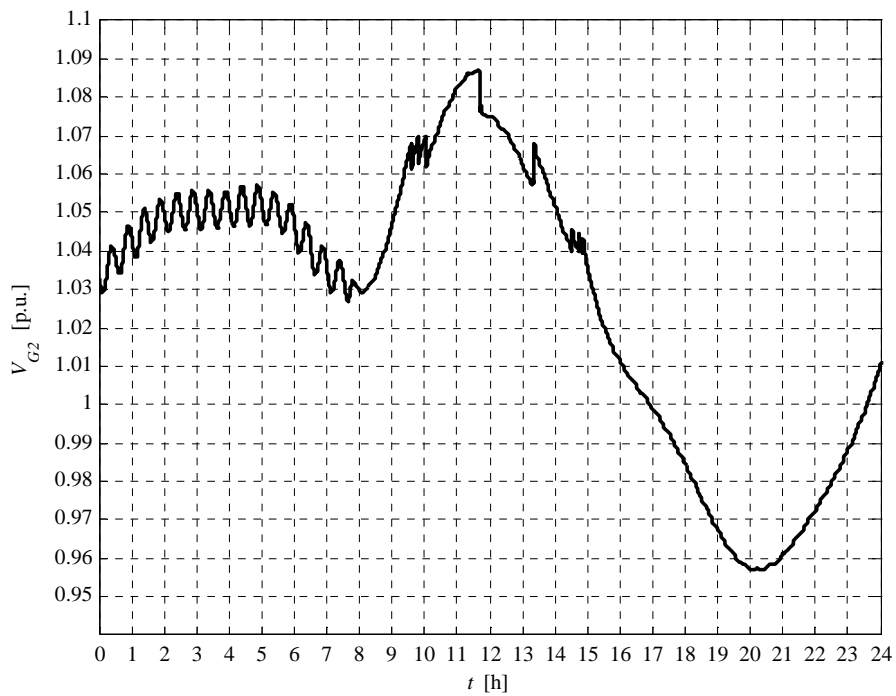
Fig. 5.12-7. G2 voltage daily profile

169
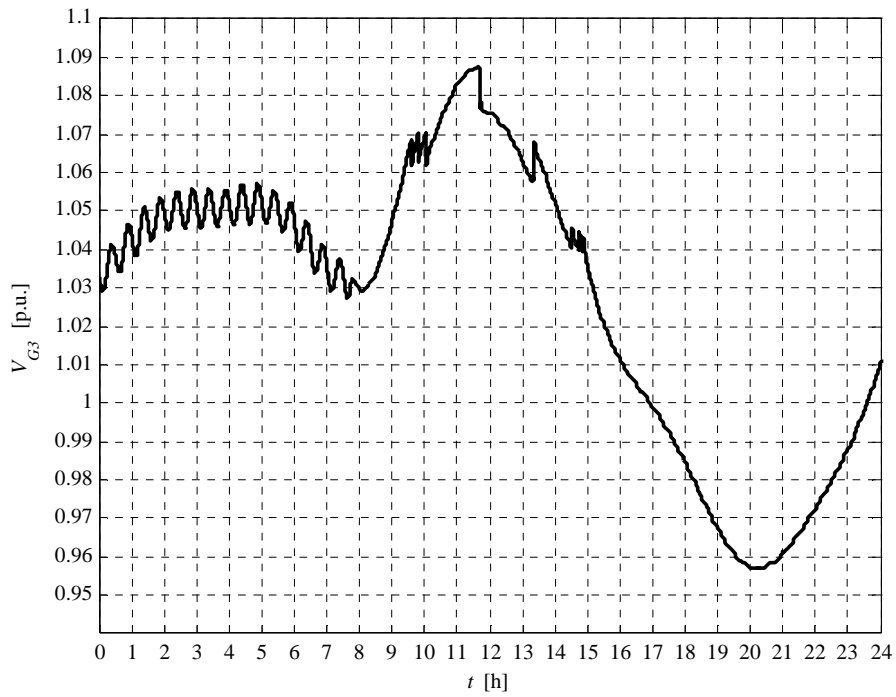
Fig. 5.12-8. G3 voltage daily profile
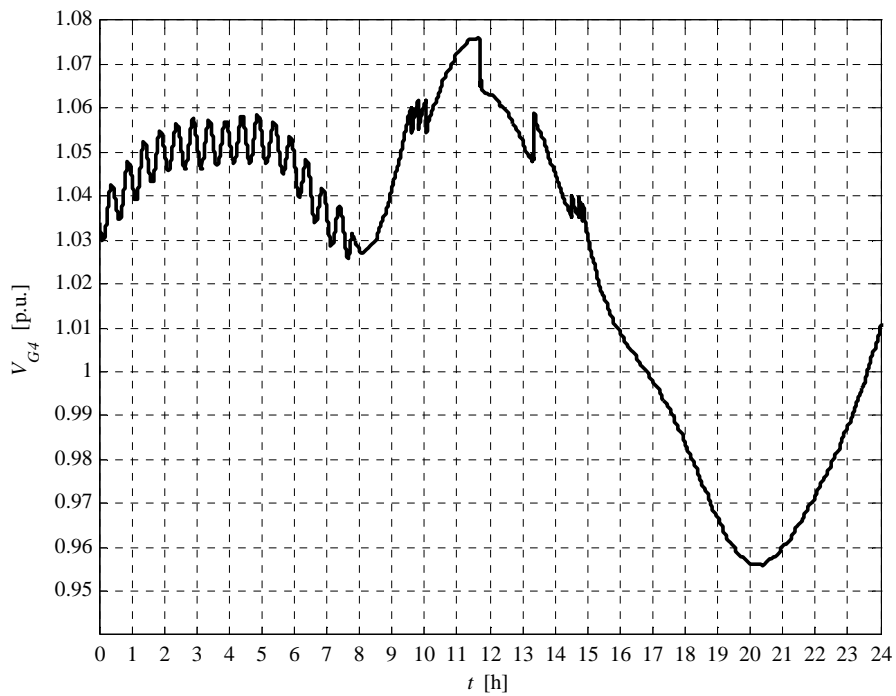
Fig. 5.12-9. G4 voltage daily profile
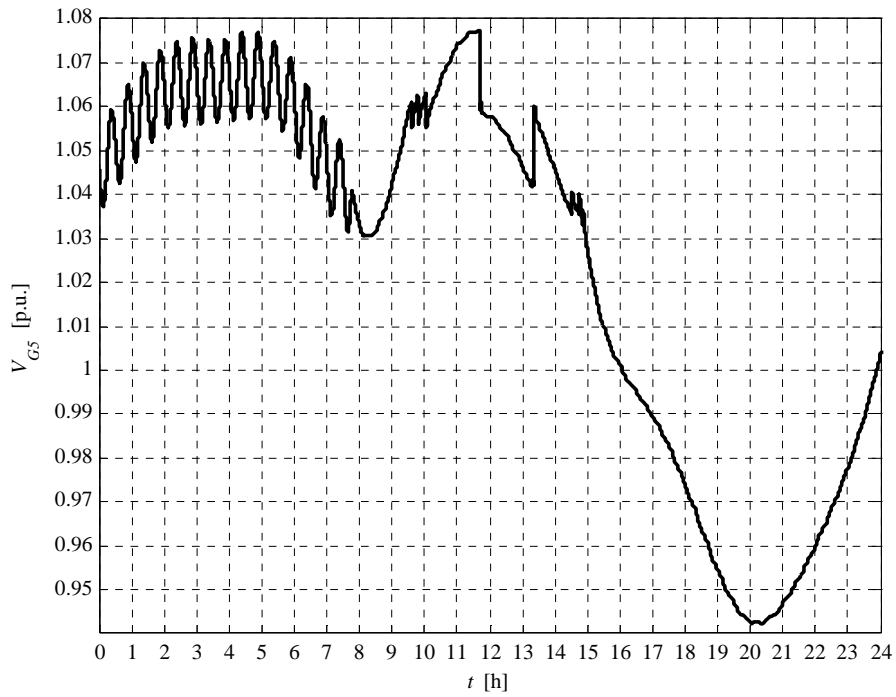
Fig. 5.12-10. G5 voltage daily profile
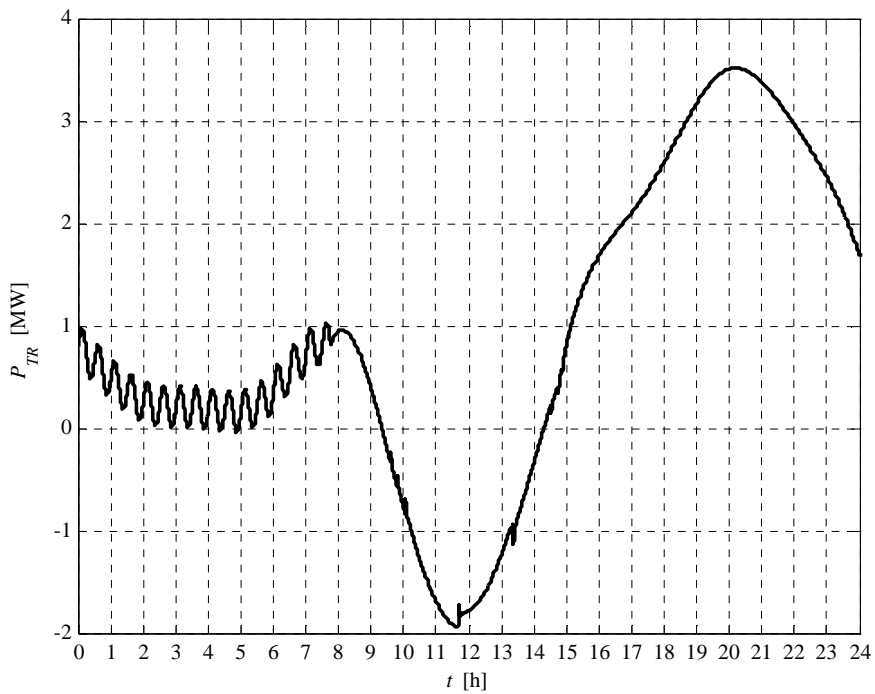
Fig. 5.12-11. HV/MV transformer daily active power profile

171
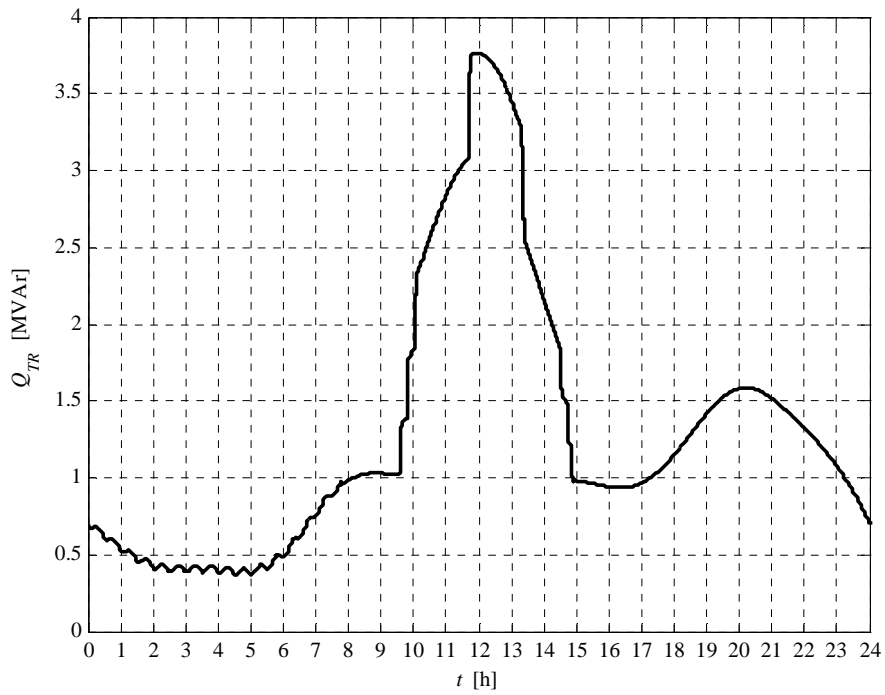
Fig. 5.12-12. HV/MV transformer daily reactive power profile
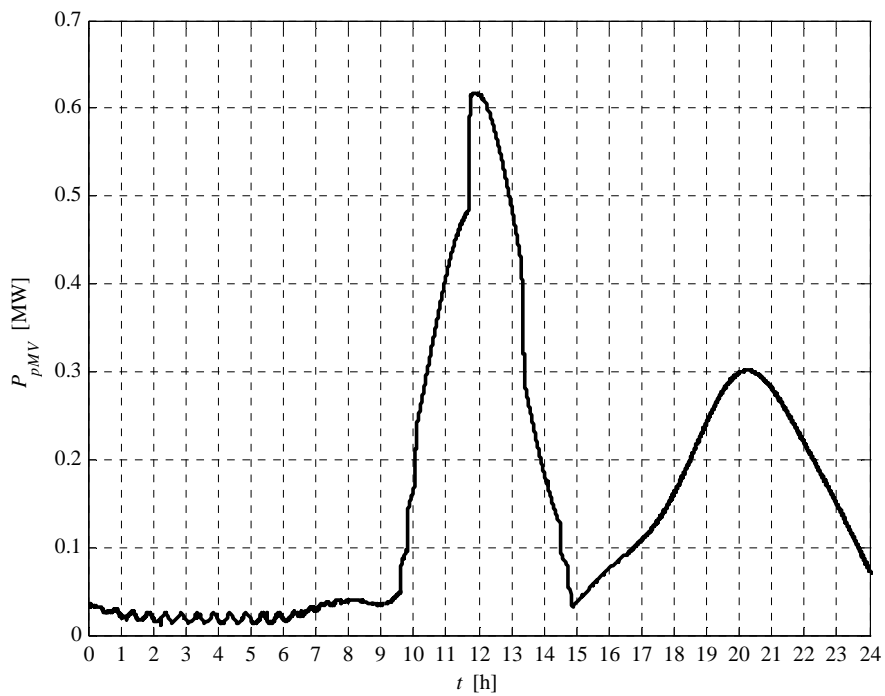
Fig. 5.12-13. MV network daily lost power profile
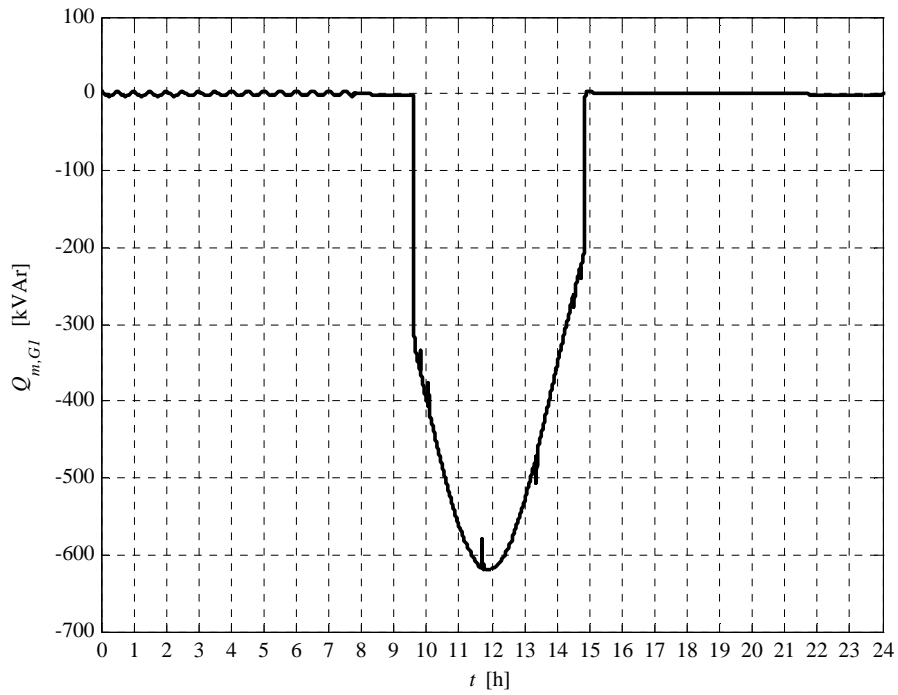
Fig. 5.12-14. G1 reactive power daily profile
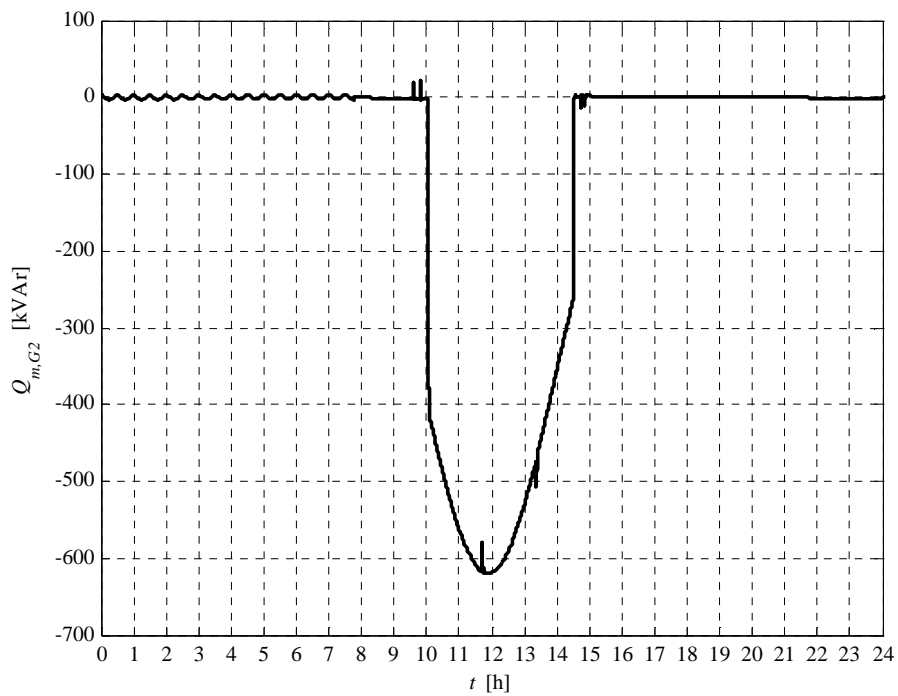
Fig. 5.12-15. G2 reactive power daily profile

173
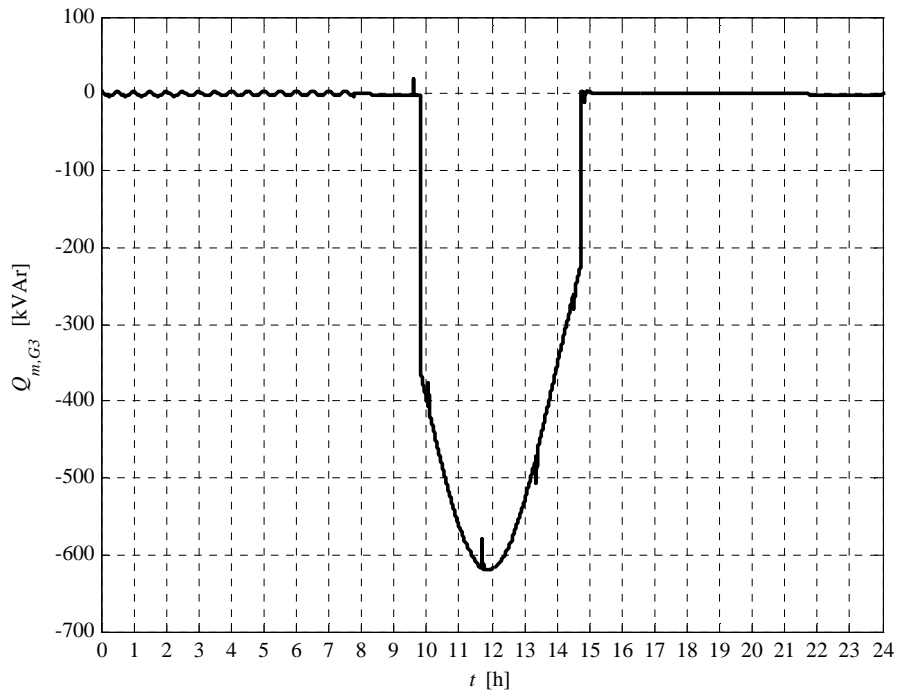
Fig. 5.12-16. G3 reactive power daily profile
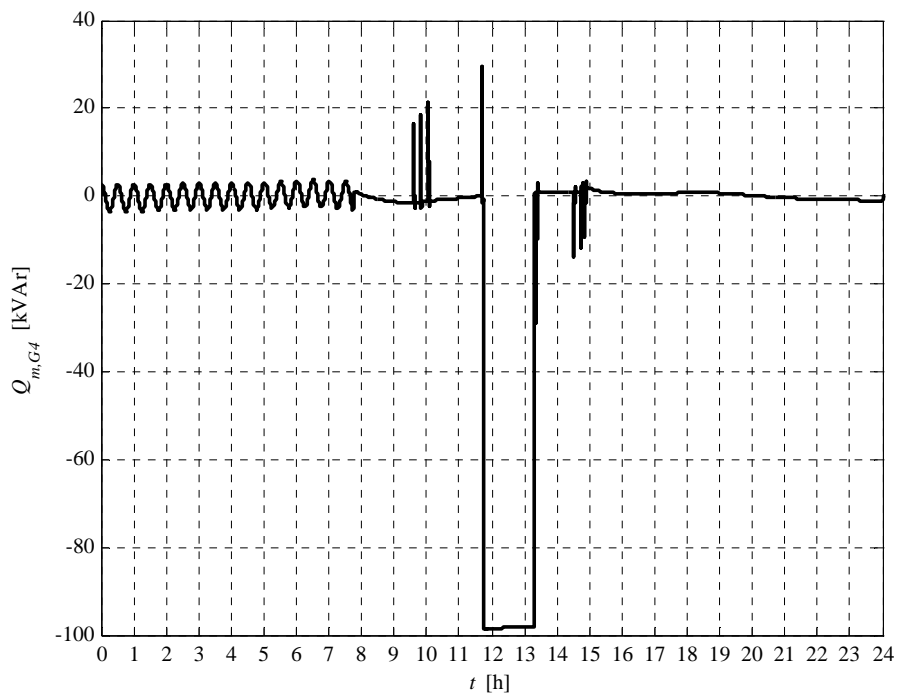
Fig. 5.12-17. G4 reactive power daily profile

174
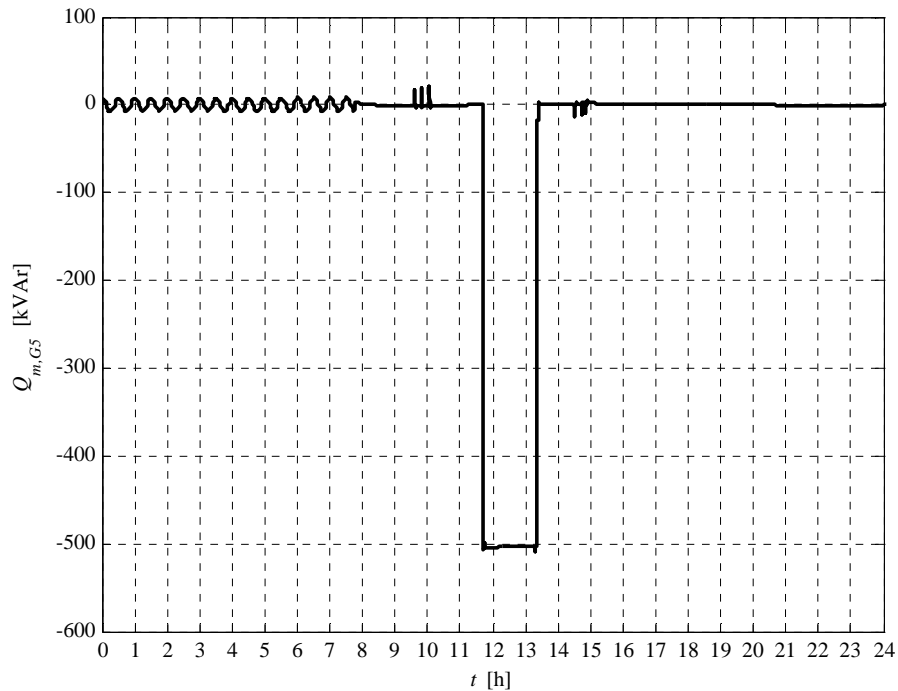
Fig. 5.12-18. G5 reactive power daily profile

From voltage plots (see figures from Fig. 5.12-6 to Fig. 5.12-10) we can observe that G1 exceeds the voltage threshold $V_{2S\text{-VCS}}$ (set to 1.09 p.u., as reported in Chapter 4). In other words G1 is the OTG[15]. After the time $T_{2S\text{-VCS}}$, G1 sent the VFLS = 1 signal to the VCS which search the BG using the reactive power Sensitivity Table presented in Chapter 4. Entering in the reactive power Sensitivity Table at the row $i = 16$, we can say that the first BG corresponds to G5[16] (node $j = 31$). The VCS request to G5 an inductive power factor 0.9. G5 reactive power is presented in Fig. 5.12-18. After the reactive power absorption, G1 voltage remains higher than $V_{1S\text{-VCS}}$ (set to 1.06 p.u., as reported in Chapter 4), then the VCS searches the second BG using the same previous row $i = 16$; the second BG corresponds to G4 (node $j = 19$). The VCS request also to G4 an inductive power factor 0.9[17]. G4 reactive power is presented in Fig. 5.12-18.

When G1 voltage became less than $V_{1S\text{-VCS}}$, the VCS firstly switches G4 and, after 1 min, G5 to work at unitary power factor. Plots demonstrates the correct Centralized Voltage Control strategy.

---

[15] From Canvas 2, attached at the end of Chapter 4, we can say that the OTG node is $i = 16$.

[16] G1, G2 and G3 must be excluded because they have been switched in RAM = ON by their UPG function.

[17] The reactive power absorption request is performed after 1 min.

175

The report referred to the presented case is:

```
Report case: 6

Maximum VG1 value = 1.0901 [p.u.]
Maximum VG2 value = 1.0872 [p.u.]
Maximum VG3 value = 1.0877 [p.u.]
Maximum VG4 value = 1.0762 [p.u.]
Maximum VG5 value = 1.0774 [p.u.]

Loads power daily peak = 3.2157 [MW]
Generators power daily peak = 4.4437 [MW]

Loads daily active energy (absorbed) = 49.2306 [MWh]
Generators daily active energy (generated) = 30.0358 [MWh]
Daily active energy absorbed from the HV grid = 22.9417 [MWh]
Daily lost active energy = 3.7469 [MWh]
Daily lost active energy (percentual) = 7.0727 [%]
```

Chapter 6

The Sensitivity Approach. Application on four-wires networks

6.1 INTRODUCTION TO CHAPTER 6

The voltage regulation criteria presented in the previous Chapters is based on reactive power variation in MV networks, both Local and Centralized Voltage Regulation. This approach can be also extended to the LV. The LV grid is characterized by a low reactive power sensitivity value, due to the low reactance/resistance ratio. Then a reactive power variation has a small influence on the voltage. However is preferable using reactive power to perform the voltage regulation in order to avoid active power reductions. This concept is also reported in the Italian technical standard CEI 0-21. For this reason the UPG and RQV local voltage regulation modalities can be extended to the LV grid[18].

Also the Centralized Voltage Control can be extended to the LV network. In this Chapter the VCS Sensitivity approach will be applied to a four-wire LV grid.

It is important to note that the main Centralized Voltage Control goal is to help the OTG. Then, in order to guarantee the voltage control effectiveness on the LV network, this regulation technique should act on generators active power. However, in this Chapter, the Sensitivity approach will be derived for the general case.

6.2 CAN THE SENSITIVITY APPROACH BE APPLIED ON FOUR-WIRES NETWORKS, LIKE THE LV GRID, IN ORDER TO CONTROL THE VOLTAGE?

In Chapter 3 the sensitivity approach has been presented. In order to apply the presented theory we needs:

- a symmetrical supply voltage system, i.e. a pure direct system voltage must feed the grid
- a balanced line current system, i.e. a pure direct system current must flows along the feeders

If the grid satisfies these hypothesis, the entire network can be represented using the single-phase equivalent circuit and the sensitivity approach can be easily applied. The MV distribution

---

[18] In a second step the UPG and RQV can perform an active power variation in order to control the voltage.

network practically satisfies the above presented hypothesis, due to the large load balancing. Instead in the LV distribution grid it is impossible to have load balancing, due to the large presence of single-phase load. Besides the neutral wire presence constitute another complication.

But now the question is: "it is possible to modify the sensitivity approach in order to apply it to the LV distribution network?" The answer is: "yes, but with some modifications". For example, as reported in the follow, it is necessary to modify the feeders equivalent circuit and consider the MV network (which feeds the LV grids via a transformer) as a slack bus.

In this chapter the sensitivity theory, applied to the LV four-wires distribution network, is presented. This approach is useful to control the voltage also in LV grids, where a large number of distributed generators, e.g. PV house-roof generators, is installed. The voltage control can be performed acting mainly on these single-phase generators.

6.2.1 Four-wires lines and uncoupled equivalent circuit

The majority of LV distributed generators is represented by single-phase generators, connected between a line conductor of the three-phase LV grid and the neutral one. This generators connection and the single-phase load presence creates a current unbalance on the phases and neutral conductors. In other words the positive, the negative and the zero-sequence system flows in a feeder section, composed by three wires with neutral. Then it is impossible to apply the single-phase equivalent circuit to the lines.

The proposed sensitivity method analyze the LV feeder "phase-by-phase", defining a "phase sensitivity matrix" (and the relative "phase sensitivity table") for the active and the reactive power. For example, if we have five generators on the phase "a", we can choose the generator to control the phase "a" voltage using the "phase "a" (active/reactive) sensitivity matrix". It is clear that a power variation on the phase "a" influences also the phase "b" and "c" voltage, due to the common connection of the generators on the neutral wire.

In the first step of the "phase-by-phase" analysis, a "magnetically uncoupled" feeder equivalent circuit must be defined. The equivalence is defined in terms of sequence impedances.

The structure of a physically symmetrical four-wires feeder is depicted in Fig. 6.2-1-a ("a", "b", "c" are the phase conductors; "n" is the neutral conductor), while its equivalent circuit is represented in Fig. 6.2-1-b, where **Errore. L'origine riferimento non è stata trovata.** (capacitances can be neglected due to the short length of the lines):

- R is the phase wire resistance
- L is the phase wire self-inductance
- M is the mutual-inductance between two phase wires
- R_n is the neutral wire resistance
- L_n is the neutral wire self-inductance
- M_n is the mutual-inductance between a phase wire and the neutral wire

In terms of sequence impedances (see Fig. 6.2-2) we can write:

$$\overline{Z}_1 = \overline{Z}_2 = R + \mathrm{j}\omega(L - M) \triangleq R + \mathrm{j}X \tag{6.1}$$

$$\overline{Z}_0 = (R + 3R_n) + \mathrm{j}\omega\left[L + 2M + 3(L_n + 2M_n)\right] \triangleq R_0 + \mathrm{j}X_0 \tag{6.2}$$

It is important to note that the neutral wire of the "black box" depicted in Fig. 6.2-2 is a "zero-impedance" conductor, because the neutral impedance (R_n, L_n and M_n) is taken into account in $\overline{Z}_1 = \overline{Z}_2$ and in $\overline{Z}_0$.

The magnetically uncoupled feeder circuit is depicted in Fig. 6.2-3. For this "fictitious" feeder we can say that:

$$\overline{Z}_{1,eq} = \overline{Z}_{2,eq} = R_{eq} + \mathrm{j}\omega L_{eq} \triangleq R_{eq} + \mathrm{j}X_{eq} \tag{6.3}$$

$$\overline{Z}_{0,eq} = R_{eq} + \mathrm{j}\omega L_{eq} + 3\left(R_{n,eq} + \mathrm{j}\omega L_{n,eq}\right) \triangleq R_{eq} + \mathrm{j}X_{eq} + 3\left(R_{n,eq} + \mathrm{j}X_{n,eq}\right) \tag{6.4}$$

The magnetically uncoupled feeder circuit of Fig. 6.2-3 is equivalent, in terms of sequence impedances, to the "original" circuit of Fig. 6.2-2 if:

$$\overline{Z}_{1,eq} = \overline{Z}_1 \left(\text{or } \overline{Z}_{2,eq} = \overline{Z}_2\right) \tag{6.5}$$

and

$$\overline{Z}_{0,eq} = \overline{Z}_0 \tag{6.6}$$

In other words, from (6.5) and (6.6), we must have:

$$R_{eq} = R \tag{6.7}$$

$$X_{eq} = X \tag{6.8}$$

$$R_{n,eq} = \frac{R_0 - R}{3} \tag{6.9}$$

$$X_{n,eq} = \frac{X_0 - X}{3} \tag{6.10}$$

Equations (6.7) to (6.10) allow to build the magnetically uncoupled feeder equivalent circuit starting from R, X, R_0 and X_0 of the "original" feeder. It is important to note that the presented model represents a fictitious feeder.

Equations (6.7) to (6.10) (summarized in Table XIII) are also valid in term of per-unit of length values (i.e. in $\left[\Omega/\text{km}\right]$ units).
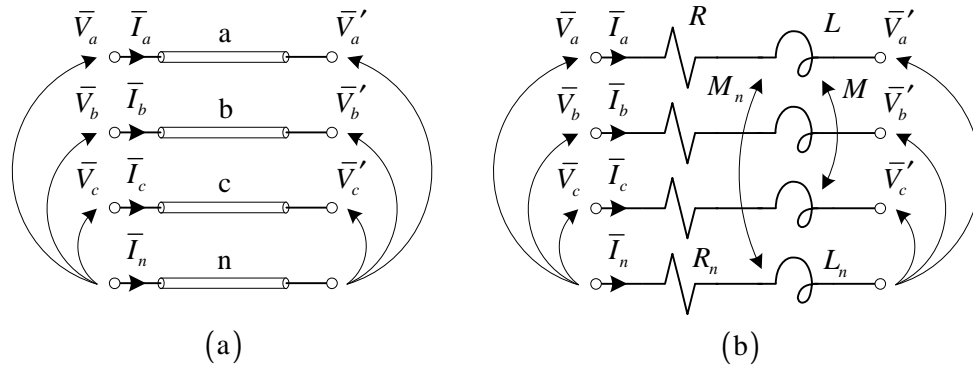
Fig. 6.2-1. The physical structure of a four-wires feeder (a), and its equivalent circuit (b)
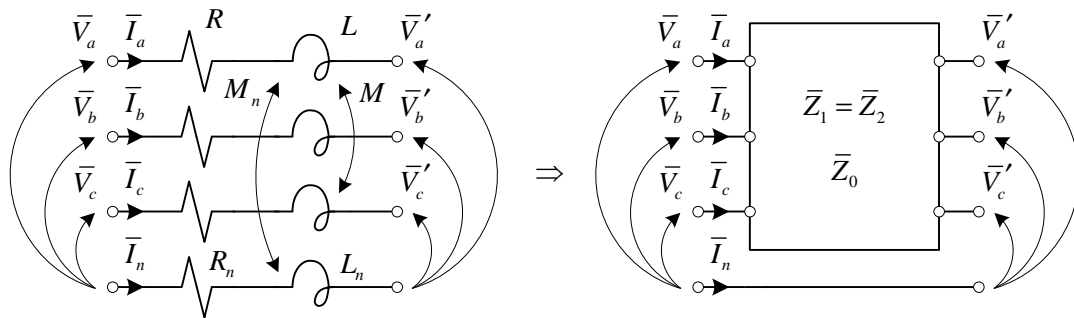
Fig. 6.2-2. The equivalent circuit of a four-wires feeder in terms of sequence impedances
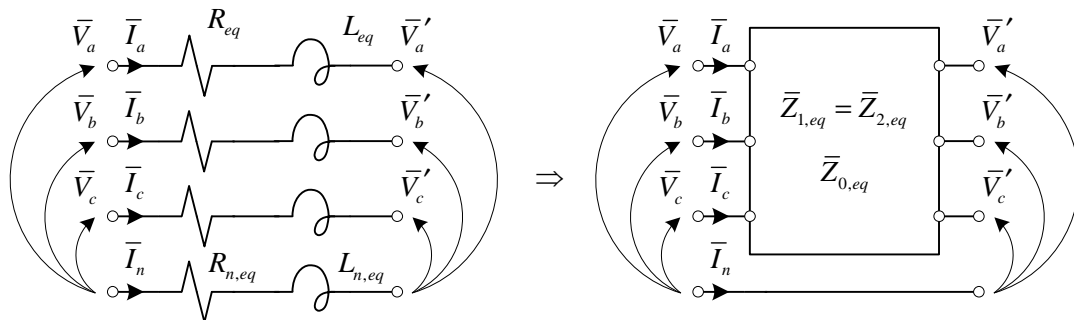
Fig. 6.2-3. The equivalent circuit of a magnetically uncoupled four-wires feeder, in terms of sequence impedances

TABLE XIII. PARAMETERS OF THE ORIGINAL AND EQUIVALENT FEEDER

Original feeder (input data)		Equivalent feeder (output data)	
R	R_0	$R_{eq} = R$	$R_{n,eq} = \dfrac{R_0 - R}{3}$
X	X_0	$X_{eq} = X$	$X_{n,eq} = \dfrac{X_0 - X}{3}$

6.2.2 Transformer uncoupled equivalent circuit

The LV grid is normally fed, by the MV network, via an MV/LV transformer. Also for this component a magnetically uncoupled circuit is necessary, because the transformer impedance plays an important role in the sensitivity matrix.

Due to the presence of single-phase load on LV network, the secondary side of the transformer must be a wye winding "y" (also the "zig-zag" winding is allowed, but this connection is not used in Enel Distribuzione grids), and the primary side must be a delta connection "D". The typical machine used in Italy by Enel Distribuzione is the Dy11 transformer. Its windings arrangement is sketched in Fig. 6.2-4.

In terms of sequence impedances, the Dy11 transformer can be represented with the secondary-side equivalent circuit reported in Fig. 6.2-5 (a and b), where:

- R_t'' is the short-circuit resistance, referred to the secondary side

- X_t'' is the short-circuit reactance, referred to the secondary side

- V_{1n} and V_{2n} are the primary and secondary rated voltages of the machine

- $\bar{Z}_{1,t}$, $\bar{Z}_{2,t}$ and $\bar{Z}_{0,t}$ are the positive, the negative and the zero sequence transformer impedances

The Dy connection separates the LV grid zero sequence circuit from the MV grid zero sequence circuit, and allows the correct operation of the single-phase loads connected to the LV side.

MV/LV Dy11 Transformer
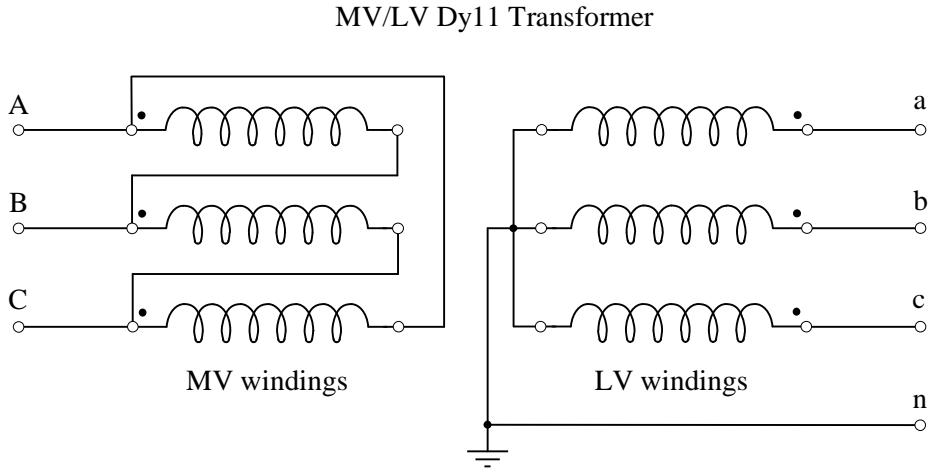
Fig. 6.2-4. MV/LV Dy11 transformer windings arrangement
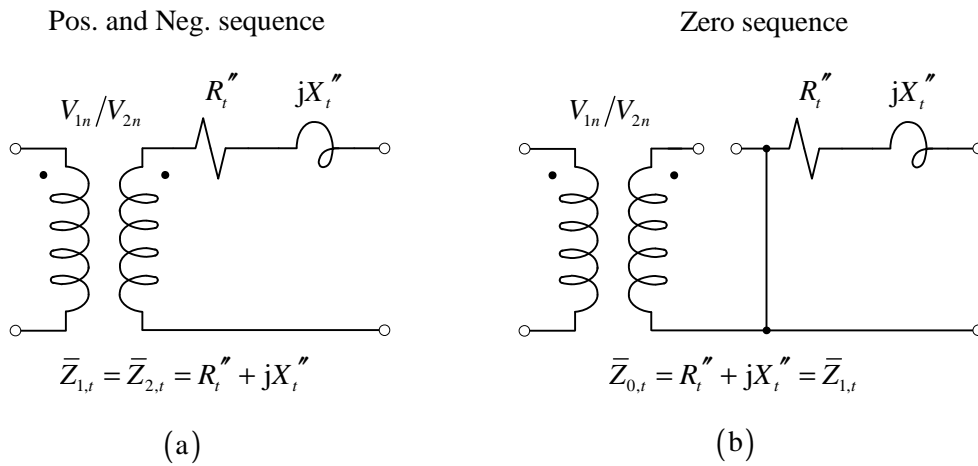
Fig. 6.2-5. Transformer secondary-side equivalent circuit in terms of sequence impedances

The transformer secondary side circuit can be substituted by an equivalent uncoupled three-phase circuit which is equivalent in terms of sequence impedances. Let us consider that the MV transformer side is fed by a three-phase positive sequence ideal voltage source (the MV short circuit power very greater than the transformer rated power, i.e. we have an MV infinite bus). Taking into account that:

$$\overline{Z}_{1,t} = \overline{Z}_{2,t} = R_t'' + jX_t'' \tag{6.11}$$

and

$$\overline{Z}_{0,t} = R_t'' + jX_t'' = \overline{Z}_{1,t} \tag{6.12}$$

The equivalent uncoupled three-phase circuit can be represented as in Fig. 6.2-6-a, where:

$$R_{t,eq} = R_t'' \tag{6.13}$$

and

$$X_{t,eq} = X_t'' \tag{6.14}$$

The sequence impedances of the circuit depicted in Fig. 6.2-6-a are:

$$\overline{Z}_{1,t,eq} = \overline{Z}_{2,t,eq} = R_{t,eq} + jX_{t,eq} = R_t'' + jX_t'' \tag{6.15}$$

and

$$\overline{Z}_{0,t,eq} = R_{t,eq} + jX_{t,eq} = R_t'' + jX_t'' \tag{6.16}$$

which are equal to (6.11) and (6.12). The equivalence has been demonstrated.

(a)   (b)
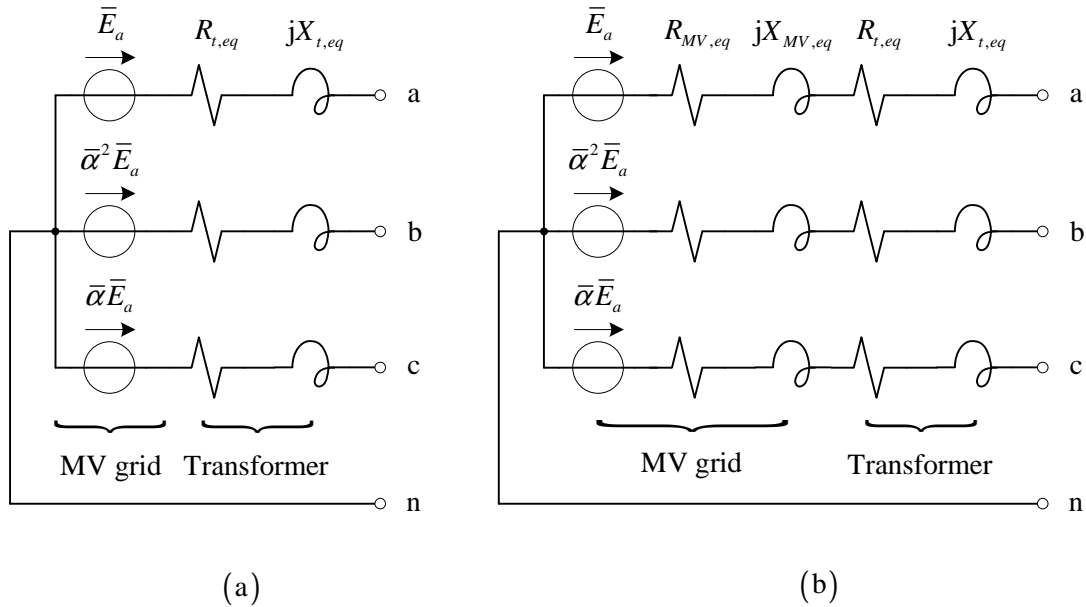
Fig. 6.2-6. Transformer secondary-side equivalent uncoupled three-phase circuit. Machine fed by a grid with infinite (a) and finite short circuit power

If the MV grid is not an infinite bus, the positive sequence MV grid impedance, referred to the LV side ($R_{MV,eq} + jX_{MV,eq}$), can be connected in series to $R_{t,eq}$ and $X_{t,eq}$, as reported in Fig. 6.2-6-b. The zero sequence MV grid impedance takes not a role in the circuit due to the separation introduced by the transformer (see Fig. 6.2-5-b).
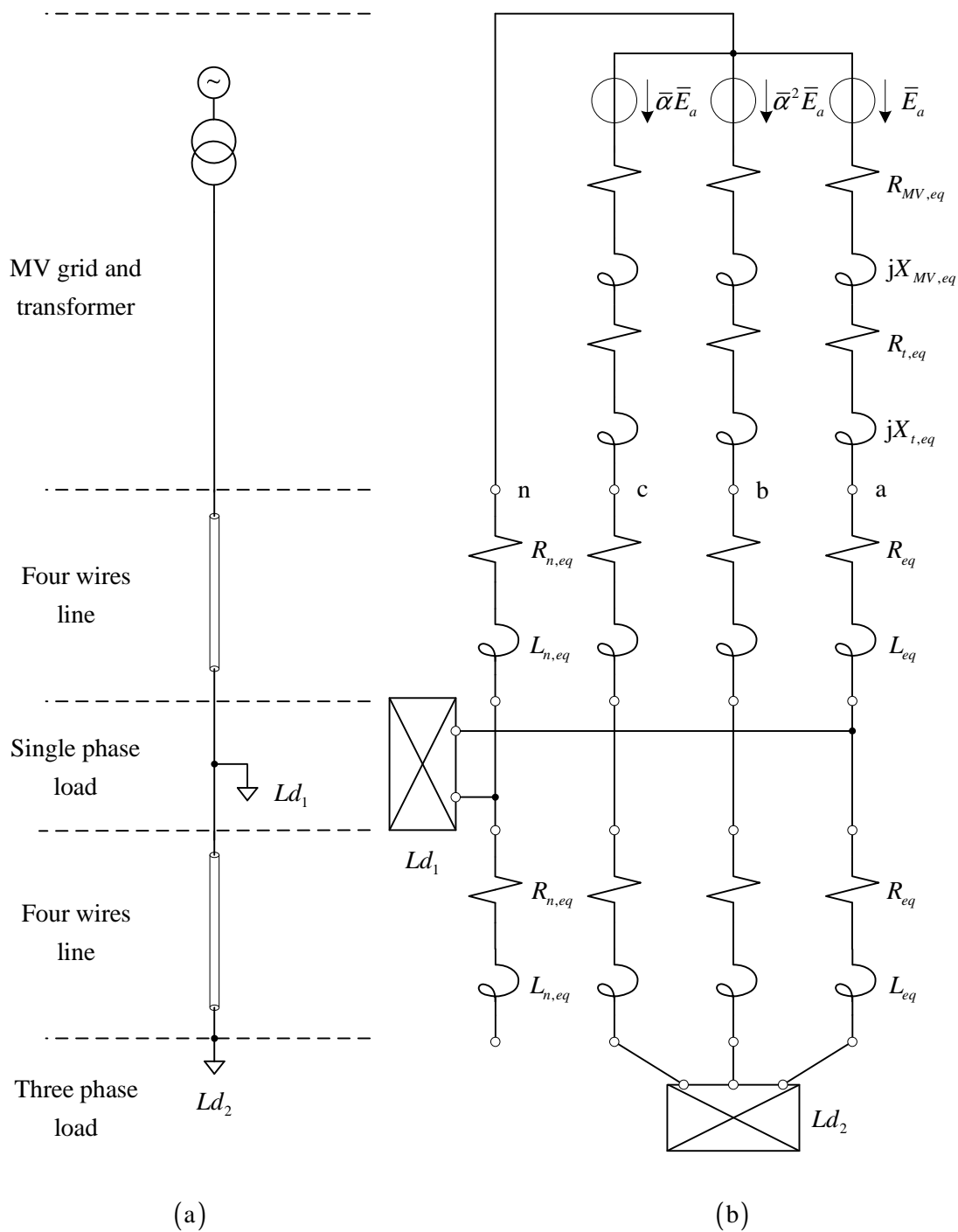
Fig. 6.2-7. A simple four-wires LV network. The single-wire diagram (a) and the equivalent uncoupled circuit referred to the LV side (b)

6.2.3 The whole LV grid representation

Let us now consider the simple LV network depicted the single-wire diagram of Fig. 6.2-7-a, where:

- both three-phase and single-phase load are present (no balanced currents are present in the lines)
- the MV grid has a finite short circuit power
- the HV/LV transformer is a Dy11 machine

According to the concepts exposed in the previous sections of this chapter, the equivalent uncoupled circuit, referred to the LV side, which takes account also the MV grid, is sketched in Fig. 6.2-7-b. This circuit can be considered as a "summary" of the concepts previously exposed.

In the next section the sensitivity approach applied on the LV network is presented.

6.3 THE SENSITIVITY APPROACH APPLIED ON A FOUR-WIRES NETWORK

As previously said, we want to control the voltages (for each phase) of a four-wires system using the sensitivity approach, acting on single-phase generators. In this way, the generators connected to the phase "a" are driven in order to control the voltage of this phase. The same occurs for the phase "b" and "c". Then, the proposed procedure will be derived analyzing only the phase "a".

Let us now consider the LV grid depicted in Fig. 6.3-1, which is topologically similar to the MV network proposed in the Chapter 3.
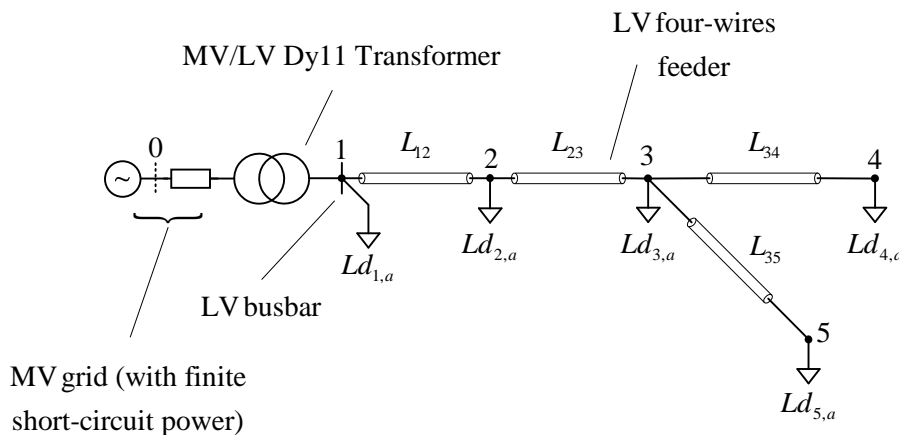
Fig. 6.3-1. LV four-wires grid used to study the sensitivity approach

In spite of generality, in each section (2 to 5) of the grid three single-phase general loads (connected to the phases "a", "b" and "c" respectively) and a three-phase general load are considered (the attribute "general" indicates that the device can be a load or a generator, in fact the treatment can be used both for loads and generators). However, in spite of simplicity, only the single-phase connected to the phase "a" has been depicted in Fig. 6.3-1. In a particular operation point, each load can be substituted, applying substitution principle, with a current generator. For example, section 2 can be represented as in Fig. 6.3-2, where the circuit

parameter has been calculated starting from the original feeder parameter using the procedure described in Section 6.2.1. Then, in the complete circuit, we can separate the generators in two groups:

- the first group is composed by the three-phase voltage source of the MV network (which can be referred to the LV side, as explained in Section 6.2.2) and all of the current sources which represent the single-phase loads connected to the phase "a" (as said before, the sensitivity approach will be derived on the phase "a")
- the second group involves all of the current sources which represent the other loads (single-phase, connected to the other phases and three-phase type)

Applying the causes and effects superimpose principle, we can calculate the node voltages (e.g. $E_{2,a}$, $E_{2,b}$, $E_{2,c}$, etc.), and its variations in function of the powers, in two steps:

- in the first step also the generators of the first group will be activated
- in the second step also the generators of the second group will be activated

Referring to the phase "a", in the first the first step we can calculate the nodal voltages variations $\left[\Delta E'\right]$, due to the power variation of the generator relative to the first group. In the second step we can calculate the nodal voltages variations $\left[\Delta E''\right]$, due to the power variation of the generator relative to the second group. Both $\left[\Delta E'\right]$ and $\left[\Delta E''\right]$ are vectors (as explained in the follow). The number of elements equals the nodes per phase. The total voltages variations $\left[\Delta E\right]$ are represented by the following algebraic sum:

$$\left[\Delta E\right]=\left[\Delta E'\right]+\left[\Delta E''\right] \tag{6.17}$$

In the follow, each "general load" must be considered as a generator.

6.3.1 Voltages calculation in the "first step"

In the first step, and for the phase "a", the entire grid of Fig. 6.3-1 can be sketched as in Fig. 6.3-3, where the circuit is referred to the LV side. All of the quantities of the first step will be marked with one apex.
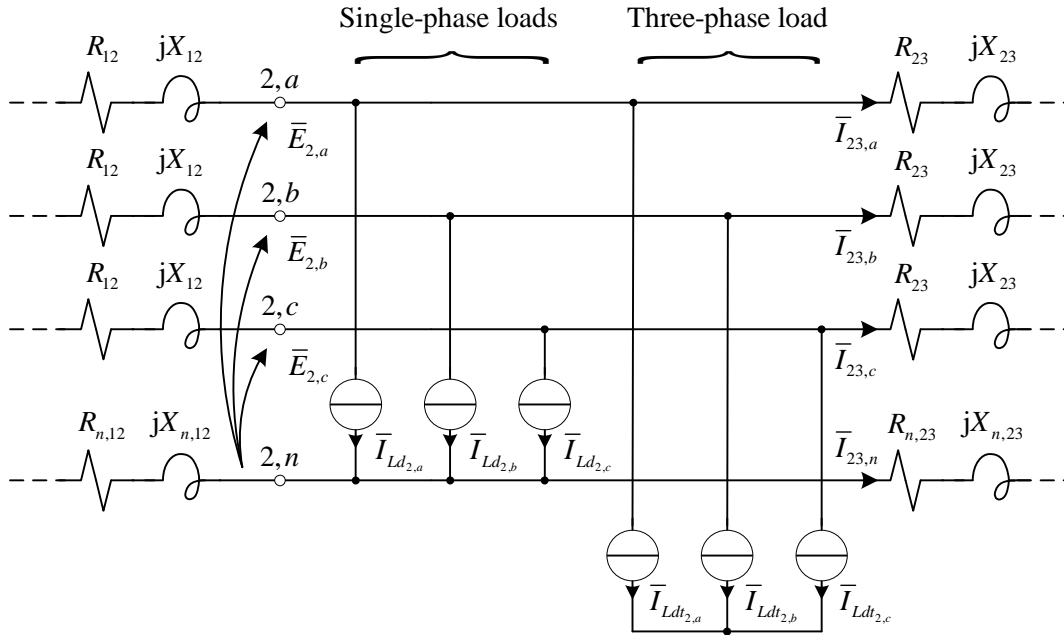
Fig. 6.3-2. LV four-wires grid used to study the sensitivity approach. Representation of section 2

The impedance $R_{01} + jX_{01}$ is composed by the transformer impedance and the MV grid impedance (both referred to the LV side), as explained in Section 6.2.2. In particular:

$$R_{01} = R_{MV,eq} + R_{t,eq} \tag{6.18}$$

$$X_{01} = X_{MV,eq} + X_{t,eq} \tag{6.19}$$

The network of Fig. 6.3-3 is very similar to which presented in Chapter 3 for the MV case. The main differences are:

- the constant voltage node, i.e. the slack node, is "0,a" (for the phase "a"). This MV node is "transported" to the LV side and its voltage is $E_{0,a} = E_a$

- the neutral conductor impedance is not zero

Then, in order to calculate the voltage variations $\Delta E'$ (the apex indicates the first step), due to a power variation ΔP and ΔQ, the sensitivity approach can be applied similarly to Chapter 3.

In spite of simplicity, in the following the reference to the phase "a" is omitted. Then, the node "0,a" will be "0", the voltage $E_{1,a}{}'$ will be $E_1{}'$ etc.

The node "0" is slack-type. Then we can characterize the generic node i using the difference $V_{0i}{}'$ between the magnitude $E_0 = E_a$ and the node voltage $E_i{}'$. In other words, we can write:

$$V_{0i}{}' = E_0 - E_i{}' \tag{6.20}$$
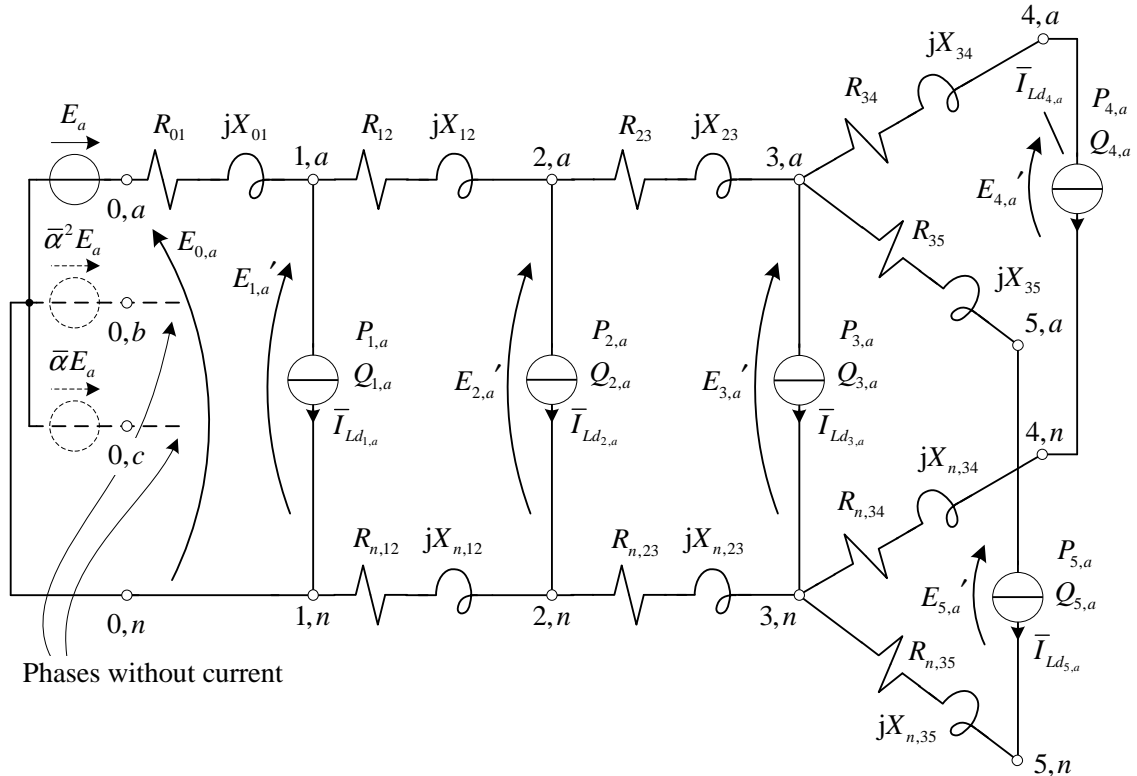
Fig. 6.3-3. First step application of the causes and effects superimpose principle

For example, if $i = 4$ (6.20) becomes:

$$V_{04}{}' = E_0 - E_4{}' \tag{6.21}$$

By adding and subtracting E_1, E_2 and E_3 we obtain:

$$V_{04}{}' = \left(E_0 - E_1{}'\right) + \left(E_1{}' - E_2{}'\right) + \left(E_2{}' - E_3{}'\right) + \left(E_3{}' - E_4{}'\right) =$$
$$= V_{01}{}' + V_{12}{}' + V_{23}{}' + V_{34}{}' \tag{6.22}$$

then $V_{04}{}'$ is the sum of the voltage differences $V_{01}{}'$, $V_{12}{}'$, $V_{23}{}'$ and $V_{34}{}'$. Then, as explained in Chapter 3, we can write:

$$V_{34}' = \frac{(R_{34} + R_{n,34})P_4 + (X_{34} + X_{n,34})Q_4}{E_4'} \cong \frac{(R_{34} + R_{n,34})P_4 + (X_{34} + X_{n,34})Q_4}{E_n} \tag{6.23}$$

where E_n is the phase-to-neutral LV grid rated voltage.

Similarly, for the other nodes we can write:

$$V_{23}' \cong \frac{(R_{23} + R_{n,23})P_{S3} + (X_{23} + X_{n,23})Q_{S3}}{E_n} \tag{6.24}$$

where P_{S3} and Q_{S3} are the active and reactive powers through the section "3,a", neglecting the power losses on resistances and reactances. In other words:

$$P_{S3} = P_3 + P_4 + P_5 \tag{6.25}$$

$$Q_{S3} = Q_3 + Q_4 + Q_5 \tag{6.26}$$

For nodes 1 and 2 we can say that:

$$V_{12}' \cong \frac{(R_{12} + R_{n,12})P_{S2} + (X_{12} + X_{n,12})Q_{S2}}{E_n} \tag{6.27}$$

where:

$$P_{S2} = P_2 + P_3 + P_4 + P_5 \tag{6.28}$$

$$Q_{S2} = Q_2 + Q_3 + Q_4 + Q_5 \tag{6.29}$$

Finally, the voltage difference V_{01}' is:

$$V_{01}' \cong \frac{R_{01}P_{S1} + X_{01}Q_{S1}}{E_n} \tag{6.30}$$

where:

$$P_{S1} \cong P_1 + P_2 + P_3 + P_4 + P_5 \tag{6.31}$$

$$Q_{S1} \cong Q_1 + Q_2 + Q_3 + Q_4 + Q_5 \tag{6.32}$$

Similarly to Chapter 3, we can say that V_{04}' is a function of all loads and (active and reactive powers). The same observation is valid for E_4' because E_0 is constant. Then:

$$E_4' = E_0 - V_{04}' = E_0 - \left(V_{01}' + V_{12}' + V_{23}' + V_{34}'\right) \tag{6.33}$$

In other words, we can write:

$$E_4' = f\left(P_1, ..., P_5, Q_1, ..., Q_5\right) \tag{6.34}$$

Equation (6.34) shows that an active/reactive power variation (in the general j node) that is defined as:

$$\Delta P_j = P_j^f - P_j^0 \tag{6.35}$$

$$\Delta Q_j = Q_j^f - Q_j^0 \tag{6.36}$$

where P_j^f (Q_j^f) and P_j^0 (Q_j^0) are the final and initial power values, respectively, produces a voltage variation in node 4 that is defined as:

$$\Delta E_4' = E_4'^f - E_4'^0 \tag{6.37}$$

Similarly to Chapter 3, we only first consider only the reactive power variations, i.e. $\Delta P_j = 0$ because we assume that only the reactive power can be used to control the node voltages.

The variation $\Delta E_4'$ can be calculated by linearizing (6.34) and considering only the reactive power variations. In particular, we can write:

$$\Delta E_4' = \frac{\partial E_4'}{\partial Q_1} \Delta Q_1 + \frac{\partial E_4'}{\partial Q_2} \Delta Q_2 + $$
$$+ \frac{\partial E_4'}{\partial Q_3} \Delta Q_3 + \frac{\partial E_4'}{\partial Q_4} \Delta Q_4 + \frac{\partial E_4'}{\partial Q_5} \Delta Q_5 \tag{6.38}$$

According to (6.33), we can obtain:

$$\frac{\partial E_4'}{\partial Q_1} = -\frac{X_{01}}{E_n} \qquad \frac{\partial E_4'}{\partial Q_2} = -\frac{X_{01} + X_{12} + X_{n,12}}{E_n} \tag{6.39}$$

$$\frac{\partial E_4'}{\partial Q_3} = -\frac{X_{01} + X_{12} + X_{n,12} + X_{23} + X_{n,23}}{E_n} \tag{6.40}$$

$$\frac{\partial E_4'}{\partial Q_4} = -\frac{X_{01} + X_{12} + X_{n,12} + X_{23} + X_{n,23} + X_{34} + X_{n,34}}{E_n} \tag{6.41}$$

$$\frac{\partial E_4'}{\partial Q_5} = -\frac{X_{01} + X_{12} + X_{n,12} + X_{23} + X_{n,23}}{E_n} \tag{6.42}$$

If the above analysis that focuses on node 4 is extended to all network nodes, we obtain a general matrix relationship:

$$
\begin{bmatrix} \Delta E_1' \\ \Delta E_2' \\ \Delta E_3' \\ \Delta E_4' \\ \Delta E_5' \end{bmatrix} =
\begin{bmatrix}
\dfrac{\partial E_1'}{\partial Q_1} & \dfrac{\partial E_1'}{\partial Q_2} & \dfrac{\partial E_1'}{\partial Q_3} & \dfrac{\partial E_1'}{\partial Q_4} & \dfrac{\partial E_1'}{\partial Q_5} \\[2mm]
\dfrac{\partial E_2'}{\partial Q_1} & \dfrac{\partial E_2'}{\partial Q_2} & \dfrac{\partial E_2'}{\partial Q_3} & \dfrac{\partial E_2'}{\partial Q_4} & \dfrac{\partial E_2'}{\partial Q_5} \\[2mm]
\dfrac{\partial E_3'}{\partial Q_1} & \dfrac{\partial E_3'}{\partial Q_2} & \dfrac{\partial E_3'}{\partial Q_3} & \dfrac{\partial E_3'}{\partial Q_4} & \dfrac{\partial E_3'}{\partial Q_5} \\[2mm]
\dfrac{\partial E_4'}{\partial Q_1} & \dfrac{\partial E_4'}{\partial Q_2} & \dfrac{\partial E_4'}{\partial Q_3} & \dfrac{\partial E_4'}{\partial Q_4} & \dfrac{\partial E_4'}{\partial Q_5} \\[2mm]
\dfrac{\partial E_5'}{\partial Q_1} & \dfrac{\partial E_5'}{\partial Q_2} & \dfrac{\partial E_5'}{\partial Q_3} & \dfrac{\partial E_5'}{\partial Q_4} & \dfrac{\partial E_5'}{\partial Q_5}
\end{bmatrix}
\begin{bmatrix} \Delta Q_1 \\ \Delta Q_2 \\ \Delta Q_3 \\ \Delta Q_4 \\ \Delta Q_5 \end{bmatrix}
\tag{6.43}
$$

which in a compact form yields:

$$
\begin{bmatrix} \Delta E' \end{bmatrix} = \begin{bmatrix} s_{Q,a} \end{bmatrix} [\Delta Q]
\tag{6.44}
$$

where $\begin{bmatrix} s_{Q,a} \end{bmatrix}$ is the reactive sensitivity matrix of the phase "a", $[\Delta Q]$ is the reactive power-variations (of the same phase) vector and $\begin{bmatrix} \Delta E' \end{bmatrix}$ is the nodal voltages vector.

Calculating the partial derivatives, $\begin{bmatrix} s_{Q,a} \end{bmatrix}$ becomes:

$$
\begin{bmatrix} s_{Q,a} \end{bmatrix} = -\frac{1}{E_n}
\begin{bmatrix}
X_{01} & X_{01} & X_{01} & \cdots \\
X_{01} & X_{01}+X_{12}+X_{n,12} & X_{01}+X_{12}+X_{n,12} & \cdots \\
X_{01} & X_{01}+X_{12}+X_{n,12} & X_{01}+X_{12}+X_{n,12}+X_{23}+X_{n,23} & \cdots \\
X_{01} & X_{01}+X_{12}+X_{n,12} & X_{01}+X_{12}+X_{n,12}+X_{23}+X_{n,23} & \cdots \\
X_{01} & X_{01}+X_{12}+X_{n,12} & X_{01}+X_{12}+X_{n,12}+X_{23}+X_{n,23} & \cdots
\end{bmatrix}
$$

$$
\begin{array}{ll}
\cdots & X_{01} \qquad\qquad\qquad\qquad\qquad X_{01} \\
\cdots & X_{01}+X_{12}+X_{n,12} \qquad\qquad\qquad X_{01}+X_{12}+X_{n,12} \\
\cdots & X_{01}+X_{12}+X_{n,12}+X_{23}+X_{n,23} \qquad X_{01}+X_{12}+X_{n,12}+X_{23}+X_{n,23} \\
\cdots & X_{01}+X_{12}+X_{n,12}+X_{23}+X_{n,23}+X_{34}+X_{n,34} \quad X_{01}+X_{12}+X_{n,12}+X_{23}+X_{n,23} \\
\cdots & X_{01}+X_{12}+X_{n,12}+X_{23}+X_{n,23} \qquad X_{01}+X_{12}+X_{n,12}+X_{23}+X_{n,23}+X_{35}+X_{n,35}
\end{array}
$$

$$
\tag{6.45}
$$

After analyzing (6.45), we can say that this matrix can be built using the following inspection rule, that is very similar to which presented in Chapter 3:

> *"The element i, j is the arithmetic sum of the reactances of all branches (including the neutral one) in which both the powers absorbed by node i and node j flow multiplied by $-1/E_n$ ".*

For example, in (6.45) the element 2,4 is $-\left(X_{01} + X_{12} + X_{n,12}\right)/E_n$ because the powers delivered by node 2 and node 4 flow in branches 01 and 12, including the neutral wire.

It is important to note that if we would consider also the active power variation effect, for the above discussions (6.44) becomes:

$$\left[\Delta E'\right] = \left[s_{Q,a}\right][\Delta Q] + \left[s_{P,a}\right][\Delta P] \tag{6.46}$$

where:

$$[\Delta P] = \begin{bmatrix} \Delta P_1 & \Delta P_2 & \Delta P_3 & \Delta P_4 & \Delta P_5 \end{bmatrix}^T \tag{6.47}$$

is the active power variations vector and $\left[s_{P,a}\right]$ is the phase "a" active power sensitivity matrix, that is formally identical to (6.45) but replacing the reactances with the resistances and maintaining the same subscript, i.e. X_{01} became R_{01} etc. Also the inspection rule is identical, considering the resistances instead of the reactances. Then the active power sensitivity matrix for the network of Fig. 6.3-1 is:

$$\left[s_{P,a}\right] = -\frac{1}{E_n} \begin{bmatrix} R_{01} & R_{01} & R_{01} & \dots \\ R_{01} & R_{01} + R_{12} + R_{n,12} & R_{01} + R_{12} + R_{n,12} & \dots \\ R_{01} & R_{01} + R_{12} + R_{n,12} & R_{01} + R_{12} + R_{n,12} + R_{23} + R_{n,23} & \dots \\ R_{01} & R_{01} + R_{12} + R_{n,12} & R_{01} + R_{12} + R_{n,12} + R_{23} + R_{n,23} & \dots \\ R_{01} & R_{01} + R_{12} + R_{n,12} & R_{01} + R_{12} + R_{n,12} + R_{23} + R_{n,23} & \dots \end{bmatrix}$$

$$\begin{matrix} \dots & R_{01} & R_{01} \\ \dots & R_{01} + R_{12} + R_{n,12} & R_{01} + R_{12} + R_{n,12} \\ \dots & R_{01} + R_{12} + R_{n,12} + R_{23} + R_{n,23} & R_{01} + R_{12} + R_{n,12} + R_{23} + R_{n,23} \\ \dots & R_{01} + R_{12} + R_{n,12} + R_{23} + R_{n,23} + R_{34} + R_{n,34} & R_{01} + R_{12} + R_{n,12} + R_{23} + R_{n,23} \\ \dots & R_{01} + R_{12} + R_{n,12} + R_{23} + R_{n,23} & R_{01} + R_{12} + R_{n,12} + R_{23} + R_{n,23} + R_{35} + R_{n,35} \end{matrix} \tag{6.48}$$

The nodal voltages variations $\left[\Delta E'\right]$ have been calculated.

6.3.2 Voltages calculation in the "second step"

In the second step the voltages variations $[\Delta E'']$ would be calculated, due to the power variations of the generators relative to the second group. However, in the practice, this contribution can be neglected.

In order to demonstrate this affirmation, let us consider a reactive power variation in the node 3, $\Delta Q_3 = Q_3{}^f - Q_3{}^0 > 0$ (the generator absorbs reactive power), by the single-phase generator connected to this node, and let us calculate the voltage variation in the same node, applying the causes and effect superimpose principle. The current of loads and generators (excluded the generator connected to the node 3) can be considered invariable with respect to ΔQ_3. Then the phasor diagram Fig. 6.3-4 can be derived, where:

- $\bar{E}_3^{0\prime}$ is the voltage of the node 3, in the first step, when the generator exchanges Q_3^0

- $\bar{E}_3{}''$ is the voltage of the node 3, in the second step. This phasor is invariant with respect to ΔQ_3, as said before

- $\bar{E}_3^0$ is the "total" voltage of the node 3, in the first step, after the application of the causes and effect superimpose principle

- $\bar{E}_3^{f\prime}$ is the voltage of the node 3, in the first step, when the generator exchanges $Q_3{}^f$

- $\bar{E}_3^f$ is the "total" voltage of the node 3, in the second step, after the application of the causes and effect superimpose principle

Besides:

- $\Delta E_3{}'$ is the voltage variation, in the node 3, due to the first step, which can be calculated using the sensitivity approach presented in Section 6.3.1

- $\Delta E_3{}''$ is the voltage variation, in the node 3, due to the second step

- ΔE_3 is the total voltage variation in the node 3 (see (6.17))

In the practice, the variation $\Delta E_3{}''$ can be neglected. In this case we can write:

$$\Delta E_3 \simeq \Delta E_3{}' \tag{6.49}$$

Then, for a practical point of view, the total voltage variation can be approximated with the voltage variation $\Delta E_3{}'$ evaluable using the sensitivity approach presented in Section 6.3.1. In other words we neglecting the influence of all other "general loads" on voltage variations due to the reactive power exchanged in the node 3.

The same conclusion can be applied to calculate the voltage variation in a node *i* when a reactive power variation occurs in a general node *j*.

These conclusions are valid also for active power.

It is important to note that if, in a particular case, $\Delta E_3{}''$ cannot be neglected, the application of the sensitivity approach presented in Section 6.3.1 to evaluate (6.49) creates error. However the sensitivity approach can be used, without problems, to choose the "best generator". In the follow we consider that $\Delta E_3{}''$ can be always negligible, and (6.49) can be used without problems. Then, the vector of the voltages variations in (6.43), can be rewritten without apexes:

$$
\begin{bmatrix} \Delta E_1 \\ \Delta E_2 \\ \Delta E_3 \\ \Delta E_4 \\ \Delta E_5 \end{bmatrix} = \begin{bmatrix} \dfrac{\partial E_1'}{\partial Q_1} & \dfrac{\partial E_1'}{\partial Q_2} & \dfrac{\partial E_1'}{\partial Q_3} & \dfrac{\partial E_1'}{\partial Q_4} & \dfrac{\partial E_1'}{\partial Q_5} \\[2ex] \dfrac{\partial E_2'}{\partial Q_1} & \dfrac{\partial E_2'}{\partial Q_2} & \dfrac{\partial E_2'}{\partial Q_3} & \dfrac{\partial E_2'}{\partial Q_4} & \dfrac{\partial E_2'}{\partial Q_5} \\[2ex] \dfrac{\partial E_3'}{\partial Q_1} & \dfrac{\partial E_3'}{\partial Q_2} & \dfrac{\partial E_3'}{\partial Q_3} & \dfrac{\partial E_3'}{\partial Q_4} & \dfrac{\partial E_3'}{\partial Q_5} \\[2ex] \dfrac{\partial E_4'}{\partial Q_1} & \dfrac{\partial E_4'}{\partial Q_2} & \dfrac{\partial E_4'}{\partial Q_3} & \dfrac{\partial E_4'}{\partial Q_4} & \dfrac{\partial E_4'}{\partial Q_5} \\[2ex] \dfrac{\partial E_5'}{\partial Q_1} & \dfrac{\partial E_5'}{\partial Q_2} & \dfrac{\partial E_5'}{\partial Q_3} & \dfrac{\partial E_5'}{\partial Q_4} & \dfrac{\partial E_5'}{\partial Q_5} \end{bmatrix} \begin{bmatrix} \Delta Q_1 \\ \Delta Q_2 \\ \Delta Q_3 \\ \Delta Q_4 \\ \Delta Q_5 \end{bmatrix} \qquad (6.50)
$$

Fig. 6.3-4. Phasor diagram derived from the causes and effects superimpose principle

6.4   THE "BEST GENERATOR" CHOICE

As said in Chapter 3, the "best generator" (BG) is the generator that has the greatest influence on a node i, which is the node where the voltage exceeds the threshold.

Thus, after analyzing (6.50), we can say that the BG is the generator that maximizes the following product, which we call the "*sensitivity product*":

$$\frac{\partial E_i{}'}{\partial Q_j} \Delta Q_j \tag{6.51}$$

As said in Chapter 3 the system must know the value ΔQ_j and it can acquire this value polling the distributed generators.

The procedure described above suggests a way of defining the "*reactive power sensitivity table*" $\left[T_{SQ,a} \right]$ (for the phase "a", in this example) that contains the single sensitivity products.

For the LV grid represented in Fig. 6.3-1, $\left[T_{SQ,a} \right]$ takes the following form:

$$\begin{bmatrix} \dfrac{\partial E_1}{\partial Q_1}\Delta Q_1 & \dfrac{\partial E_1}{\partial Q_2}\Delta Q_2 & \dfrac{\partial E_1}{\partial Q_3}\Delta Q_3 & \dfrac{\partial E_1}{\partial Q_4}\Delta Q_4 & \dfrac{\partial E_1}{\partial Q_5}\Delta Q_5 \\[2mm] \dfrac{\partial E_2}{\partial Q_1}\Delta Q_1 & \dfrac{\partial E_2}{\partial Q_2}\Delta Q_2 & \dfrac{\partial E_2}{\partial Q_3}\Delta Q_3 & \dfrac{\partial E_2}{\partial Q_4}\Delta Q_4 & \dfrac{\partial E_2}{\partial Q_5}\Delta Q_5 \\[2mm] \dfrac{\partial E_3}{\partial Q_1}\Delta Q_1 & \dfrac{\partial E_3}{\partial Q_2}\Delta Q_2 & \dfrac{\partial E_3}{\partial Q_3}\Delta Q_3 & \dfrac{\partial E_3}{\partial Q_4}\Delta Q_4 & \dfrac{\partial E_3}{\partial Q_5}\Delta Q_5 \\[2mm] \dfrac{\partial E_4}{\partial Q_1}\Delta Q_1 & \dfrac{\partial E_4}{\partial Q_2}\Delta Q_2 & \dfrac{\partial E_4}{\partial Q_3}\Delta Q_3 & \dfrac{\partial E_4}{\partial Q_4}\Delta Q_4 & \dfrac{\partial E_4}{\partial Q_5}\Delta Q_5 \\[2mm] \dfrac{\partial E_5}{\partial Q_1}\Delta Q_1 & \dfrac{\partial E_5}{\partial Q_2}\Delta Q_2 & \dfrac{\partial E_5}{\partial Q_3}\Delta Q_3 & \dfrac{\partial E_5}{\partial Q_4}\Delta Q_4 & \dfrac{\partial E_5}{\partial Q_5}\Delta Q_5 \end{bmatrix} \tag{6.52}$$

Row i represents the node in which we want to control the voltage, and column j represents the nodes in which we can control the reactive power. The BG is the generator connected to node j that has the maximum absolute value of the sensitivity product in position i,j. By finding the maximum sensitivity product in row i, we automatically choose the BG because the location corresponds to column j of the maximum sensitivity product.

It is clear that, for a general network with N nodes (per phase), the sensitivity table takes the following form:

$$\begin{bmatrix} \dfrac{\partial E_1}{\partial Q_1}\Delta Q_1 & \dfrac{\partial E_1}{\partial Q_2}\Delta Q_2 & \dots & \dfrac{\partial E_1}{\partial Q_N}\Delta Q_N \\[2mm] \dfrac{\partial E_2}{\partial Q_1}\Delta Q_1 & \dots & \dots & \dots \\[2mm] \dots & \dots & \dots & \dots \\[2mm] \dfrac{\partial E_N}{\partial Q_1}\Delta Q_1 & \dots & \dots & \dfrac{\partial E_N}{\partial Q_N}\Delta Q_N \end{bmatrix} \tag{6.53}$$

It is important to note that, if it is not possible to regulate the reactive power (e.g., if in that node there is a load or a non-controllable generator) in a node j, then $\Delta Q_j = 0$ and, consequently, the sensitivity product in the position i,j of the sensitivity table is 0.

Comparing (6.52) with (6.50), we can say that each element i, j of $\left[T_{SQ,a}\right]$ represents the line-to-neutral voltage variation in node i when a reactive power variation occurs in node j.

It is clear that also the "*active power sensitivity table*" $\left[T_{SP,a}\right]$ can be defined. The elements of this table are $\left(\partial E_i' \big/ \partial P_j\right)\Delta P_j$.

It is clear that, for the entire LV grid, two sensitivity tables per phase (for the reactive and active power), and matrixes, can be defined, as summarized in Table III.

TABLE XIV. SENSITIVITY TABLES OF THE ENTIRE LV GRID

Phase	Reactive power sensitivity table	Active power sensitivity table
a	$\left[T_{SQ,a}\right]$	$\left[T_{SP,a}\right]$
b	$\left[T_{SQ,b}\right]$	$\left[T_{SP,b}\right]$
c	$\left[T_{SQ,c}\right]$	$\left[T_{SP,c}\right]$

6.5 REFERENCES

[1] R. Marconato, "Electric Power Systems Vol. II" CEI, Milano, 2008.

[2] M. Brenna, E. De Berardinis, L. Delli Carpini, F. Foiadelli Member, P. Paulon, P. Petroni, G. Sapienza, G. Scrosati, D. Zaninelli, " Automatic Distributed Voltage Control Algorithm in Smart Grids applications", IEEE Transaction on Smart Grids, in publication.

[3] M. Brenna, E. De Berardinis, F. Foiadelli, G. Sapienza, D. Zaninelli, "Voltage Control in Smart Grids: an Approach Based On Sensitivity Theory", J. Electromagnetic Analysis & Applications, 2010.

[4] F. Cottignoli, A. Baccarini, "Elettrotecnica Generale", Edizioni Calderini, Bologna.

[5] F. Cottignoli, A. Baccarini, "Macchine Elettriche", Edizioni Calderini, Bologna.

[6] F. Cottignoli, A. Baccarini, "Misure elettriche ed elettrotecniche", 3 voll., Edizioni Calderini, Bologna, 1970.

[7] F. Cottignoli, A. Baccarini, "Guida al laboratorio di misure elettriche", 2 voll., E-dizioni Calderini, Bologna, 1971.

[8] S. Conti, S. A. Rizzo, "Voltages Sensitivity Analysis in Radial Active Distribution Networks using Novel Closed-Form Approximate Equations", International Review of Electrical Engineering (I.R.E.E.).

[9] S. Conti, S. Raiti, G. Vagliasindi, "A Simplified Approach to Voltage Sensitivity Analysis in Radial MV Distribution Networks with Constant Current Models for Loads and Generators", Industrial Electronics (ISIE), 2010 IEEE International Symposium on, Issue Date: 4-7 July 2010, On page(s): 2548 - 2554.

[10]   P. Kundur, "Power System Stability and Control" McGraw-Hill, 1994.

[11]   Y. Rosales Hernandez, T. Hiyama, "Distance Measure Based Rules for Voltage Regulation with Loss Reduction"

[12]   F. Saccomanno, "Electric Power Systems" Wiley-Interscience IEEE Press, Piscataway, NJ, 2003.

[13]   G. Andersson, "Modeling and Analysis of Electric Power Systems" Lecture 227-0526-00, ITET ETH Zürich, 2008, Zürich.

[14]   Y. Abdel-Rady I. Mohamed E. F. El-Saadany "A Control Scheme for PWM Voltage-Source Distributed-Generation Inverters for Fast Load-Voltage Regulation and Effective Mitigation of Unbalanced Voltage Disturbances" IEEE Transactions on Industrial Electronics, Vol. 55, N. 5, May 2008 Page(s): 2072 – 2084.

[15]   P. M. S. Carvalho, P. F. Correia, L. A. F. M. Ferreira, "Distributed Reactive Power Generation Control for Voltage Rise Mitigation in Distribution Networks," Power Systems, IEEE Transactions on Volume: 23 , Issue: 2, 2008 , Page(s): 766 – 772.

[16]   P. N. Vovos, A. E. Kiprakis, A. R. Wallace, G. P. Harrison, "Centralized and Distributed Voltage Control: Impact on Distributed Generation Penetration," Power Systems, IEEE Transactions on Volume: 22, Issue: 1, 2007 , Page(s): 476 – 483.

[17]   P.M. Anderson, "Power System Protection," IEEE Press, Piscataway, NJ, 1999.

[18]   N. Mohan, T. M. Undeland, W. P. Robbins, "Power electronics: converters, applications, and design", Wiley, 1995.

[19]   M. H. Rashid, "Power Electronics Handbook", Academic Press-Elsevier, 2007.

[20]   L. L. Grigsby, "Electric Power Generation, Transmission and Distribution", CRC Press-Taylor & Francis Group, Boca Raton, 2006.

[21]   F. A. Viawan, D. Karlsson, "Coordinated Voltage and Reactive Power Control in the Presence of Distributed Generation," PES General Meeting - Conversion and Delivery of Electrical Energy in the 21st Century, 2008 IEEE.

[22]   S. Corsi, "Wide Area Voltage Regulation & Protection" Paper accepted for presentation at 2009 IEEE Bucharest Power Tech Conference, June 28th - July 2nd, Bucharest, Romania.

[23]   A. Gandelli, S. Leva, A. P. Morando, "Topological Considerations on the Symmetrical Components Transformation, "Circuits and Systems I: Fundamental Theory and Applications, IEEE Transactions on Vol. 47, Issue 8, Aug. 2000 Page(s): 1202 – 1211.

[24]   Radial Distribution Test Feeders, Distribution System Analysis Subcommittee Report.

[25]   H. M. Ayres, L. C. P. da Silva, W. Freitas, M. C. de Almeida V. F. da Costa, "Evaluation of the Impact of Distributed Generation on Power Losses by Using a Sensitivity-Based Method," PES General Meeting, 2009 IEEE.

[26]   A. Kishore, E. F. Hill, "Static optimization of Reactive Power Sources by use of Sensitivity Parameters", Power Apparatus and Systems, IEEE Transactions on, Volume: PAS-90, Issue: 3, 1971, Page(s): 1166 – 1173.

Conclusions

In this PhD Thesis, developed in collaboration with Enel Distribuzione S.p.A., new MV distribution grid voltage control criteria has been analyzed, in order to improve the network operation in presence of high Distributed Generation installation.

The Distributed Generation presence in distribution networks completely changes the voltage control criteria both in Primary Substation and along feeders because lines voltage profile is not more decaying in monotone way. In fact, due to active power injections, DG can increase node voltages up to exceeding voltage limits stated by European Standards.

Therefore a new voltage control strategy is necessary both to avoid over/under voltages conditions and to increase MV network hosting capacity.

Real-Time Digital Simulator (RTDS) has been used to test the new voltage control criteria applied:

- to MV busbar voltage regulation in Primary Substation
- locally, along feeders
- centrally, involving the entire MV grid

Obtained results, detailed in Chapter 5, can be summarized as follows:

1. Using the actual voltage control, without involving new voltage control criteria, generators G1, G2, G3 and G5 daily violate, for about two hours, voltage limits imposed by the European Standard EN 50160 ($\pm$ 10 %). It is important to note that the generators nominal power that should be disconnected amounts to 3.814 MW, referred to a total 3.974 MW connected to the grid. It is important to note that the presence of DG decrease active power losses from 2.99 MWh to 1.74 MWh. This phenomenon occurs because generated energy is quite close to the load so reducing power flows along line sections.

2. Activating the new Local Voltage Control criteria, presented in Chapter 2, all generators do not violate EN 50160 limits. In this conditions, daily grid losses increase, passing from 1.74 MWh to 2.57 MWh (UPG voltage control function) or 2.41 MWh (RQV voltage control function) due to the reactive power exchange necessary to the voltage control. It is worth noting that the UPG and the RQV have quite the same effect, even if

the UPG function seems to be more efficient in terms of hosting capacity. In fact, it is able to decrease the voltage to some percent less than RQV function.

Further analysis showed that up to 5 MW can be connected to the network without violating EN 50160 limits, which corresponds to +28 % hosting capacity more.

3. Modifying the criteria actually used for the MV busbar voltage control, presented in Chapter 1, the nominal power that could be connected reaches 6.95 MW so increasing of +75 % the grid hosting capacity. In this conditions daily grid losses increase significantly, passing from 1.74 MWh to 5.77 MWh (UPG voltage control function) or 5.51 MWh (RQV voltage control function) due to great amount of reactive power exchange necessary to the voltage control. On the other hand, daily energy flowing through HV/MV transformer is quite zero due to the high DG penetration compared to the load.

4. Finally, activating the new Centralized Voltage Control function, presented in Chapter 3, different condition have been considered. In particular, a condition where two generators (G4 and G5) don't activate any local voltage control has been considered. In this condition, G1 voltage exceeds voltage limits and local voltage control is activated. Nevertheless G1 voltage reaches the highest value so requiring an help to the central Voltage Control System (VCS). The VCS call the "closest" generators to operate, at first G5 and then G4. It's important to note that the closet generator firstly called (G5) is geographically farer than G4 but more efficient from the Sensitivity Table.

Results showed in this PhD Thesis have been obtained analyzing a real MV line (named "Ciccalento"). They demonstrated the effectiveness of the proposed voltage control criteria that can be therefore used for an efficient voltage control of MV grids.

However, numerical results obtained for the "Ciccalento" line can't be used to evaluate the effectiveness of the proposed voltage control for different lines because it strongly depends on network electric characteristics (resistance, reactance, capacitance, etc.), network topology, load and generation power, point of connection. In other words, only analysis on each line could give numerical results to quantify the effectiveness of the proposed voltage control criteria.

Un Grazie...

Un grazie di cuore a tutte le persone che direttamente o indirettamente hanno fatto si che questo lavoro potesse vedere la luce, assistendomi, consigliandomi e supportandomi sia dal punto di vista scientifico che umano.

Ringrazio, con una forte stretta di mano, tutte le persone che istituzionalmente hanno permesso l'avvio ed il temine di questo percorso di Dottorato di Ricerca, nato e portato avanti in collaborazione con Enel Distribuzione S.p.A.

Un sentito grazie è rivolto agli Amici dell'Enel, del CESI e del Politecnico di Milano. I loro preziosi consigli, la loro esperienza e soprattutto la loro Amicizia, hanno funzionato da motore per svolgimento e la conclusione di questa Attività di Ricerca.

Ringrazio la mia Famiglia per tutto il supporto datomi in questi anni.
Infine un forte abbraccio è rivolto ad Alessandra che, ancora una volta, ha avuto la pazienza di aspettarmi e credere in me.

Un grazie di cuore, a tutti,

Gianluca